



This work is protected by copyright and other intellectual property rights and duplication or sale of all or part is not permitted, except that material may be duplicated by you for research, private study, criticism/review or educational purposes. Electronic or print copies are for your own personal, non-commercial use and shall not be passed to any other individual. No quotation may be published without proper acknowledgement. For any other use, or to quote extensively from the work, permission must be obtained from the copyright holder/s.

**A novel *in vitro* bioluminescence rate-of-kill  
(BRoK) assay to study the pharmacodynamic properties of  
antimalarial drug action in *Plasmodium falciparum***

**Imran Ullah**

**Ph.D thesis**

**June, 2016**

**Keele University**

## DECLARATION

---

### SUBMISSION OF THESIS FOR A RESEARCH DEGREE

#### Part I. DECLARATION by the candidate for a research degree.

Degree for which thesis being submitted: **Ph.D**

Title of thesis: **A novel *in vitro* bioluminescence rate-of-kill (BRoK) assay to study the pharmacodynamic properties of antimalarial drug action in *Plasmodium falciparum***

Date of submission: **21/12/2015**

Original registration date: **19/09/2012**

Name of candidate : **Imran Ullah**

Research Institute: **rISTM**

Name of Lead Supervisor: **Prof. Paul Horrocks**

I certify that:

- (a) The thesis being submitted for examination is my own account of my own research
- (b) My research has been conducted ethically. Where relevant a letter from the approving body confirming that ethical approval has been given has been bound in the thesis as an Annex
- (c) The data and results presented are the genuine data and results actually obtained by me during the conduct of the research
- (d) Where I have drawn on the work, ideas and results of others this has been appropriately acknowledged in the thesis
- (e) Where any collaboration has taken place with one or more other researchers, I have included within an 'Acknowledgments' section in the thesis a clear statement of their contributions, in line with the relevant statement in the Code of Practice (see Note overleaf).
- (f) The greater portion of the work described in the thesis has been undertaken subsequent to my registration for the higher degree for which I am submitting for examination
- (g) Where part of the work described in the thesis has previously been incorporated in another thesis submitted by me for a higher degree (if any), this has been identified and acknowledged in the thesis
- (h) The thesis submitted is within the required word limit as specified in the Regulations

Total words in submitted thesis (including text and footnotes, but excluding references and appendices) **41,299.**

Signature of candidate .....

Date: **21/12/2015**

## ABSTRACT

---

Massive screens of chemical libraries for antimalarial activity have identified thousands of compounds that exhibit sub-micromolar potency against the blood stage of the malaria parasite *Plasmodium falciparum*. Triaging these compounds to establish priorities to take forward for development requires additional information regarding their activity. Key amongst their pharmacodynamics (PD) properties is the rate of kill– with a rapid cytocidal effect specifically identified as a key requirement for a Single Exposure Radical Cure and Prophylaxis (SERCaP) product. Compounds that exert an immediate cytocidal effect rapidly reduce parasite burden to ameliorate the morbidity and mortality of disease. With the overall aim to accelerate drug screening by validating a rapid rate of kill, the validation of a novel, quick (6hr) and potentially scalable bioluminescence rate of kill (BRoK) assay is described here that demonstrates a good correlation with *in vitro* recrudescence-based rate of kill data and available *in vivo* clinical findings. The BRoK assay was used to screen the Medicine for Malaria Venture Malaria Box to identify compounds with rapid cytocidal activity. Seventeen compounds have an initial rate of kill greater than artemisinins, with a further 39 compounds exhibiting a rate of kill between chloroquine and artemisinins. These compounds represent potential Target Candidate Profile, compounds for a SERCaP product. This work highlights the opportunity for the BRoK assay as a hit discovery tool. In addition, the potential for this assay in lead validation through structure activity relationship studies are highlighted.

## TABLE OF CONTENTS

DECLARATION .....	II
ABSTRACT .....	III
LIST OF FIGURES .....	VII
LIST OF TABLES .....	X
ABBREVIATIONS .....	XI
ACKNOWLEDGEMENTS .....	XV
<b>CHAPTER 1: Introduction.....</b>	<b>1</b>
1.1 Malaria: a major public health challenge.....	1
1.2 The genus <i>Plasmodium</i> .....	4
1.2.1 <i>Plasmodium falciparum</i> .....	4
1.2.2 <i>Plasmodium vivax</i> .....	5
1.2.3 <i>Plasmodium ovale</i> .....	6
1.2.4 <i>Plasmodium malariae</i> .....	7
1.2.5 <i>Plasmodium knowlesi</i> .....	7
1.3 Malaria transmission .....	8
1.3.1 The <i>Anopheles</i> vector and factors affecting transmission.....	8
1.4 Life cycle and biology of <i>P. falciparum</i> .....	13
1.4.1 Asexual life cycle of <i>P. falciparum</i> .....	14
1.4.1.1 Hepatic stage/ pre-erythrocytic phase.....	14
1.4.1.2 Erythrocytic stage.....	14
1.4.1.2.1 Erythrocytes invasion.....	14
1.4.1.2.2 Ring forms.....	15
1.4.1.2.3 Parasite-induced changes to the host erythrocyte: its associated virulence and pathology.....	17
1.4.1.2.4 Late trophozoite and schizogony.....	19
1.4.2 Sexual differentiation .....	19
1.5 Clinical features .....	20
1.5.1 Uncomplicated malaria .....	21
1.5.2 Severe malaria .....	21
1.6 Malaria control strategies.....	23
1.6.1 Diagnosis of malaria .....	23
1.6.2 Vector control.....	24
1.6.3 Vaccine development .....	25
1.7 Antimalarial drugs.....	27

1.8 The search for novel scaffolds/chemotypes .....	34
1.8.1 Target product profiles .....	39
1.9 Moving forward: determining key pharmacodynamic properties.....	41
Aims of this study .....	48
<b>CHAPTER 2: Materials and Methods.....</b>	<b>50</b>
2.1 Materials (stocks and reagents).....	50
2.2 Cell culture methods.....	51
2.2.1 Human blood and serum .....	51
2.2.2 <i>P. falciparum</i> clone .....	52
2.2.3 Preparation of normal human red blood cells .....	52
2.2.4 Continuous cell culture of <i>P. falciparum</i> .....	53
2.2.5 <i>P. falciparum</i> cell culture synchronisation with sorbitol .....	53
2.2.6 Long term storage of <i>P. falciparum</i> cell culture .....	53
2.2.7 Thawing of glycerolyte-frozen <i>P. falciparum</i> with NaCl .....	54
2.3 Drug assays .....	54
2.3.1 Drug stocks preparation .....	54
2.3.2 Standard cell culture conditions and format of 96-well microplates for drug assays .....	55
2.3.3 Standard protocol for luciferase assay .....	58
2.3.4 Standard protocol for Malaria Sybr Green I Fluorescence (MSF) assay .....	58
2.3.5 Determination of the 50% inhibition concentration (IC <sub>50</sub> ) .....	59
2.3.6 Determination of the 50% lethal dose concentration (LD <sub>50</sub> ) .....	59
2.3.7 Bioluminescent rate-of-kill assays .....	62
2.3.8 Bioluminescence rate of kill assay quality parameters .....	64
2.4 Data management .....	64
<b>CHAPTER 3: Development and Validation of a Rapid <i>In Vitro</i> Bioluminescence-Based Rate of Kill Assay ..</b>	<b>66</b>
3.1 Introduction .....	66
3.2. Results.....	73
3.2.1 The bioluminescence response following drug treatment is both time and dose-dependent .....	73
3.2.2 Correlating the loss of bioluminescence signal following drug treatment with the loss of parasite viability .....	74
3.2.3 The dose and time-dependent loss of bioluminescence following drug treatment correlates with the known rate of kill of benchmark antimalarial drugs .....	84
3.3 Discussion .....	89
<b>CHAPTER 4: Screening the Malaria Box Using a Rapid <i>In Vitro</i> Bioluminescence Rate of Kill Assay .....</b>	<b>98</b>
4.1 Introduction .....	98
4.2 Results.....	103

4.2.1 Determination of the 50% inhibition concentration (IC <sub>50</sub> ) using the Malaria Sybr .....	103
4.2.2 Screening the Malaria Box for compounds that exert an immediate rapid rate of kill using a single-dose/single timepoint triage assay .....	108
4.2.3 Exploring the fast acting compounds .....	110
4.2.4 Principle Component Analysis (PCA) of bioluminescence rate of kill assay data .....	117
4.2.5 Single point assays using 3D7 IC <sub>50</sub> data: A simpler way forward? .....	128
4.3 Discussion .....	134
<b>CHAPTER 5: Exploring the Slow Acting Compounds in the Malaria Box Using a 48-Hours Bioluminescence-Rate of Kill (BRoK) Assay .....</b>	<b>154</b>
5.1 Introduction .....	154
5.2 Results.....	159
5.2.1 Summary of the experimental approach.....	159
5.2.2 Provision of a full 6hr BRoK assay dataset for the MMV Malaria Box.....	161
5.2.2 Exploring the slow acting compounds in a 48hr assay format .....	165
5.3 Discussion .....	173
<b>CHAPTER: 6 Discussion .....</b>	<b>183</b>
<b>References .....</b>	<b>204</b>
Appendix 1 (Chapter 4, Chapter 5).....	226
Appendix 2 (Chapter 4) .....	252
Appendix 3 (Chapter 5) .....	254
Appendix 4 (Chapter 5) .....	257

## LIST OF FIGURES

---

Figure 1.1: The global distribution of malaria .....	1
Figure 1.2: Global malaria mortality trends .....	3
Figure 1.3: The immuno-epidemiology of malaria in relation to age.....	12
Figure 1.4: The life cycle of the human malaria parasite <i>P. falciparum</i> .....	13
Figure 1.5: Intraerythrocytic development (48 hour cycle) of <i>P. falciparum</i> .....	16
Figure 1.6: The malaria vaccine pipeline .....	26
Figure 1.7: The main antimalarial drugs classes approved for use in humans. ....	31
Figure 1.8: MMV selection process for the 400 Malaria Box compounds .....	38
Figure 1.9: Target candidate profiles (TCP) for future antimalarial drugs .....	41
Figure 1.10: Schematic representation of luciferase and SyBr-Green-I reactions.....	46
Figure 1.11: The immediate dynamic response of bioluminescence and fluorescence assays of drug activity.....	48
Figure 2.1: Schematic representation of the plate set-up used for drug assays.....	57
Figure 2.2: Schematic representation of the modified bioluminescence protocol. ....	61
Figure 2.3: Schematic representation of the BRoK protocol.....	63
Figure 3.1 In vivo PRR and PCT data .....	68
Figure 3.2: In vitro log PRR and PCT data .....	70
Figure 3.3: Bioluminescence signal loss following drug perturbation is time-dependent .....	71
Figure 3.4: Dose and time-dependent effect on luciferase signal following drug perturbation.....	74
Figure 3.5: Protocols for the determination of in vitro LD <sub>50</sub> . ....	76
Figure 3.6: In vitro ED <sub>50</sub> <sup>6hr</sup> , LD <sub>50</sub> <sup>48hr</sup> and IC <sub>50</sub> <sup>48hr</sup> determination using luciferase and SyBr-Green-I (MSF) assay formats. ....	79
Figure 3.7: Loss of bioluminescence correlates with loss of viability.....	82
Figure 3.8: Morphological inspection of drug-treated parasites .....	84
Figure 3.9: The dose and time-dependent effects of different antimalarial drugs.....	85
Figure 3.10: Correlation of the bioluminescence against in vitro PCT and PRR .....	88
Figure 3.11: Comparison of ED <sub>50</sub> <sup>6hr</sup> against LD <sub>50</sub> <sup>48hr</sup> .....	92
Figure 3.12: Comparison of rate of kill against IC <sub>50</sub> and LD <sub>50</sub> .....	94
Figure 3.13: Comparison of LD <sub>50</sub> /IC <sub>50</sub> ratios against Rate of kill .....	96
Figure 4.1: The initial selection process of St Jude's, GSK and Novartis antimalarial datasets.....	100
Figure 4.2: The MMV selection process for the 400 Malaria Box compounds .....	101
Figure 4.3: Exemplars of log dose response curves for the Malaria Box compounds ...	104
Figure 4.4: Initial rate of kill against the IC <sub>50</sub> potency for the Malaria Box compounds	109
Figure 4.5: Exemplars of estimated fast and slow RoK .....	111

Figure 4.6: Correlation between time and dose dependent effects in the BRoK assay	116
Figure 4.7: Principle component Analysis	119
Figure 4.8: Comparison between PC1 and loss of bioluminescent signal in the BRoK assay	120
Figure 4.9: Exploring RoK (PC1) against the IC <sub>50</sub> potency of the MMV Malaria Box compounds	123
Figure 4.10: Comparison of Dd2 <sup>luc</sup> and 3D7 IC <sub>50</sub> data	129
Figure 4.11: Comparison of two independent 3D7 IC <sub>50</sub> datasets	130
Figure 4.12: Correlating the RoK against the corresponding IC <sub>50</sub> data from 3D7	131
Figure 4.13: Comparison between the RoK obtained using Dd2 <sup>luc</sup> and 3D7 IC <sub>50</sub> values	132
Figure 4.14: Single dose and single timepoint triage assay	133
Figure 4.15: Correlation of PC1 against PCT and PRR	136
Figure 4.16: Physicochemical property radar plot of the 17 hits compounds	141
Figure 4.17: Stage specific action of MMV Malaria Box compounds	142
Figure 4.18: Comparison of Tanimoto similarity score against differences in PC1	145
Figure 4.19: Correlation of Tanimoto similarity score against difference in RoK	151
Figure 4.20: Comparison of PC1 dataset ( $\Delta$ PC1) against the fold-IC <sub>50</sub> difference	152
Figure 5.1: Strong temporal regulation of the Pfp <sub>pcna</sub> -luciferase promoter cassette during intraerythrocytic development.	155
Figure 5.2: A schematic for the analysis of the BRoK data	159
Figure 5.3: Dose-dependent rate of kill of the Malaria Box candidates	160
Figure 5.4: Correlation between dose-dependent effects in a 6hr BRoK assay	162
Figure 5.5: Correlating RoK (PC1) for 370 Malaria Box compounds with IC <sub>50</sub> and PC2	164
Figure 5.6: Correlation between dose-dependent effects in the 48hr BRoK assay	167
Figure 5.7: PC1 (48hr) data plotted against their IC <sub>50</sub> potency- separating “slow-cytocidal” from those with no appreciable cytotoxic effect	169
Figure 5.8: Exploring the top 20 compounds with “slow-cytocidal” activity or no appreciable cytotoxic effect	172
Figure 5.9: Correlating biophysical properties against the RoK	178
Figure 5.10: Stage specific action of Group A and B compounds	180
Figure 6.1: Comparison between BroK and reinvasion rate of kill assay data	185
Figure 6.2: Metabolic fingerprints of selected Malaria Box compounds	190
Figure 6.3: Correlation between RoK and fold-changes in the metabolites DHO and NCLA	191
Figure 6.4: Stereoisomers (R,S) of 4-aminoalcohol quinolines show the same rate of kill in the BRoK assay	193
Figure 6.5: Examples illustrating related compounds in the Malaria Box that share a similar rate of kill	196

Figure 6.6: Examples illustrating related compounds in the Malaria Box that show variation in their rates of kill.....	199
Figure 6.7: Correlating biophysical data against rates of kill for Acridine and Tetrahydroisoquinoline scaffolds in the Malaria Box.....	202

## LIST OF TABLES

Table 1.1: Malaria morbidity and mortality rates .....	3
Table 1.2.: Antimalarials and resistance .....	28
Table 1.3: Antimalarial drug classes; their mode of action and mechanism of resistance .....	32
Table 1.4: Common artemisinin-based combination therapies .....	33
Table 1.5: The antimalarial drug pipeline over the past five years .....	38
Table 2.1: Preparation of drug stocks .....	55
Table 2.2: Bioluminescence assay quality parameters .....	64
Table 3.1: Target Candidate Profile 1 (TCP1) .....	66
Table 3.2: Estimates of $ED_{50}^{6hr}$ , $LD_{50}^{48hr}$ and $LD_{50}^{48hr}$ using the bioluminescence and MSF assay formats .....	80
Table 3.3: Ratios of $IC_{50}$ and $LD_{50}/ED_{50}$ .....	95
Table 4.1: Reports $IC_{50}$ data of the 396 Malaria Box compounds obtained using host strain Dd2 <sup>luc</sup> .....	107
Table 4.2: PCA on the estimates of rate of kill data .....	119
Table 4.3: TCP1 candidates in the MMV Malaria Box .....	124
Table 4.4: Biophysical parameters of hits .....	127
Table 4.5: Seven outliers in the Malaria Box compounds .....	139
Table 4.6: Similarity scores for 22 pairs of the Malaria Box compounds .....	150
Table 5.1: The in vitro lag phase of known antimalarial drugs .....	156
Table 5.2: Stage specific activity of known antimalarial drugs .....	157
Table 5.3: Principle Component for 370 MMV Malaria Box compounds (6hr) .....	163
Table 5.4: Comparison TCP1 candidates (Chapter 4 vs 5) .....	165
Table 5.5: Principle Component for 370 MMV Malaria Box compounds (48hr) .....	168
Table 5.6: Ranking of the 48hr PC1 data .....	170
Table 6.1: Advantages and disadvantages of current in vitro rate of kill assays for P. falciparum. ....	187
Table 6.2: Structure of compounds within the acridines and tetrahydroisoquinoline clusters .....	198

## ABBREVIATIONS

---

ACTD	Actinomycin-D
ACTs	Artemisinin Combination Therapies
AQ	Amodiaquine
ART	Artemether
AS	Artesunate
ASAQ	Artesunate-Amodiaquine
ASMQ	Artesunate-Mefloquine
ATOVA	Atovaquone
AZ	Azithromycin
BOC	British Oxygen Company
BRoK	Bioluminescence Rate of Kill
BSD	Blasticidin S hydrochloride
CC <sub>50</sub>	Cytotoxicity 50%
CDC	Centers for Disease Control and Prevention
CHMP	Committee for Medicinal Products for Human Use
CHX	Cycloheximide
CQ	Chloroquine
CQR	Chloroquine Resistant
CQS	Chloroquine Sensitive
CSA	Chondroitin Sulphate
DAPI	40, 60-Diamidino-2-Phenylindole
DDT	Dichlorodiphenyltrichloroethane
DHA	Dihydroartemisinin
DHFR	Dihydrofolate Reductase
DHODase	Dihydroorotate Dehydrogenase
DHPS	Dihydropteroate Synthase
DMSO	Dimethyl Sulfoxide
DNDi	Drugs for Neglected Diseases initiative
DXP	1-Deoxy-D-Xylulose 5-Phosphate
ED <sub>50</sub> <sup>6hr</sup>	Effective dose at 6hr
EBI	European Bioinformatics Institute
ECFP4	Extended Connectivity Fingerprint
ECG	Electrocardiogram
EDTA	Ethylene Diamine Tetraacetic Acid
EIR	Entomological Inoculation Rate
ELAM-1	Endothelial Leukocyte Adhesion Molecule-1
EMA	European Medicines Agency

EBI	European Bioinformatics Institute
Farmanguinhos	Institute of Drug Technology Brazil
FDA	Food and Drug Administration
Fe (III) PPIX	Ferrous-Protoporphyrin IX
FV	Food Vacuole
G6PDH	Glucose-6-Phosphate Dehydrogenase
GM	Genetically Modified Parasites
GNF	Novartis Research Foundation
GSK	GlaxoSmithKline
HCT	Haematocrit
HIV	Human Immunodeficiency Virus
HL	Horrocks laboratory
hpi	Hours Post Infection
HRP2	Histidine-Rich Protein 2
hrs	Hours
HSE	Health and Safety Executive
HTA	Human Tissue Authority
HTS	High Throughput Screening
IC <sub>50</sub>	50% Inhibition Concentration
ICAM-1	Intercellular Adhesion Molecule-1
IE	Infected Erythrocytes
IFN- $\gamma$	Interferon-Gamma
IFN- $\gamma$	Interferon-Gamma
iRBCs	Infected Red Blood Cells
IRS	Indoor Residual Spraying
ISTM	Institute for Science and Technology in Medicine
ITNs	Vector controls Insecticide Treated Nets
KAHRP	knob-Associated Histidine Rich Protein
L	litres
LD <sub>50</sub>	50% Lethal Dose Concentration
LLINs	Long Lasting Insecticide Nets
LSTM	Liverpool School of Tropical Medicine
Luc	Luciferase
M	Molar
MDGs	Millennium Development Goals
MDR	Multi Drug Resistant
MEF	Mefloquine
mins	minutes
mL	millilitre
mM	milliMolar

MMV	Medicine for Malaria Venture
MSF	Malaria Sybr Green I Fluorescence
MSPs	Merozoites Surface Proteins
NBTS	National Blood and Transfusion Service
nM	nanoMolar
ORh+	Type-O-Rhesus Positive
PABA	P-Aminobenzoic Acid
PAINS	Pan Assay Interference Compounds
PCA	Principal Component Analysis
PCR	Polymerase chain reaction
PCs	Principle components
PCT	Parasite Clearance Time
<i>PfEMP1</i>	<i>P. falciparum</i> Erythrocyte Membrane Protein 1
<i>PfHRP2</i>	<i>P. falciparum</i> Histidine-Rich Protein 2
pLDH	Parasite lactate dehydrogenase
PQ	Primaquine
PRR	Parasite Reduction Ratio
PSA	Polar Surface Area
PV	Parasitophorous Vacuole
PYR	Pyronaridine
QN	Quinine
RBCs	Human Red Blood cells
RBM	Roll Back Malaria
RDTs	Rapid Diagnostic Tests
REOS	Rapid Elimination of Swill
RLU	Relative Light Units
RNA	Ribonucleic acid
Ro5	Lipinski's Rule of five
RoK	Rate of Kill
RPMI	Roswell Park Memorial Institute
RT	Room Temperature
S/N	Signal-to-Noise
SAR	Structure-activity relationship
sdH <sub>2</sub> O	Sterile Distilled Water
SEC	Single Exposure Chemoprotection
secs	Seconds
SERCaP	Single Exposure, Radical Cure and Prophylaxis
SL	Luciferase Substrate
SP	Sulfadoxine-Pyrimethamine
TBV	Transmission Blocking Vaccines

TCAMS	Tres Cantos Antimalarial Set (GlaxoSmithKline)
TCPs	Target Candidate Profiles
TFQ	Tafenoquine
TPP	Target Product Profiles
TSP	Thrombospondin
U/mL	Unit Per millilitre
UNDP	United Nations Development Programme
v/v	Volume per volume
VCAM-1	Vascular Cell Adhesion Molecule
w/v	Weight per volume
WBCs	White Blood cells
WHO	World Health Organization
$\alpha$	Alpha
$\beta$	Beta
$\gamma$	Gamma
$^{\circ}\text{C}$	Degrees Celsius
$\mu\text{L}$	microllilitre
$\mu\text{M}$	micromolar

## ACKNOWLEDGEMENTS

---

Firstly, I would like to express my sincere gratitude to my supervisor Professor Dr. Paul Horrocks for his great supervision, encouragement, unstinting moral and technical support. I am privileged to have been a part of Prof. Horrocks' research team; which has allowed me to work with an inspiring scientist who dwells deep into research questions and as an individual; he has been very friendly and caring. I could not have imagined having a better supervisor for my Ph.D. studies – the most inspiring, outstanding and selfless scientist I have ever worked with.

I am thankful to my advisor Dr. Catherine Merrick for her guidance and encouragement in general and in particular, I have greatly benefited from her feedbacks and insightful comments and suggestions on my presentations and reports. I am grateful to Dr. Colin Sutherland, Dr. Mark Skidmore and Dr. Clare Hoskins for their willingness to serve on my dissertation research committee. I would like to offer my special thanks to Dr. Sandra Hasenkamp who initially trained me in the laboratory.

Principle Component Analysis (PCA), chemical informatics and medicinal chemistry analysis of the Malaria Box compounds were carried out in collaboration with Prof. Giancarlo Biagini and Dr. Raman Sharma of the Liverpool School of Tropical Medicine (LSTM) and Dr. Tony Mete of the Medsyndesign Ltd – A huge thank you to all of you for providing insight and expertise in data analysis

My sincere thanks go to Dr. Srabasti Chakravorty, Dr. Lynne Harris and Dr. James Edwards-Smallbone for their stimulating discussions and constant motivation.

I acknowledge the financial support provided by Keele University for my Ph.D. I also acknowledge the support provided by the Charles Wallace Trust during the final year of my Ph.D. I am indebted to Prof. Trevor Greenhough for providing additional financial support when I needed it most.

Thanks are also due to fellow Ph.D. students, Douglas Paton, Esther Ekechukwu, Hiba Nadhim, Rowida Baeshan and both past and present MSc and BSc project students, and all other colleagues of the Keele Life Sciences department for their cooperation.

I would like to thank my family for their unconditional love and encouragement with particular thanks to my father who served for four decades within the Malaria Control Programme in Pakistan and inspired me to study malaria.

I wish to express a sincere thank you to Hurmat Sami for her unwavering support and endless patience during my Ph.D studies at Keele.

Last, but not the least, I owe my deepest gratitude to my elder brother, Dr. Sami Ullah, for his generous support, guidance and persistent help throughout my life and particularly during my Ph.D. studies at Keele, without which I would not have been able to reach this level of academic achievement.

## CHAPTER 1: Introduction

---

### 1.1 Malaria: a major public health challenge

Malaria is an infectious disease caused by the obligate intracellular protozoan parasite *Plasmodium falciparum* and transmitted by the mosquito vector *Anopheles*. It is a significant public health problem, transmitted in 97 countries (Figure 1.1) with approximately 3.3 billion people at risk which amounts to half of the world population (Roll Back Malaria, 2014; White *et al.*, 2014; WHO, 2014). Approximately 198 million malaria cases (range between 124 to 283 million) were reported in 2013 with 584,000 deaths (range between 367,000-755,000), of which 86% of the morbidity and 90% of the mortality occurred in Africa, mainly in young children under 5 years of age (Roll Back Malaria, 2014; White *et al.*, 2014; WHO, 2014). Malaria is a leading cause of death of children in endemic areas and the most significant parasitic disease in tropical and sub-tropical regions of Africa (White *et al.*, 2014).

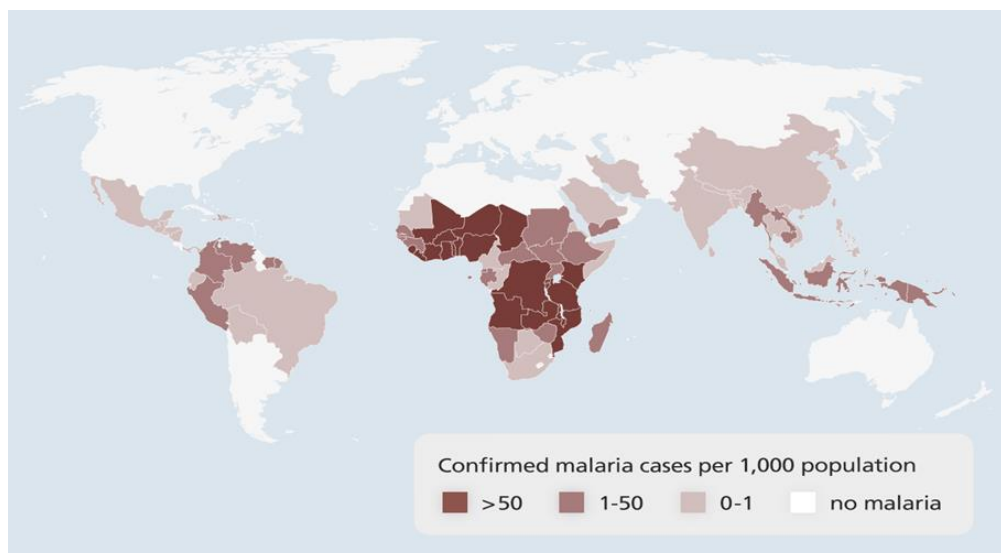


**Figure 1.1: The global distribution of malaria**  
A world map showing the global distribution of malaria burden (source- modified from WHO, 2014).

These figures, however, are based upon WHO reports and it is thought that mortality rates could be as high as one million per year (Murray *et al.*, 2012; Verma *et al.*, 2013). Malaria has been recognised as a major public health problem from the early 20th century. It was once prevalent in 178 countries across the globe (Faechem *et al.*, 2010). World Health Organization (WHO) launched the Global Malaria Eradication Program in the 1950s in all parts of the world apart from Africa. This campaign relied on vector control with the use of insecticide dichlorodiphenyltrichloroethane (DDT) and mass administration of chloroquine (CQ) chemoprophylaxis, which succeeded in eliminating malaria from Europe, Canada, Russia, the Caribbean and parts of Asia (Hay *et al.*, 2004; Faechem *et al.*, 2010; Najera *et al.*, 2011; White, 2014). However, because of the technical, financial and administrative issues, this campaign was abandoned in 1969 leaving Africa, facing a significant health burden from malaria. Chloroquine (CQ) and DDT resistance also emerged during this time in Africa, which led to a three-fold increase in recorded deaths from malaria through the 1980s and 1990s to a peak in 2004 (Figure 1.2) (Faechem *et al.*, 2010; Hay *et al.*, 2004; Murray *et al.*, 2012; White, 2014). Despite these setbacks, control efforts have recently focused on technical developments that have led to renew a global focus on malaria control scale-up activities and, as a result, malaria deaths have declined significantly over the last decade (Table 1.1). These achievements were propelled by the Roll Back Malaria (RBM) initiative (in partnership with WHO, UNDP, UNICEF and the World Bank), launched in 1998, which designed control strategies to eliminate malaria. Whilst emphasizing the strengthening of local health systems, several control intervention coverages were provided, including the wider availability of rapid diagnostic tests (RDTs), treatments and chemoprophylaxis with artemisinin combination

therapies (ACTs), and vector controls such as Insecticide Treated Nets (ITNs) and Long Lasting Insecticide Nets (LLINs).

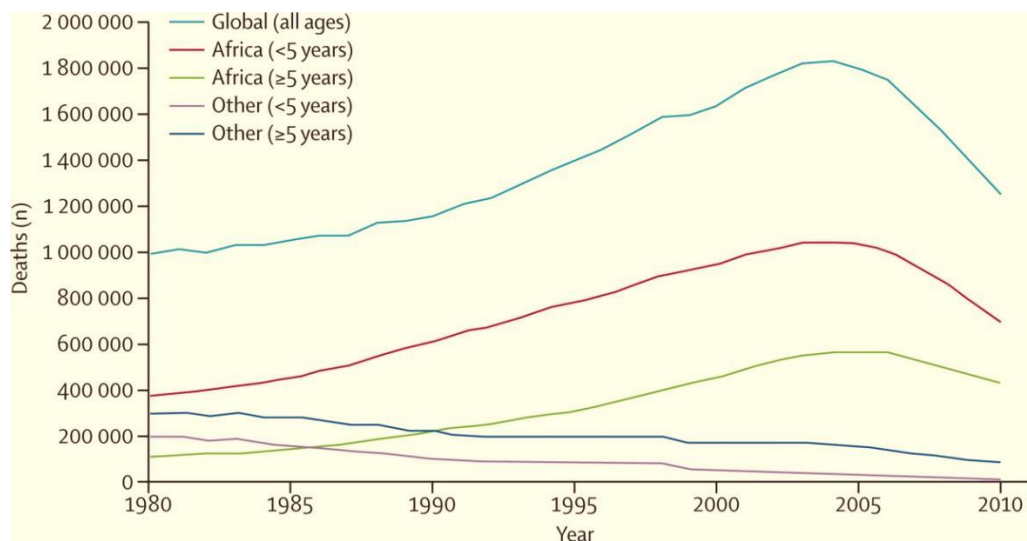


**Figure 1.2: Global malaria mortality trends**

Different curves (color coded) show malaria mortality trends by age and geographical region over time. Malaria mortality rates raised through the 1980s and early 1990s to a peak in 2004 with a 32% from this peak by 2010 (source- Murray et al., 2012).

KEY MALARIA STATISTICS FROM 2000 TO 2013		
Average malaria infection prevalence declined 46% in children aged 2–10, from 26% to 14% in 2013	The number of malaria infections at any one time dropped 26%, from 173 million to 128 million in 2013	Malaria mortality rates have decreased by 47% worldwide and by 54% in the WHO Africa Region
MILLENNIUM DEVELOPMENT GOALS (MDG) BY 2015		
Malaria mortality rates are projected to decrease by 55% globally and by 62% in the WHO Africa Region.	Malaria mortality rates in children aged under 5 years are projected to decrease by 61% globally and 67% in the WHO Africa Region.	

**Table 1.1: Malaria morbidity and mortality rates**

Significant reduction in overall morbidity and mortality of malaria over the last 13 years and the millennium development goals set for 2015 (source- WHO, 2014).

As mentioned earlier, malaria transmission is restricted to 97 countries of which 67 countries are reversing the incidence of malaria. Of these, 55 countries are likely to meet the Millennium Development Goals (MDGs) set by RBM and World Health Assembly, which aim at a 75% reduction in malaria case incidence by 2015 (WHO, 2014). However, the recent global economic crisis has led to reduction in funding and resources for malaria

control and this underscores a real and imminent threat to the striking reversal of malaria mortality. Furthermore, emerging resistance to ACTs and insecticides in malaria endemic countries pose a direct threat to the huge inroads made recently (WHO, 2014). These challenges, together with poor local health systems, lack of sufficient data on the real impact of malaria case incidence and administrative issues raise enormous doubts, if not addressed promptly, that will make it unlikely to achieve the MDGs established for malaria control by 2015 and even harder to meet the ambitious future targets set for elimination.

## **1.2 The genus *Plasmodium***

*Plasmodium* is a genus of Apicomplexa, which are unicellular eukaryotic organisms (protozoa). Apicomplexa are a diverse group that also includes organisms such as *Cryptosporidium*, *Coccidia* and *Haematozoa*. A large proportion of Apicomplexa are parasitic organisms of vertebrate hosts. *Plasmodium* is the aetiological agent of human malaria. Five species of this genus are known to cause malarial infections in human; *P. vivax*, *P. malariae*, *P. ovale*, *P. knowlesi* and *P. falciparum* (Sutherland *et al.*, 2010).

### **1.2.1 *Plasmodium falciparum***

*P. falciparum* is the most virulent of malaria parasites that infect humans. *P. falciparum* is not as widespread as *P. vivax* (Gething *et al.*, 2011), but it is responsible for almost all malaria deaths (Gething *et al.*, 2011; White, 2014). Sub-Saharan Africa has the heaviest malaria burden due to the predominance of *P. falciparum* in this continent where it accounts for some 70% of cases. *P. falciparum* causes malignant, tertian or falciparum malaria in humans which leads to serious life threatening pathological conditions such as

severe anaemia, respiratory distress, organ failure, and intrauterine growth retardation in pregnancy and cerebral malaria (White, 2014). Due to such potential consequences of *P. falciparum* infection, rapid and effective treatment is vital. However, due to the spread of the multi-drug resistant (MDR) parasite strains globally in general, and in particular, recent reports of evolving resistance to artemisinins in South-East Asia, treatment of *P. falciparum* is becoming increasingly difficult and continues to be responsible for thousands of deaths each year, particularly in children under 5 years of age (Dondorp *et al.*, 2008).

### **1.2.2 *Plasmodium vivax***

*P. vivax* is the most widely distributed of the malaria parasites and accounts for a significant morbidity burden (Gething *et al.*, 2012), with an estimated 2.49 billion people at risk of acquiring infection (Battle *et al.*, 2012). Infection with *P. vivax* occurs predominantly in South East Asia and the Western Pacific, although a number of cases are also found across Africa and South America (Hey *et al.*, 2004). *P. vivax* forms an asymptomatic dormant liver stage (hypnozoites) with an incubation period ranging between weeks to months and may last for years (Price *et al.*, 2007). These dormant stages often result in relapses causing infection (Walker *et al.*, 2014). *P. vivax* has a preference for the invasion of reticulocytes, as opposed to *P. falciparum* which has a broader erythrocyte age invasion range (Price *et al.*, 2007; Simpson *et al.*, 1999) and this might be one of the reasons for limiting its infectious potential. Whilst not normally associated with the severe manifestations of *P. falciparum* malaria, *P. vivax* infection can be serious in the event of a splenic rupture. Nevertheless, it can cause respiratory distress, severe anaemia, coma (Genton *et al.*, 2005) and intrauterine growth retardation

similar to *P. falciparum* (White, 2014). *P. vivax* blood stage infections can be treated with CQ and ACTs where CQ is resistant. The current gold standard for preventing *P. vivax* relapse is Primaquine (PQ), which has hypnozoitocidal activity. However, significant concerns are associated with this drug due to its haemolytic activity in glucose-6-phosphate dehydrogenase (G6PDH) deficient humans.

### **1.2.3 *Plasmodium ovale***

*P. ovale* is a rare protozoan parasite; closely related to *P. falciparum* and *P. vivax* and distributed across South East Asia, sub-Saharan Africa, the Indian subcontinent and the Western Pacific (Fuehrer *et al.*, 2010; Kawamoto *et al.*, 1996; Sutherland *et al.*, 2010). *P. ovale* has a typical incubation time between 12 to 20 days, and like *P. vivax*, it is also characterised by dormant liver stage hypnozoites (with incubation time from weeks, months to years) which can subsequently lead to a relapse after infection (Sutherland *et al.*, 2010). It is responsible for causing tertian malaria in humans; however, assessment of its actual malaria burden is difficult to estimate due its problematic diagnosis. Co-infections of *P. ovale* can be encountered together with *P. falciparum*, *P. vivax* and *P. malariae* (Win *et al.*, 2002) although most *P. ovale* infections last for less than two weeks and parasitaemia rarely reaches a sufficient level which is required to induce clinical episodes. This, in combination with a 49-hour erythrocytic stage, results in *P. ovale* infections often remaining asymptomatic (Mueller *et al.*, 2007). CQ is the current gold standard for the treatment of uncomplicated malaria caused by *P. ovale*, and as described above, PQ is required to eliminate hypnozoites (Kantele and Jokiranta, 2011; Walker *et al.*, 2014).

#### **1.2.4 *Plasmodium malariae***

*P. malariae* is responsible for the mildest and most persistent form of malaria infection, often called benign malaria. Its infection can be found in combinations with *P. falciparum* and *P. vivax* (Westling *et al.*, 1997); however a typical infection caused by this species shows synchronised schizogony from the beginning, with febrile paroxysms normally occurring in the late afternoon, separated by 72 hour intervals, and is known as quartan malaria. The parasitaemia in erythrocytes rarely exceeds 1% due to the spontaneous remission of parasites and thus remains asymptomatic in the blood and, if not treated, infection can even persist for decades (Bartolini and Zammarchi 2012; White, 2014). Due to its low prevalence, milder clinical manifestations, difficulty in diagnosis and lack of *in vitro* studies, *P. malariae* is perhaps the least studied human malarial parasite species and the reason why it is frequently under reported (Mueller *et al.*, 2007; Singh *et al.*, 2004; Smith *et al.*, 1993). CQ or ACTs are the recommended medication for the infections caused by *P. malariae* (CDC, 2013).

#### **1.2.5 *Plasmodium knowlesi***

*P. knowlesi* is a parasite primarily thought to be of primate origin causing infection in *Macaca fascicularis* (Lee *et al.*, 2009). The vectors of this parasite are *Anopheles latens* and *Anopheles cracens* (subgroups of the leucosphyrus group of *Anopheles*) which are zoophilic in nature (Singh and Daneshvar, 2013) and thus naturally acquired human infections of this species were consequently considered rare in South-East Asia until a 2004 outbreak in Sarawak, Malaysia (Antinori *et al.*, 2013; Singh *et al.*, 2004; Singh and Daneshvar, 2013; White, 2008). It was reported that *P. knowlesi* was responsible for about ~60-70% of human malaria cases in Borneo, Malaysia in 2008 (Antinori *et al.*, 2013).

These infections can now be found in almost all other countries in South East Asia, and consequently, *P. knowlesi* is now classified as the fifth human malaria species (Antinori *et al.*, 2013; Figtree *et al.*, 2010; Singh and Danesh, 2013; Van-Hellemond *et al.*, 2009; White, 2008). *P. knowlesi* has a relatively short 24 hour erythrocytic stage cycle (Antinori *et al.*, 2013; Singh and Danesh, 2013) and can, however, attain a high parasitaemia quickly, which results in severe symptoms. The symptoms of infection are comparable to severe malaria caused by *P. falciparum* with the exceptions of severe anaemia and cerebral malaria (Singh and Danesh, 2013; Antinori *et al.*, 2013). *P. knowlesi* shares certain morphological features with *P. falciparum* and *P. malariae*, thus making it difficult to accurately identify it by microscopy. PCR is the most reliable source for detecting and diagnosing *P. knowlesi* infection (Kantele and Jokiranta, 2011), although this is not a rapid diagnostic method. Microscopy still remains the most widely used method in rural areas, and this could affect our understanding of the epidemiology of this species. Since there is no evidence of drug resistance in *P. knowlesi*, CQ is very effective in the treatment of uncomplicated knowlesi malaria infections in humans (Daneshvar *et al.*, 2010).

### **1.3 Malaria transmission**

#### **1.3.1 The *Anopheles* vector and factors affecting transmission**

Malaria is transmitted almost exclusively to human hosts through the bite of an infected *Anopheles* mosquito, which belongs to the subfamily *Anophelinae* (Autino *et al.*, 2012; Su *et al.*, 2007; Toure *et al.*, 2004). There are over 400 species of the *Anopheles* genus, of which over 100 are vectors for malaria (CDC, 2012). Malaria transmission intensity depends on various factors related to the parasite, the vector, the human host, and the environment and thus, only around 20 of the 400 *Anopheline* species are regarded as

good vectors of human infection (White *et al.*, 2013; WHO, 2014). The main *Anopheles* vectors *Anopheles gambiae*, *Anopheles arabiensis* and *Anopheles funestus* are strictly anthropophilic in nature and thus recognised as the most effective vectors of human malaria (CDC, 2012). These vectors are long-lived, occur in high densities in tropical climates, adaptable to environmental change and robust against them, breed readily and are anthropophilic. Their widespread distribution in Sub-Saharan Africa explains why 90% of malaria mortalities are reported in this region (White *et al.*, 2013). These species bite during the night and are most active at dusk and just before dawn mostly endophagic (feed indoors), although some might be both endophagic and exophagic (feed outdoors) (Pates and Curtis, 2012; Zimmerman *et al.*, 2013). The first three stages of the mosquito's life cycle occurs in water; although dependent on the preference of each *Anopheles* mosquito, however, in general, they are capable of breeding in most locations with slow moving water. As this may be fresh or saline water, lakes or small pools, rice paddies or rivers, effects to curtail the breeding of mosquitoes are difficult to implement (CDC, 2012; Zimmerman *et al.*, 2013).

Many factors affect the rate of malaria transmission, including temperature and humidity, time of the season, the longevity of the mosquito's life cycle and its feeding habits. Insect and parasite physiology limits malarial transmission to temperatures between 17-34°C. This temperature range with humidity in temperate regions provide optimum conditions for *Anopheles* mosquitoes to hatch eggs in a few days as opposed to cold or very hot regions where it may take longer (e.g. weeks) or may be detrimental to parasite development. This explains the high transmission burden of parasite in tropical regions compared to colder regions and further elucidates the trend of parasite transmission that

often peaks in autumn as opposed to summer (Mordecai *et al.*, 2013; Yamana and Eltahi, 2013). Malaria transmission peaks during and directly after the rainy season. This is due to the availability of temporary rain pools to the mosquito, which they use as a breeding ground (CDC, 2012). Depending upon environmental conditions, malarial parasites have an extrinsic incubation period (parasite development inside the mosquito host) of between 10-21 days. Thus, long-lived vectors have higher disease transmission rates in endemic regions as the parasite goes through an extrinsic incubation phase ensuring the vectors have sufficient time to transmit the parasite to the human host (White *et al.*, 2014).

The majority of *Anopheles* mosquitoes are both anthropophilic and zoophilic. Areas, where anthropophilic species are prominent have been demonstrated to have higher transmission intensity as compared to those where zoophilic tendencies are more common (CDC, 2012). Transmission intensity is generally measured by determining the Entomological Inoculation Rate (EIR) which is the average number of infectious bites per individual per unit time (Okello *et al.*, 2006; Smith *et al.*, 2001; Talisuna *et al.*, 2012). In low malaria transmission areas, transmission intensity can also be estimated by parasite prevalence (Beier *et al.*, 1999). Malaria transmission is more likely to be seasonal and less intense across (unstable transmission) Asia and South and Central America where people may receive up to 1 infectious bite per year, explaining almost the same prevalence of *P. falciparum* and *P. vivax* although the latter is more common in these areas (Gething *et al.*, 2011). The cooler temperatures in these areas explain why *P. vivax* is more prevalent, since *P. vivax* can survive at lower temperatures and higher altitudes as compared to *P. falciparum* (WHO, 2013). More intense, stable malaria transmission occurs in Africa,

south of the Sahara and in parts of Oceania. These regions are warmer where *P. falciparum* predominates and thus EIR is much higher (i.e. >200 infectious bites per year) (CDC, 2012; Gething *et al.*, 2011).

In those regions where malaria transmission is stable, malaria mortality and morbidity are pronounced in early childhood (i.e. children under five years of age), because the younger children are considered immunologically naive to the malaria parasite. As age increases subsequent malarial infections become milder leading to asymptomatic infections in adulthood (Dondorp *et al.*, 2008, Sarda *et al.*, 2009). This is reflected by the fact that those who live in malaria endemic countries with high transmission rates develop premunition through recurrent exposure (Figure 1.3). Although this protection does not ensure sterile immunity to the disease, it provides partial protection for those regularly exposed to the parasite and thus it prevents symptomatic disease despite the persistent presence of malarial parasites (Doolan *et al.*, 2009; Weatherall *et al.*, 2002). Although the acquired immunity develops rapidly in infants, children under five account for the majority of the malaria incidences especially in holoendemic nations (Aponte *et al.*, 2007). This is because the children under five have not yet acquired a sufficient level of natural immunity offered through repeated exposure so experience the severe and often fatal symptoms (White *et al.*, 2014).

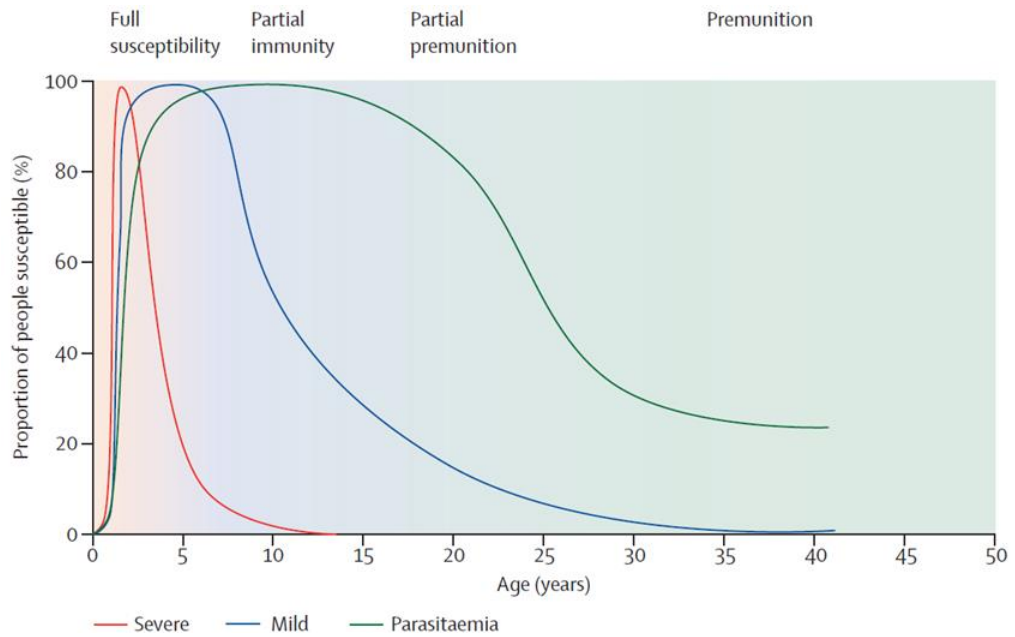


**Figure 1.3: The immuno-epidemiology of malaria in relation to age**  
 The different age groups at which, severe, mild and asymptomatic malaria parasitaemia occurs in areas of high malaria transmission. The stages of infection state are shown above the graph. Full susceptibility is pre-infection, partial immunity is post a single infection while partial premunition and premunition occurs after ~2-3 and 4 or more infections respectively (Source- White et al., 2014).

For non-immune travelers visiting endemic states or people living in unstable malaria transmission regions, full protective immunity from malaria is not acquired. This lack of protective immunity leads to symptomatic disease in all age groups (Crawley et al., 2010; White et al., 2013). Within unstable malaria transmission regions, environmental, economic and social challenges render the regions prone to epidemics, which can result in substantial mortality at all age groups (White et al., 2013). Pregnant women are also prone to malaria infection due to pregnancy related immunosuppression and this explains why they have an elevated rate of stillborn and maternal deaths whilst semi-immune pregnant women have an elevated rate of miscarriage and low birth weight in areas of stable malaria transmission (Kakkilya, 2011). Malaria and HIV are inextricably linked; children born from mothers with both human immunodeficiency virus (HIV) and malaria

have an increased chance of contracting HIV, as placental parasitaemia increases the chance of HIV crossing the placenta (Newman *et al.*, 2009). Similarly, those with HIV are at a greater risk of contracting malaria due to immunosuppression and a reduction in efficiency of antimalarial medication as a result of the virus (Cuadros *et al.*, 2011).

#### 1.4 Life cycle and biology of *P. falciparum*

The life cycle of *P. falciparum* is complex (Figure 1.4), requiring a human host and Anopheline vector for its completion. Within both the host and the vector, the life cycle is characterized by multiple morphological changes as the parasite invades, colonises and then replicates within a diverse range of host environments.

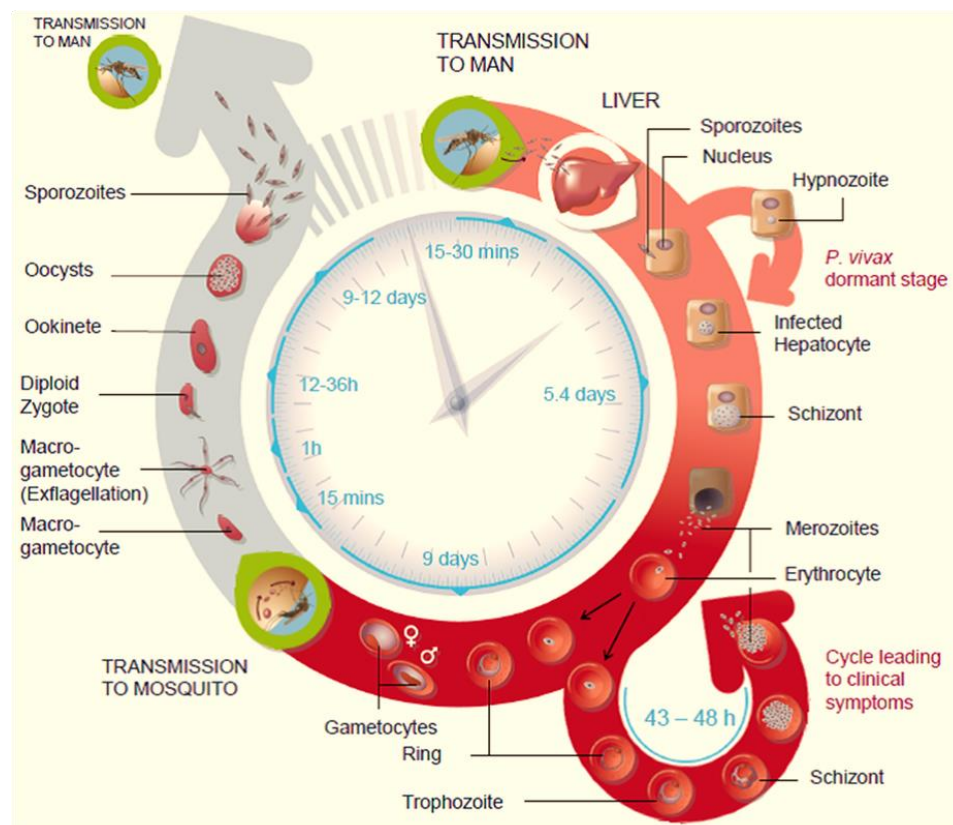


**Figure 1.4: The life cycle of the human malaria parasite *P. falciparum***  
 Female *Anopheles* mosquitoes serve as a vector and humans as the vertebrate host, with different stages in both vector and human host are shown (Source- MMV website <http://www.mmv.org>).

### **1.4.1 Asexual life cycle of *P. falciparum***

#### **1.4.1.1 Hepatic stage/ pre-erythrocytic phase**

The life cycle begins with the bite of an infected female Anopheline mosquito (Figure 1.4). The mosquito injects an anticoagulant and sporozoites into the bloodstream of a human (Amino *et al.*, 2006; Bannister and Mitchell, 2009; Frevert, 2004). Sporozoites migrate into the microvasculature and are carried through the blood system to the liver. Here, sporozoites transverse through multiple hepatocytes before they infect a final one, and form a parasitophorous vacuole (PV) (Prudêncio *et al.*, 2006). With the help of PV or by disrupting the cell membrane, sporozoites cross the liver sinusoid barrier by evading the host's immune defense (i.e. remains hidden from attacks by phagocytic cells and kuppfer cells) (Amino *et al.*, 2008). Following hepatocyte invasion, sporozoites multiply asexually to produce thousands of merozoites within the PV membrane (Meister *et al.*, 2011; Prudêncio *et al.*, 2006). This process of replication and maturation within the liver takes between 5-8 days (White *et al.*, 2014) and this process is called intrahepatic schizogony or the pre-erythrocytic phase. The schizont within the hepatocytes ruptures through mediation by cysteine proteases, releasing thousands of merozoites into the sinusoidal lumen ready to invade erythrocytes (Frevert, 2004). The hepatic/pre-erythrocytic phase of *P. falciparum* life cycle is asymptomatic in humans.

#### **1.4.1.2 Erythrocytic stage**

##### **1.4.1.2.1 Erythrocytes invasion**

The asexual erythrocytic stage of *P. falciparum* commences when small extracellular merozoites invade erythrocytes (Figure 1.5) This is a multi-stage complex process facilitated by the interaction of merozoites surface proteins (MSPs) and invasion

organelles (i.e. dense granules, rhoptries and micronemes) present at the apical end of the parasite (Bannister *and* Mitchell, 2009; Cowman and Crabb, 2006; Morrissette and Sibley, 2002; Silvie *et al.*, 2008). These invasion organelles, rhoptries and micronemes are orientated towards the erythrocyte. The content of these organelles (adhesive proteins and membrane altering agents) help in erythrocyte capture, junction formation, migration through RBC membrane to create a PV with host erythrocyte. As the merozoites move through a moving junction, adhesins and other surface proteins are shed and finally the parasite reside within a PV located within the host RBC (Cowman and Crabb, 2006; Haldar *et al.*, 2006).

#### **1.4.1.2.2 Ring forms**

Following RBC invasion, the dense granules are pushed towards the surface of the parasite to further increase the area by releasing their contents to the PV (Bannister *et al.*, 2000) and thus the parasite enlarges, loses the invasive organelles and start intraerythrocytic development (Bannister *and* Mitchell, 2009). Based on the morphology of the early intraerythrocytic parasite, it's often referred as ring forms and/or "ring" cells, for up to the first 24 hours post invasion (Figure 1.5) (Bannister *and* Mitchell, 2009; Haldar *et al.*, 2006).

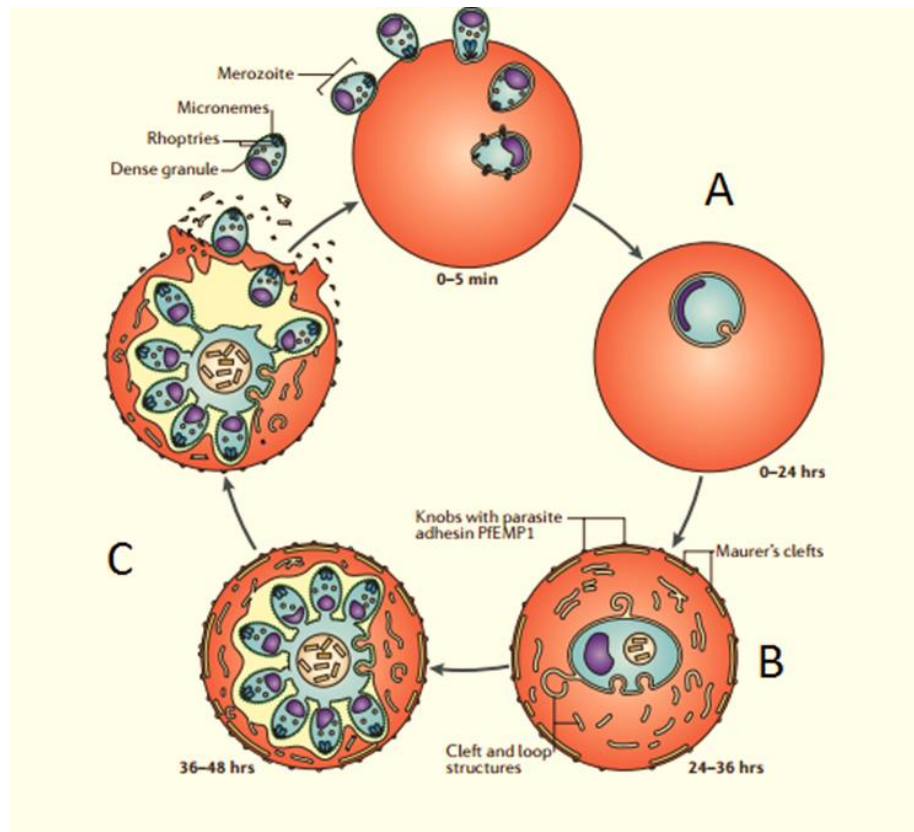


**Figure 1.5: Intraerythrocytic development (48 hour cycle) of *P. falciparum***

The image shows different stages of *P. falciparum* inside the human host from extracellular merozoites invading mature RBCs to schizont burst (Source- Halder *et al.*, 2006).

Over the first 24 hours, the parasite starts a programme of host erythrocyte modification. The parasite ingests the cytoplasm and transfers the cell's haemoglobin to the parasites acidic digestive vacuole where it is degraded by the proteases (Bray *et al.*, 2005; Tilley *et al.*, 2011). This digestion result in potentially toxic haem waste product (haematin) that is converted to biologically inert haemozoin by the parasite through lipid mediated crystallization (Tilley *et al.*, 2011; White *et al.*, 2014). The parasite goes through a major remodeling of the host RBCs as essential for its survival. During the ring and trophozoite development, the parasites feed on host cells; it also exports numerous proteins in the host cell cytoplasm and membrane of the erythrocyte and into structures called the Maurer's clefts (Haldar *et al.*, 2006). As a result, this transforms the erythrocyte surface,

which allows the parasite to consume nutrients and export waste product (Bannister *and* Mitchell, 2009; Goldberg and Cowman, 2010).

#### **1.4.1.2.3 Parasite-induced changes to the host erythrocyte: its associated virulence and pathology**

Adherence of mature infected erythrocytes (IE) (schizonts/trophozoite stages) of *P. falciparum* to microvascular endothelial cells is directly responsible for the virulence and pathology of human malaria. The pathogenesis of *P. falciparum* is a complex interplay of parasite-induced structural, biochemical and mechanical modifications of the RBCs and microcirculatory abnormalities along with local and systemic immune reactions that lead to life-threatening complications in humans (Grau *et al.*, 2003; Maier *et al.*, 2009). There are several pathophysiological factors that are responsible for the development of severe malaria and life-threatening complications in humans, which include the parasite biomass, cytoadherence, altered erythrocyte deformability and fragility of parasitized erythrocytes, malaria toxins and inflammatory response, thrombocytosis, endothelial injury and activation (Chen *et al.*, 2000).

*P. falciparum* has the ability to evade the host's immune system through clonal antigenic variation of a key virulence factor, *P. falciparum* erythrocyte membrane protein 1 (PfEMP1). PfEMP1 is exported to electron dense knob structures anchored into the infected erythrocyte plasma membrane. Here, PfEMP1 acts as an adhesive ligand for a wide range of host proteins (Pasternak and Dzikowski, 2009; Kyes *et al.*, 2001), critical of these is adhesion to proteins expressed on the surface of endothelial cells of the microvasculature. *P. falciparum* also adheres IE to uninfected erythrocytes called rosetting (David *et al.*, 1988). Mild modification of adherence and deformability can be

observed in the ring stage IE, which can, however, circulate in the blood vessels, but this is substantially developed in trophozoite and schizonts stage where these mature forms sequester and block the microvasculature, ultimately preventing circulation in the peripheral vasculature (Buffet *et al.*, 2011; Maier *et al.*, 2009). The sequestration of the schizonts/trophozoite (mature forms) of *P. falciparum* is determined by their adherence to different blood and endothelial cells, platelets and fresh uninfected RBCs while multiple host receptors are responsible for recognizing and mediating these interactions. As a result, of all these pathophysiological factors, cerebral malaria, hypoglycaemia, metabolic acidosis, renal failure, and respiratory distress can be observed mostly in infections with *P. falciparum* (Miller *et al.*, 2002).

Several molecules present at the plasma membrane of the IE are known to contribute in adherence, several of whose function is not entirely known. However, it is evident that some of these proteins (e.g. knob-associated histidine rich protein, KAHRP and PfEMP3), are essential for the parasite's survival as studies that cause gene disruption have resulted in parasite death but the reason for this still remains unclear (Cowman *et al.*, 2012; Crabb *et al.*, 1997a; Crabb *et al.*, 1997b). Nevertheless, *P. falciparum* erythrocyte membrane protein 1 (PfEMP1), encoded by the large and diverse *Var* multigene family, is the key parasite adherence receptor for *P. falciparum* (Barusch *et al.*, 1995; Buffet *et al.*, 2011; Pasternak and Dzikowski, 2009; Kyes *et al.*, 2001 Smith *et al.*, 1995). PfEMP1 is perhaps best known to mediate adhesion to the CD36 receptor present on endothelial cells of the microvasculature (Rowe *et al.*, 2009). Adherence of IE to endothelial cells is also mediated by several other molecules which includes intercellular adhesion molecule-1 (ICAM-1), Thrombospondin (TSP), a endothelial leukocyte adhesion molecule-1 (ELAM-

1) vascular cell adhesion molecule-1 (VCAM-1) and chondroitin sulphate (CSA) (Hasler *et al.*, 1990; Ockenhouse *et al.*, 1991; Rogerson *et al.*, 1995) but CD36 appears to be the key receptor for adhesion of IE to the microvascular endothelium cells (Baruch *et al.*, 1997). PfEMP1-mediated adherence results in tissue sequestration of IE, which removes them from the peripheral blood circulation (Barusch *et al.*, 1995; Pasternak and Dzikowski, 2009; Kyes *et al.*, 2001; Scherf *et al.*, 2008). Parasite sequestration, leading to adhesion of the microvasculature, ultimately leads to the pathology of severe disease (see below). Further, the clonal antigenic variation of PfEMP1 facilitates the development of chronic infection of a human host in the face of the host immune response to IE (Kyes *et al.*, 2001; Scherf *et al.*, 2008).

#### **1.4.1.2.4 Late trophozoite and schizogony**

Multiple rounds of nuclear division occur in late trophozoites (24-36 hours post infection, hpi), resulting in the segmented schizont stage (36-48 hpi). The parasite goes through many rounds of mitosis to generate 16-32 nuclei around which daughter merozoites are formed. Once the schizont matures, the infected erythrocyte ruptures at 44-48 hpi releasing merozoites into the blood stream ready to invade erythrocytes to restart the cycle (Haldar *et al.*, 2006).

#### **1.4.2 Sexual differentiation**

During the erythrocytic stage, a few reinvading merozoites commit to differentiate into gametocytes to start the sexual life cycle (Bousema and Drakeley, 2011). Gametogenesis takes some 10 days within the IE, resulting in the development of male (microgametocytes) and female (macrogamocytes) stages that circulates in the blood and are taken up by the mosquito vector during a blood meal (Figure 1.4). The male

gametocyte divides to rapidly produce many motile flagellated microgametes with long motile flagella within 8- 15 minutes in a process termed exflagellation. This motility enables them to make contact with female macrogametes for fertilization (Simonetti, 1996; Vlachou *et al.*, 2006). Fusion of the male microgametes and female macrogametes takes place within the midgut of the mosquitoes forming a zygote within 60 minutes of taking the blood meal (Hurd *et al.*, 2005). The zygote (after about 10-25 hours) undergoes meiotic nuclear division, elongates and develops into a motile ookinete. This ookinete penetrates the midgut epithelial cells of the mosquito and develops into a sessile oocyst (Anand and Puri, 2005). During the early stage, oocysts are covered by amorphous thick capsules that become thinner and stretch when the oocyst matures (Simonetti, 1996). Hereafter, the oocyst undergoes multiple rounds of asexual replication that results in the production of thousands of sporozoites in the intercellular space between the basal lamina and mid-gut epithelium. Further maturation occurs and the oocyst ruptures, releasing sporozoites into the haemolymph of the mosquito within a period of 7-12 days (Simonetti, 1996). The mature sporozoites migrate within the haemocoel finally invading the salivary glands of the mosquito within two days and hereafter reach the mosquito's stored saliva in readiness for transmission to a vertebrate during a subsequent blood meal.

### **1.5 Clinical features**

The WHO classified malaria into two categories, uncomplicated (mild) and complicated (severe) disease (WHO, 2014). Severe and mild infections are caused by *P. falciparum*, *P. vivax* and *P. knowlesi*, whereas *P. malariae* and *P. ovale* only induce mild infection.

### **1.5.1 Uncomplicated malaria**

Uncomplicated malaria is the most common form of the disease. It is not immediately life threatening, however, rapid and effective treatment is required to avoid disease progression into severe malaria. Generally, individuals with a history of exposure (premunition) typically remain asymptomatic or may present with uncomplicated malaria with the typical symptoms such as headache, fatigue, muscle aches, abdominal discomfort, chills, sweating and irregular fever (Bartolini and Zammarchi, 2012; Rubin and Strayer, 2011; White *et al.*, 2014). These symptoms arise as a result of pyrogens (haemozoin and GPI-linked proteins) released into the blood stream as the merozoites rupture (Chen *et al.*, 2000; Grobusch and Kremsner 2005).

### **1.5.2 Severe malaria**

Severe malaria is a medical emergency which induces several complex and life threatening complications. It involves any of the central nervous system, pulmonary system, renal system or haematopoietic system alone or in combination and, if not treated promptly and aggressively, 10 to 20% cases are fatal (Bartolini and Zammarchi 2012; Shanks, 2010). Severe malaria is associated with the presence of three overlapping clinical symptoms; cerebral malaria, severe anaemia and respiratory distress (Cunnington, 2013). One of the most prominent causes of death is due to IE sequestration in the microvasculature of crucial organs such as the brain (cerebral malaria), heart and lungs (Idro *et al.*, 2007). As indicated above, during an infection with *P. falciparum* PfEMP1 mediates adherence to endothelial surfaces of blood vessels via receptors such as ICAM1 in the brain, CSA in the placenta and CD36 in most other organs (Cooke *et al.*, 2000; Buffet *et al.*, 2011; Barusch *et al.*, 1995; Tilleya *et al.*, 2011). This results in the

development of fibrin, thrombus and micro infarcts, which can cause encephalopathy, congestive heart failure and pulmonary oedema (Rubin and Strayer, 2011). Moreover, significant amounts of cytokines, such as interferon-gamma (IFN- $\gamma$ ), are produced during the infection. This causes the suppression of erythropoiesis, therefore, inducing hypoxia and high levels of nitric acid. This further promotes rosetting of the parasitized RBCs, resulting in sequestration in specific organs like the brain for cerebral malaria (Weatherall *et al.*, 2002) or may cause damage to other tissues (Clark *et al.*, 2006). Acute anaemia is the main manifestation of severe malaria in young children (White *et al.*, 2014). It is caused by erythrocytic destruction and decreased erythrocyte production due to the disruption of multiple pathways (i.e. failure of bone marrow to produce more erythrocytes) (Menendez *et al.*, 2000). Infected erythrocytes are destroyed by the parasite whilst non-infected erythrocytes are phagocytised by a complement induced immune response (Autino *et al.*, 2012; Stoute *et al.*, 2003). Thus, the level of circulating reticulocytes is reduced, indicating a decreased response to erythropoietin and, therefore, a decline in the production of RBCs (Makintosh *et al.*, 2004).

Metabolic acidosis is a one of the key clinical features of severe malaria, which results in respiratory distress. Hypovolaemia, due to anaemia and capillary obstruction, results in decreased oxygen delivery. Consequentially, cells are unable to metabolise aerobically thus anaerobic metabolism results (White *et al.*, 2014). This leads to the accumulation of lactic acid causing metabolic acidosis and respiratory distress (Makintosh *et al.*, 2004; White *et al.*, 2014).

## 1.6 Malaria control strategies

The past decade has seen unprecedented efforts undertaken for malaria control that include RDTs, treatments, earlier chemoprophylaxis, vector control and vaccine trials. With all these efforts, as described, the overall morbidity and mortality rates for malaria have fallen (Alonso and Tanner, 2013; WHO, 2014).

### 1.6.1 Diagnosis of malaria

The gold standard for the diagnosis of malaria is microscopic examination of Giemsa-stained thin or thick blood smears (Wongsrichanalai *et al.*, 2007). This is a simple, inexpensive and commonly used method in low to moderate transmission regions (Wongsrichanalai *et al.*, 2007). However, a lack of quality control and poorly maintained laboratory equipment has led to degraded diagnostic smears, which has significantly affected both sensitivity and specificity of routine diagnosis (Guerin *et al.*, 2002; Wongsrichanalai *et al.*, 2007). Alternative diagnostics using molecular methods (i.e. DNA probes, detection of malaria antibodies and PCR) have been developed over the last two decades (Wongsrichanalai *et al.*, 2007), which provides a high degree of sensitivity and accurate speciation of *Plasmodium spp* compared to microscopic techniques (Walker *et al.*, 2014). Whilst these techniques are more sensitive and reproducible than conventional microscopy, their high cost and complicated procedures has limited their use in the field (Coleman *et al.*, 2006; Makler *et al.*, 1998; Perandin *et al.*, 2004). RDTs require minimum training and skills and thus serves as a useful tool in rural areas (Crawley and Nahlen, 2004). The principle of RDTs relies on an immunochromatography method with monoclonal antibodies that target species-specific malarial antigens such as *P. falciparum*

Histidine-Rich Protein 2 (*PfHRP2*). *PfHRP2*-based RDTs are better, or at least as good as, conventional microscopic methods in the diagnosis of falciparum malaria (White *et al.*, 2014). However, the latest generation of tests has been developed based on the detection of parasite lactate dehydrogenase (pLDH). These tests are highly effective in the diagnosis of both *P. falciparum* and *P. vivax* infections, although it shows low sensitivity at *P. vivax* densities of lower than 200/ $\mu$ L in blood (White *et al.*, 2014). Although RDTs are very useful because of their simplicity and speed, their high unit cost, inability to quantify parasitaemia and low sensitivity to other *Plasmodium* infections identifies a need to advance diagnostic tools alongside other control interventions (Chong *et al.*, 2013; Gatti *et al.*, 2007).

### **1.6.2 Vector control**

Vector control is a cornerstone in any control policy- the key being a break in the transmission cycle. It is particularly important in areas of high transmission, such as Africa, where resistance to antimalarial drugs is common (White *et al.*, 2014). Different approaches have been adapted to scale-up vector-control interventions; however, only insecticide-based vector-control stands out as a conventionally applied methodology. These methods include the use of indoor residual spraying (IRS) and ITNs (The malERA Consultative Group on Vector Control, 2011), which rely on insecticides such as DDT, pyrethroids, organophosphates and carbamates. IRS is an effective malaria control method that was widely used during the late 20<sup>th</sup> century, which led to malaria elimination from many temperate regions across the globe (Karunamoorthi, 2011; Pates and Curtis, 2005). Despite the contribution of IRS to malaria control and elimination efforts over the last 60 years, IRS use has declined in recent years due to various concerns

such as reduced funding, harmful effects of DDT on the environment and human health and insecticide resistance (WHO, 2006). ITNs have evolved to become the most widely used vector control method after the reduction in IRS use. Among the four classes of insecticides being used, pyrethroids are the only option available for treating bed nets due to its fast action and non-toxic properties (Balmert *et al.*, 2014; White *et al.*, 2014). The deployment of pyrethroid-treated LLINs in endemic regions has made significant inroads in controlling malaria transmission over the past decade in Asia and Africa (Balmert *et al.*, 2014; Karunamoorthi, 2011; White *et al.*, 2014). LLINs are thought to have a mass effect and hence serve as the current gold standard in control methods (Godfray, 2013). LLINs are only useful against those Anopheline species that bite at night and hence this limits its use against those which bite in the early evening/morning. In those regions where LLINs are useful and are regularly used, concerns have arisen that mosquitoes will adapt different biting trends. Furthermore, the use of DDT and pyrethroids in agriculture in West Africa has been shown in recent studies to provide selection pressure that has driven mosquitoes to develop resistance (Ranson *et al.*, 2011).

### **1.6.3 Vaccine development**

Vaccine development against malaria is a challenge, although many lines of evidence indicate that humans can be vaccinated against malaria (Schwartz *et al.*, 2012). The premunition (Figure 1.3) normally developed against malaria and the observed protective immunity in murine models are examples that have encouraged many attempts at vaccination against *P. falciparum* (Hill, 2011; Heppner, 2013; Finney *et al.*, 2014). Whilst knowing that vaccine development against malaria is a difficult task, many design strategies and approaches have been adopted. Owing to the multistage complex life cycle

of *Plasmodium*, three different approaches have been employed in an attempt to develop an effective vaccine. These approaches include Pre-erythrocytic stage, erythrocytic stage and transmission blocking vaccines (TBV) against the sexual stage (Birkett *et al.*, 2013; Hill, 2011; Guilbride *et al.*, 2010; Targett and Greenwood, 2008). Currently, RTS, S/AS01 (Pre-erythrocytic stage) is the most promising candidate (Figure 1.6) under development. Modern pre-erythrocyte vaccine development stems from immunization studies of mice in the 1960s using irradiated sporozoites to induce immunity against *Plasmodium* infection (Hill, 2011; Schwenk and Richie, 2011). The identification and cloning of CSP (the major component of the sporozoites coat) in the early 1980s with subsequent studies led to the development of Spf66, a peptide-based vaccine as the first sporozoites based vaccine (Hill, 2011).

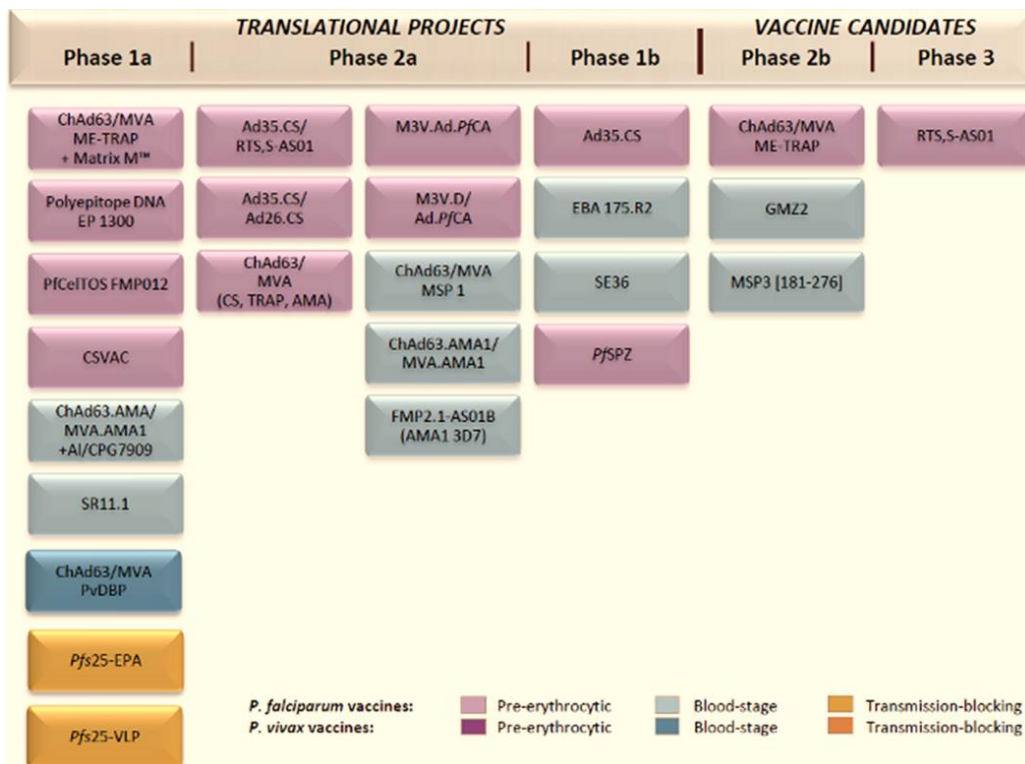


**Figure 1.6: The malaria vaccine pipeline**  
 The candidate malaria vaccines pipeline target different stages of *P. falciparum* and *P. vivax* (Source-WHO, 2014).

Apparently this candidate showed efficacy in monkeys and human, but failed to demonstrate any protection during successive field trials in Asia and Africa (Hill, 2011). However, these field trials of SPf66 has set a platform in terms of improved field technologies for successive studies, which led to the development of a new formulation of the *P. falciparum* CS protein called RTS, S (Hill, 2011). Following subsequent trials, this hybrid protein was formulated a multi-component adjuvant named AS01. Its central repeat region flanked by conserved motifs of CSP (R) and C-terminal region known to contain T cell epitopes (T) fused in turn to the hepatitis B surface antigen (S) that yielded a yeast-expressed protein RTS (Stoute *et al.*, 1997). To enhance immunogenicity and efficacy, RTS was co-expressed with unfused S protein and adjuvants AS01/AS02 (contains liposomes) (Hill, 2011; Schwenk and Richie, 2011; Targett and Greenwood, 2008; Heppner, 2013). RTS, S when administered with the AS01 (the most effective adjuvant), showed sterile efficacy of 30-50%, although with some concerns regarding the longevity of this protection (Bejon *et al.*, 2013; Moorthy *et al.*, 2013; Hill, 2011). RTS, S/AS01 is the most effective vaccine candidate that has led the way over the past decade. It has been evaluated in Phase-III clinical trials in seven endemic countries and is currently under regulatory review (WHO, 2014; Bejon *et al.*, 2013; Hill, 2011).

### **1.7 Antimalarial drugs**

In the absence of an effective vaccine, antimalarial drugs are critical components of any programme directed at the control and eradication of malaria. However, continued evolving resistance to antimalarial drugs is a recurring problem (Table 1.2). The first drug introduced widely for the treatment of malaria was Quinine (QN), which dates back to the early 1800s. However, the bark of Cinchona tree (original source of QN) had already been

used in the treatment of fever since the beginning of the 17th century (Meshnick and Dobson, 2001; Wiesner *et al.*, 2003). QN remained an important and effective treatment for malaria (and is still used in the UK today), but the first case of resistance was encountered in 1910. This resistance was widely feared and scientists initiated a search to discover a substitute for QN to treat severe malaria. As a result, chloroquine (CQ) was synthesised in 1934 but was not used clinically until 1945 as initially it was considered toxic. CQ was the first drug to be discovered in 4-aminoquinolines class. CQ safety, effectiveness and importantly its cheapness, led to its worldwide adaptation for the treatment of malaria (Famin and Ginsburg, 2002; Famin *et al.*, 1999; Wiesner *et al.*, 2003).

Antimalarials	Resistance
Quinine	
- introduced in 1632	- 1st case of resistance: 1910
Chloroquine	
- introduced in 1945	- 1st case of resistance: 1957
Proguanil	
- introduced in 1948	- 1st case of resistance: 1949
Sulfadoxine- Pyrimethamine	
- introduced in 1967	- 1st case of resistance: 1967
Mefloquine	
- introduced in 1977	- 1st case of resistance: 1982
Atovaquone	
- introduced in 1996	- 1st case of resistance: 1996

**Table 1.2.: Antimalarials and resistance**

This list provides common antimalarials, with the year they were first introduced in and their first case of resistance encountered (Source- MMV website <http://www.mmv.org>).

In 1957, however, the first case of CQ resistance was encountered (Table 1.2). Currently, CQ resistant strains of *P. falciparum* are common in all endemic countries and pose a significant problem for malaria control. During World War II, proguanil (pyrimidine derivative) also emerged from the antimalarial pipeline (MMV, 2015). Proguanil was a very effective drug and further studies of its chemical class led to the development of pyrimethamine. Resistance to both monotherapies appeared very quickly (MMV, 2015).

The subsequent resistance to these antimalarial drugs was widely feared. As a result in hopes of forestalling resistance and increasing drug efficacy, sulfones and sulfonamides were combined with proguanil and/or pyrimethamine; however, *P. falciparum* resistance had already emerged by 1953 in Tanzania (MMV, 2015). The combination of Sulfadoxine/Pyrimethamine was then introduced in 1967 in Thailand, but resistance was encountered in the same year (MMV, 2015). Although at a low level until 1990s, resistance to Sulfadoxine/Pyrimethamine spread rapidly throughout South-East Asia. A synthetic analogue of QN called mefloquine (MEF) was developed in the 1970s (MMV, 2015). It was introduced in 1977 and used as a potential agent for the treatment of *falciparum* malaria, however; the first case of resistance was encountered in 1982 in Asia. Thereafter, another drug atovaquone (ATOVA) was introduced in 1996 but resistance also appeared in the same year (MMV, 2015). Following the treatment failure of the aforementioned drugs due to resistance, many new antimalarial drug classes and their derivatives were discovered (Figure 1.7). However, due to multidrug resistance and other safety issues, many classes of these drugs (i.e. sulfonamides and antifolates) failed and are no longer used clinically. Being from different drug classes, all these drugs have a different mode of actions and hence the mechanism of resistance also differs (Table 1.3). The antimalarial properties of artemisinin and their derivatives i.e. artemether (ART), artesunate (AS) and dihydroartemisinin (DHA) were identified by Chinese scientists in the 1970s (Lin *et al.*, 2010). Their potential as antimalarial compounds was acknowledged and appreciated by the rest of the world in 1990s. Since then, artemisinin derivatives have served as the frontline antimalarial drug and are used in combination with other drugs in artemisinin combination therapies (ACTs). Keeping in view the resistance developed by *P.*

*falciparum* to other conventional antimalarial drugs, the WHO in 2001 recommended the use of ACTs to reduce the load of morbidity, mortality and drug resistance (Table 1.4). Currently, ACTs are the foremost option for the treatment of uncomplicated malaria, however, non-ACT treatments are still effective up to some extent and should not be ignored (Lin *et al.*, 2010; WHO, 2012). The non-ACTs, such as the combination of amodiaquine (AQ) and sulfadoxine-pyrimethamine (AQ-SP), used to be effective before ACTs and hence the WHO still recommends this combination when ACTs are not available.

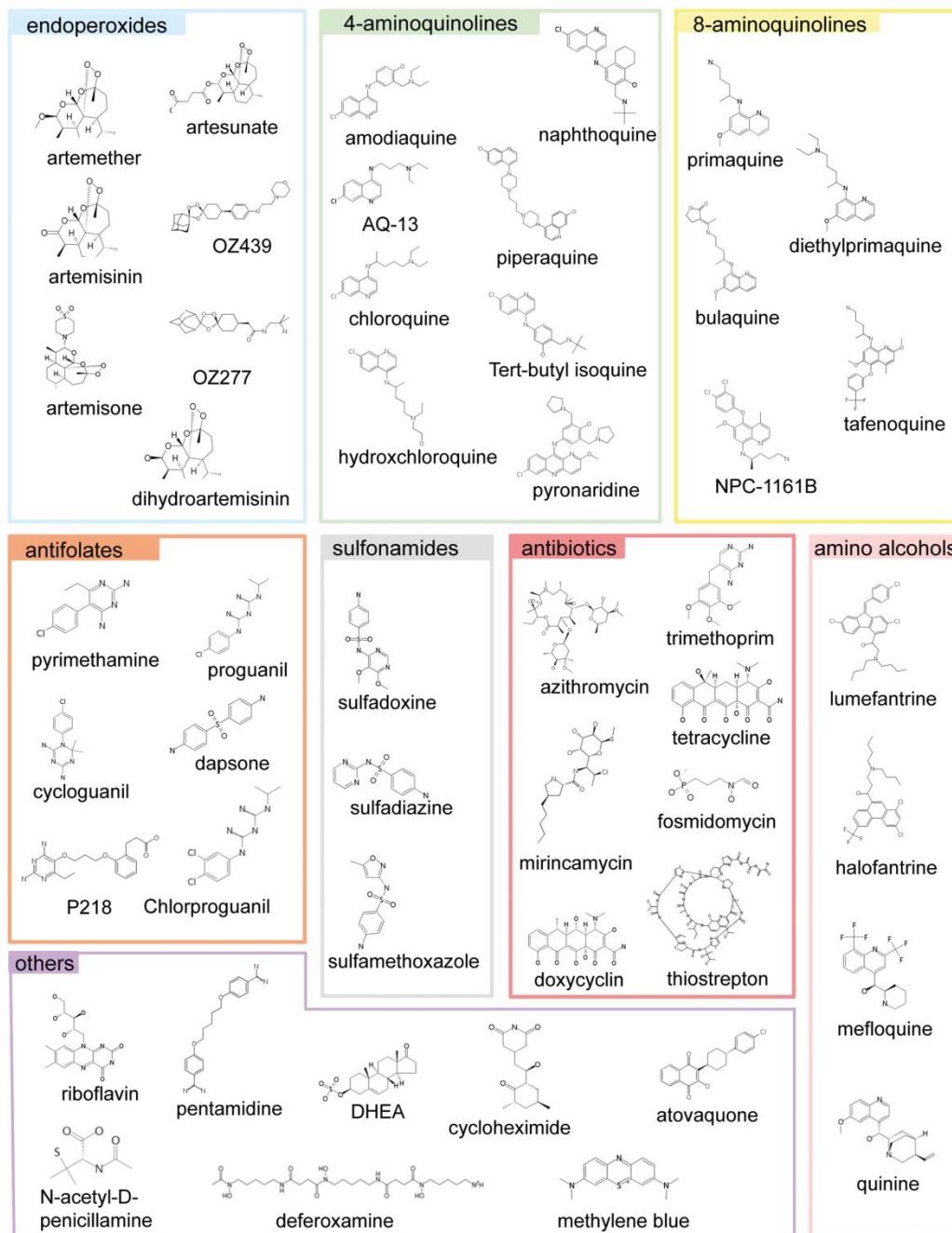


**Figure 1.7: The main antimalarial drugs classes approved for use in humans.** These classes are either based on antimalarials chemical composition (endoperoxides, 4- and 8-aminoquinolines, amino-alcohols) or their function (antifolates, antibiotics) and/or both chemical composition and function (e.g., sulfonamides, a chemical class of antibiotic used in combined antimalarial therapies) (Source-Delves et al., 2012).

Pathway	Drug class	Target	Mechanisms of action	Selectivity	Mechanisms of resistance
<b>Nucleic acid metabolism</b>	Type-1 antifolates: Sulfonamides, sulfones	Formation of dihydropteroate from PABA <sup>1</sup> + pteridine catalysed by DHPS <sup>2</sup>	Mimic PABA: compete for active site of DHPS	Parasite can either synthesize or salvage folate precursors	Mutations at binding site
	Type-2 antifolates: Pyrimethamine, biguanides (proguanil, cycloguanil), trimethoprim	Reduction of di- to tetra-hydrofolate (cofactor for the biosynthesis of thymidylate, purine nucleotides, amino acids) by DHFR <sup>3</sup> using NADPH as cofactor	Mimic dihydrofolate: compete for active site of DHFR	Mammals have no de novo synthesis and must rely on dietary sources	Mutations at binding site)
	Naphthoquinones (atovaquone)	Mitochondrial functions (electron transport chain), blockade of pyrimidine synthesis	Inhibits DHODase <sup>4</sup> ; mimics ubiquinone: competes for complex III	Different binding constant for parasite enzyme	Mutations at coenzyme Q binding site
<b>Haem detoxification</b>	Type-1 quinolines (4-amino-quinolines)	Haem crystallization	Inhibition/termination of $\beta$ -haematin formation	Mechanism unique to the parasite	Multi-gene: altered accumulation at FV <sup>5</sup> (reduced influx or increased efflux)
	Type-2 quinolines (aryl-amino alcohols)	Same as Type-1	Same as Type-1	Same as Type-1	Same as Type-1
<b>Oxidative stress</b>	Artemisinin-type compounds	Alkylation of unidentified target? Hydroxylation?	Free radical formation through activation of the peroxide by binding with Fe(II)PPIX <sup>6</sup>	Environment (FV, Fe <sup>2+</sup> ) unique to the parasite	Unknown

<sup>1</sup>PABA=p-aminobenzoic acid-<sup>2</sup>DHPS= dihydropteroate synthase-<sup>3</sup>DHFR= dihydrofolate reductase-<sup>4</sup>DHODase, dihydroorotate dehydrogenase  
<sup>5</sup>FV= food vacuole-<sup>6</sup>Fe (III) PPIX=ferrous-protoporphyrin IX

**Table 1.3: Antimalarial drug classes; their mode of action and mechanism of resistance**  
 (Source-Modified from Olliaro, 2001).

Artemisinin component	Partner drug	Coformulation	Elimination half-life of partner drug	Areas where ACT is commonly deployed
<b>Artesunate</b>	Mefloquine	ASMQ <sup>1</sup> (Far-Manguinhos Institute of Pharmaceutical Technology, Brazil)	2–3 weeks	Southeast Asia, South America
<b>Artemether</b>	Lumefantrine	Coartem (Coartem; Novartis AG, Basel, Switzerland)	3–4 days	Africa, South Asia, Middle East, South America
<b>Artesunate</b>	Amodiaquine	ASAQ <sup>2</sup>	~10 days	West Africa
<b>Artesunate</b>	Sulfadoxine-pyrimethamine	None	3–7 days	South Asia, Middle East, South America
<b>Dihydroartemisinin</b>	Piperaquine (PPQ)	Artekin (Holleykin, Guangzhou, China); Duocotecxin (Beijing Holley-Cotec, Beijing, China); Eurartesim (Sigma-tau Industrie Farmaceutiche Riunite S.p.A., Rome, Italy)	4–5 weeks	Southeast Asia, China, Africa

<sup>1</sup>ASMQ=artesunate-mefloquine-<sup>2</sup>ASAQ=artesunate-amodiaquine

**Table 1.4: Common artemisinin-based combination therapies**  
(Source-modified from Lin et al., 2010).

However, current reports of artemisinin treatment failure in South-East Asia is yet another issue and a significant threat to malaria control (Dondorp *et al.*, 2009). The number of existing front line antimalarials seems to be rapidly declining and hence, there is an urgent need to identify new small molecule drugs (Burrows *et al.*, 2011; Grimberg and Mehlotra, 2011) to seed the antimalarial drug development pipeline.

### **1.8 The search for novel scaffolds/chemotypes**

Phenotypic screening of massive chemical libraries (over six million compounds) for antimalarial activity has been conducted by the Genomics Institute of the Novartis Research Foundation (GNF, San Diego, California, USA), GlaxoSmithKline (GSK, Tres Cantos, Spain) and St. Jude Children's Research Hospital, Memphis, USA which yielded some 20,000 hits that exhibit sub-micromolar potency against the blood stage of malaria parasite *P. falciparum* (Gamo *et al.*, 2010; Spangenberg *et al.*, 2013). This search resulted in a significant progress over the past decade, with many new chemical entities entering the pipeline for antimalarial drug development (Table, 1.5) (Wells *et al.*, 2015), However, to make this collection accessible for researchers across the globe, a collection of 400 chemotypes has been assembled and finalised by the Medicine for Malaria Venture (MMV) called the "Malaria Box" (Figure 1.8). MMV freely provides this "Malaria Box" resource, containing 200 diverse drug-like compounds as starting points for oral drug discovery and development and 200 diverse probe-like compounds, for use as biological tools in malaria research (<http://www.mmv.org>; Gamo *et al.*, 2010; Spangenberg *et al.*, 2013).

Agent (alternative names)	Class	Comments
<b>DISCONTINUED OR ON HOLD</b>		
(+)-Mefloquine (AD-452, RS(+)-mefloquine, (+)-erythro-mefloquine)	Quinine, an amine alcohol	<ul style="list-style-type: none"> <li>• Studies in healthy volunteers showed that the safety of the single enantiomer was similar to that of the racemate and the project was discontinued</li> </ul>
Artemisone (BAY-44-9585)	Artemisinin derivative	<ul style="list-style-type: none"> <li>• Showed promising efficacy for the treatment of uncomplicated falciparum malaria in Phase II trials in Thailand (R. K. Haynes, personal communication), but no further development has been reported</li> <li>• A plan to test it clinically in western Cambodia for activity against artemisinin-insensitive strains (ClinicalTrials.gov identifier: NCT00936767) was withdrawn for operational reasons</li> </ul>
N-tert butyl isoquine (GSK369796)	4-aminoquinoline	<ul style="list-style-type: none"> <li>• Investigated in human volunteers (ClinicalTrials.gov identifier: NCT00675064) but showed evidence of ECG changes and lower-than-expected plasma exposure</li> <li>• GlaxoSmithKline thus returned the project to the Liverpool School of Tropical Medicine, UK, and no further development has been reported</li> </ul>
GSK932121	4(1H)pyridine	<ul style="list-style-type: none"> <li>• An electron transport inhibitor related to atovaquone; was tested in human volunteers</li> <li>• The project was terminated based on safety data from a soluble phosphate prodrug of the candidate, and work on other members of this series was also stopped <ul style="list-style-type: none"> <li>• It was recently suggested that these safety liabilities are associated with GSK932121 binding at the cytochrome <i>bc</i> Q site rather than the Q site</li> </ul> </li> </ul>
MK4815 (2-amino- methyl-3,5-di-tert-	Aminocresol	<ul style="list-style-type: none"> <li>• Characterized, but preclinical safety studies in 2010 showed a relatively small safety window, even in higher species</li> <li>• There are no current plans to move to first-in-human studies</li> </ul>
SAR97276 (albitiazolium	Bisthiazolium	<ul style="list-style-type: none"> <li>• This choline transport inhibitor was discontinued after failing to meet its primary end point in Phase II (<a href="#">Sanofi press release</a>; see Further information)</li> </ul>
Tinidazole	Nitroimidazole	<ul style="list-style-type: none"> <li>• This approved antibiotic for amoebae, giardia and trichomonas infections was found to be ineffective in preventing relapse</li> <li>• This result was in line with previous primate data but contradicted anecdotal reports in patients</li> </ul>

Trioxaquine (PA1103, SAR116242)	4-aminoquinoline with a synthetic endoperoxide	<ul style="list-style-type: none"> <li>• This is a fusion molecule of an endoperoxide and a 4-aminoquinoline that had entered preclinical development in 2007</li> <li>• Palumed has stopped working on this series for malaria in 2010 owing to a lack of financial support (<a href="#">company website</a>; see Further information)</li> </ul>
<b>IN DEVELOPMENT OR LAUNCHED</b>		
AQ13	Aminoquinoline	<ul style="list-style-type: none"> <li>• In 2006, AQ13 was examined in a single-dose healthy volunteer study</li> <li>• In 2013, a Phase IIa study comparing it with the artemether–lumefantrine combination (ClinicalTrials.gov identifier: NCT01614964) was started, funded by the US FDA's Office of Orphan Product Development, with a completion date of 2015</li> </ul>
Arterolane– piperaquine combination (Synriam)	Synthetic endoperoxide plus a 4-aminoquinoline	<ul style="list-style-type: none"> <li>• Launched in India in 2012</li> <li>• Current development plans include trials in African children, the development of a paediatric dose strength and discussions on WHO prequalification</li> <li>• By December 2014, Synriam was approved in seven African countries</li> </ul>
Artesunate– mefloquine combination  CDRI 97/78 (REFS 132–134)	Artemisinin derivative plus a 4-aminoquinoline  1,2,4 trioxane	<ul style="list-style-type: none"> <li>• Prequalified as a fixed-dose combination by DNDi and its Brazilian partner Farmanguinhos in 2012</li> <li>• Now manufactured by CIPLA Global</li> <li>• Originally developed by India's Central Drug Research Institute, which recently completed a healthy volunteer study</li> <li>• Has a plasma half-life of 12 hours</li> <li>• Work is ongoing to prepare for a multiple-dose study and test the activity against resistant malaria strains</li> </ul>
Dihydroartemisinin– piperaquine combination  Ferroquine (SSR97193)	Artemisinin derivative plus a 4-aminoquinoline  Ferrocene– 4-aminoquinoline	<ul style="list-style-type: none"> <li>• Recommended for approval by the EMA's CHMP in June 2011, and then by the EMA in Oct 2011</li> <li>• Developed by the Institut Pasteur in Lille, France; this drug was being developed by Sanofi in a Phase II trial in combination with artesunate (ClinicalTrials.gov identifier: NCT00988507)</li> <li>• This project has since been put on hold, and a new project was started combining ferroquine with OZ439 (artefenomel)</li> <li>• The Phase I drug interaction study is completed and a Phase IIb study is expected to start early in 2015</li> </ul>
Fosmidomycin	Antibiotic	<ul style="list-style-type: none"> <li>• Inhibits DXP reductoisomerase, a key enzyme in the non-mevalonate pathway of isoprenoid biosynthesis</li> <li>• A clinical trial of fosmidomycin with clindamycin showed poor efficacy in children younger than 3 years</li> <li>• Subsequent studies have switched to using piperaquine as a partner drug (ClinicalTrials.gov identifier: NCT02198807) with a currently ongoing trial in patients over the age of 5 years</li> </ul>

KAE609 (cipargamin, NITD-609) and KAF156 (GNF156)	Spiroindolone (KAE609) and imidazolopiperazine (KAF156)	<ul style="list-style-type: none"> <li>• Developed by Novartis and still in clinical development</li> <li>• Both have been tested in early Phase II clinical trials as monotherapies</li> </ul>
Methylene blue	Phenothiazin dye	<ul style="list-style-type: none"> <li>• This compound, first proposed for the treatment of malaria more than a century ago, is now being prioritized for its potential role as a transmission-blocking compound, to be used in combination with ACTs</li> <li>• A trial is ongoing to evaluate its safety in G6PD-deficient subjects in Thailand versus a single high dose (0.75 mg per kg) of primaquine (ClinicalTrials.gov identifier: NCT01668433)</li> </ul>
Pyronaridine–artesunate (Pyramax)	Chloroquine analogue plus an artemisinin derivative	<ul style="list-style-type: none"> <li>• Approved first by the Korean FDA in August 2011, followed by positive scientific opinion from the EMA under Article 58 in Feb 2012, for single use in countries with low malaria endemicity <ul style="list-style-type: none"> <li>• It was then added to the WHO list of prequalified medicines in May 2012</li> </ul> </li> </ul>
<b>COMPOUNDS THAT HAVE ENTERED THE PIPELINE SINCE 2012†</b>		
ACT451840	A hydroxy-ethyl-amine scaffold-based peptidomimetic protease inhibitor	<ul style="list-style-type: none"> <li>• Developed by Actelion</li> <li>• In a recently published Phase I trial it was well tolerated at all doses tested<sup>143</sup></li> </ul>
DF02 (Sevuparin)	Heparin analogue with low anticoagulant activity	<ul style="list-style-type: none"> <li>• Phase I/II studies failed to meet their primary end point for uncomplicated <i>P. falciparum</i> malaria and were prematurely ended</li> <li>• A Phase I trial for severe malaria was completed in 2009, and Dilaforette is planning to continue development</li> </ul>
GSK369796	Isoquine	<ul style="list-style-type: none"> <li>• Development is on hold after the first-in-human study (ClinicalTrials.gov identifier: NCT00675064), the only clinical study performed with GSK369796</li> <li>• Two factors contributed to this decision: first, a drug-related serious adverse event (generalized tonic-clonic seizure accompanied by hypotension and ECG changes (QTc prolongation and T-wave abnormalities)) occurred in one subject during the study approximately 2 hours after oral administration of 2,000 mg GSK369796; the subject recovered fully</li> <li>• Second, lower plasma exposures were observed for GSK369796 compared with other 4-aminoquinolines (based on the literature) and compared with other 4-aminoquinolines at equivalent doses (N. Cammack, personal communication)</li> </ul>
NPC1161B	8-aminoquinoline	<ul style="list-style-type: none"> <li>• Discovered and developed at the University of Mississippi, USA</li> <li>• Basic discovery papers have been published, and preclinical activity assessments have been completed</li> <li>• The compound has been tested in the huSCID<sup>5</sup> model with G6PD-deficient erythrocytes</li> <li>• NPC1161B was more potent, but the margin for safety in causing haemolysis was not significantly better than that for tafenoquine (L. Walker, personal communication)</li> </ul>

RKA182

Tetraoxane

- Initially planned for full preclinical development, and a Phase I study was initiated in 2011
- Some safety issues were reported, and the compound has been replaced by a new tetraoxane TDD E209

CHMP, Committee for Medicinal Products for Human Use; DNDi, Drugs for Neglected Diseases initiative; DXP, 1-deoxy-d-xylulose 5-phosphate; ECG, electrocardiogram; EMA, European Medicines Agency; Farmanguinhos, The Institute of Drug Technology, Brazil; FDA, Food and Drug Administration

**Table 1.5: The antimalarial drug pipeline over the past five years**

(Source- wells et al., 2015).

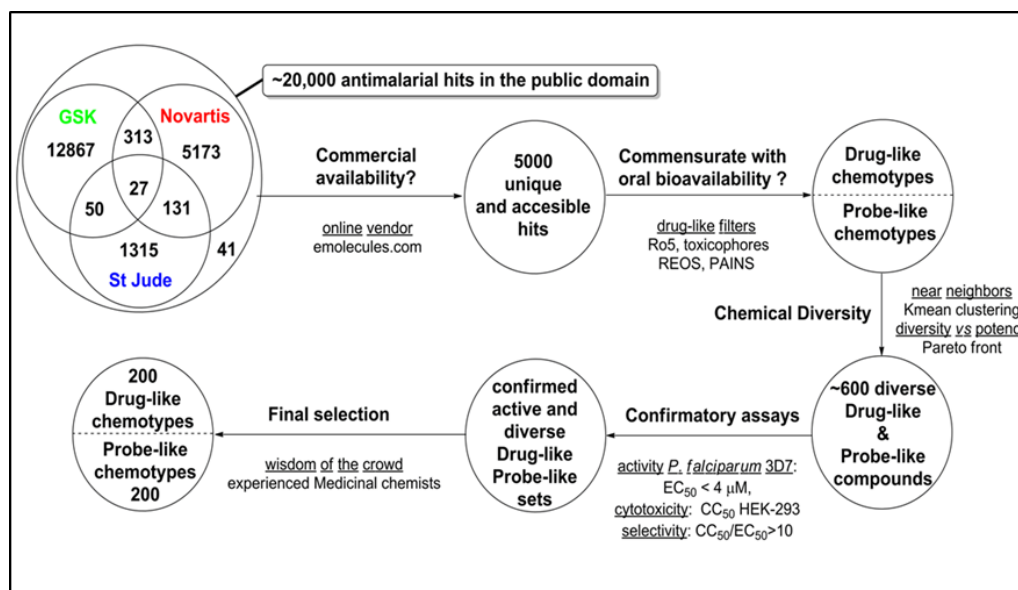


**Figure 1.8: MMV selection process for the 400 Malaria Box compounds**

The resource is freely available from the MMV on request (Spangenberg et al., 2013).

This significant progress and development are commendable, however, to eradicate the disease, searching for new candidate drugs to cure malaria rapidly and efficiently are no longer sufficient (Leroy *et al.*, 2014; White *et al.*, 2014). The new candidate drugs need to go beyond treating acute infections to additionally interrupt transmission cycle to help support malaria control and elimination strategy (White *et al.*, 2014). To support this, four different goals have been set that includes efficient elimination of the liver stage hypnozoites, targeting the IE sexual stages in human blood to block disease transmission, identification of new small molecule drugs to avoid cross-resistance and minimise the risk of emerging resistance and development of molecules that protect vulnerable populations (Leroy *et al.*, 2014).

Typically, drug development for malaria is a lengthy process that takes some 13-15 years from finding a hit to registration (<http://www.mmv.org>). Keeping in view the long timelines for the discovery and development of new antimalarial drugs, there is a real need to underline the description of the desired product profile of an ideal clinical candidate molecule. This will not only accelerate the overall drug discovery and development process but also will impact on the cost in this expensive development process (Burrows *et al.*, 2013). To support this, MMV has recently defined requirements for the potential antimalarial drug candidates called the target product profiles (TPP).

### **1.8.1 Target product profiles**

With the overall aim to rapidly discover, develop, and deliver safe, efficient, and inexpensive new antimalarials to support malaria elimination and eradication agenda, the

MMV underlined the description for four-five types of molecules under TPPs that are required. These new molecules will have to be suitable for incorporation into combination therapies which aim to efficiently cure the disease by rapid clearance of parasitaemia in patients. This will not only reduce the risk of resistance but will also prevent recrudescence. Furthermore, these new molecules will block transmission and eliminate all liver forms of the parasite including dormant hypnozoites (Burrows *et al.*, 2013; Leroy *et al.*, 2014). This profile corresponds to an “**ideal**” drug candidate that has to be administered for the treatment of uncomplicated malaria in children and adult as a single exposure, radical cure and prophylaxis (SERCaP), defined under TPP1. In addition to this, a second TPP (TPP2) was also defined. TPP2 should provide Single Exposure Chemoprotection (SEC), a new medicine to offer long-lasting chemoprotection. The goal of SERCaP to be met by a single molecule looks very ambitious and thus in line with the WHO recommendation, this medicine is likely to be a combination of several molecules. Thus, this led to the development of Target Candidate Profiles (TCPs) to reduce the risk of resistance, whilst SEC will likely need separate molecules (Burrows *et al.*, 2013; Leroy *et al.*, 2014). A TCP1 candidate corresponds to “**fast clearance**” to quickly reduce the initial parasite burden. TCP1 will ideally as good or better than artemisinin and at least as good as chloroquine and thus, if resistance renders artemisinin ineffective, TCP1 will ideally replace them. TCP2 represents candidate drug that could be either fast or slow acting, but should maintain a plasma concentration above the minimum parasitocidal concentration for 2-4 weeks. TCP2 act as a long-duration partner to complete the clearance of the residual parasites not eliminated by TCP-1 medicine. A TCP3 candidate will target *Plasmodium spp* in the non-dividing stages such as TCP3a will prevent relapses from

hypnozoites and TCP3b will block transmission to the mosquito. TCP4 also describes a compound or compounds that will provide chemoprotection by killing sporozoites and liver schizonts or eliminating parasites upon entering the blood stream from the liver (Figure 1.9) (Burrows *et al.*, 2013).

**MMV's Target Candidate Profiles (TCPs) define a stringent set of biological attributes to select and prioritize NCEs**

TPP	SERCaP			SEC
TCP	Fast Parasite Clearance	Long Duration	Transmission Blocking/ Relapse Prevention	Chemoprotection
<b>Critical Attributes</b>	<ul style="list-style-type: none"> <li>Minimum 99.9% parasite clearance over 48 hours</li> <li>&gt;6 log total parasite reduction</li> </ul>	<ul style="list-style-type: none"> <li>Time &gt; MPC* critical</li> <li>&gt;80% ACPR Day 28 monotherapy</li> <li>Delivers &gt;95% ACPR Day 28 when combined with TCP1</li> </ul>	<ul style="list-style-type: none"> <li>Gametocytocidal activity</li> <li>Hypnozoitocidal activity without G6PD liability</li> </ul>	<ul style="list-style-type: none"> <li>Liver schizontocide</li> <li>Slow onset asexual blood stage</li> <li>Supports 1x/ month use (min.: 1x/ week)</li> <li>High safety</li> </ul>
<b>Desirable Attributes</b>	<ul style="list-style-type: none"> <li>Gametocytocidal activity</li> <li>Hypnozoitocidal activity</li> </ul>	<ul style="list-style-type: none"> <li>Gametocytocidal activity</li> <li>Hypnozoitocidal activity</li> </ul>	<ul style="list-style-type: none"> <li>Vector-stage activity**</li> </ul>	<ul style="list-style-type: none"> <li>Vector-stage activity to deplete mosquito reservoir</li> <li>Gametocytocidal activity</li> <li>Orthogonal MoA to minimize resistance development to drugs used for treatment</li> </ul>
<b>Current Gold Standard</b>	<i>Artemisinin</i>	<i>4-aminoquinolines</i>	<i>Primaquine</i>	<i>Atovaquone/ Proguanil</i> <i>Mefloquine</i>

\* Minimum Parasitocidal Concentration  
 \*\* Delivering a molecule that will remain in human blood for as long as mature gametocytes circulate is extremely challenging in the absence of a rapid gametocytocide; therefore, vector-stage parasite killing is seen as a desirable rather than critical activity

**Figure 1.9: Target candidate profiles (TCP) for future antimalarial drugs**  
 TCPs are necessary for the proposed target product profiles (TPP) for future antimalarial drug development (Source- Burrows *et al.*, 2013).

### 1.9 Moving forward: determining key pharmacodynamic properties

To triage the 20,000 candidates that resulted from the massive chemical screens to establish priorities to take them forward for development requires additional information regarding their activity. Key features among their pharmacodynamic properties are Lethal Dose (LD<sub>50</sub>) and rate-of-kill (RoK) (Paguio *et al.*, 2011; Sanz *et al.*, 2012). To support this, a rapid, inexpensive and reliable quantification of the precise potencies and interactions of

new and existing drugs is essential to accelerate the drug discovery process and protect the efficacy of the current front line drugs against severe disease. To date, virtually all *in vitro* quantifications of antimalarial drugs or drug combination potency have been performed using a growth inhibition assay that quantifies *in vitro* drug potency as an IC<sub>50</sub> value (Bell, 2005; Foley and Tilley, 1998; Foley and Tilley, 1997). IC<sub>50</sub> values report the concentration of a drug that inhibits the growth of a mass population of parasites by 50% relative to untreated control. This means that all previous quantifications of IC<sub>50</sub> potency were based on both determining the cytostatic and cytotoxic potency of antimalarial drugs in the absence of additional information regarding their mode of killing. Depending upon specific antimalarial drug classes, these may inhibit proliferation by killing some of the parasites in a time-dependent fashion while others act by alternative ways, either slowing the metabolism and the cell cycle, impeding DNA replication and parasite egress etc., without killing the cell. However, this means it cannot be conclusively determined from these standard assays whether the IC<sub>50</sub> value reveals cytostatic or cytotoxic potency for distinct classes of antimalarial drugs. That said, it might be useful to develop a precise and applicable assay in high throughput screening (HTS) platforms to distinguish between cytostatic and cytotoxic activities of antimalarial drugs. Thus, the cytotoxic activity of antimalarial drugs must be quantified by LD<sub>50</sub> that is the concentration of drug that kills 50% of a bulk population of parasites relative to untreated control. In 2011, a probe-wash high throughput assay was developed to measure LD<sub>50</sub> using the DNA intercalating dye Sybr Green-1. Using this approach, Paguio *et al.*, (2011) demonstrated that the LD<sub>50</sub> of quinoline drugs may be as much as 20-50 fold higher than the IC<sub>50</sub>. Critically, LD<sub>50</sub> potency in CQR parasites is not subject to verapamil- reversal, unlike IC<sub>50</sub>. Moreover, the LD<sub>50</sub> is

not wholly linked to CQ concentration in the digestive vacuole, but additionally linked to genetic loci other than PfCRT (chloroquine resistance gene) in genome-wide association studies (Gaviria *et al.*, 2013). Thus, even for a well characterized antimalarial drug action/resistance model offered by CQ, LD<sub>50</sub> data may provide new insights into the mechanism of lethal drug action.

The RoK has been explicitly identified by MMV as a vital requisite (TCP1) in the TPPs for future antimalarial drugs (Burrows *et al.*, 2013; Leroy *et al.*, 2014). RoK is important because compounds that kill quickly not only rapidly reduce parasite burden, ameliorating the morbidity and mortality of the disease, but also may offer a narrower window of suboptimal drug levels during which resistance may evolve. The RoK is currently determined *in vivo* using mouse models or phase IIa humans clinical trials. It is determined in terms of two parameters; the parasite reduction ratio (PRR, the reduction from the starting parasitaemia after 48 hours of drug action corresponding to one cycle of erythrocyte-stage growth) or parasite clearance time (PCT, time to reduce parasitaemia by 99.9%). However, there is an urgent demand to identify RoK earlier in the drug discovery process, i.e. during *in vitro* laboratory studies. Earlier accesses to pharmacodynamic properties (RoK) would substantially accelerate the antimalarial drug discovery process (Sanz *et al.*, 2012).

To examine the effect of drug treatment on the asexual stages of the parasite, a number of *in vitro* standard techniques have been developed. These are used today for both drug development and monitoring resistance (Sanz *et al.*, 2012). These antimalarial drug assays typically rely on incorporation of radiolabeled hypoxanthine/ethanolamine and/or metabolic precursor as a measure of parasite growth, providing a standard assay format

with excellent signal-to-noise (S/N) ratio (Desjardins *et al.*, 1979; Elabbadi *et al.*, 1992; Sanz *et al.*, 2012). However, problems regarding the safe disposal of the radiolabeled material have restricted these assay formats. Further assays have been recently developed which are based on the measurement of enzyme activity or an immunological assay of its presence. These assays are relatively expensive although, they avoid use of the radiolabeled materials. The enzyme lactate dehydrogenase (pLDH), which is involved in the glycolysis pathway, can be used as a marker for parasite presence. In order to measure this protein either *in vitro* and/or *in vivo*, both colorimetric and immunodetection-based assays have been developed (Makler and Hinrichs, 1993; Piper *et al.*, 1999). Parasite growth rate can also be accurately estimated by using histidine-rich protein 2 (HRP2) measured by immunodetection (Noedl *et al.*, 2002; Sanz *et al.*, 2012). New methods such as flow cytometry have also been used to measure light depolarization by haemozoin or a determination of DNA content to evaluate drug potency. All these commonly used techniques measure the metabolic activity as a proxy for parasite viability. However, these approaches are vulnerable to artefacts because parasite metabolism and viability are two parameters that are coupled during the life cycle of the parasite, but may be uncoupled following drug treatment (Sanz *et al.*, 2012). Considering the limitations of traditional approaches, fluorescence-based platforms have been developed which use DNA intercalating agents such as Sybr Green I and/or 40, 60-diamidino-2-phenylindole (DAPI) (Johnson *et al.*, 2007; Ndiaye *et al.*, 2010; Sanz *et al.*, 2012). Fluorescence-based platforms offer inexpensive, sensitive assay formats and the utility of the Malaria Sybr Green I Fluorescence (MSF) assay for single-dose HTS has readily been demonstrated (Gamo *et al.*, 2010). Using a fluorescence-based assay of

parasite recrudescence, RoK was measured *in vitro* by Sanz *et al.*, (2012) based on the re-growth of drug-treated parasites. Following different times and doses of drug treatment, this assay provides high-quality RoK data that correlates with *in vivo* data. However, this format is very laborious as the re-growth of parasites over 3-4 weeks poses a significant limitation on its feasibility as a medium to HTS assay.

Keeping in view the limitations of the above-mentioned assay formats; there is a significant demand within the drug development community for a quantitative and rapid *in vitro* methodology to provide LD<sub>50</sub> and RoK data in a HTS system. Towards this aim, the Dd2 strain of *P. falciparum* has been genetically modified by the insertion of a luciferase reporter cassette (Hasenkamp *et al.*, 2012; Hasenkamp *et al.*, 2013; Wong *et al.*, 2011). This cassette expresses the bioluminescent reporter luciferase under the control of *Pfpcna* flanking sequence (Wong *et al.*, 2011). This parasite clone exhibit a strong temporal peak of luciferase expression during the S-phase of intraerythrocytic DNA replication (i.e. mature trophozoites stage), thus acting as a marker of cell proliferation (Hasenkamp *et al.*, 2012) (Figure 1.10) distinct to that using a fluorescent DNA intercalating agents.

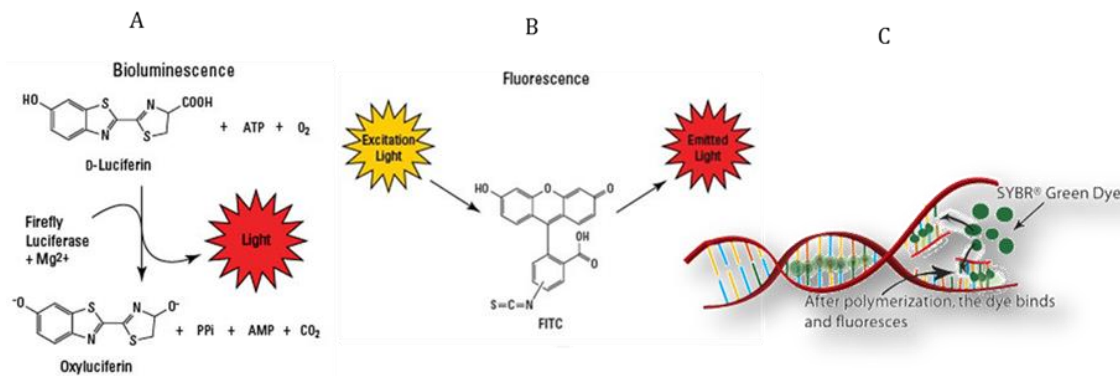


**Figure 1.10: Schematic representation of luciferase and SyBr-Green-I reactions**

**(A)** Illustrates the reaction of the firefly Luciferase. The Luciferase enzyme is detected following lysis of parasite-infected erythrocytes. In the presence of co-factors, the released luciferase oxidizes a luminogenic substrate releasing energy in the form of light. **(B)** Shows the action of fluorescence (i.e. that is the product of a fluorophore-FITC, DyLight dyes) which absorbs the energy from a light source and emits light energy at a different wavelength. **(C)** The action of the DNA intercalating dye SyBr-Green-I dye incorporated into DNA (Source: modified from Thermo Fisher Scientific, 2009).

This novel bioluminescent assay, when compared against the current standard drug action assay, based on the fluorescence of a DNA intercalating dye, MSF (Figure 1.11c), reveals high concordance in determining IC<sub>50</sub> values of antimalarial drugs (Hasenkamp *et al.*, 2013). Essentially, both luciferase and the MSF monitor parasite proliferation via DNA replication, however, the biomarkers are different. The MSF assay measures DNA content directly and the luciferase assay monitors induction of DNA replication proteins (Hasenkamp *et al.*, 2012) and thus has distinct properties following death induced by drug action. Whilst the MSF assay can be problematic due to the low (4-5) S/N ratio resulting from high background signals while the S/N ratio for bioluminescence is between 2500-17,000 depending upon the luminogenic agent used (Hasenkamp *et al.*, 2012). This enhanced working range of bioluminescent assay demonstrates a wide range in the limits for reliable detection. The applications of bioluminescence have been readily demonstrated in single-dose HTS, small- to medium-sized chemical libraries providing evidence that this assay format is a robust and reliable platform for antimalarial drug

discovery (Adjalley *et al.*, 2011; Che *et al.*, 2012; Cui *et al.*, 2008; Ekland *et al.*, 2011; Franke-Fayard *et al.*, 2008; Lucumi *et al.*, 2010). However, this assay format is more expensive and only applicable in genetically modified parasites expressing the luciferase reporter gene whilst the MSF assay can be performed in any parasite line. Despite these limitations, the bioluminescent assay provides a significantly improved dynamic measurement of temporal parasite viability following drug exposure. This immediate dynamic response of bioluminescence was previously demonstrated by Hasenkamp *et al.*, (2013). When death was induced using super-lethal doses of either the RNA polymerase II inhibitor actinomycin-D or the ribosome inhibitor cyclohexamide, the bioluminescence assay provided a more dynamic response than fluorescence-based DNA intercalating dyes as the expression of luciferase ceases and the protein is turned over. By contrast, the intrinsic stability of DNA hampers any attempt at short-term fluorescence-based monitoring of cell death. This means that whilst the dead parasite doesn't express protein, it still retains DNA (Figure 1.11). This study also provided evidence that the bioluminescence assay can determine relative RoK by investigating the effect of four antimalarial drugs, azithromycin (AZ), CQ, DHA and ART at a fixed dose of  $3 \times \text{IC}_{50}$  concentration. This initial **"Proof of Principle"** suggests that bioluminescence assay can be developed into a rapid *in vitro* RoK assay (Hasenkamp *et al.*, 2013).

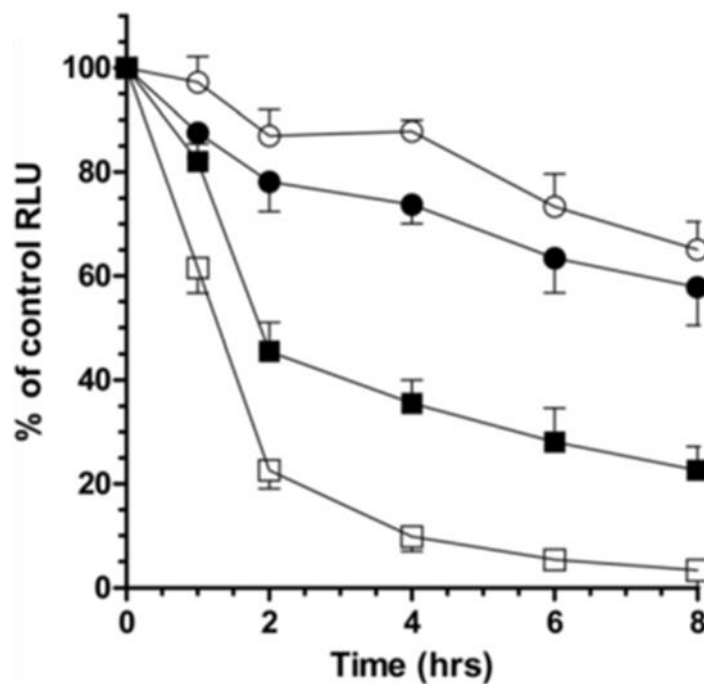


**Figure 1.11: The immediate dynamic response of bioluminescence and fluorescence assays of drug activity.**

Plot of the time-dependent changes in relative light units (RLU) (bioluminescent and fluorescence when compared to untreated control) measured from trophozoite stage  $Dd2^{luc}$  (2% parasitaemia, 2% HCT) exposed to a supralethal  $1\mu M$  dose of actinomycin D (filled symbol) or cyclohexamide (open symbol). The fraction of mean RLU  $\pm$  stdev ( $n = 3$ ) at each time point are shown for a luciferase assay (square) or MSF assay (circle).

### Aims of this study

Following the demonstration of proof-of-principle that a bioluminescence assay has the potential to rapidly provide evidence for the relative Rate-of-Kill of antimalarial drug action, this thesis proposes to;

1. Validate the hypothesis that bioluminescence can be used to monitor a time and dose dependent decrease in parasite viability following drug treatment.

2. Develop a medium to high-throughput plate based assay format for a bioluminescence Rate-of-Kill assay, benchmarked against known antimalarial drugs and their *in vitro* rate of Kill.
3. Utilize this bioluminescence Rate-of-Kill (BRoK) assay against the compounds present in the MMV Malaria Box to establish their relative rate of kill against known standards.
4. Explore the utility of the BRoK assay for longer term, i.e. 48hr, assays of rate of kill

This work will conclude with a discussion of the relative strengths, weaknesses, opportunities and threats to the representation of the BRoK assay in the antimalarial drug development pipeline.

## CHAPTER 2: Materials and Methods

---

### 2.1 Materials (stocks and reagents)

**Note:** The chemicals mentioned in this section and/or elsewhere in this thesis, were sourced commercially from either Sigma-Aldrich or VWR unless stated otherwise. Plasticware for tissue culture and biological assays were sourced from Star Lab, Greiner Bio-One and Sarstedt.

**Blasticidin S hydrochloride:** A 10 mg/mL stock concentration was achieved by adding 0.05 g of Blasticidin S hydrochloride to 5 mL sterile distilled water (sdH<sub>2</sub>O) (filter sterilised-0.45 µM). This was stored in 0.5 mL aliquots at -20°C. 125 µL of 10 mg/mL Blasticidin S hydrochloride was added to 500 mL complete growth medium to give a final working concentration of 2.5 µg/mL.

**Growth medium for *P. falciparum* culture:** To make an incomplete growth medium 500 mL of Roswell Park Memorial Institute (RPMI) 1640 medium was supplemented with 37.5 mM HEPES buffer solution, 5 mM sodium hydroxide solution, filter sterilised (0.5 µM) 10 mM D-glucose, 2 mM L-Glutamine, 100 µM hypoxanthine solution (Sigma) and 25 µg/mL gentamicin sulfate (Sigma). For a complete growth medium, the incomplete growth medium was supplemented with 8% v/v pooled human serum and 0.2 % albumax-II (w/v filter sterilised-0.45 µM in sdH<sub>2</sub>O) (Invitrogen).

**Glucose solution:** To make a 45% w/v glucose solution, 90 g of D-glucose was added to 200 mL sdH<sub>2</sub>O and dissolved with the help of a magnetic stirrer. The solution was filter sterilised (0.45µM filter) and stored in 10 mL aliquots at 4°C.

**Glycerolyte freezing solution:** Stocks of glycerolyte freezing solution were prepared in advance by supplementing 200 mL sdH<sub>2</sub>O with 142.5 g glycerol, 4 g sodium lactate, 0.075 g potassium chloride, 0.311 g disodium phosphate (Na<sub>2</sub>HPO<sub>4</sub>) and 0.129 g monosodium phosphate (NaH<sub>2</sub>PO<sub>4</sub>). The pH (6.8) and final volume (250 mL) were adjusted using 10 M NaOH and sdH<sub>2</sub>O, respectively. The solution was filter sterilised (0.45µM filter) and stored at 4°C.

**Hypoxanthine solution:** To make 1000X hypoxanthine solution, 340 mg hypoxanthine was added to a volume of 25 mL 1M sodium hydroxide. The solution was filter sterilised (0.45µM filter) and stored in 0.5 mL aliquots at -20°C.

**Malaria Sybr-Green-I Fluorescence (MSF) assay buffer:** An appropriate volume of MSF lysis buffer was prepared in advance that contained 20 mM Tris pH 7.5, 5 mM EDTA, 0.008% w/v saponin and 0.08% v/v Triton -100 at final concentrations and stored at room temperature (RT).

**WR99210 drug:** A 25 mM long-term stock solution was achieved by adding 0.05 g of WR99210 to 1 mL DMSO and was stored at -20°C. This was further diluted 1/1000 in complete growth medium to achieve a 25 µM short-term stock solution, which was stored at 4°C for a week. The required 5 nM final concentration of WR99210 was achieved by adding 100 µL of the 25 µM stock solution to 500 mL of complete growth medium.

## **2.2 Cell culture methods**

### **2.2.1 Human blood and serum**

The Institute for Science and Technology in Medicine (ISTM) at Keele University holds a Human Tissue Authority (HTA) license for the use, storage and disposal of human blood.

The Horrocks laboratory (HL) within ISTM is an approved user of the National Blood and Transfusion Service (NBTS), UK. The HL CAT-III cell culture suite facility is approved by the Health and Safety Executive (HSE) for the use and generation of genetically modified parasites (GM) and the users of this facility are pre-trained as per rules laid out in the CAT-III suite code of practice. Human blood and serum were supplied by NBTS and 50 mL aliquots stored at 4°C and -20°C, respectively, until further use.

### **2.2.2 *P. falciparum* clone**

The *P. falciparum* chloroquine resistant (CQR) parasite clone Dd2<sup>luc</sup> was used throughout this study. The Dd2<sup>luc</sup> transgenic parasite line is a clone of Dd2 which expresses high levels of luciferase during the trophozoite stage under the control of *Pfpcna* flanking sequences (Wong *et al.*, 2011). Drug selections of 5 nM WR99210 and 2.5 µg/mL Blasticidin S hydrochloride were applied throughout cell culturing to maintain the stability of the *attB* site (Hasenkamp *et al.*, 2013).

### **2.2.3 Preparation of normal human red blood cells**

NBTS, UK provided whole blood type-O-Rhesus positive (ORh<sup>+</sup>) human red blood cells (RBCs). The blood was aliquoted into 50 mL tubes and stored at 4°C for 2-3 weeks. To make a 50 % v/v haematocrit (HCT) solution, the aliquots were centrifuged for 8 minutes at 1160 g RT and the serum was removed. An equal volume of the incomplete growth medium was added to the packed RBCs. This was resuspended and centrifuged for 5 minutes at 850 g RT and the supernatant removed. The same centrifugation step was repeated to ensure the complete removal of serum, preservatives and white blood cells (WBCs). The packed RBCs were resuspended in an equal volume of incomplete growth medium and stored at 4°C for up to 10 days.

#### **2.2.4 Continuous cell culture of *P. falciparum***

All the cultures were maintained by standard continuous culture as originally described by Trager and Jensen, (1976) and later modified by Freese *et al.*, (1988). On a daily basis, thin blood smears were prepared, fixed with absolute methanol and stained with 10 % v/v Giemsa. Subsequent assessment of parasitaemia and parasite staging were established by light microscopy (oil immersion objective lens) at x1000 magnification (Olympus). The appropriate amount of complete growth medium and fresh 50 % v/v HCT washed RBCs were added to maintain the cultures between 1-5 % parasitaemia at a 2-4 % HCT. The cultures were gassed to maintain an atmosphere of 1 % O<sub>2</sub>, 3 % CO<sub>2</sub> and 96 % N<sub>2</sub> (BOC special gas) and returned to the incubator at 37°C.

#### **2.2.5 *P. falciparum* cell culture synchronisation with sorbitol**

A standard sorbitol-lysis protocol, first described by Lambros and Vanderberg, (1979) with minor modifications was used for the synchronisation of parasite cultures. Predominantly ring stage parasite cultures were collected by centrifugation at 850 g for 5 minutes at RT, suspended in 5 volumes of pre-warmed D-sorbitol 5 % w/v (Sigma) and incubated at 37°C for 5 minutes. The culture was centrifuged again at 300 g, RT for 5 minutes, the supernatant was aspirated, and following this treatment standard cell culture conditions were employed.

#### **2.2.6 Long term storage of *P. falciparum* cell culture**

A predominantly ring stage parasite culture (high parasitaemia ~10%) is suitable for long-term storage in liquid nitrogen. The ring stage culture was pelleted by centrifugation for 5 minutes RT at 300 g, the supernatant was aspirated, leaving about 500 µL on top, and gently resuspended. The volume of the packed cells was estimated and five volumes of

glycerolyte were added to three volumes of cell pellet (i.e. drop by drop) using a sterile dispenser or pipette. Following the addition of first volume of glycerolyte, the parasite culture was allowed to stand upright for 5 minutes to allow glycerol to permeate cells. The remaining 4 volumes of glycerolyte were added slowly to the parasite culture, and 0.8 mL samples were aliquoted into sterile freezing vials (NUNC). The vials were stored for at least 24 hours (hrs) in  $-80^{\circ}\text{C}$  before transferring to liquid nitrogen for long term storage.

### **2.2.7 Thawing of glycerolyte-frozen *P. falciparum* with NaCl**

A freezing vial was removed from the liquid nitrogen and placed at  $37^{\circ}\text{C}$  to thaw. The infected red blood cells (iRBCs) was transferred from vials to 50 mL sterile tubes and a  $1/5^{\text{th}}$  volume of 12% NaCl was added slowly and incubated at RT for 5 minutes followed by gently adding 10 volumes of 1.8 % NaCl. Thereafter, 10 volumes of 0.9% NaCl in 0.2% glucose were added, mixed and centrifuged for 5 minutes at 850 g, RT to collect the cell pellet. The cell pellet was then transferred to a small flask containing 10 mL complete growth medium, gassed and returned to the incubator at  $37^{\circ}\text{C}$ .

## **2.3 Drug assays**

### **2.3.1 Drug stocks preparation**

Drug stocks were prepared in their required solvents (Table 2.1) and stored at  $-20^{\circ}\text{C}$ . Antimalarial drugs were sourced from Sigma-Aldrich unless stated otherwise whilst PG-227 was kindly provided by the Biagini group of the Liverpool School of Tropical Medicine (LSTM). All the 400 compounds (200 drug-like and 200 probe-like) of the Malaria Box were sourced from the Medicine for Malaria Ventures (MMV) formatted as 20  $\mu\text{L}$  solutions at 10 mM concentration in dimethyl sulfoxide (DMSO) ([www.mmv.org](http://www.mmv.org)). The

Malaria Box compounds were diluted into 1 mM concentrations, stored at -20°C and working stocks were prepared when needed.

Drug	Group of drug	Solvent	Stock concentration
Dihydroartemisinin (DHA) <sup>1</sup>	Endoperoxides	Methanol	100 mM
Artemether (ART)	Endoperoxides	Ethanol	50 mM
Primaquine (PQ)	8- aminoquinolines	DMSO	50 mM
Tafenoquine (TFQ)	8- aminoquinolines	DMSO	50 mM
Chloroquine (CQ)	4- aminoquinolines	H <sub>2</sub> O	100 mM
Amodiaquine (AQ)	4- aminoquinolines	H <sub>2</sub> O	50 mM
Piperaquine (PPQ)	4- aminoquinolines	Ethanol	100 mM
Pyronaridine (PYR)	4- aminoquinolines	H <sub>2</sub> O	50 mM
Quinine (QN)	amino-alcohols	Ethanol	100 mM
Mefloquine (MEF)	amino-alcohols	DMSO	100 mM
Atovaquone (ATOVA)	others	DMSO	10 mM
PG-227 (PG)	others	DMSO	10 mM
Actinomycin-D (ACTD)	Antibiotics	DMSO	500 µg/mL
Cycloheximide (CHX)	Antibiotics	DMSO	1 mg/mL
Malaria Box compounds	Novel	DMSO	10 mM

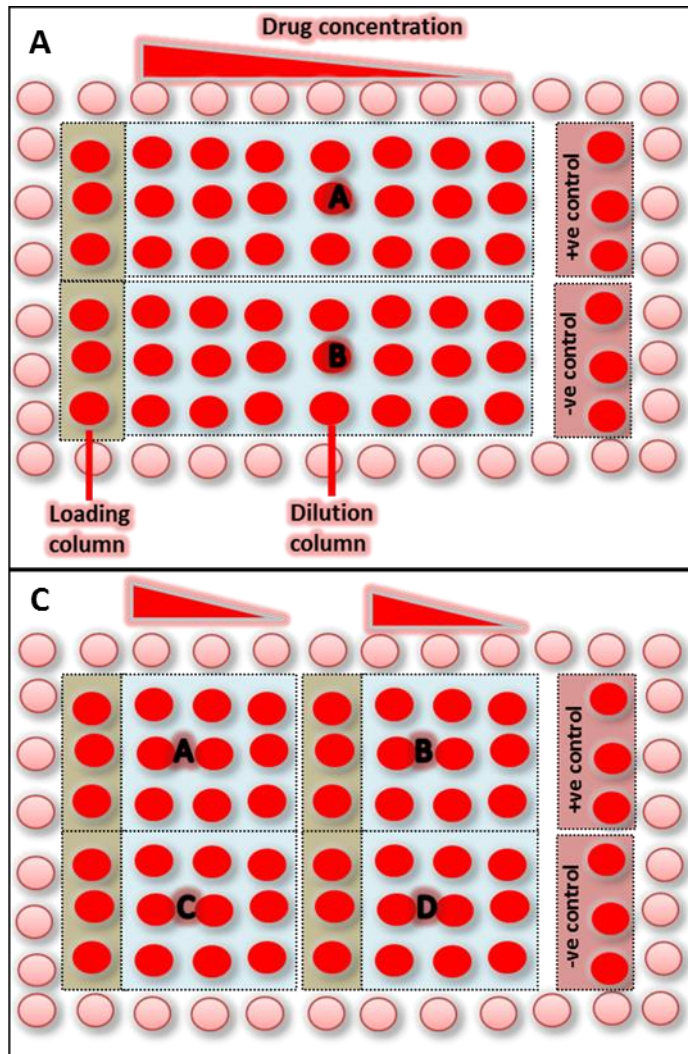
**Table 2.1: Preparation of drug stocks.**

The different drug classes are either based on the antimalarials chemical composition (endoperoxides, 4- and 8- aminoquinolines, and amino alcohols), their function (antibiotics) or novel compounds from the Malaria Box (200 diverse drug-like and 200 diverse probe-like compounds) are recorded with the solvent used and concentration prepared to. <sup>1</sup>Common abbreviations shown in brackets and used throughout this thesis.

### 2.3.2 Standard cell culture conditions and format of 96-well microplates for drug assays

Experiments were typically conducted using synchronised early trophozoite stage [17-24 hours post infection (hpi)] parasites unless stated otherwise. All the drug assays were initially set-up in a 96-multiwell tissue culture plate (SARSTEDT, UK). To minimize edge effects from evaporation, 200 µL of incomplete growth medium was added to the outermost wells on each plate for each assay. The remaining wells on a 96-multiwell tissue culture plate were supplied with 100 µL complete growth medium except the first column where appropriate volumes of complete growth medium were added depending upon the dilution series of the drug under investigation. An appropriate amount of drug was added to the first column, mixed completely by repeated pipetting and serial dilution

performed. An equal volume (100  $\mu$ L) of mastermix containing 1% synchronous trophozoite stage culture at a haematocrit was added to each well and homogenised by repeated pipetting to give a final 2 % HCT. The same mastermix without drugs served as a positive control (i.e. 100 % parasite growth under the same condition) while 2% HCT (RBCs) was typically used as a negative control (background signal) on each plate. In addition, an internal control of benchmark antimalarial drug was also included (Figure 2.1). The plate was transferred to a humidified airtight box and the chamber was flushed with gas to maintain an atmosphere of 1% O<sub>2</sub>, 3% CO<sub>2</sub> and 96% N<sub>2</sub>. This was incubated at 37°C for the appropriate time depending upon the type of assay. For each experiment, three technical and three biological replicates were typically employed.



**B**

Dilution series	Loading column <sup>1</sup>	Dilution column	Volume used
5-fold	125	100	25
3-fold	150	100	50
2-fold	200	100	100

<sup>1</sup>Loading drug DMSO not > 1% of total volume

**Figure 2.1: Schematic representation of the plate set-up used for drug assays**

Trophozoite stage parasites (at 1 % parasitaemia and 2 % final HCT) were exposed to multiple concentrations of the compound/drug under investigation. Drugs were added (2x final concentration) to the loading column and depending on the assay type and drugs, two, three or five-fold dilution series were employed as per table B. 100 µL of mastermix was added to each well, which reduced the concentration into half (required 1X concentration). A known antimalarial drug (usually CQ) was also included as an internal control. **(A)** This assay format (eight to nine drug doses where initial concentration was dependent on the  $IC_{50}$  value of the drug under investigation) was mainly adopted for  $IC_{50}$  and  $LD_{50}$  assays and/or unless stated otherwise. **(C)** This assay format was used for the RoK assays. Loading column was supplemented with  $18 \times IC_{50}$  dose of the drug (DMSO  $\leq$  1% of total volume) under investigation and 3-fold dilution was performed as per table B. 100 µL of mastermix was added to each well, which reduced the concentration to  $9 \times IC_{50}$ ,  $3 \times IC_{50}$ ,  $1 \times IC_{50}$  and  $0.3 \times IC_{50}$ .

### **2.3.3 Standard protocol for luciferase assay**

An improved single-step lysis protocol previously described by Hasenkamp *et al.*, 2012 was used for all luciferase assays. 40 µL samples of Dd2<sup>luc</sup> culture were transferred to wells of a white 96-multiwell plate (Greiner, UK) and 10 µL of 5X Passive Lysis Buffer (Promega, UK) was added to each well and homogenised gently by shaking. An equal volume (50 µL) of luciferase substrate (SL) was added and mixed by repeated pipetting with the lysed parasites. The resultant bioluminescence signal in relative light units (RLU) was immediately measured for 2 seconds on a Glomax Multi Detection System (Promega, UK). Data were exported into an excel spreadsheet using Instinct™ software (Promega). “Graphit” software was used for the normalization of the data and all the graphs were plotted in GraphPad Prism v5.0 (GraphPad Software, Inc., San Diego, CA).

### **2.3.4 Standard protocol for Malaria Sybr Green I Fluorescence (MSF) assay**

This protocol was initially described by Smilkstein *et al.*, (2004). SYBR Green I (1X final concentration, from 5000x stock) (Invitrogen, UK) was added to the MSF assay buffer, mixed by inversion and placed in an opaque dark box until ready to use. Immediately prior to the start of the experiment, 100 µL of MSF assay buffer was added to each well on a black 96-multiwell plate (Greiner, UK). To each well an equal volume (100 µL) of parasite culture was added with repeated pipetting to lyse and homogenize the cellular contents. This was incubated for one hour at RT in the dark (opaque dark box). The fluorescent signal, in RLU, was measured using the blue fluorescent module (excitation 490nm: emission 510–570nm) of a Glomax Multi Detection System (Promega, UK). Data

were exported into an excel spreadsheet using Instinct™ software (Promega). “Graphit” software was used for the normalization of the data and all the graphs were plotted in GraphPad Prism v5.0 (GraphPad Software, Inc., San Diego, CA).

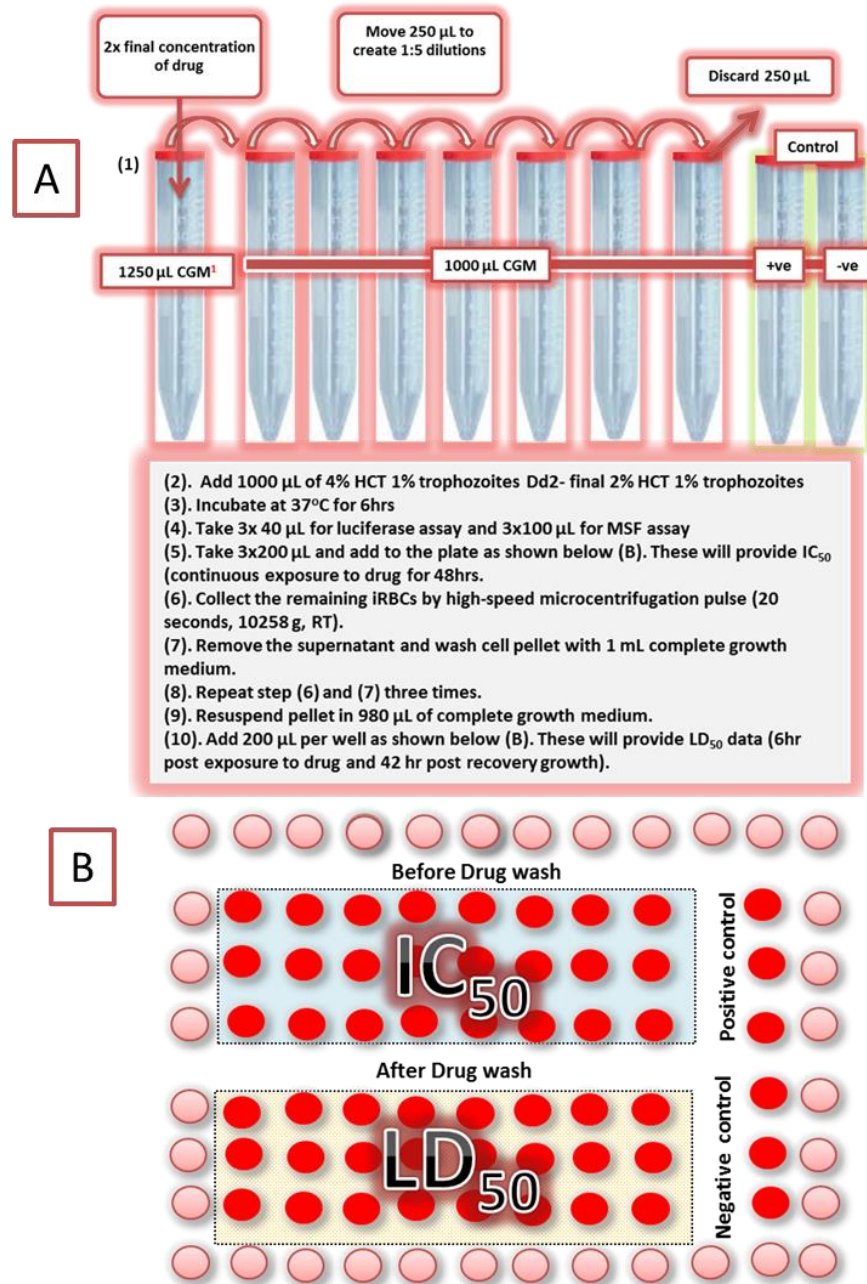
### **2.3.5 Determination of the 50% inhibition concentration (IC<sub>50</sub>)**

The protocol used is an adaptation of that originally described by Smilkstein *et al.*, (2004) as modified in Hasenkamp *et al.*, (2012). These experiments were employed using the Dd2<sup>luc</sup> *P. falciparum* strain. For these assays, a two-fold dilution series (unless stated otherwise) was employed for a 48hr assay (trophozoite to trophozoite). Each biological replicate recorded here comprises three technical replicates on the same 96-well plate. Following capture of the fluorescent or bioluminescent signal using standard MSF and luciferase assay protocols described above, the percentage growth was calculated as follows:  $100 \times [\mu(S) - \mu(-) / \mu(+) - \mu(-)]$  where  $\mu(S)$ ,  $\mu(+)$  and  $\mu(-)$  represent the means for the sample in question and 100 % and 0 % controls, respectively (Hasenkamp *et al.*, 2013). The percentage growth was plotted against log<sub>10</sub> transformed drug concentration and the IC<sub>50</sub> determined using a nonlinear regression (sigmoidal dose–response/variable slope equation) in GraphPad Prism v5.0 (GraphPad Software, Inc., San Diego, CA).

### **2.3.6 Determination of the 50% lethal dose concentration (LD<sub>50</sub>)**

The protocol used is an adaptation of that originally described by Paguio *et al.*, (2010). These experiments were performed using the Dd2<sup>luc</sup> *P. falciparum* strain. Initial starting conditions employed were: 1% trophozoite-synchronised culture at a final 4% haematocrit. Five-fold dilution series were employed unless stated otherwise (Figure 2.1a). Following a 6hr drug bolus, the signal was immediately measured (prior to drug washing step) using both the standard MSF and luciferase assay protocols described

above. Appropriate volumes (200  $\mu$ L n=3) were transferred to a 96-multiwell tissue culture plate (SARSTEDT, UK). The remaining infected erythrocytes were washed three times with 5 volumes of complete growth medium, with infected erythrocytes collected by high-speed microcentrifugation pulse (20 seconds, 10258 g, RT). Following the last wash, parasites were resuspended to the initial 2% haematocrit and 200  $\mu$ L in triplicates were transferred to the same plate as shown in figure 2.2B. The plate was incubated for an additional 42hrs at 37°C (for a total of 48hrs) prior to being processed for their fluorescent or bioluminescence signal using the MSF and luciferase assay standard protocols. The percentage growth was plotted against  $\log_{10}$  transformed drug concentration and the LD<sub>50</sub> determined using a nonlinear regression (sigmoidal dose–response/variable slope equation) in GraphPad Prism v5.0 (GraphPad Software, Inc., San Diego, CA).



<sup>1</sup>CGM= Complete growth medium

**Figure 2.2: Schematic representation of the modified bioluminescence protocol.**  
 (A) Outline the method for measuring *In vitro* 6hr LD<sub>50</sub> and 48hr IC<sub>50</sub> and LD<sub>50</sub> using both Luciferase and Sybr-Green-I biomarkers. (B) The plate was incubated for an additional 42hrs at 37°C (total 48hrs).

### 2.3.7 Bioluminescent rate-of-kill assays

The Dd2<sup>Luc</sup> parasite line used throughout. The parasitaemia of early trophozoite stage (17-24 hpi) Dd2<sup>Luc</sup> culture was assessed by microscopy. A mastermix of 1% trophozoite-synchronised culture at a final 2% HCT was prepared, with 200 µL aliquots exposed to multiples of the IC<sub>50</sub> of the compound under investigation (9x IC<sub>50</sub>, 3x IC<sub>50</sub>, 1x IC<sub>50</sub> and 0.3x IC<sub>50</sub> unless stated otherwise). Following exposure to these concentrations of compound after 3hr and 6hr at 37°C (with the exception of assays performed in chapter 5, where a 6hr and 48hr assay format was adopted), 40 µL samples were removed and the bioluminescent signal was measured using the standard luciferase protocol described above. The bioluminescent signal obtained was plotted as a percentage of the same volume of an untreated iRBC control. For each experiment three technical repeats were employed, the final data plotted is the mean and standard deviation of these data from three independent biological replicates (n=9) (Figure 2.3).

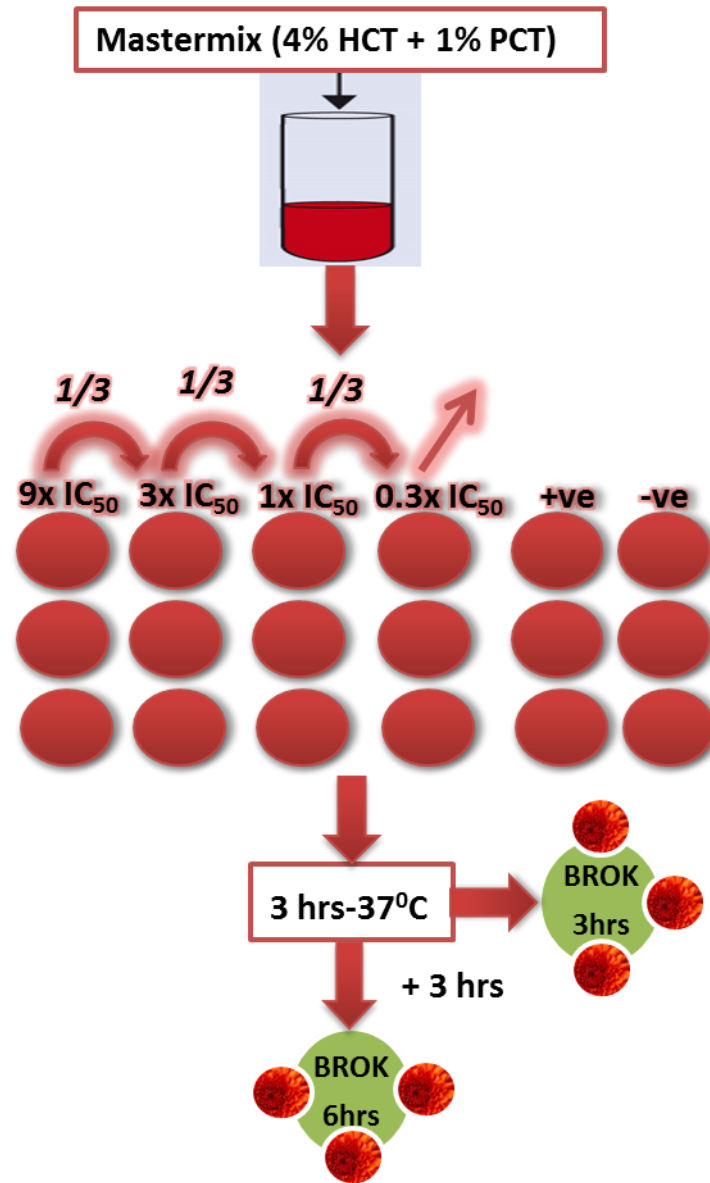


**Figure 2.3: Schematic representation of the BRoK protocol.**  
 A mastermix at 1% parasitaemia and 2 % final HCT was prepared and added to a 96-multiwell tissue culture plate contained serially diluted (three-fold dilution series was employed) drug in complete growth medium (9x IC<sub>50</sub>, 3x IC<sub>50</sub>, 1x IC<sub>50</sub> and 0.3x IC<sub>50</sub>). Positive and negative controls were used on each plate and an addition benchmark drugs were included on each plate as internal controls. The plate was incubated at 37°C and the bioluminescent signal was captured at 3hrs and 6hrs respectively.

### 2.3.8 Bioluminescence rate of kill assay quality parameters

The assay quality parameters for bioluminescence assays were previously determined by Horrocks laboratory and are reported in Hasenkamp *et al.*, (2013). To ensure the reliability of drug screening in this study, the following parameters such as Z-Factor, coefficient of variation (%CV MAX), Signal-to-background (S/B) and Signal-to-noise (S/N) were determined for benchmark drugs and Malaria Box compounds (Table 2.2) using the formulas previously reported by Zhang *et al.*, (1999). These parameters are used to assess the quality and suitability of an assay for a HTS. For a reasonable HTS assay, its Z-factor should be greater than 0.5, low %CV (i.e. indicates high precision), low S/B ratios and high S/N ratios.

	Z-Factor	%CV MAX	S/B	S/N
	$1 - [(3\sigma (+) + 3\sigma (-))/\mu (+) - \mu (-)]$	$\%CV\ MAX = 100 \times [\sigma(+)/\mu(+)]$	$\mu (+) \text{ signal} / \mu(-) \text{ background signal}$	$[\mu (+) - \mu (-)] / \sigma (-)$
	95% CI	95% CI	95% CI	95% CI
3hr	0.76-0.93	0.25-3.44	450.3-929.8	36018-74381
6hr	0.90-0.97	0.86-2.98	805.8-993	64464-79433
48h	0.85-0.95	0.9-2.84	2580-5001	206420-400048

**Table 2.2: Bioluminescence assay quality parameters**  
 $\mu (+)$  and  $\sigma (+)$  = mean and standard deviation of the positive control (parasites only, no drug) respectively.  
 $\mu (-)$  and  $\sigma (-)$  = mean and standard deviation of a negative control (RBCs only or super lethal dose of CQ).

### 2.4 Data management

All bioluminescence and fluorescence data developed using Glomax Multi Detection System (Promega, UK). These data exported as Instinct software files (Promega) and converted into excel (Windows 8.0) spreadsheets for analysis. These raw sequence files shared on University desktop and a copy saved on University network. Data from

different biological repeats of assays combined in GraphPad Prism v5.0 (GraphPad Software, Inc., San Diego, CA) software for production of graphs, regression analyses and determination of IC<sub>50</sub>, LD<sub>50</sub> and rate of kill data.

IC<sub>50</sub> data for 396 compounds have been compiled in excel spreadsheet and have been submitted to Dr. George Papadatos of EBI for forthcoming release on ChEMBL data repository ([www.ebi.ac.uk/chembl/malaria/](http://www.ebi.ac.uk/chembl/malaria/)).

Principle component analysis (PCA) of the 3hr, 6hr and 48hr rate of kill data was performed by Dr. Raman Sharma, LSTM. PCA was performed on the 0.3x, 1x, 3x and 9x IC<sub>50</sub> variables for the 3, 6 and 48hrs bioluminescence assay endpoints using the KNIME analytics platform to reduce the dimensionality of these data set, allowing the concentration rate Relationship to be captured in one parameter (Michael *et al.*, 2007). I then carried out the correlation of PC1 components with IC<sub>50</sub> data in GraphPad Prism v5.0 (GraphPad Software, Inc., San Diego, CA) software. This data will be submitted to ChEMBL data repository.

## CHAPTER 3: Development and Validation of a Rapid *In Vitro* Bioluminescence-Based Rate of Kill Assay

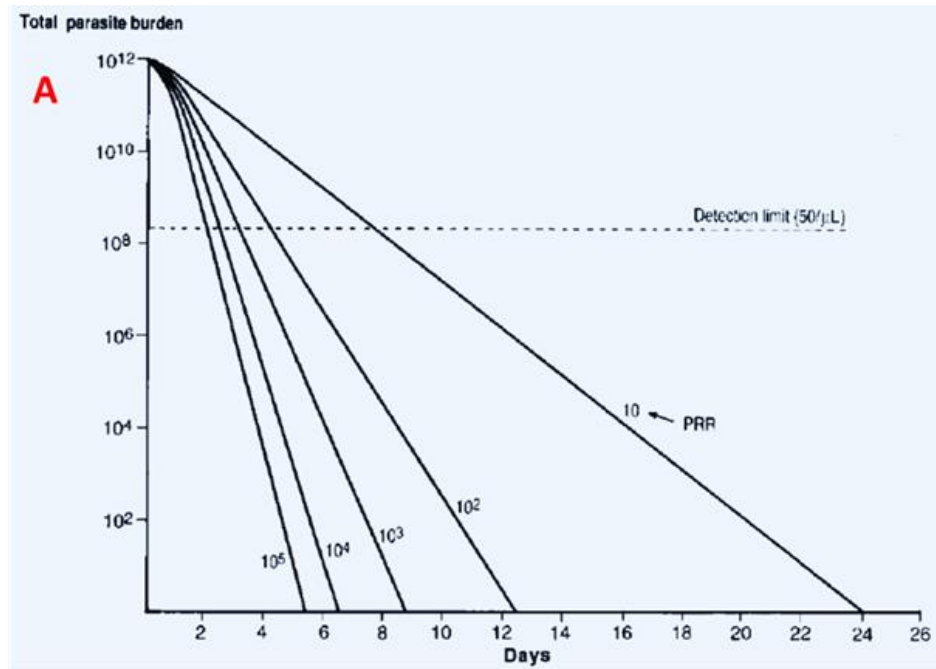
### 3.1 Introduction

The Medicines for Malaria Venture (MMV) has defined the attributes of a future combination therapy for the treatment of uncomplicated malaria – a Single Exposure Radical Cure and Prophylaxis (SERCaP). To meet this challenge, candidates for inclusion in this combination therapy must meet at least one of four Target Candidate Profiles (Burrows *et al.*, 2013; Leroy *et al.*, 2014). Target Candidate Profile 1 (TCP1) emphasizes fast clearance of the initial parasite burden (Table 3.1).

TCP-1 criteria at human proof of concept	Minimum essential	Ideal
Dosing regimen: adult dose*	Oral, one-three doses; <1,000 mg	Oral, single dose; <100 mg
Rate of onset of action and clinical parasite reduction ratio from single dose	Immediate and rapid clearance of parasites at least as fast as chloroquine; > 6 log unit total reduction in parasites	Immediate and rapid clearance of parasites at least as fast as artesunate; > 6 log unit total reduction in parasites
Susceptibility to loss of efficacy due to acquired resistance	Low (better than atovaquone); no cross resistance with TCP-2	Very low (similar to chloroquine); no cross resistance with TCP-2. Resistance markers identified
Clinical efficacy from single dose (day 7) including patients from areas known to be drug-resistant to current first line medications	100%	
Clinical efficacy from single dose (ACPR at day 28 or more, per protocol, PCR-corrected)	>50%	>95%
Bioavailability / Food Effect - human data	>30%, <3-fold	>50%, none
Drug- drug interactions	No unmanageable risks	No interactions with other anti-malarial, anti-retroviral or TB medicines
Safety - clinical	Acceptable therapeutic ratio based on human volunteer studies between exposure at human effective dose and NOAEL, dependent on nature of toxicity	Therapeutic ratio >50 fold based on human volunteer studies between exposure at human effective dose and NOAEL; benign safety signal
G6PD (Glucose-6-phosphate dehydrogenase) deficiency status	Measured - No enhanced risk in preclinical data from relevant G6PD deficient animal models	Measured - No enhanced risk in G6PD deficient subjects
Formulation	Acceptable clinical formulation identified	
Cost of active ingredient in final medicine	Similar to current medication: ≤\$0.5 for adults, \$0.1 for infants under two years	Similar to older medications: <\$0.25 for adults, \$0.05 for infants under two years
Projected stability of final product under Zone IVb conditions (37°C 75% humidity)	≥ 6–24 months	≥1-5 years

**Table 3.1: Target Candidate Profile 1 (TCP1)**  
The minimum essential and ideal attributes required for TCP1 candidate antimalarial drug (reproduced from- Burrows *et al.*, 2013).

TCP1 defines both a “minimum essential” and an “ideal” criterion for the rate of onset of drug action. Ideally a candidate has to be as effective, or better, than the very rapidly-acting artemisinin and at least as effective as rapid-acting 4-aminoquinolines (Burrows *et al.*, 2013; <http://www.mmv.org/>). TCP1 is important because compounds that kill quickly not only rapidly reduce parasite burden, ameliorating the morbidity and mortality of the disease, but also may offer a narrower window of suboptimal drug levels during which resistance may evolve. The rate of kill is currently determined *in vivo* using mouse malaria models or during phase IIa human clinical trials (Burrows *et al.*, 2013; White, 1997). It is clinically defined in terms of two parameters; (i) the parasite reduction ratio (PRR), the fold-reduction from the starting parasitaemia after 48-hours of drug action (corresponding to one cycle of erythrocyte stage growth) and (ii) the parasite clearance time (PCT), time to reduce parasites until they are no longer detectable in the peripheral blood film, i.e. by 99.9% (Figure 3.1a) (White, 1997). Typically, the PRR and PCT are estimated by measuring a change in the peripheral parasitaemia over time by microscopy. To characterize the PCT profile during therapeutic assessments, parasite counts at  $\leq 6$  hr intervals are required (White, 2011). However, the precision of this assay depends on a range of factors such as parasite burden, sequestration of parasites and expertise of the observer (White, 2011; White, 1997). By contrast, PRR estimation is much easier, requiring only two counts 48hrs apart (White, 1997). The PCT and the PRR are closely related as antimalarial drugs with high PRR take less time to eliminate parasites from the blood (Figure 3.1). However, PRR varies greatly depending upon the type of infection (i.e. sequestering malaria caused by *P. falciparum* and non-sequestering by *P. vivax*, *P. ovale*, and *P. malariae*) and the overall efficacy of antimalarial drugs (White, 2011; White, 1997).



B	Antimalarial drugs	Estimated PRR in vivo <sup>a</sup>
	Artemisinin, artesunate, artemether .....	10 <sup>3</sup> –10 <sup>5</sup>
	4-Aminoquinolines, halofantrine .....	10 <sup>2</sup> –10 <sup>4</sup>
	Quinine, mefloquine, pyrimethamine-sulfadoxine .....	10–10 <sup>3</sup>
	Antimalarial antibiotics, desferrioxamine .....	5–10

<sup>a</sup> PRR = baseline parasite count/parasite count 48 h later; this rises if there is background immunity and falls with resistance.

**Figure 3.1 In vivo PRR and PCT data**  
 (A) Schematic representation of the PRR and PCT. Essentially antimalarial drugs with  $\leq 10^3$  PRR should be administered for more than a week to effectively eliminate parasites. (B) In vivo PRR values of different drug classes (reproduced from White, 1997).

Most antimalarial drugs are predominantly active against the mature trophozoite stages of parasite development (schizonticides). Antimalarial drugs such as cycloguanil and pyrimethamine, the quinolones and mefloquine have little or no efficiency against the early stage circulating parasites (i.e. rings) and thus they are less likely to significantly prevent sequestration. Parasitemia-time profiles are affected by the magnitude of infection, stage and synchronicity, but generally, those antimalarial drugs that are effective against the young parasites (particularly artemisinin and CQ to some extent)

rapidly reduce the initial parasite burden. The fast acting drug artemisinin exerts *in vivo* PRR in the order of  $10^3$ – $10^5$  whilst slow acting drugs such as antimalarial antibiotics have a PRR of 5-10 (Figure 3.1) (Hien and White, 1993; White, 1997).

The “fast killing” and “slow killing” profiles, share a link with the cytotoxic and cytostatic potential of antimalarial drugs as described in chapter I (see section 1.9) (Gorka *et al.*, 2013; Paguio *et al.*, 2011). Cytotoxic antimalarial drugs (i.e. artemisinin, CQ) actively kill the parasite and hence display a high efficacious profile. In contrast, the cytostatic drugs (i.e. ATOVA) may not completely eliminate circulating parasites and this may open a window to treatment failure and subsequent resistance (Paguio *et al.*, 2011). Therefore, it is important to consider the cytotoxic potential profile in the search of future antimalarial drugs.

Antimalarial drug development is a slow process that takes some 13-15 years. Earlier access to pharmacodynamic properties, such as rate of kill, could substantially accelerate the antimalarial drug discovery process (Sanz *et al.*, 2012). Towards this aim, rate of kill was measured *in vitro* by Sanz *et al.* (2012), using a fluorescence-based assay of parasite recrudescence, which is based on the re-growth of drug-treated parasites. Briefly, this assay establishes an initial inoculum corresponding to  $10^6$ /mL of parasites at 0.5% parasitaemia and 2% haematocrit, which are treated with a  $10\times C_{50}$  concentration of an antimalarial drug. The effect on parasite viability is monitored by removing an aliquot corresponding to  $10^5$  parasites every 24 hours, washing away the drug before adding fresh erythrocytes and performing a limiting serial dilutions into a microtiter plate. This plate is maintained for 3-4 weeks and parasite growth determined in each well to enable an estimate of the number of viable cells that were present prior to the drug wash step

(Sanz *et al.*, 2012). This recrudescence assay provides high quality *in vitro* rate of kill data, i.e. PRR, PCT and information about the lag-phase for onset of drug action (Figure 3.2).

	lag phase (h)	log(PRR)	99.9% PCT (h)
artemisinin	0	>8.0 <sup>a</sup>	<24.0
pyronaridine	0	4.8	29
lumefantrine	0	4.8	32
piperaquine	0	4.6	33
chloroquine	0	4.5	32
mefloquine	0	3.7	43
pyrimethamine	24	3.5	55
atovaquone	48	2.9	90

<sup>a</sup>estimation based on the first 24 hours of treatment.  
doi:10.1371/journal.pone.0030949.t001

**Figure 3.2: In vitro log PRR and PCT data**  
Classic antimalarial drugs and their associated lag phase, PRR and PCT (reproduced from-Sanz *et al.*, 2012).

This *in vitro* recrudescence assay data, as shown in Figure 3.2, correlates with *in vivo* clinical data, showing the same relative order of antimalarial drugs in terms of their rate of kill i.e. ART > 4 aminoquinolines > QN and MEF (Sanz *et al.*, 2012). However, the necessary re-growth of parasites over 21-28 days poses a significant limitation on the recrudescence assays feasibility as a medium to high throughput assay. This issue identifies a development gap for a quantitative and rapid *in vitro* assay to provide *in vitro* rate of kill data in a HTS system – a gap that is addressed here.

As described in chapter 1, a genetically modified (GM) parasite line (Dd2<sup>luc</sup>) is available in the Horrocks laboratory that expresses high levels of luciferase during the S-phase (trophozoite stage) of the *P. falciparum* life cycle and thus acting as a marker of cell proliferation (Wong *et al.*, 2011). Hasenkamp *et al.*, (2013) have previously shown that luciferase is a more dynamic reporter of immediate drug action than commonly used fluorescence based assays of DNA content. The high turnover rate of the bioluminescence

reporter protein luciferase provides an opportunity to develop a rapid *in vitro* assay to explore the pharmacodynamic properties of antimalarial drugs. Hasenkamp *et al.*, (2013) exploited the immediate dynamic response of bioluminescence against known antimalarial drugs to show a time-dependent effect on luciferase signal following drug treatment (Figure 1.11B). Critically, this data suggests that the loss of bioluminescence for the drugs tested correlates with our available understanding of their relative rates of kill from both clinical *in vivo* studies and the *in vitro* recrudescence assay.

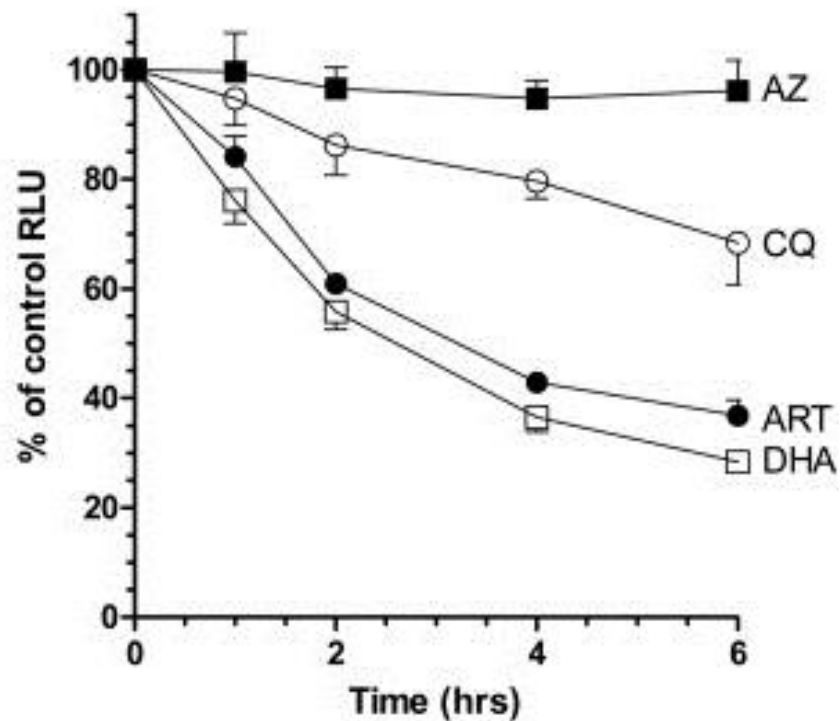


**Figure 3.3: Bioluminescence signal loss following drug perturbation is time-dependent**  
 Plot of the time-dependent changes in mean fraction of Luciferase RLU  $\pm$  stdev ( $n = 3$ ) exposed to  $3 \times IC_{50}$  doses of the indicated antimalarial drug; artemether (ART, rapid rate of kill), azithromycin (AZ, slow rate of kill), dihydroartemisinin (DHA, rapid rate of kill) and chloroquine (CQ, fast rate of kill) (Hasenkamp *et al.*, 2013).

Based on this proof-of-principle regarding the potential application of a bioluminescence-based monitoring of initial rate of kill, the work described in the following chapter sets out to;

1. Validate that the bioluminescence response immediately following antimalarial drug treatment reflects an actual loss in viability of parasites, and
2. develop and test a plate-based assay format to estimate the initial rate of kill using this bioluminescence assay.

## 3.2. Results

### 3.2.1 The bioluminescence response following drug treatment is both time and dose-dependent

Hasenkamp *et al.* (2013) have previously shown a time-dependent loss of bioluminescence signal following Dd2<sup>luc</sup> exposure to the rapid acting cytotoxic drugs DHA, ART and CQ for 6 hours. By contrast, the same study reports that exposure to the cytostatic drug AZ results in no apparent loss in bioluminescence signal over the same timeframe. To extend this observation to include the dose-dependent effect, Dd2<sup>luc</sup> parasites were exposed to equipotent doses of two antimalarial drugs, CQ and ATOVA. CQ is a fast acting compound known to exert an immediate cytotoxic effect on trophozoites. ATOVA is a slow acting compound, with a 48hr lag in its action during which it is primarily cytostatic. During drug incubation, samples were removed at 2hr intervals and the loss of bioluminescence signal, compared to an untreated control plotted (Figure 3.4). As expected, Dd2<sup>luc</sup> exposure to the rapid acting cytotoxic drug CQ for eight hours showed both a dose and time-dependent loss of bioluminescence signal, whilst the bioluminescence signal from parasites exposed to increasing doses of the cytostatic drug ATOVA is essentially unaffected over this time. These data supports the contention that the bioluminescence assay can differentiate between the cytotoxic and cytostatic effect of antimalarial drugs.

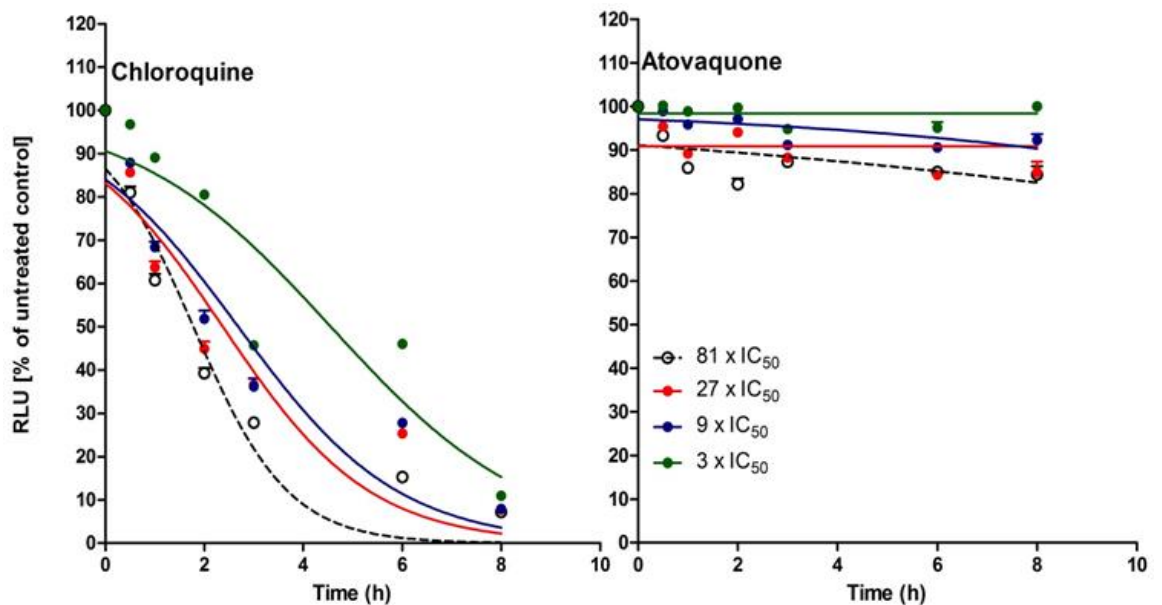
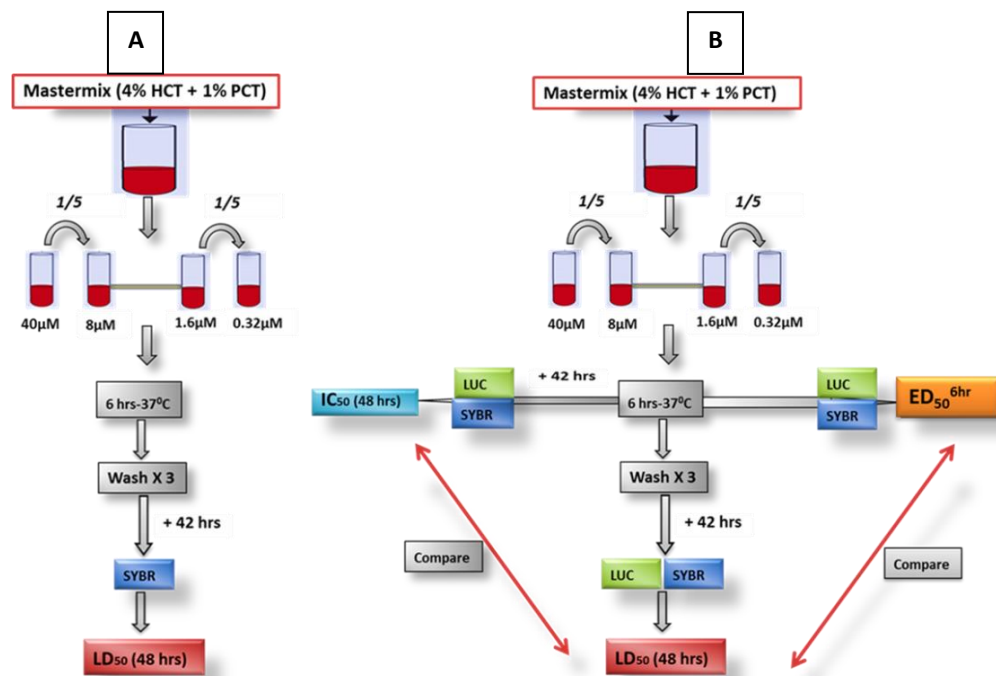


**Figure 3.4: Dose and time-dependent effect on luciferase signal following drug perturbation**  
 The dose and time-dependent effect on luciferase signal exposed to multiples of  $IC_{50}$  doses (i.e.  $81 \times IC_{50}$ ,  $27 \times IC_{50}$ ,  $9 \times IC_{50}$ ,  $3 \times IC_{50}$ ,  $1 \times IC_{50}$ ) for a fast acting cytotoxic CQ ( $IC_{50} = 208.8nM$ ) and slow acting cytostatic ATOVA ( $IC_{50} = 4nM$ ). Samples were removed and luciferase signal was measured at 0hr, 30minutes, 1hr, 2hr, 3hr, 6hr and 8hrs respectively. The luciferase signal obtained in relative light units (RLU) was normalised to untreated control and the dose/time response curves were plotted in GraphPad Prism v5.0 (GraphPad Software, Inc., San Diego, CA). Each data point represents mean RLU  $\pm$  stdev ( $n \geq 9$ ).

### 3.2.2 Correlating the loss of bioluminescence signal following drug treatment with the loss of parasite viability

As described in chapter 1, and illustrated by Sanz *et al.*, (2012), the assumption that *in vitro* measurements of metabolic activity act as a direct proxy for parasite viability is vulnerable to artefacts; whilst parasite metabolism and viability are apparently coupled during the life cycle of the parasite, these may be uncoupled following drug treatment. Recently, *in vitro* assays to measure the loss of parasite viability following drug treatment have been reported by Sanz *et al.*, (2012) and Paguio *et al.*, (2011). The Sanz assay utilises a drug bolus (multiples of 24 hours), washing off the drug and regrowth of viable parasites. This assay provides a low to medium throughput of PRR, PCT and lag phase

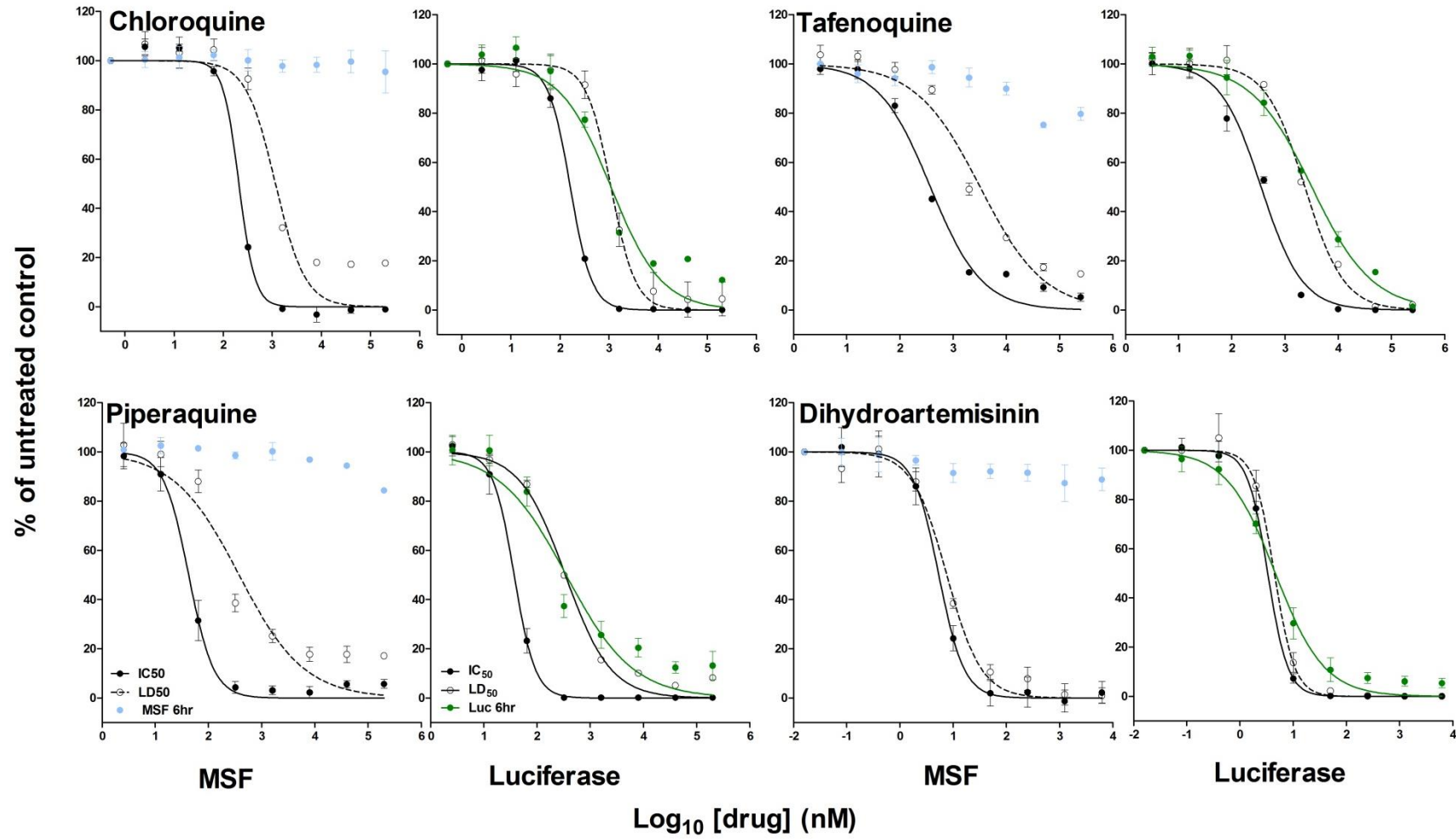
data for antimalarial compounds. By contrast, Paguio reports a 6hr drug bolus-wash assay more amenable to scale up for high throughput screening that measures the 50% lethal dose ( $LD_{50}$ ) concentration using a fluorescent DNA intercalating dye SyBr Green-1. The drug is extensively washed and the surviving parasites are allowed to recommence growth in the absence of drug pressure (+42 hours) for one cell cycle (Figure 3.5A). Thus, both these assays measure parasite viability as opposed to metabolic activity.



**Figure 3.5: Protocols for the determination of *in vitro* LD<sub>50</sub>.**

(A) Illustrates schematic of the Paguio's protocol for the determination of *in vitro* LD<sub>50</sub>. (B) Modified bioluminescence protocol to measure *in vitro* effective dose (ED<sub>50</sub><sup>6hr</sup>), Lethal dose (LD<sub>50</sub><sup>48hr</sup>) and Inhibitory concentration (IC<sub>50</sub><sup>48hr</sup>) using both luciferase and SyBr-Green-I fluorescence. Both bioluminescence (Luc) and fluorescence (SYBR) green signals for ED<sub>50</sub><sup>6hr</sup> were immediately captured following drug bolus (6hr incubation at 37°C). Samples for IC<sub>50</sub><sup>48hr</sup> (before drug wash step .e.g. IC<sub>50</sub> requires continuous presence of drug for full 48hrs), was removed (incubated for an additional 42hrs). The remaining sample was washed to remove the drug and was also incubated for an additional 42hrs to determine LD<sub>50</sub><sup>48hr</sup> (LD<sub>50</sub> only requires a drug bolus for 6hrs)

To determine here whether the immediate loss of bioluminescence measures a loss in parasite viability, Paguio's protocol was modified (Figure 3.5B). This modified experimental approach offers an opportunity to compare and contrast a range of experimental variables; e.g.  $LD_{50}^{48hr}$  against  $IC_{50}^{48hr}$  as well as bioluminescence against fluorescence assay and provide an additional opportunity to correlate how the immediate loss of bioluminescence signal  $ED_{50}^{6hr}$  (effective dose at 6hr) compares to these variables. To reflect a range of chemotypes and mode of drug action, different antimalarial drugs were selected which includes the 4-aminoquinoline CQ, the 8-aminoquinoline TFN, the 4-methanolquinolines mefloquine MEF and QN, the bisquinoline piperazine PPQ, the sesquiterpene lactones DHA and ART and a naphthoquinone ATOVA. Using this protocol, early trophozoite stage  $Dd2^{luc}$  parasites were exposed to a serial dilution of the selected antimalarial drugs in a 6hr drug bolus. The drugs were extensively washed after this period and the remaining parasites were allowed to recommence growth in the absence of drug pressure for an additional 42 hours (48 hours in total) as described above. The principle of this assay is that parasites killed during the drug bolus will not divide after removal of the drug, whereas those inhibited by the drug will recommence growth on removal of drug pressure. Three log dose-response curves, normalised against untreated controls, were fitted using data derived from either a bioluminescence assay (Luc) or malaria SyBr Green I fluorescence (MSF) assay of DNA content. These curves (Figure 3.6) report the following parameters (Table 3.2); a 50% effective dose recorded immediately following the drug bolus but prior to drug wash-out ( $ED_{50}^{6hr}$ ), a 50% lethal dose estimate following drug wash out and re-culture ( $LD_{50}^{48hr}$ ) and a 50% inhibitory concentration estimate following 48hr of continuous culture in the presence of the drug ( $IC_{50}^{48hr}$ ).



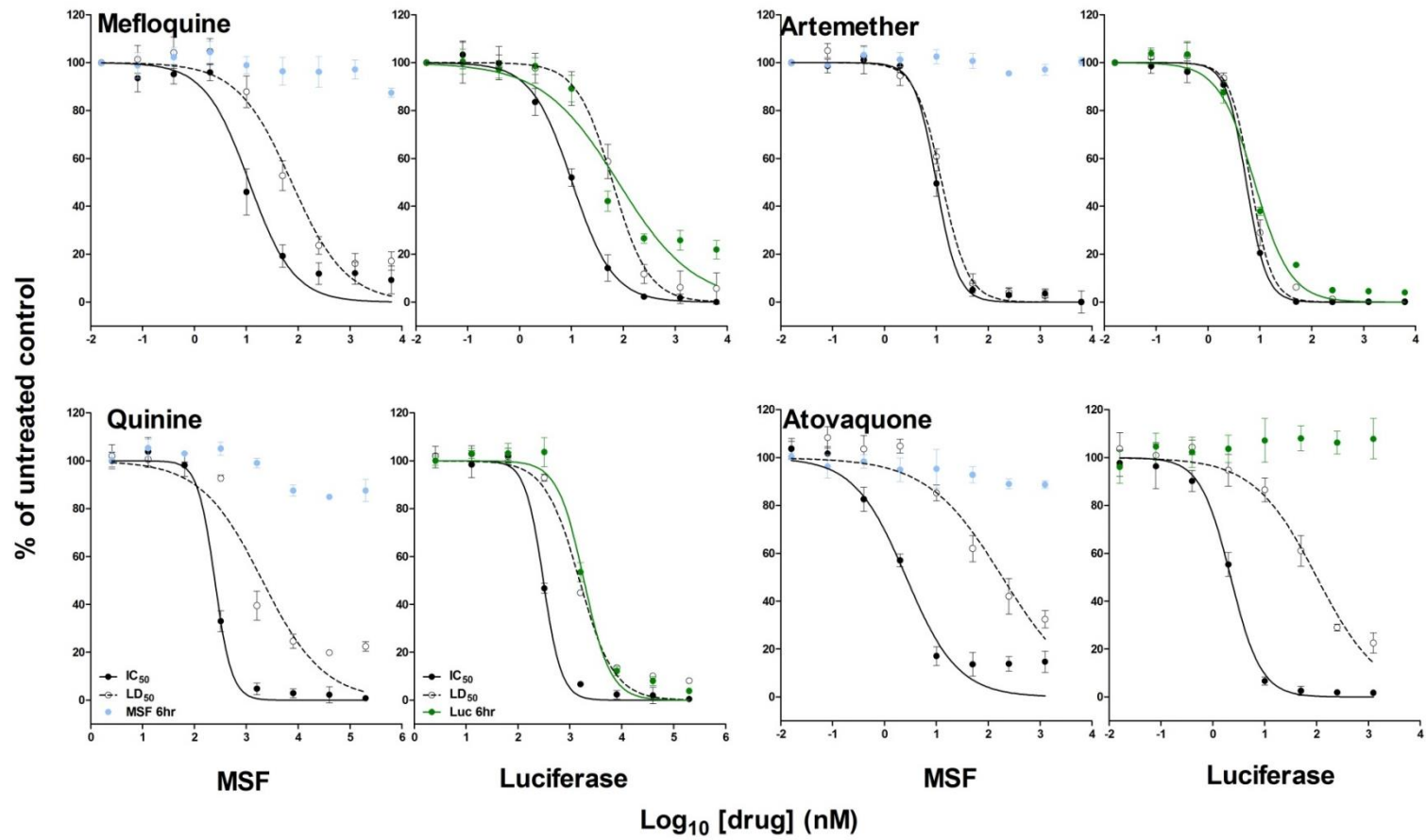


**Figure 3.6: In vitro  $ED_{50}^{6hr}$ ,  $LD_{50}^{48hr}$  and  $IC_{50}^{48hr}$  determination using luciferase and SyBr-Green-I (MSF) assay formats.** Each page reports four drugs (indicated on the left-hand panel in each pair), with pairs of graphs reporting the bioluminescent (Luciferase) and Malaria Sybr Green-I fluorescence (MSF) data normalised to an untreated control. The data shown is a mean  $\pm$  Stdev from three biological replicates ( $n \geq 9$  measurements in nM, nd-not determined). See also Table 3.2.

Drug	IC <sub>50</sub> (nM) <sup>48hr</sup>		LD <sub>50</sub> (nM) <sup>48hr</sup>		ED <sub>50</sub> (nM) <sup>6hr</sup>	
	MSF	luciferase	MSF	luciferase	MSF	luciferase
Chloroquine	208.8	162	1163	1093	nd	1091
Piperaquine	42.45	37	376.4	339	nd	351.4
Mefloquine	11.4	10.3	74.7	62.3	nd	79.8
Quinine	245.9	306	2031	1532	nd	1865
Tafenoquine	372.5	354.2	3207	2356	nd	3169
Dihydroartemisinin	4.1	3.3	5.8	4.4	nd	4.6
Artemether	10	5.5	12.77	6.7	nd	7.8
Atovaquone	2.6	2.2	187.4	101.2	nd	nd

**Table 3.2: Estimates of ED<sub>50</sub><sup>6hr</sup>, LD<sub>50</sub><sup>48hr</sup> and LD<sub>50</sub><sup>48hr</sup> using the bioluminescence and MSF assay formats**  
 These data for ED<sub>50</sub><sup>6hr</sup>, LD<sub>50</sub><sup>48hr</sup> and LD<sub>50</sub><sup>48hr</sup> obtained from the curves plotted of luciferase and MSF assays of indicated antimalarials in Figure 3.6.

As expected, the majority of drugs show a right shift in the lethal dose curve compared to that of the inhibitory dose, reflecting the shorter duration of action of the drug. The lack of an apparent shift for the artemisinins DHA and ART likely reflects their formation of covalent adducts with their target(s), rendering them resistant to the wash steps (Paguio *et al.*, 2012). The  $IC_{50}^{48hr}$  and  $LD_{50}^{48hr}$  assay data developed using either the MSF or bioluminescence assay are essentially identical, unlike those data reported immediately following the 6hr drug bolus ( $ED_{50}^{6hr}$ ). Here, the intrinsic instability of the luciferase reporter protein ( $t_{1/2}$  of approximately 1.5hr) compared to that of the far more stable DNA biomarker, offers a more dynamic report of drug action (Hasenkamp *et al.*, 2013). Critically, the  $ED_{50}^{6hr}$  values determined using bioluminescence assay is almost identical to the  $LD_{50}^{48hr}$  estimated using either assay formats. This, and the observation that the 6hr bioluminescence curve closely fits that of the lethal dose curve for the majority of drugs, suggests that the 6hr bioluminescence response provides a rapid surrogate determination of the lethal action of these drugs. The sole exception, ATOVA, shows no reduction in the bioluminescence signal within 6hr, a reflection of its cytostatic action within the first intraerythrocytic cycle of its application, commonly reported as a delayed death phenotype (Sanz *et al.*, 2012).

To provide additional confirmation that loss of bioluminescence correlates with loss of viability, the assay was repeated using CQ, QN, MEF, DHA and ATOVA at three equipotent doses corresponding to 1x, 3x and 9x $IC_{50}$  for a 6hr bolus and the luciferase signal measured at this time. The drug then removed by extensive washing before replacing the parasites into culture for an additional 42hr to complete a cycle of intraerythrocytic development and the luciferase signal was remeasured. The bioluminescent signal was

normalised to an untreated control at the same time point, plotted against drug dose (Figure 3.7). The expectation here is that the 6hr luciferase signal immediately following drug treatment will be the same as that after the drug wash and regrowth i.e. the apparent 6hr lethal effect is the same as the real lethal effect observed after regrowth of parasites on removal of drug pressure.

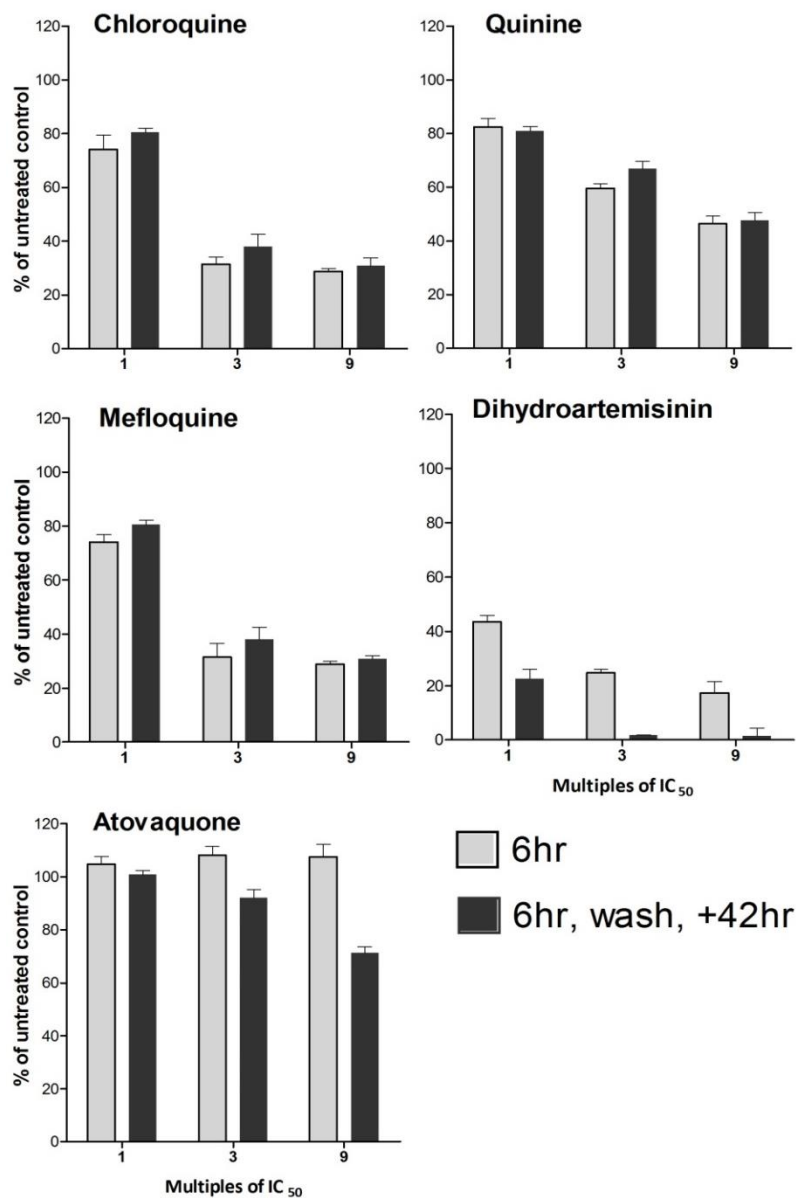


**Figure 3.7: Loss of bioluminescence correlates with loss of viability**  
The bioluminescence<sup>6hr</sup> signal compared against the bioluminescence<sup>48hr</sup> signal, obtained after drug removal using equipotent doses. Each data point represents mean RLU ± stdev (n=9).

The 6hr bioluminescence response appears to provide a rapid surrogate determination of the lethal action of CQ, MEF and QN. As expected (i) ATOVA shows no reduction in the bioluminescence signal within 6hr, with only moderate effects after 48hr mirroring what is known about the delayed death phenotype for this class of drug and (ii) the resistance of DHA to removal is illustrated by the continued loss of bioluminescence signal at 48hr. Importantly, comparison of the loss of bioluminescence for drugs used at equipotent doses suggests that a ranking order for their effect on loss of viability (at both 6hr and 48hr) can be measured, and these apparently correlate with their known relative rates of kill.

Finally, confirmation of the loss of parasite viability during the 6hr drug bolus was independently verified following morphological inspection of Giemsa-stained thin smears of drug-treated parasites. Early trophozoite stage parasites under the same experimental conditions were exposed to a fixed dose of  $9 \times IC_{50}$  of the drug under investigation for 6hr and images were obtained by light microscopy. In comparison to the untreated control, DHA and CQ reveal almost exclusively condensed pyknotic parasites (Figure 3.8). Thus, the observed loss of viability as determined using the bioluminescence assay is mirrored in the very poor morphology of parasites after this length and dose of drug treatment. Parasites treated with ATOVA for the same length and equipotent dose (Figure 3.8), however, show little difference in gross morphology compared to the untreated control – again mirroring the observation in no apparent loss in bioluminescence at this time and dose of drug. This independent evidence offers a cautionary tale in the applications of the bioluminescent assay for slow acting drugs (i.e. ATOVA) but further strengthens the hypothesis that the loss of bioluminescence is a measure of loss of parasite viability.

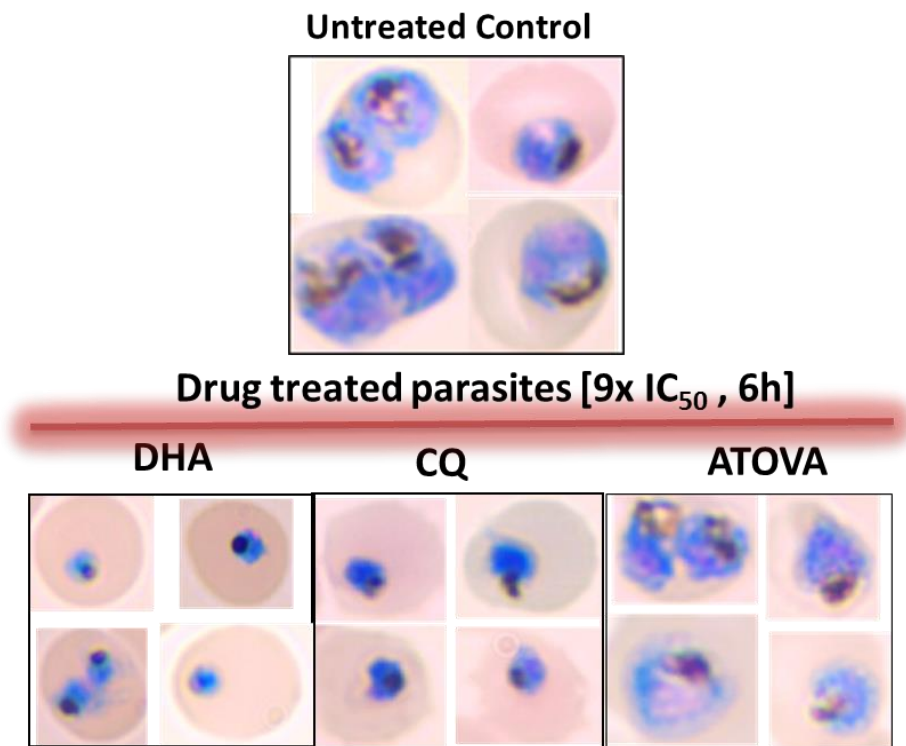


**Figure 3.8: Morphological inspection of drug-treated parasites**  
 Light microscopy images of Geimsa-stained thin blood smears of an untreated control and drug-treated trophozoite stage parasites (9xIC<sub>50</sub> for 6hr).

### 3.2.3 The dose and time-dependent loss of bioluminescence following drug treatment correlates with the known rate of kill of benchmark antimalarial drugs

As shown above in figure 3.4, a saturation effect is apparent beyond the 6hr window (i.e. 8 hours) at higher concentrations. This suggests that the 6hr window is sufficient to obtain the most useful information regarding the activity of rapid acting drugs. Notably some discrimination between the rapid killing profiles of DHA and CQ is apparent, an important observation given the specific noting of these drugs in the TCP1 of SERCaP. To effectively capture these killing profiles and compare the relative time and dose-dependent effects of different antimalarial drugs within the 6hr window, a revised bioluminescence assay was devised that utilised fold-changes in IC<sub>50</sub> concentrations to ensure exposure to equipotent doses of drug. Dd2<sup>luc</sup> parasites were exposed to a three-

fold serial dilution ( $81$  to  $0.33 \times IC_{50}$ ) for either 3 or 6 hrs, plotted against drug dose. Bioluminescent signal was normalised to an untreated control at the same time point (Figure 3.9).

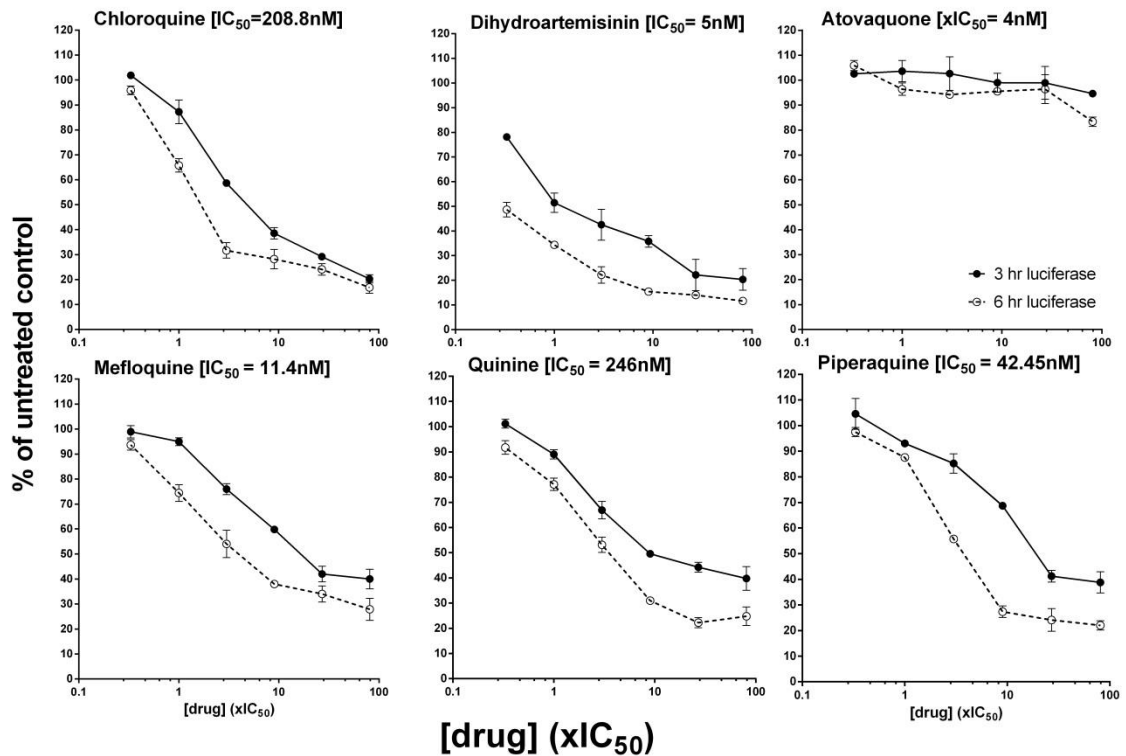
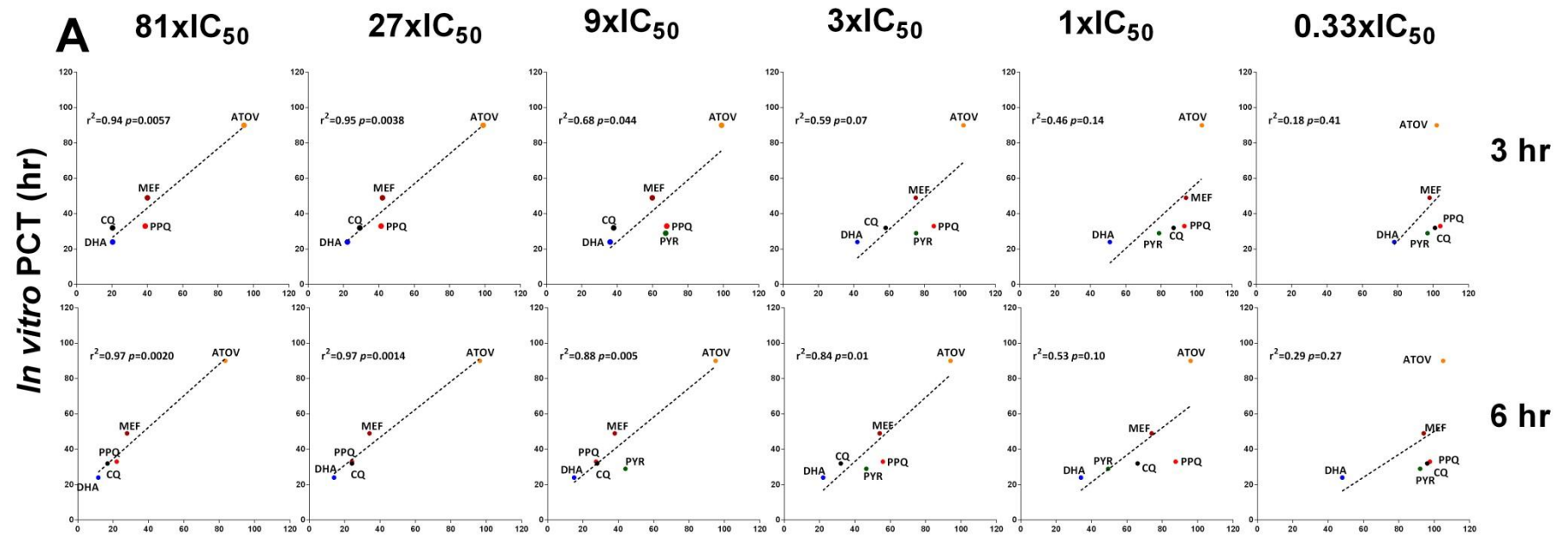


**Figure 3.9: The dose and time-dependent effects of different antimalarial drugs**  
The dose and time-dependent response curves for the indicated antimalarial drugs at 3hr (closed circles) and 6hr (open circles) using multiples of  $IC_{50}$  doses (i.e.  $81 \times IC_{50}$ ,  $27 \times IC_{50}$ ,  $9 \times IC_{50}$ ,  $3 \times IC_{50}$ ,  $1 \times IC_{50}$  and  $0.33 \times IC_{50}$ ). Each data point represents mean RLU  $\pm$  stdev ( $n=9$ ).

These data illustrate an apparent saturation in the lethal effect of drug doses greater than  $9 \times IC_{50}$  for all, except ATOVA, of the drugs tested. This observation is in agreement with the findings of Sanz *et al.*, (2012) who suggest that a  $10 \times IC_{50}$  dose produces the maximal rate of kill for the drugs they tested. Direct comparison between the data shown in figure 3.9 describes an apparent relative ranking order of artemisinins > CQ > 4-methanolquinolines > ATOVA. This is identical to the relative order of rates-of-kills described both *in vivo* and *in vitro* for the same drugs. To explore this correlation further,

the *in vitro* estimates of Log PRR and PCT available from Sanz *et al.* (2012) were plotted against the bioluminescent signals produced at each time point and drug concentration and a linear regression analysis performed (Figure 3.10).

Comparison of bioluminescence data against the PCT shows a strong and significant correlation at higher doses of the drug and on longer treatment i.e. 81 to 3XIC<sub>50</sub> at 6hrs with p-values <0.01 (Figure 3.10A). Interestingly, the slope and intercept of the regression analysis is essentially unchanged at greater than 9XIC<sub>50</sub> doses reflecting an apparent saturation in the rate of kill achieved at these doses. Similarly, comparisons with the Log PRR show a strengthening trend with higher doses of drug and longer exposure times i.e. 81 to 3XIC<sub>50</sub> at 6hrs although these just fail to reach a level of significance (p values >0.05) (Figure 3.10B). One possible explanation for this is the relative lack of data for the PRR comparison as DHA is excluded from the analysis as it is reported as >10<sup>8</sup> in Sanz *et al.*, (2012) and cannot be plotted here (whilst noting that it's pseudo-positioning at 81XIC<sub>50</sub> follows the general observable trend).



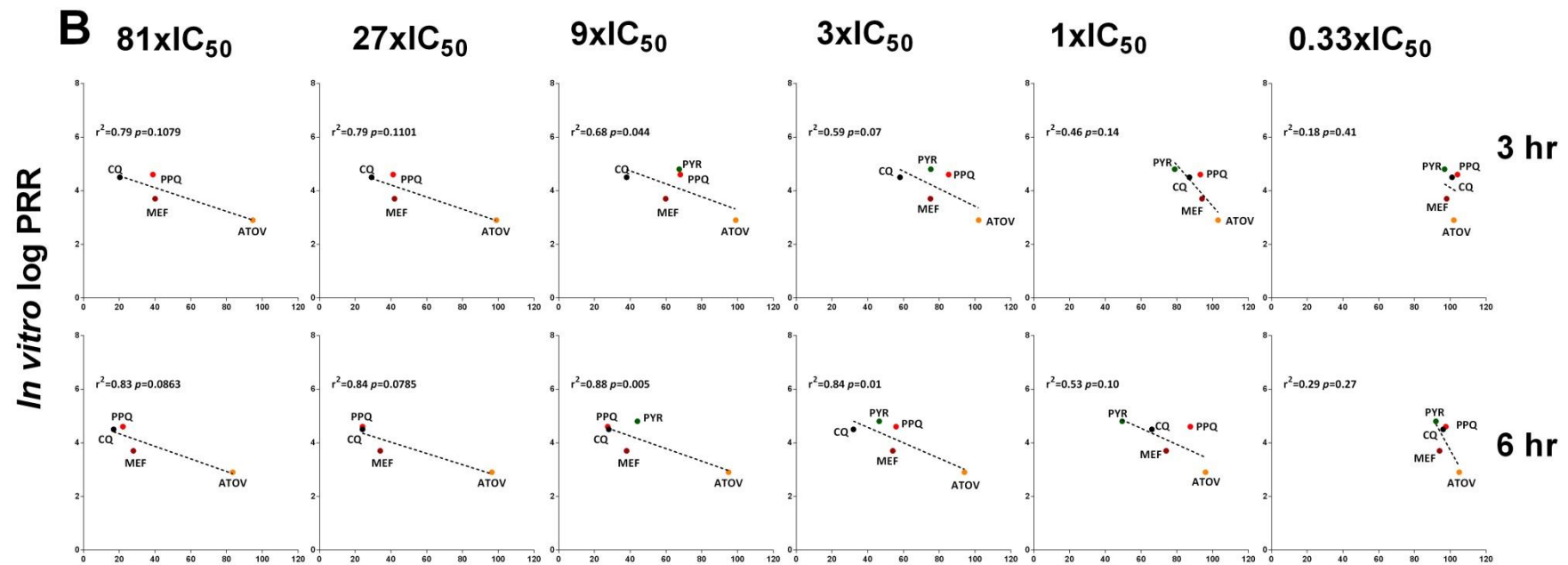


**Figure 3.10: Correlation of the bioluminescence against in vitro PCT and PRR**  
 Bioluminescence data (% of untreated control) plotted against available in vitro (A) PCT and (B) PRR (Sanz et al., 2012).

### 3.3 Discussion

This chapter set out to demonstrate that the dynamic response of a bioluminescence assay offers a useful biomarker of parasite viability following drug treatment. The principle here is that a more dynamic response would be obtained in a bioluminescence assay upon initial drug perturbation as a result of the cessation of luciferase expression in dead and dying parasites, coupled with the turnover of the intrinsically unstable luciferase reporter protein ( $t_{1/2}$  of approximately 1.5hr, Hasenkamp *et al.*, 2013). By contrast, the intrinsic stability of DNA, monitored using the fluorescent DNA-intercalating dye SyBr Green I, hampers any attempt at a short-term fluorescence-based monitoring of cell death. Simply put, dead parasites don't make new protein, but they still retain (at least for 6hr) DNA.

Previous work in the Horrocks laboratory has evaluated, compared and contrasted the application of MSF and luciferase assays in the determination of  $IC_{50}$  (Hasenkamp *et al.*, 2012 and Hasenkamp *et al.*, 2013). Moreover, the application of luciferase assays to measure  $IC_{50}$  in medium throughput screens of both intraerythrocytic and gametocyte stage *P. falciparum* have been described (Adjalley *et al.*, 2011; Che *et al.*, 2012; Cui *et al.*, 2008; Ekland *et al.*, 2011; Franke-Fayard *et al.*, 2008; Lucumi *et al.*, 2010; Lucantoni *et al.*, 2013). The luciferase assay format, compared to fluorescent assays of DNA content, offers significant advantages in terms of the signal to noise ratio with the luciferase assay offering dynamic ranges typically exceeding 250 compared to 4-5 achieved using MSF assay (Hasenkamp *et al.*, 2013). Critically, however, in screening for  $IC_{50}$  potency, the reliability of the MSF assay format (determined as  $Z'$  scores), being essentially the same as that for luciferase assays, coupled with its much cheaper cost means that high throughput screening with luciferase is economically unfeasible. Another key limitation is the need to GM the parasite strain for

luciferase assays; a limitation that is shared in the bioluminescence rate of kill assay described here, and will be discussed below.

The object of the work described in this chapter was to evaluate the potential for a bioluminescence assay to measure a distinct pharmacodynamics property, the rate of kill. Here, the dynamic response offered by the luciferase reporter offers an opportunity to quickly monitor the initial rate of kill – something which cannot be offered by the available, albeit cheaper, fluorescence assay. A number of key observations were made.

First, that ***the loss of bioluminescence signal is both time and dose-dependent***. This provides for a means to compare the loss of bioluminescence exposed to equipotent doses of different drugs, allowing for a ranking order to be determined. The assay, as described here, doesn't provide a rate of kill in terms of the currently used parameters of PRR and PCT, rather it provides for a relative rank of initial rate of kill. The incorporation of benchmark drugs, current antimalarials with known PRR and PCT, does provide for an opportunity to rank an unknown drug against these benchmarks (and is the topic of the rest of this thesis).

A limitation revealed here is the apparent lack of response in this assay to drugs that affect a slow rate of kill – whether intrinsically slow in mediating their cytotoxic effect or displaying a lag-phase (i.e. ATOVA). Here, the maximal 6hr window of the assay doesn't offer sufficient time for slower acting drugs to affect a loss in bioluminescence. Thus, the utility of the 6hr assay appears limited to drugs with a moderate to fast rate of kill (i.e.  $PPR > 10^{3.5}$ ). This limit is imposed by the temporal luciferase expression at the trophozoites stage. The 6hr window was extended to 12 hours (data not shown). However, analysis of a fall in bioluminescence signal caused by loss of viability overlapping with the concurrent temporal loss of luciferase expression as the parasites complete S-phase and move into schizogony was difficult (Wong

*et al.*, 2011; Hasenkamp *et al.*, 2013). This suggests that whilst the current 6hr assay is useful to estimate the rate of kill of fast acting schizonticide antimalarial drugs, it cannot currently be used to measure rate of kill in other stages (i.e. rings stage). This issue will be picked up again in chapter 5. That said, this assay does provide a means to identify and discriminate between the initial rates of kill of moderate to fast-acting drugs – the intended class of compounds of interest for a TCP1 component of a potential future SERCaP.

Second, that ***the loss in bioluminescence reports the loss in parasite viability***. Confirmation of the loss of parasite viability during the 6hr drug bolus was independently verified exposing Dd2<sup>luc</sup> parasites to a modified lethality assay adapted from that originally described by Paguio *et al.*, (2011) as well as following gross morphological examination of the drug-treated parasites. In the Paguio bolus-wash-regrowth assay, the LD<sub>50</sub><sup>48hr</sup> was measured using both a luciferase and MSF assay and compared to the ED<sub>50</sub><sup>6hr</sup> i.e. the bioluminescence response immediately following drug treatment (and before any drug washing steps). LD<sub>50</sub><sup>48hr</sup> strongly and significantly correlates with the ED<sub>50</sub><sup>6hr</sup> (Figure 3.11). In other work in the laboratory (Ali and Horrocks, *pers comm*), the cytotoxic effect of CQ at 9XIC<sub>50</sub> has been confirmed using both a TUNEL assay of DNA fragmentation and by ultrastructure examination using transmission electron microscopy. This latter study reveals extensive vacuolization in cytoplasm and loss of digestive vacuole integrity as previously described by Ch'Ng *et al.* (2011) following exposure of *P. falciparum* to high doses of CQ. Together, this evidence suggests that the cytotoxic potential of antimalarial drugs certainly plays a role in the rate of kill. This also validates that the 6hr bioluminescence response curves are a characteristic of “lethal effect” of a drug rather than an “inhibitory effect” on the parasites. Importantly, given previous issues regarding the uncoupling of parasite metabolism and

growth following drug perturbation (Sanz *et al.*, 2012), the bioluminescence assay described here directly measures antimalarial drug activity - providing a rapid distinction between cytotoxic fast acting and cytostatic slow acting drugs.

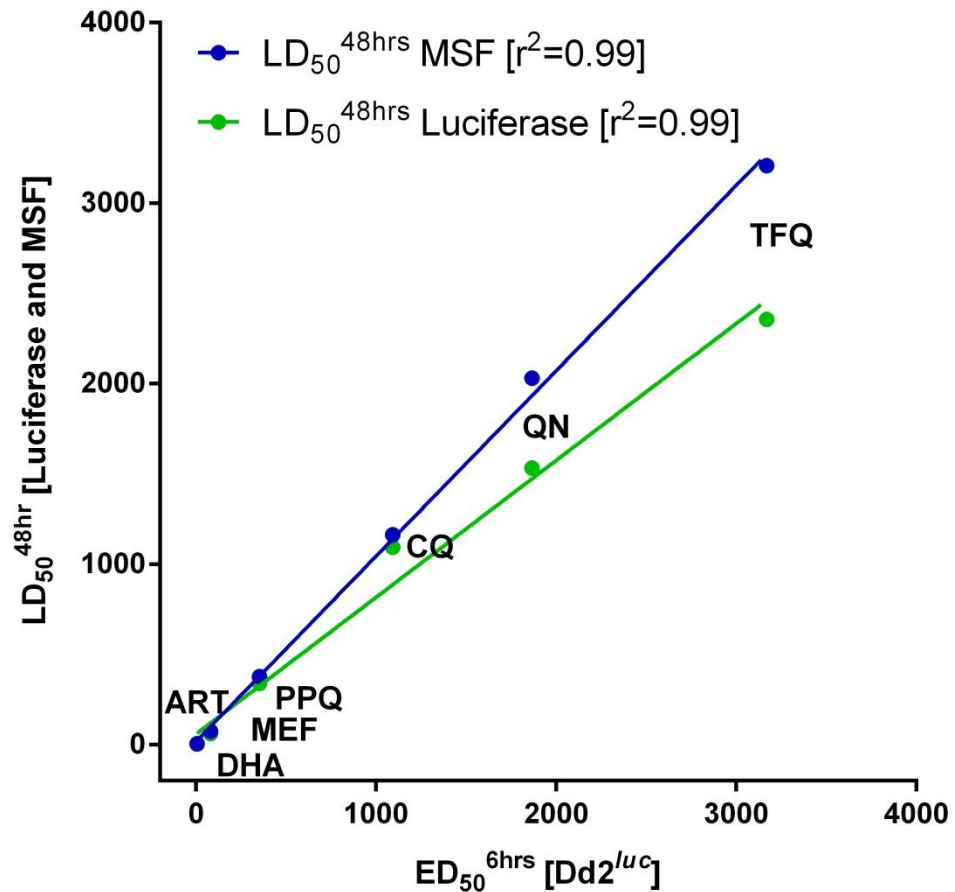


**Figure 3.11: Comparison of  $ED_{50}^{6hr}$  against  $LD_{50}^{48hr}$**   
 Linear regression analysis of the bioluminescence  $ED_{50}^{6hr}$  against  $LD_{50}^{48hr}$  in Dd2 parasite clone obtained using either MSF (blue) or luciferase (green) assays.

Third, **the relative order in rate of kill provided by the bioluminescence assay correlates with available *in vitro* and *in vivo* PRR and PCT data.** The bioluminescence assay data describes an apparent relative ranking order of artemisinins > CQ > 4-methanolquinolines > ATOVA. This relative ranking has been observed in both *in vitro* and *in vivo* studies of the pharmacodynamics of antimalarial drug action in *P. falciparum* (Sanz *et al.*, 2012; White, 1997). Pukrittayakamee *et al.* (2000) evaluated the therapeutic responses of known

antimalarial drugs in *P. vivax*, which illustrates the same relative order as indicated above. *P. vivax* is not sequestered markedly in the microcirculation and thus PRR represents a more readily determined measure of antimalarial drug activity. The relative order of bioluminescence data also correlates with the *in vivo* PRR data of Pukrittayakamee *et al.*, (2000) and this essentially suggests that bioluminescence directly measures parasite viability. Sanz *et al.*, (2012) has shown that *in vitro* rate of kill data of antimalarial drugs correlate with the standard *in vivo* PRR and PCT data. The bioluminescence data developed here shows a direct correlation with Sanz *et al.*, (2012) *in vitro* PCT and PRR data (Figure 3.10). At 6hrs, comparison against PCT data illustrates a strong and significant correlation at higher doses of the drug as described above (Figure, 3.10A). Comparisons with the Log PRR show a strengthening trend with higher doses of drug and longer exposure times, although these just fail to reach a level of significance. The limitations here appear to be the available shared data (artemisinins are excluded as Log PRR only reported as >8) and the limited distribution in Log PRR for the quinoline drugs used here.

It has been previously shown by Sanz *et al.*, (2012) that rate of kill has no correlation with  $IC_{50}$  values. This is perhaps best illustrated by artemisinin and atovaquone, both drugs with single digit nM  $IC_{50}$ , yet very different rates of kill. To further explore this correlation, the *in vitro* estimates of Log PRR and PCT were correlated against the  $IC_{50}^{48hr}$  and  $LD_{50}^{48hr}$  data developed using the MSF assay (Figure 3.12). Note only MSF data used here because the  $IC_{50}^{48hr}$  and  $LD_{50}^{48hr}$  assay data developed using either the MSF or bioluminescence assay are identical as described above (Figure 3.6, see also Table 3.2).

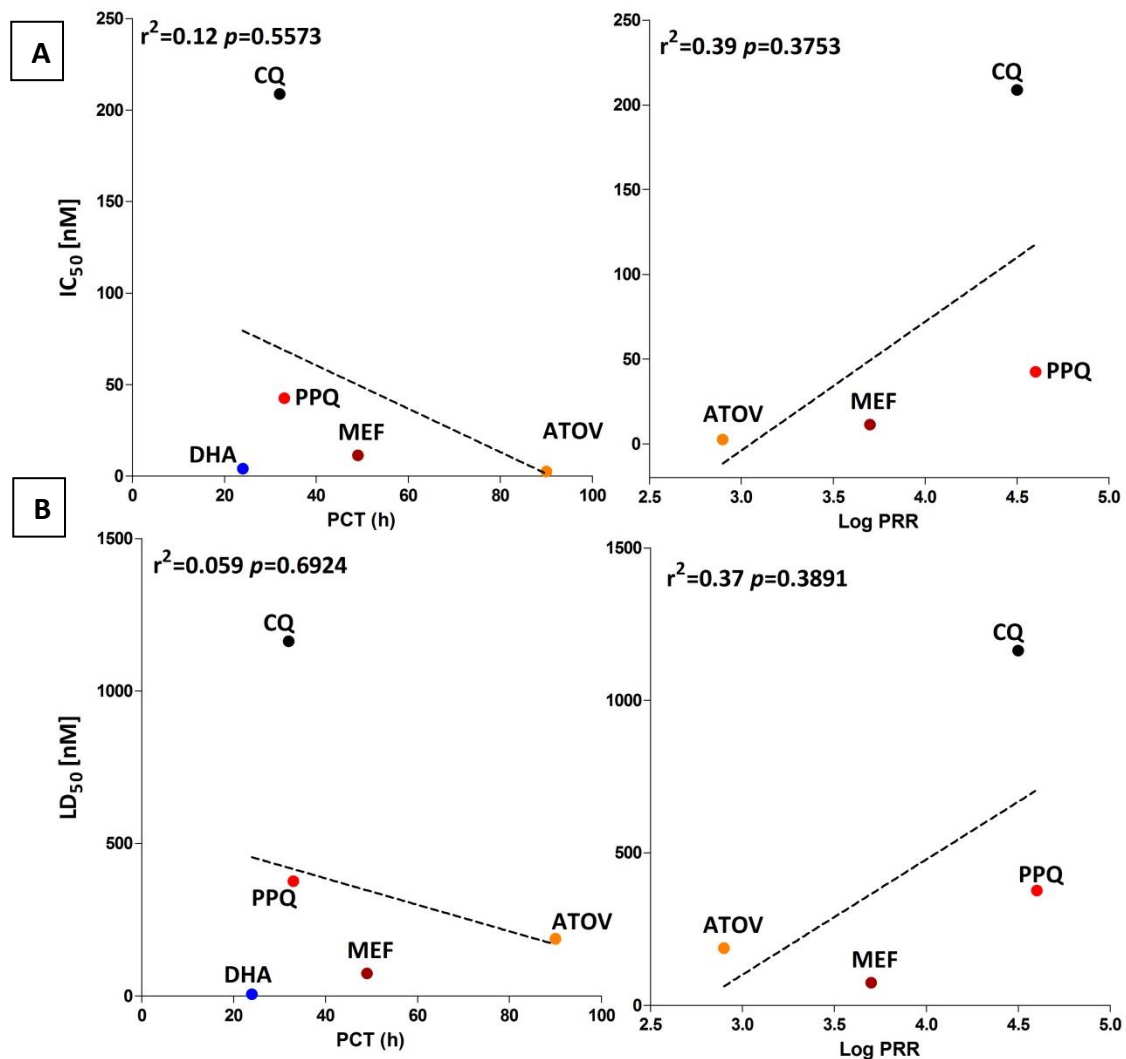


**Figure 3.12: Comparison of rate of kill against  $IC_{50}$  and  $LD_{50}$**   
 Linear regression plots of (A)  $IC_{50}$  and (B)  $LD_{50}$  plotted against available in vitro PCT and Log PRR data (Sanz *et al.*, 2012).

Comparison of this PCT/ PRR data illustrates no significant correlation with the  $IC_{50}$  potency of antimalarial drugs (Figure 3.12A). The finding with respect to  $IC_{50}$  is, not unexpectedly, in agreement with that originally described in Sanz *et al.*, (2012). Comparison with  $LD_{50}$ , however, extends this analysis, and also shows no significant correlation with the available PCT and PRR data (Figure 3.12B). Whilst the action of the drug in 6hrs likely solely represents the immediate cytotoxic activity of antimalarial drugs (remembering that  $ED_{50}^{6hr}$  is essentially the  $LD_{50}$ ), the  $IC_{50}$  reports a mixture of both the cytostatic and cytotoxic activity of

drugs over 48hrs (See section 1.9 in introduction). In table 3.2, the LD<sub>50</sub> for the artemisinins DHA and ART is reported as the same as their IC<sub>50</sub>. One explanation for this is that the drug binds covalently to its target and is thus resistant to washing – however, the ED<sub>50</sub><sup>6hr</sup> (i.e. LD<sub>50</sub>) is determined before the wash steps and suggests that the profound rate of kill has already been achieved within the first 6 hours. This contrast with atovaquone, where the LD<sub>50</sub> is many-fold higher than the IC<sub>50</sub>, primarily as a result of the delay in kill. The other benchmark drugs apparently fall between these two extremes. To explore whether a ratio of LD<sub>50</sub>/IC<sub>50</sub>, capturing the inherent differences between cytotoxic and cytostatic effects of drugs (as proposed by Paguio *et al.*, 2011) instead correlates with rate of kill, these ratios were determined (Table 3.3) and correlated with the available PRR and PCT data (Figure 3.13).

Drug	LD <sub>50</sub> <sup>48hr</sup> / IC <sub>50</sub> <sup>48hr</sup> ratio		ED <sub>50</sub> <sup>6hr</sup> / IC <sub>50</sub> <sup>48hr</sup> ratio	
	MSF	luciferase	MSF	luciferase
Chloroquine	5.6	6.7	5.2	6.7
Piperaquine	8.9	9.2	8.3	9.5
Mefloquine	6.6	6.0	7.0	7.7
Quinine	8.3	5.0	7.6	6.1
Tafenoquine	8.6	6.7	8.5	8.9
Dihydroartemisinin	1.4	1.3	1.1	1.4
Artemether	1.3	1.2	0.8	1.4
Atovaquone	72.1	46.0	nd	nd

**Table 3.3: Ratios of IC<sub>50</sub> and LD<sub>50</sub>/ED<sub>50</sub>**  
Ratios of IC<sub>50</sub> and LD<sub>50</sub>/ED<sub>50</sub> (in Dd2 clone) for the given antimalarial drugs are reported. The data shown is a mean ± Stdev from three biological replicates (n>9 measurements in nM, nd-not determined).

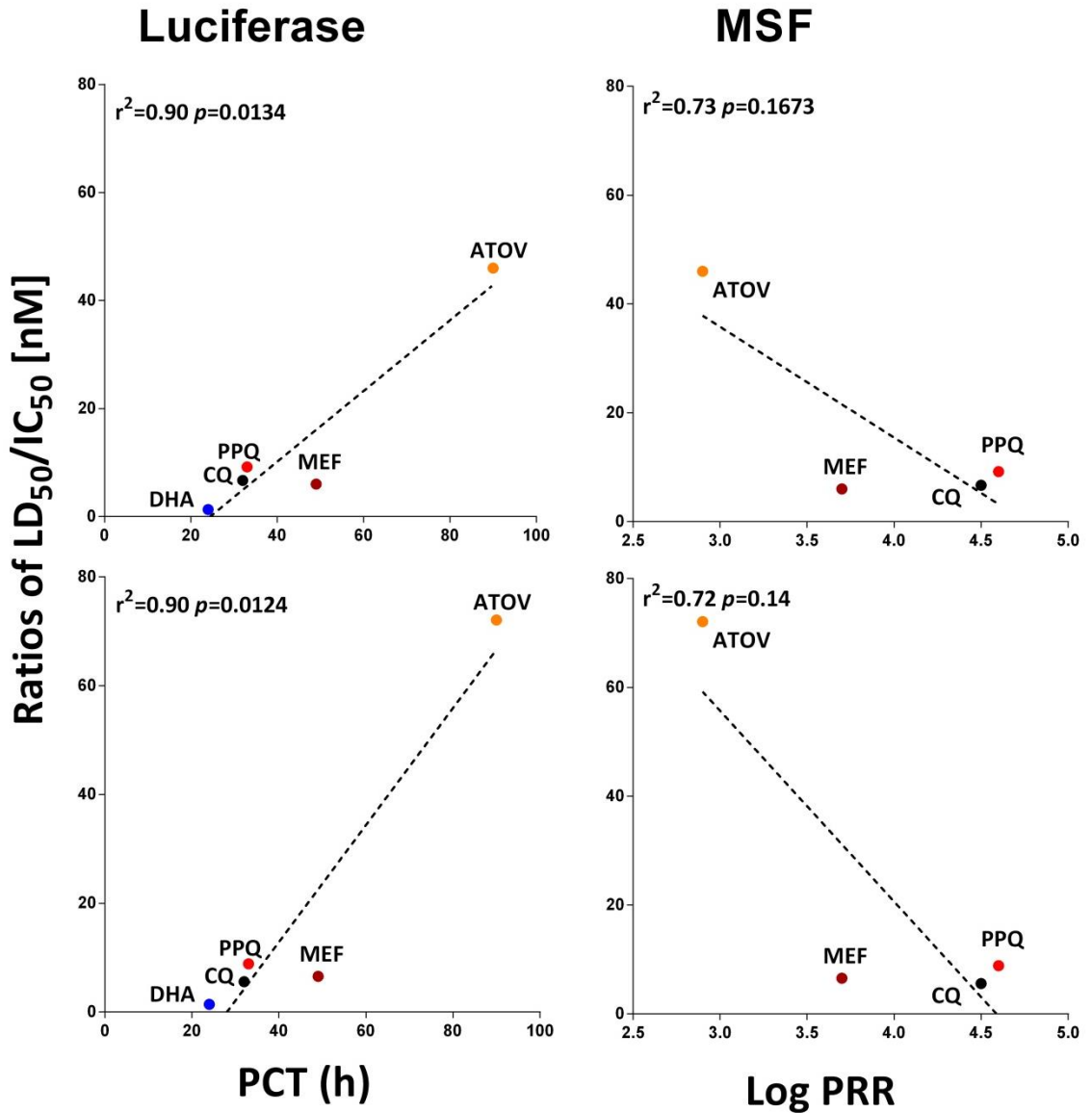


**Figure 3.13: Comparison of LD<sub>50</sub>/IC<sub>50</sub> ratios against Rate of kill**  
 Linear regression plots of available in vitro PCT and Log PRR compared against both the luciferase and MSF ratios of IC<sub>50</sub><sup>48hr</sup> and LD<sub>50</sub><sup>48hr</sup> - Note all the ratios determined either using MSF or luciferase data are obtained using Dd2 clone (see Table 3.3).

Comparison of PCT against the IC<sub>50</sub>/LD<sub>50</sub> ratios illustrates a strong and significant correlation (Figure 3.13). As expected, based on previous correlations of limited PRR data, there is a clearly emerging trend between IC<sub>50</sub>/LD<sub>50</sub> ratios and PRR (Figure 3.13). Nevertheless, this PRR correlation is clearly stronger than that observed against either IC<sub>50</sub> or LD<sub>50</sub> data alone. This observation is potentially promising. The bioluminescence assay is only applicable in GM parasites expressing the luciferase reporter gene and thus, it cannot be adapted as a

screening tool against field isolates. The LD<sub>50</sub>/IC<sub>50</sub> fold change in non-GM parasites could, however, provide a surrogate measure of rate of kill. However, given the requirements for multiple wash steps and plating it will not be readily applicable for a HTS system.

Work described here provides a validation of a bioluminescence rate of kill assay that can quickly and reliably provide relative ranking data for fast to moderately acting drugs that could identify leads for TCP1 compounds. The simplicity of the assay and its inherent capacity to be scaled suggests that it offers a tool that would assist in the identification of leads for further development. This opportunity is explored in subsequent work described in this thesis that utilises the “MMV Malaria Box”.

## CHAPTER 4: Screening the Malaria Box Using a Rapid *In Vitro* Bioluminescence Rate of Kill Assay

---

### 4.1 Introduction

The demonstration of rapid development and global spread of resistance by *P. falciparum* to front-line therapeutics identifies a constant need for the discovery of new chemotypes to feed the pipeline of antimalarial drug development (Burrows *et al.*, 2012; Kim *et al.*, 2015; Spangenberg *et al.*, 2013). This pressing need has been supported over the last five years by the Genomics Institute of the Novartis Research Foundation (GNF, San Diego, California, USA), GlaxoSmithKline (GSK, Tres Cantos, Spain) and St. Jude Children's Research Hospital through the phenotypic screening of over six million compounds. This screen yielded some 20,000 hits (Spangenberg *et al.*, 2013) that exhibit sub-micromolar potency against the blood stage of the malaria parasite *P. falciparum* and have been made available to the wider scientific community (Gamo *et al.*, 2010; Guiguemde *et al.*, 2010; Meister *et al.*, 2011; Plouffe *et al.*, 2008; Spangenberg *et al.*, 2013). To support academic and industry efforts in antimalarial drug discovery, the structure of these chemical starting points have been deposited in the open access ChEMBL database ([www.ebi.ac.uk/chembl/ntd](http://www.ebi.ac.uk/chembl/ntd)). These efforts have resulted in significant progress over the past decade, with many new chemical entities entering the pipeline for antimalarial drug development (see Table 1.5 in introduction) (Wells *et al.*, 2015).

However, exploiting these screening efforts have been hampered by the unavailability of physical samples of these compounds to the wider research community for further validation and follow-on studies. To make this collection of over 20,000 compounds more accessible for researchers across the globe and to offer a more manageable and presentable

set of compounds, the MMV implemented a step-by-step approach to refine a pool of these compounds as a freely available community resource termed the “Malaria Box”. The initial resource included compounds from St Jude’s (1536 compounds), GSK (13519 compounds) and Novartis (5708 compounds) (Gamo *et al.*, 2010; Guiguemde *et al.*, 2010; Meister *et al.*, 2011). Initially, any compound with a molecular weight >1000 and/or any compound with greater than 20 rotatable bonds was removed from these libraries. These datasets were then compared to remove any interdataset structure duplicates and some 19876 structurally unique compounds present in the three libraries were identified as a compound pool for further selection (Figure 4.1A). Analysis of the chemical diversity within these three libraries showed that they occupied an almost similar property space. The GSK library, however, showed the greatest chemical diversity, explained simply by it being the largest dataset among the three of them (Spangenberg *et al.*, 2013). To ensure commercial availability, these compounds were searched using the eMolecules website (Rishton, 1997), identifying 5034 to be readily accessible for follow-up experiments (Spangenberg *et al.*, 2013).

The drug-like compounds were selected from the commercially available hits (Figure 4.1B) considering their compliance with the Lipinski's Rule of 5 (Ro5); physiochemical properties that predict acceptable oral absorption (Lipinski *et al.*, 2001; Spangenberg *et al.*, 2013). Known toxicophores were removed applying substructure filters and compounds which met the criteria of these filters were included in the drug-like set while those failing one or more of these filters were assigned to the probe-like category (Spangenberg *et al.*, 2013). This analysis split the compounds into drug-like and probe-like categories, each representing 2693 and 2341 compounds, respectively.

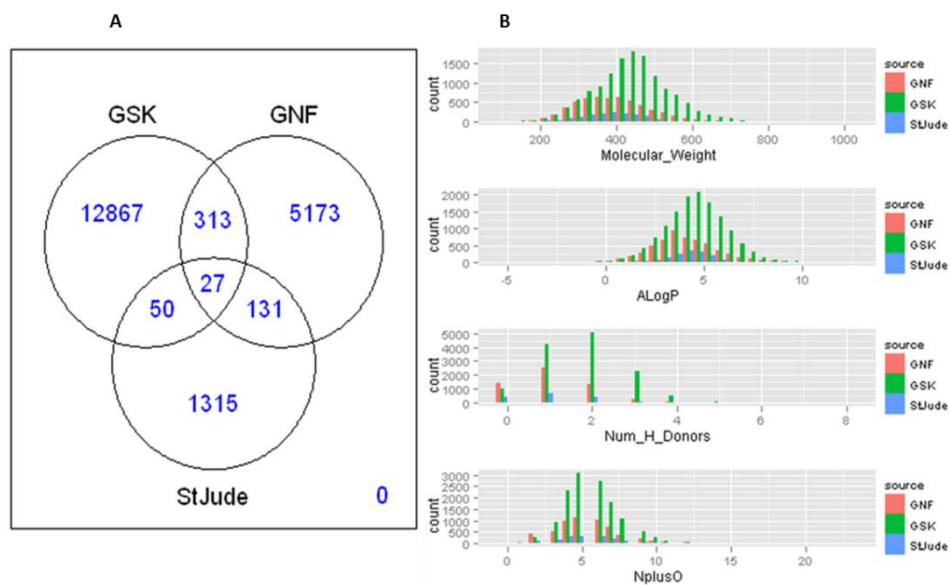


**Figure 4.1: The initial selection process of St Jude's, GSK and Novartis antimalarial datasets** (A) Shows the overlap of structures within each screening library and (B), profiling of the compounds based on physicochemical properties between the three available libraries (Source modified from Spangenberg *et al.*, 2013).

To provide a manageable, representative library, the drug-like and probe-like compounds were subjected to further analysis with the aim to provide a good balance between potency and chemical diversity. With the emphasis on maximising chemical diversity, the inclusion of near neighbours or matched molecular pairs was attempted given that they display a significant distinct antiplasmodial activity. Finally the ability of 300 drug-like and 300 probe-like compounds to inhibit the growth of *P. falciparum* 3D7 and K1 strains was tested using a DAPI (4-6-diamidino-2-phenylindole) stain and fluorescent high content imaging assays (Duffy and Avery, 2012; Spangenberg *et al.*, 2013).

Following confirmatory screening of the over 600 compounds in *P. falciparum*, their cytotoxicity (CC<sub>50</sub>) was measured in the HEK-293 cell line. Of these, a total of 459 compounds showed an activity of at least 4  $\mu$ M against *P. falciparum* 3D7 and a selectivity ratio of at least a 10-fold over the cytotoxicity assay, thus meeting the criteria set by the MMV. Firstly, a collection of 200 drug-like were selected through consultation with a group of experienced

medicinal chemists (a process termed “wisdom of the crowd”) from the drug-like confirmatory set and then the remaining 200 compounds were assigned to the probe-like category. This collection was finally assembled into the “Malaria Box (Figure 4.2).

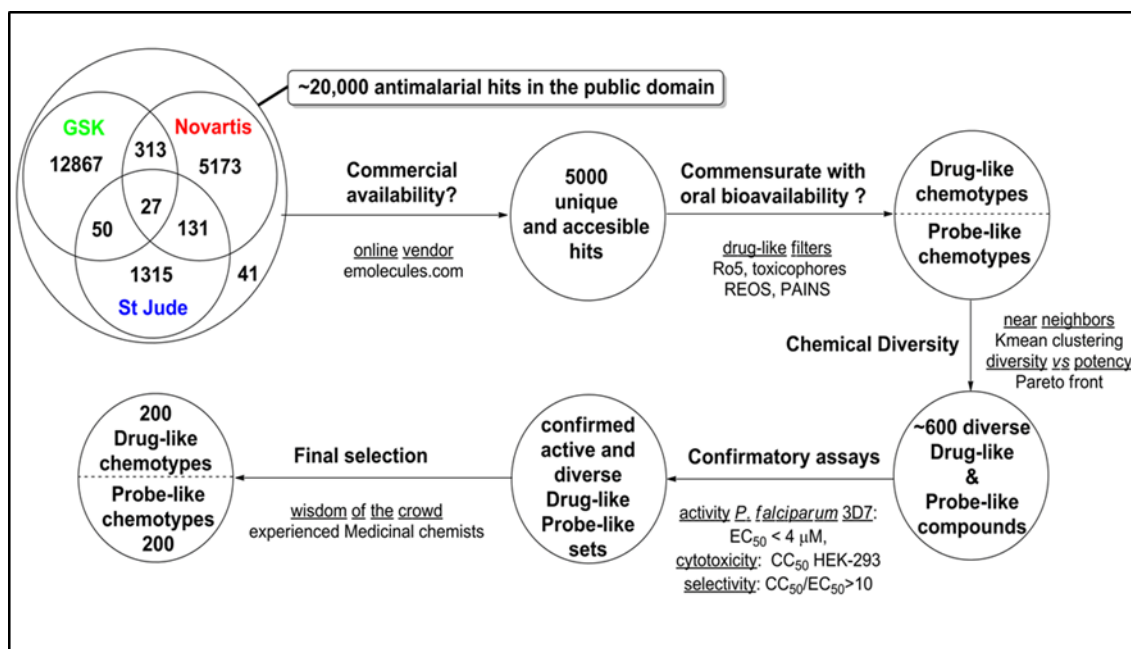


**Figure 4.2: The MMV selection process for the 400 Malaria Box compounds**  
(Source- Spangenberg *et al.*, 2013).

MMV provides this “Malaria Box” resource, containing 200 diverse drug-like compounds as a freely available resource of starting points for oral drug discovery and development with the 200 diverse probe-like compounds provided for use as biological tools in malaria research (Burrows *et al.*, 2012; Paiardini *et al.*, 2015; Spangenberg *et al.*, 2013). However, it is noted that some of the probe-like compounds might be compliant with the Lipinski's Rule of 5 and hence could serve as starting points for drug discovery programmes (Spangenberg *et al.*, 2013).

Given the importance of the MMV Malaria Box as a resource to the drug discovery community, and an interest of this study in exploring the potential for scaling up the application of bioluminescence rate of kill assay, here the use of this assay to identify

compounds in this resource that are most likely to meet the TCP1 criteria (rapid rate of action) is described. This study also explores the potential for scaling the bioluminescence rate of kill assay to enable initial screens of larger sets of compounds, for which only limited  $IC_{50}$  data is available, in an attempt to reconcile where this assay could fall in future hit and/or lead discovery programmes.

## 4.2 Results

### 4.2.1 Determination of the 50% inhibition concentration (IC<sub>50</sub>) using the Malaria Sybr Green I Fluorescence (MSF) assay

The application of a microplate-based bioluminescence assay to rapidly identify compounds that exert an immediate and rapid rate of-kill against Dd2<sup>luc</sup> was explored using the compounds set available in the MMV Malaria Box. For these 400 compounds the only IC<sub>50</sub> data available is that for genetically-distinct *P. falciparum* clone 3D7 ([www.mmv.org](http://www.mmv.org)). Using a 48hrs MSF assay (see section 2.3.5), IC<sub>50</sub> data were developed in the Dd2<sup>luc</sup> clone for 396 of these compounds; the remaining four compounds omitted as insufficient material was available. The IC<sub>50</sub> values were obtained from log dose-response curves, with example data shown in Figure 4.3. The full set of IC<sub>50</sub> data are reported in Table 4.1. These IC<sub>50</sub> data have been submitted to ChEMBL –Neglected Tropical Disease Open Access Repository.

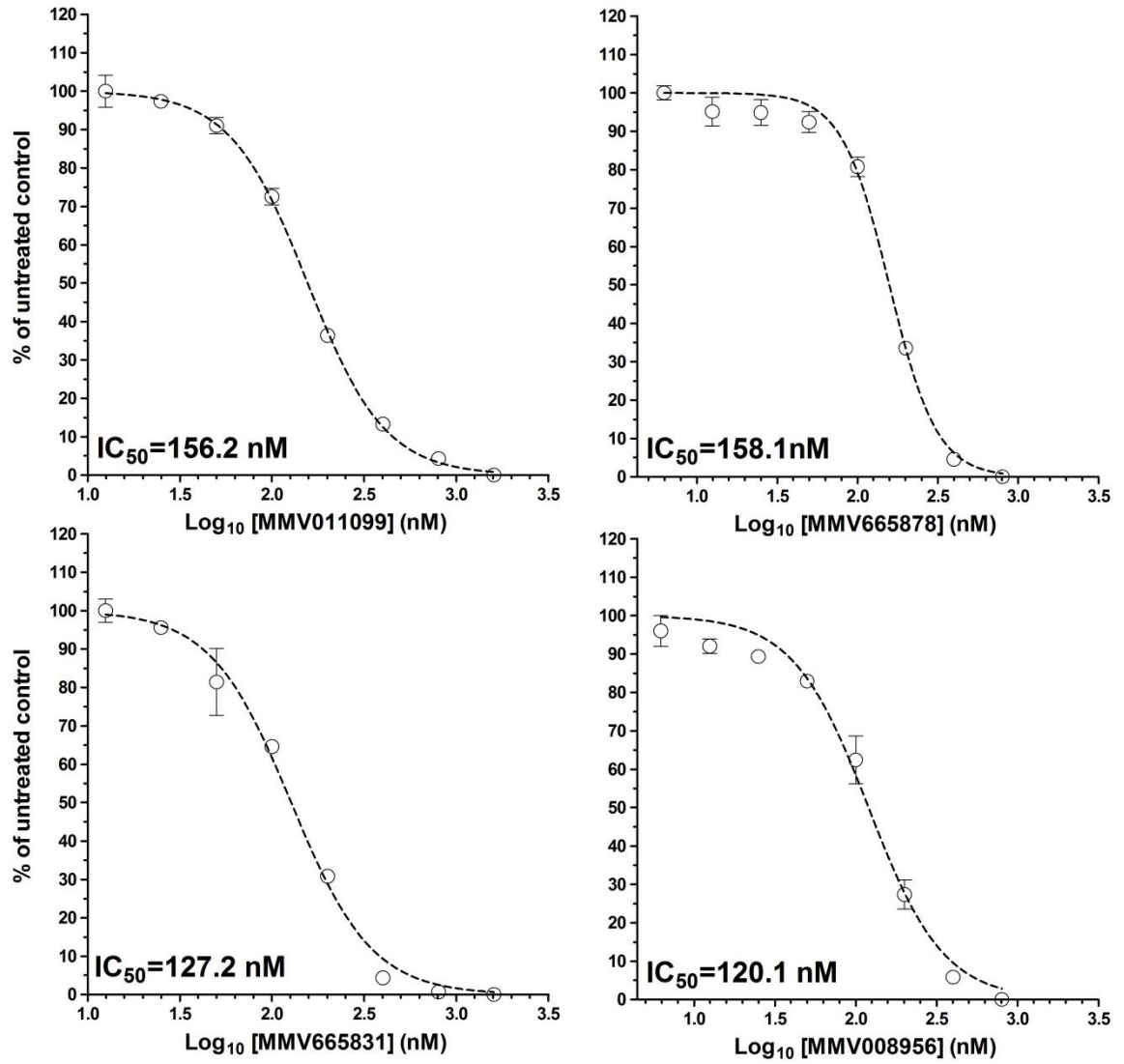


**Figure 4.3: Exemplars of log dose response curves for the Malaria Box compounds**  
 Log dose response curves show determination of IC<sub>50</sub> for the indicated Malaria Box compounds. Each data point represents the mean with standard deviation (from three biological repeats n=9) indicated by error bars.

COMPOUND_ID	IC <sub>50</sub> (nM)								
MMV019066	976.8	MMV665876	337.7	MMV665891	2001	MMV007617	1494	MMV018984	775.1
MMV665941	217.6	MMV666023	40.91	MMV665899	1189	MMV665796	1445	MMV000911	1207
MMV396680	327.7	MMV009063	277.9	MMV665961	424.8	MMV665906	2354	MMV007430	901.3
MMV666601	489.3	MMV006558	296.8	MMV665929	420.5	MMV665954	1694	MMV007977	1186
MMV008294	538.5	MMV007160	38.19	MMV666108	1026	MMV019738	1672	MMV020654	701.2
MMV011259	136.9	MMV006429	160	MMV665948	2992	MMV666075	1100	MMV665883	506.3
MMV019406	141.3	MMV396703	373	MMV006188	878.1	MMV666070	468	MMV084940	732.5
MMV006278	2769	MMV006937	1780	MMV001230	2701	MMV142383	4146	MMV396715	262.8
MMV666688	594.3	MMV085203	9.98	MMV665918	541.2	MMV000788	573.2	MMV000963	90.59
MMV019110	3500	MMV665820	958.5	MMV665799	810.5	MMV000561	1159	MMV006319	543.8
MMV006427	298.3	MMV665841	2573	MMV665826	1266	MMV000248	403.8	MMV000972	1027
MMV666062	397.1	MMV007116	646.9	MMV665807	1088	MMV665879	752.8	MMV020490	1225
MMV020885	366.5	MMV007384	715.3	MMV665946	1240	MMV665890	903.8	MMV001318	3587
MMV000570	316.1	MMV020548	664.9	MMV665935	3991	MMV666116	646.7	MMV007978	2719
MMV020439	468.1	MMV019258	351.4	MMV666102	1239	MMV006913	1484	MMV020660	1328
MMV396672	466.7	MMV007686	7278	MMV666061	501.8	MMV008127	1487	MMV665904	929.8
MMV019871	334.7	MMV011256	302.4	MMV008149	82.67	MMV403679	993.8	MMV396632	1301
MMV085583	179.4	MMV666693	426.4	MMV019074	1854	MMV006545	870.5	MMV007875	1181
MMV008416	825.3	MMV008956	120.1	MMV665914	913	MMV019700	559.2	MMV006820	1413
MMV665874	1241	MMV665827	276.3	MMV665798	885.1	MMV019670	741.8	MMV396749	239.4
MMV006203	308.9	MMV001038	986.6	MMV665902	1106	MMV001344	1883	MMV011576	512
MMV665977	447.6	MMV007839	369.5	MMV665888	201.7	MMV011795	959.3	MMV020651	1739
MMV020549	242.1	MMV000662	1258	MMV666067	1188	MMV019124	521	MMV000483	653.5
MMV001246	1798	MMV396678	1451	MMV665939	1045	MMV006767	883.6	MMV019266	844.4
MMV666607	241.6	MMV006861	586.7	MMV009060	513.9	MMV007808	365.1	MMV001049	1076
MMV665915	514.6	MMV006457	719.8	MMV666110	1462	MMV019017	651.8	MMV665806	483.5
MMV007695	244.4	MMV396693	606.9	MMV019758	614.1	MMV396681	2181	MMV667487	158.3

COMPOUND_ID	IC <sub>50</sub> (nM)								
MMV000448	236.8	MMV007907	479.1	MMV000498	2772	MMV006587	617.4	MMV000356	1287
MMV020500	437	MMV665805	153.8	MMV665913	1439	MMV019202	1207	MMV396705	1154
MMV665878	158.1	MMV666021	1259	MMV665789	498.3	MMV000848	452.7	MMV006704	3653
MMV666101	190.3	MMV665800	827.8	MMV665901	957.5	MMV020275	1480	MMV000760	1345
MMV666596	184.2	MMV000634	558.9	MMV666069	2678	MMV019918	596	MMV007881	1155
MMV396679	2300	MMV666103	902.8	MMV666080	426.3	MMV075490	904.2	MMV008212	941.4
MMV396797	304.7	MMV666057	866.2	MMV666081	636.8	MMV396633	1908	MMV007363	1286
MMV665916	517.6	MMV007564	825.6	MMV666009	1146	MMV007374	691.2	MMV007791	2900
MMV020788	283.1	MMV001255	3679	MMV019313	366.4	MMV396719	1406	MMV665843	876
MMV666691	603.9	MMV665917	1039	MMV019746	1299	MMV396744	680.3	MMV396595	1225
MMV665785	180.6	MMV000563	723	MMV019064	1913	MMV006706	915.5	MMV396669	1262
MMV665831	127.2	MMV665850	1001	MMV011944	885.4	MMV009108	932.9	MMV396704	1181
MMV011099	156.2	MMV665817	1756	MMV665803	649.4	MMV020700	794.2	MMV019762	831.5
MMV000642	46.27	MMV665979	490.3	MMV665857	1362	MMV007906	783	MMV020505	1163
MMV666600	613.7	MMV665928	550.6	MMV666071	459	MMV008270	1556	MMV020942	704.5
MMV006172	1596	MMV666105	975.4	MMV019780	1281	MMV019127	603.2	MMV000839	1096
MMV006309	32.51	MMV666072	754.3	MMV666093	518.3	MMV396794	493.5	MMV666599	5930
MMV006087	44.01	MMV000653	1220	MMV665953	1828	MMV396736	733.6	MMV000481	1607
MMV020492	104.2	MMV000620	314.4	MMV000648	1143	MMV306025	691.1	MMV665897	1871
MMV006455	209	MMV665909	1613	MMV019662	569.1	MMV056726	3947	MMV665908	2495
MMV665782	418	MMV665940	739.8	MMV007571	549.9	MMV274073	1099	MMV665924	3291
MMV011438	540.4	MMV020243	972.9	MMV011895	315.1	MMV001041	418.7	MMV665840	1244
MMV665894	1973	MMV396770	1301	MMV665812	1866	MMV009015	1093	MMV666597	5723
MMV665944	1135	MMV006513	200	MMV665881	1228	MMV000720	962.8	MMV007224	1511
MMV666054	511.9	MMV666095	1218	MMV665875	196.7	MMV000619	3573	MMV020912	1700
MMV008474	3337	MMV665943	1818	MMV007020	997.7	MMV006753	606.7	MMV007181	296.5
MMV000445	1805	MMV019555	545.3	MMV006656	458.1	MMV006787	906.6	MMV007113	638

COMPOUND_ID	IC <sub>50</sub> (nM)								
MMV006882	1183	MMV019741	1156	MMV396726	803.4	MMV665794	739.1	MMV007228	1695
MMV007127	818.2	MMV019690	1207	MMV006522	791.3	MMV000917	1693	MMV665972	4212
MMV666123	7329	MMV000621	3419	MMV666686	4022	MMV666125	129.4	MMV073843	345.3
MMV006389	766.4	MMV008173	5018	MMV007474	691.5	MMV665987	567.5	MMV006303	464.9
MMV665949	1906	MMV019241	659.3	MMV006962	863.9	MMV007574	1145	MMV667490	1227
MMV665934	874.2	MMV665783	60.75	MMV665813	4887	MMV000326	1393	MMV667492	268.3
MMV665994	601.4	MMV000787	961	MMV080034	2366	MMV000604	850.7	MMV019881	263.8
MMV665980	127.1	MMV666106	883.4	MMV019199	3108	MMV007557	1329	MMV000478	1699
MMV007577	1473	MMV666022	977.9	MMV396652	956.4	MMV000699	935.7	MMV020403	4912
MMV019995	965	MMV498479	1312	MMV000704	769.1	MMV009127	499.3	MMV007764	1288
MMV007208	2978	MMV007396	808.3	MMV396635	5173	MMV665786	542.8	MMV665830	475.6
MMV000442	195.6	MMV000617	3553	MMV000986	1412	MMV006250	684	MMV665886	1095
MMV666124	1692	MMV006764	789.1	MMV008160	891.8	MMV666079	1445	MMV396664	217.8
MMV000444	2346	MMV007275	558	MMV000753	683.1	MMV665969	939.5	MMV667491	443.2
MMV666109	2199	MMV007273	734.5	MMV011436	1989	MMV000304	1668	MMV006169	897.4
MMV665936	5069	MMV666026	730.7	MMV665882	436.4	MMV000443	617.2	MMV086103	846.4
MMV666020	2479	MMV665923	241.5	MMV665809	1523	MMV666604	1521	MMV084434	993.6
MMV665971	527	MMV666025	2028	MMV665810	332.2	MMV008455	2340	MMV666692	255.6
MMV001241	9328	MMV666060	635.4	MMV665927	806	MMV007199	808.9	MMV665836	311.5
MMV667486	8132	MMV396665	1037	MMV396663	1335	MMV085471	1153	MMV008829	1637
MMV667488	271.7	MMV396723	1541	MMV007041	751.4	MMV665797	2157	MMV666689	1533
MMV006825	311.4	MMV007654	1049	MMV000340	3938	MMV667489	1215	MMV645672	289.7
MMV009085	891.6	MMV011832	629.4	MMV666687	3945	MMV011522	1105	MMV007285	768.3
MMV007591	1598	MMV020750	1544	MMV396594	1467	MMV665898	1671	MMV396717	3188
MMV128432	1867	MMV007092	948.3	MMV665852	3876	MMV665864	892.6	MMV638723	221
MMV665814	1070								

**Table 4.1: Reports IC<sub>50</sub> data of the 396 Malaria Box compounds obtained using host strain Dd2<sup>luc</sup>.**  
*These data have been reported back to MMV and provided to the ChEMBL database.*

#### **4.2.2 Screening the Malaria Box for compounds that exert an immediate rapid rate of kill using a single-dose/single timepoint triage assay**

Data shown in chapter 3 indicates that compounds that exert a slow rate of kill report little or no change in the bioluminescence signal over the 6hr window used in this assay. To identify, and exclude, these apparently slow-acting compounds, 370 compounds from the MMV Malaria Box were subjected to an initial single-dose/single-time point triage assay utilizing a  $9 \times IC_{50}$  concentration of drug for 6hrs, with normalised bioluminescence signal then plotted against the corresponding  $IC_{50}$  (Figure 4.4). A total of 30 compounds were omitted from this screen as insufficient material was available from the MMV Malaria Box for this and subsequent experiments as the  $IC_{50}$  of these compounds were very high (i.e.  $>2500nM$ ). To prioritise the rapid rate of kill compounds to take them forward for a full analysis, a threshold of 70% of the normalised bioluminescence signal was used (i.e. compounds that exert an apparent  $>30\%$  loss in viability in 6hrs). This threshold was selected because it reflects the midway response between quinolones and atovaquone and provided an exclusion criterion for approximately half of the available compounds.

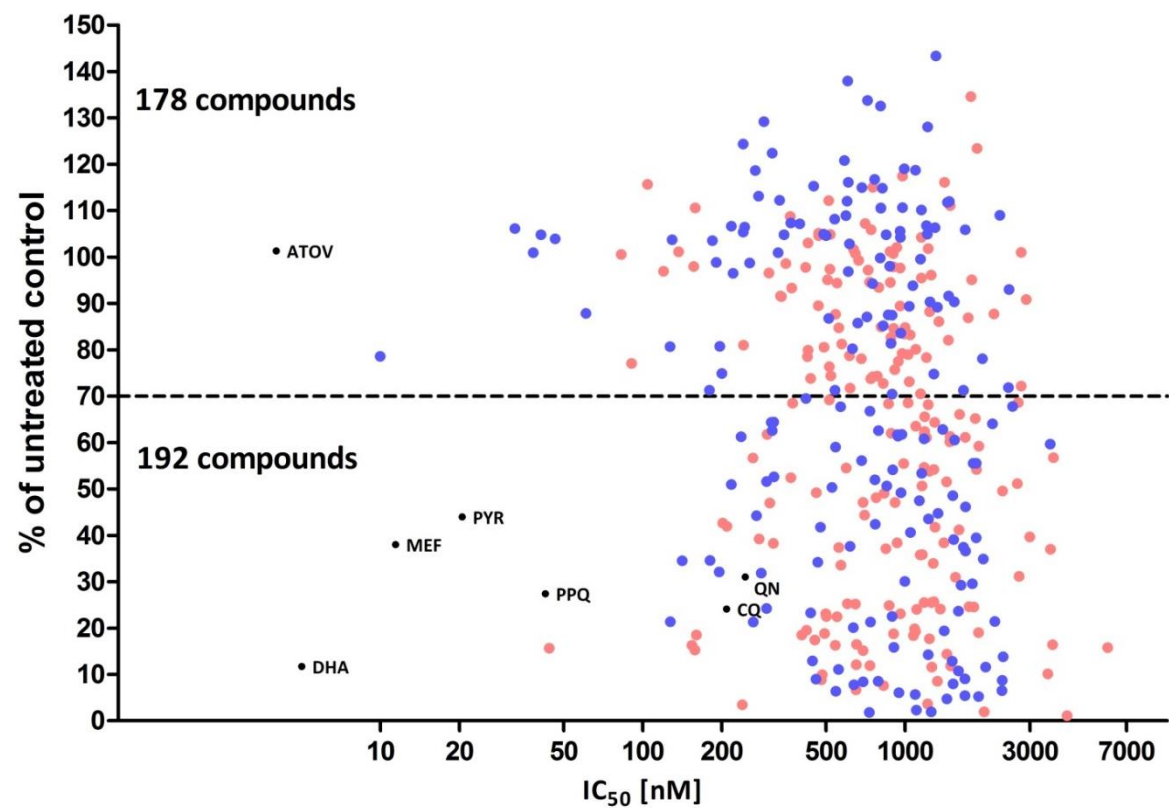


**Figure 4.4: Initial rate of kill against the IC<sub>50</sub> potency for the Malaria Box compounds**

Scatterplot indicating the initial rate of kill data (9XIC<sub>50</sub> concentration of drug for 6hrs) against the IC<sub>50</sub> potency for 370 compounds in the Malaria Box. The threshold line (70% of untreated control) is indicated using a dotted line. The filled black circles represent known antimalarial drugs, pink and blue circles shows drug-like and probe-like compounds, respectively. Each data point represents mean from three biological repeats (n=9).

As expected, based on a similar observation by Sanz *et al.* (2012), there is no apparent correlation ( $r^2=0.041$ ) between these initial estimates of rate of kill using the single time/dose triage assay and the  $IC_{50}$  of these compounds. Based on this single triage assay, 31 compounds in the MMV Malaria Box would appear to initially meet the ideal target of a rate of kill at least as fast as artemisinins (i.e. data points falls below DHA on y-axis). Of note, however, is the limited potency of these compounds, with a mean  $IC_{50}$  of 1340nM (range 239-4156) with only four compounds with an  $IC_{50}$  of less than 500nM.

#### **4.2.3 Exploring the fast acting compounds**

To fully explore the relative rate of kill of these 192 faster acting compounds, bioluminescence assays were carried out at 3 and 6hrs, using a three-fold serial dilution of compounds between 9 to  $0.33 \times IC_{50}$ . This range was selected to monitor the range of rates of kill without the saturation effects observed at higher concentrations as previously described in Chapter 3 (Section 3.2.3). An additional 25 compounds from above this threshold (i.e. exerted less than a 30% reduction in bioluminescence signal in the triage assay) were included in the full analysis with the aim of confirming their apparent slow rate of kill in the full bioluminescence rate of kill assay. Log dose-normalised bioluminescence signal plots for all 217 MMV Malaria Box compounds, as well as 7 antimalarial drugs, to act as benchmarks were determined. Representative data are shown in Figure 4.5, with the full dataset provided at the end of this thesis in appendix 1.

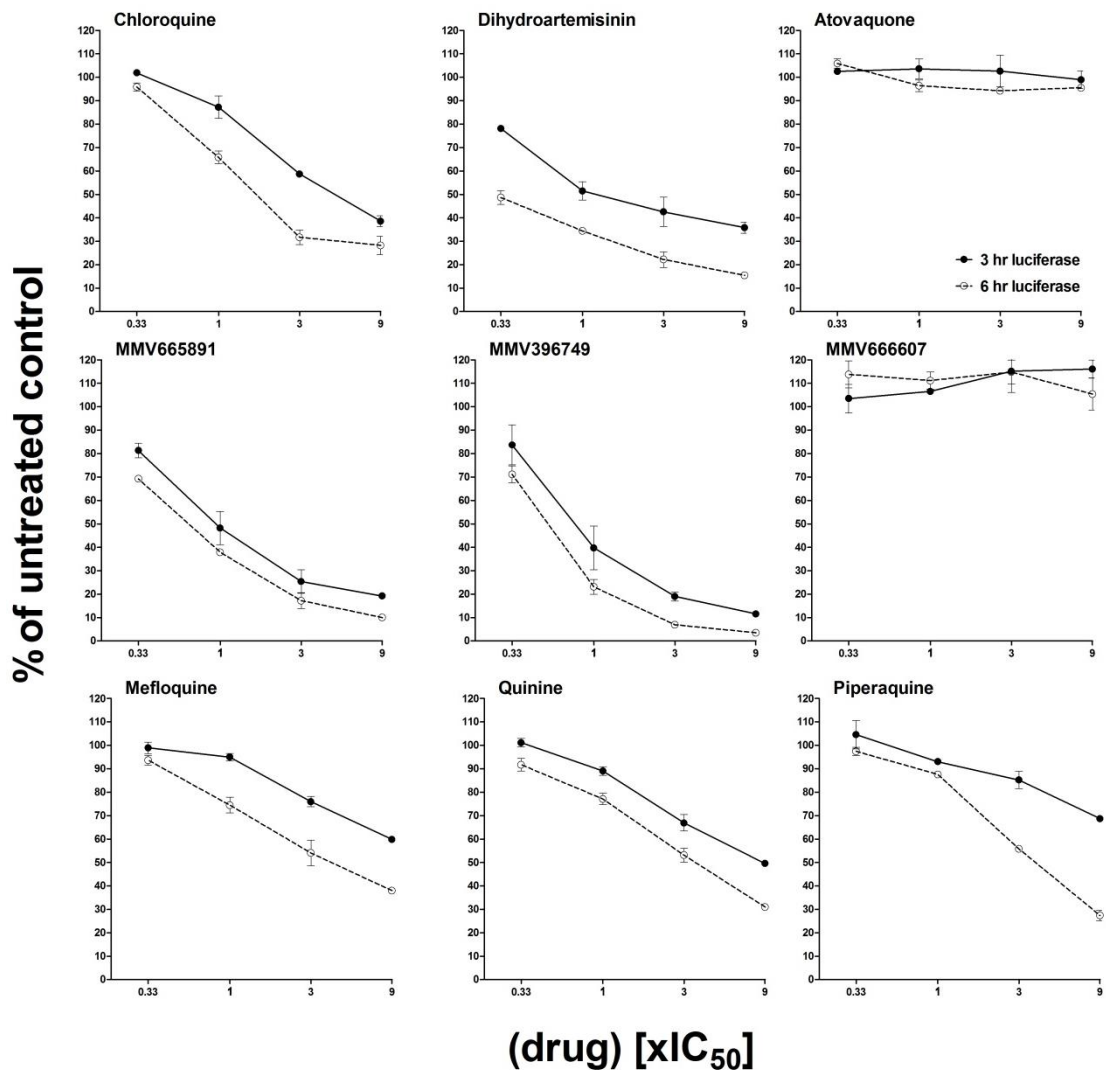


**Figure 4.5: Exemplars of estimated fast and slow RoK**  
 Exemplars of estimated “fast RoK” (MMV665891 and MMV396749) and “slow RoK” (MMV666607). MMV Malaria Box candidates against a set of benchmark controls (chloroquine, dihydroartemisinin, atovaquone, mefloquine, quinine and piperaquine) are shown. Note – the full dataset developed for 217 MMV Malaria Box compounds is provided in Appendix 1.

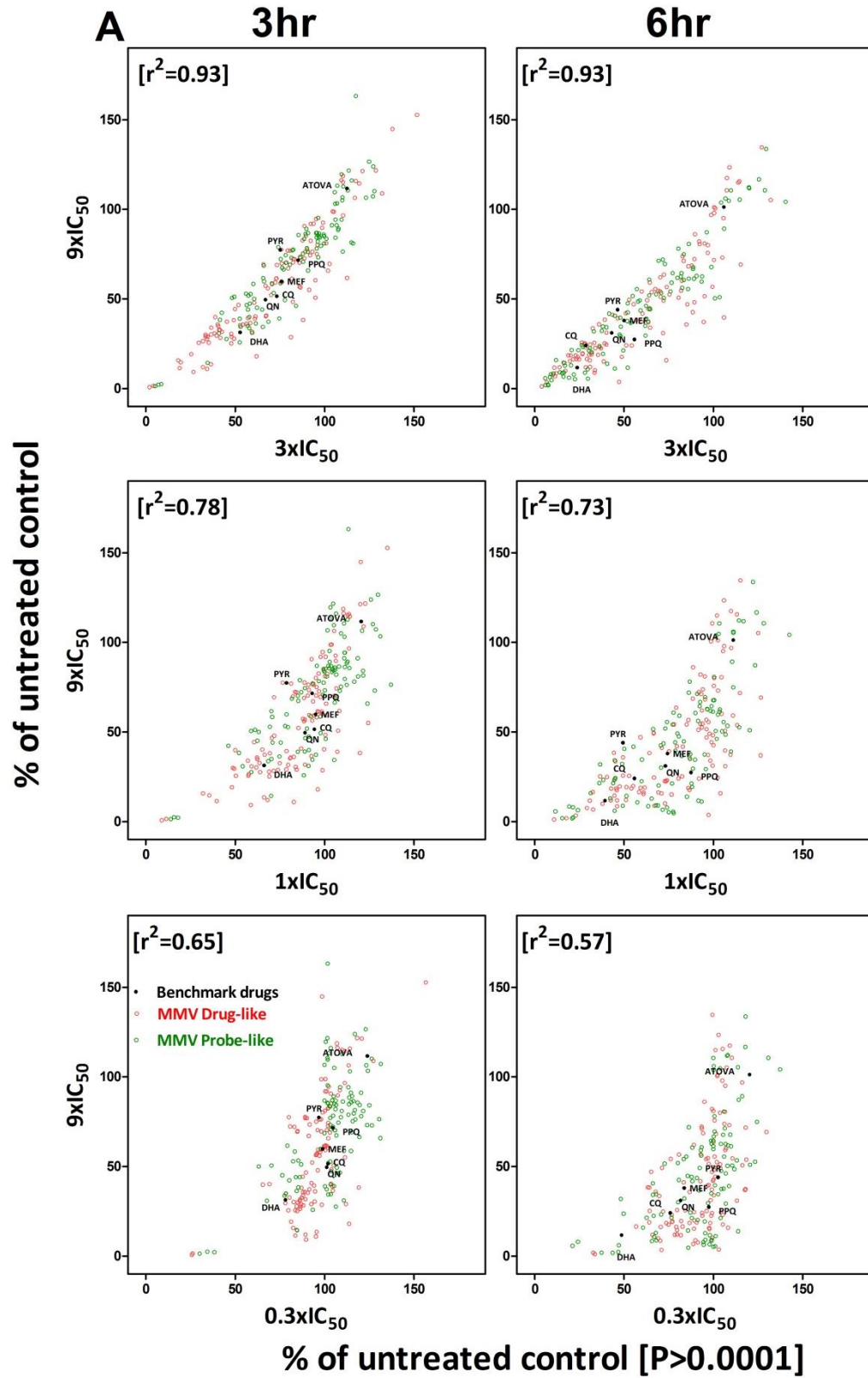
As expected, the selected fast acting Malaria Box compounds (below the 70% threshold) showed a time and dose-dependent loss of bioluminescence signal when exposed to the compound (e.g. MMV665891 and MMV396749). By contrast, all the 25 compounds predicted to have an initial slow rate of kill were confirmed as such in this more complete

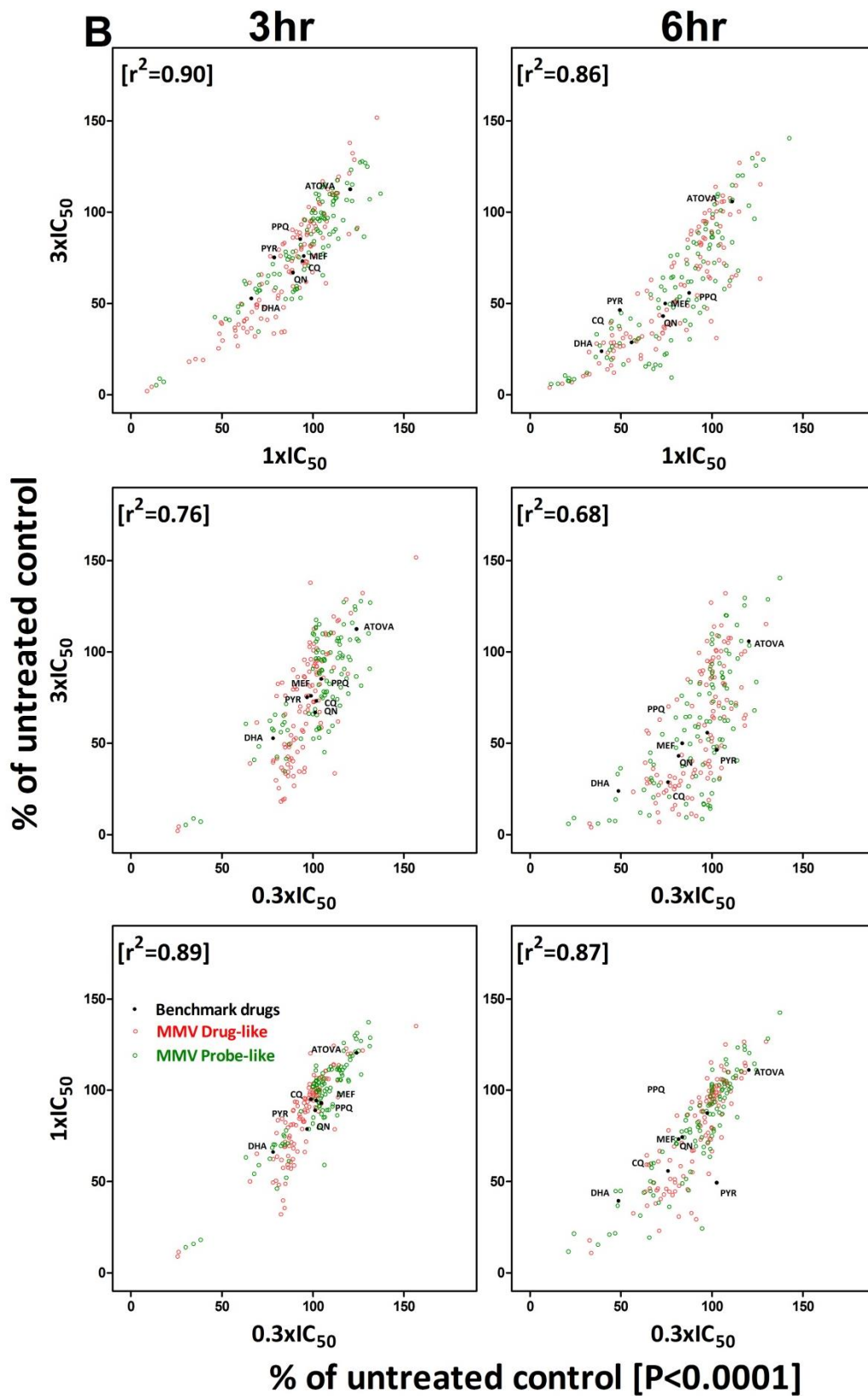
analysis, with the normalised bioluminescence signal above 70% at both time points at all drug doses (e.g. MMV666607 in Figure 4.5 and a completed list provided in appendix 1).

With data available for four concentrations at two timepoints for 217 compounds, a more meaningful analysis of the correlation between time and dose-dependent effects in this assay could be explored. Initially, correlations between bioluminescent signals following exposure to different doses of drugs were explored (Figure 4.6A and B); separating the data by their timepoint e.g. data developed for each concentration at 3hrs was compared against each other. Interestingly, whilst all correlations were highly significant ( $P < 0.001$ ), a clear pattern regarding the strength of each correlation emerged. Correlations were strongest when datasets for each concentration were compared to those closest to them, e.g. the  $3 \times IC_{50}$  at both 3hr and 6hr correlates well with  $9 \times IC_{50}$  and  $1 \times IC_{50}$  than at  $0.33 \times IC_{50}$ . This is perhaps not unexpected given the previous observations regarding the dose-dependent effect of the benchmark antimalarial drugs (except atovaquone) in this assay (See chapter 3, Figure 3.9).

Correlation of bioluminescent signals following exposure to the same concentration of drug at the two different endpoints (3 and 6hr), show a strong ( $r^2$  between 0.82-0.83) and significant (all  $P < 0.001$ ) correlation between 3 and 6hr endpoints at  $9 \times IC_{50}$ ,  $3 \times IC_{50}$  and  $1 \times IC_{50}$  concentrations (Figure 4.6C). At  $0.33 \times IC_{50}$  this correlation is weaker, with an  $r^2$  of 0.6, with the data clearly clustering together. This would suggest that at this low concentration of drug only minimal changes in the bioluminescence signal are achieved over the time of the assay. Inclusion of this dose, however, does reveal that very fast acting compounds (i.e. show a loss in bioluminescent signal greater than that for dihydroartemisinin) can be discriminated using this dose over the 3hr and 6hr used in this

assay (see datapoints distributed below and to left of dihydroartemisinin in Figure 4.6C  
0.33xIC<sub>50</sub> graph).





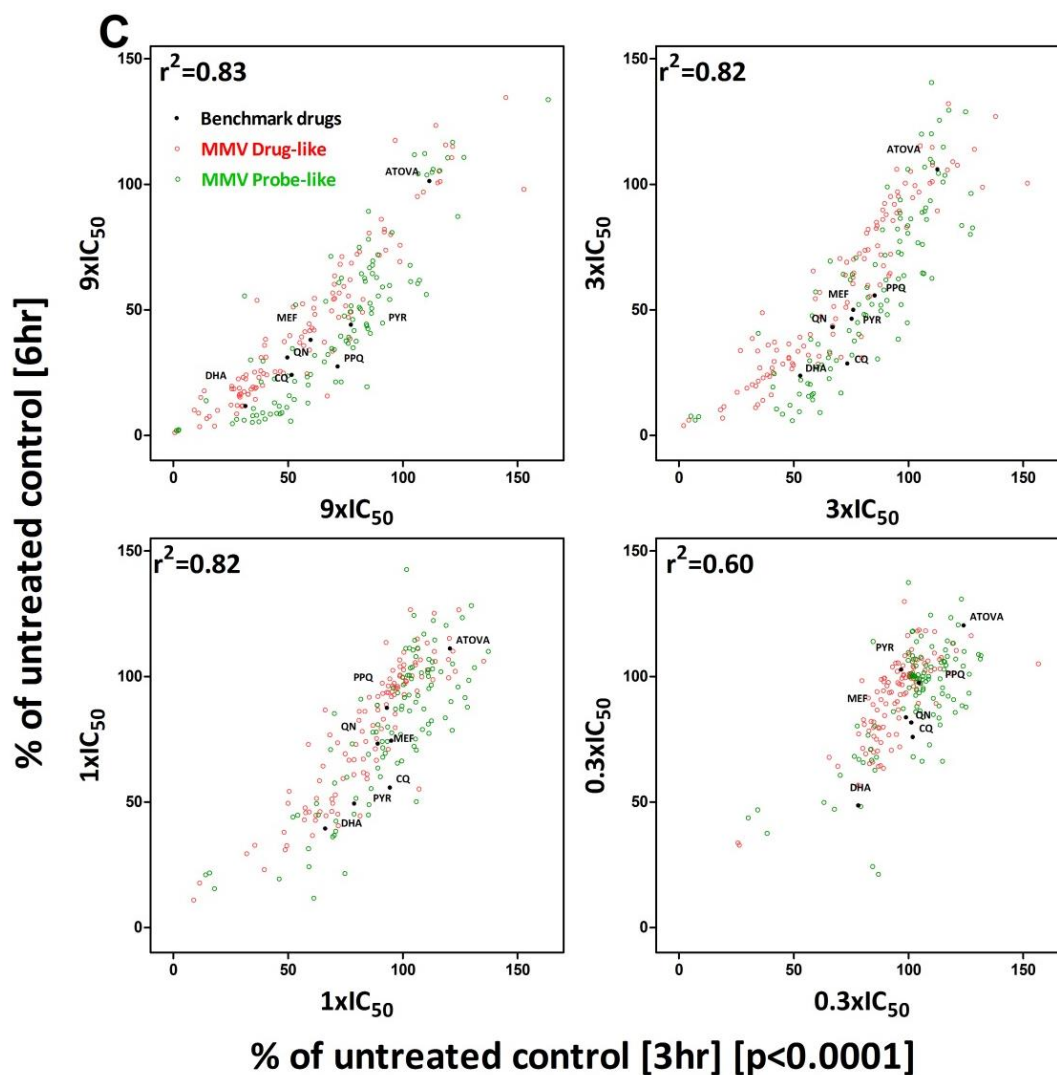


**Figure 4.6: Correlation between time and dose dependent effects in the BRoK assay**  
 (A-B) Illustrates correlation between  $9x IC_{50}$ ,  $3x IC_{50}$ ,  $1x IC_{50}$  and  $0.3x IC_{50}$  at 3 and 6hrs respectively. (C) Comparisons of each concentration across 3 and 6hr endpoints. The filled black circles represent known antimalarial drugs, red and green open circles shows drug-like and probe-like compounds respectively. Note all correlations are significant i.e.  $p < 0.0001$ .

Together, these analyses support data presented in chapter 3 regarding the time and dose dependent loss of bioluminescence signal for compounds that affect a kill within 6hr of exposure to these trophozoite stage parasites. This assay appears to provide a rapid means to identify and rank fast acting compounds from the Malaria Box. However, to enable a simpler means to utilise the bioluminescence data derived at these different

doses and timepoints, a single value is needed that is representative of all four concentrations used at each timepoint would be preferred. To achieve this, a Principle Component Analysis (PCA) was carried out in collaboration with Dr Raman Sharma of the Liverpool School of Tropical Medicine (LSTM).

#### **4.2.4 Principle Component Analysis (PCA) of bioluminescence rate of kill assay data**

**Note:** All the PCA analyses shown in this work were conducted by Raman Sharma (LSTM), using data prepared and formatted by me. Subsequent analyses were done by me and Dr Sharma with all data presentation done by me.

To capture the concentration rate relationship in a single parameter, the dose/time/drug data was collected in a standard format and sent over to Prof. Biagini's team with Raman Sharma conducting the PCA analysis. PCA transforms the original variable set into a new variable set of principle component's that are totally uncorrelated to each other (Figure 4.7). Principle components (PCs) are ordered by how much variability in the data they explain, with the first few PCs usually explaining the majority of the variance in all the variables. PCA is used to reduce dimensionality in the data set and also analyze the relationship between the variables. PCA was performed on the 0.3x, 1x, 3x and 9x IC<sub>50</sub> variables for the 3 and 6hrs bioluminescence assay endpoints using a KNIME analytics platform to reduce the dimensionality of these data sets (Michael *et al.*, 2007), allowing the concentration rate relationship to be captured in one parameter.

As suggested above, the first principle components should represent the majority of the variance in the data set, with the last representing the least. Table 4.2 reports the proportion of variance in each of the four principle components for PCA carried out on the 3hr and 6hr datasets, along with their cumulative sum of variance. Importantly here,

PC1 reports the vast majority of the variance in the bioluminescence rate of kill assays. PC1 explains 89% of the variance at 3hr end point and has roughly equal positive contributions from 9x and 3xIC<sub>50</sub> outputs ( $PC1 = 0.61(9X IC_{50}) + 0.58(3X IC_{50}) + 0.45(1X IC_{50}) + 0.29(0.3X IC_{50})$ ). Similarly, PC1 explains 86% of the variance at 6hr end point and has large positive contributions from 9X and 3X IC<sub>50</sub> outputs ( $PC1 = 0.56 (9X IC_{50}) + 0.61 (3X IC_{50}) + 0.48 (1X IC_{50}) + 0.29 (0.3X IC_{50})$ ) (Table 4.2).

PC1 determined for each of the 217 Malaria Box compounds and seven benchmark antimalarial drugs were plotted against each equipotent dose (9 to 0.33xIC<sub>50</sub> at 6 hrs) (Figure 4.8). Interestingly, whilst all the correlations were highly significant ( $P > 0.0001$ ), a clear pattern regarding the strength of each concentration emerged. As expected, the correlation was strong at 3XIC<sub>50</sub> doses ( $r^2 = 0.91$ ), 9XIC<sub>50</sub> ( $r^2 = 0.82$ ) and 1XIC<sub>50</sub> ( $r^2 = 0.78$ ) and relatively less correlated at 0.33XIC<sub>50</sub> ( $r^2 = 0.53$ ). Note that PC1 plotted against 9XIC<sub>50</sub> illustrated a relatively lower correlation than that of 3XIC<sub>50</sub> because of the saturation effect of very rapid acting drugs at this concentration – the data clusters at bottom of the plot (9xIC<sub>50</sub>) stretching the regression line towards right and thus affecting slope of the curve. Based on my experience, the most useful information regarding the activity of drugs in a single-dose/time point triage assay could be obtained using 9XIC<sub>50</sub> concentration.

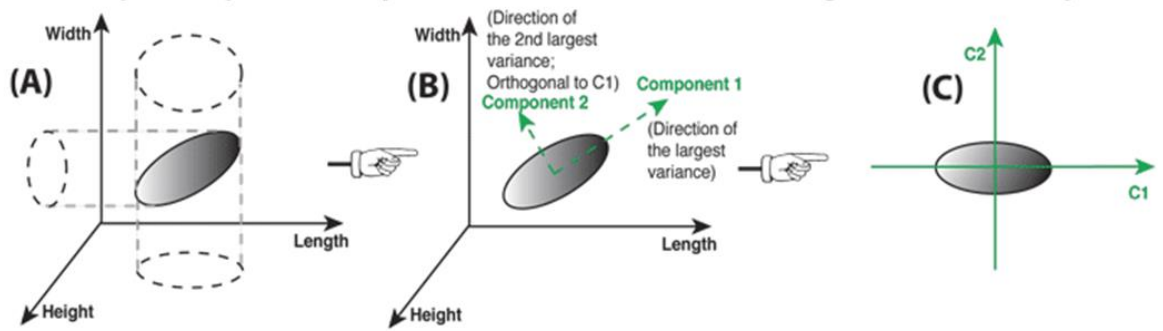


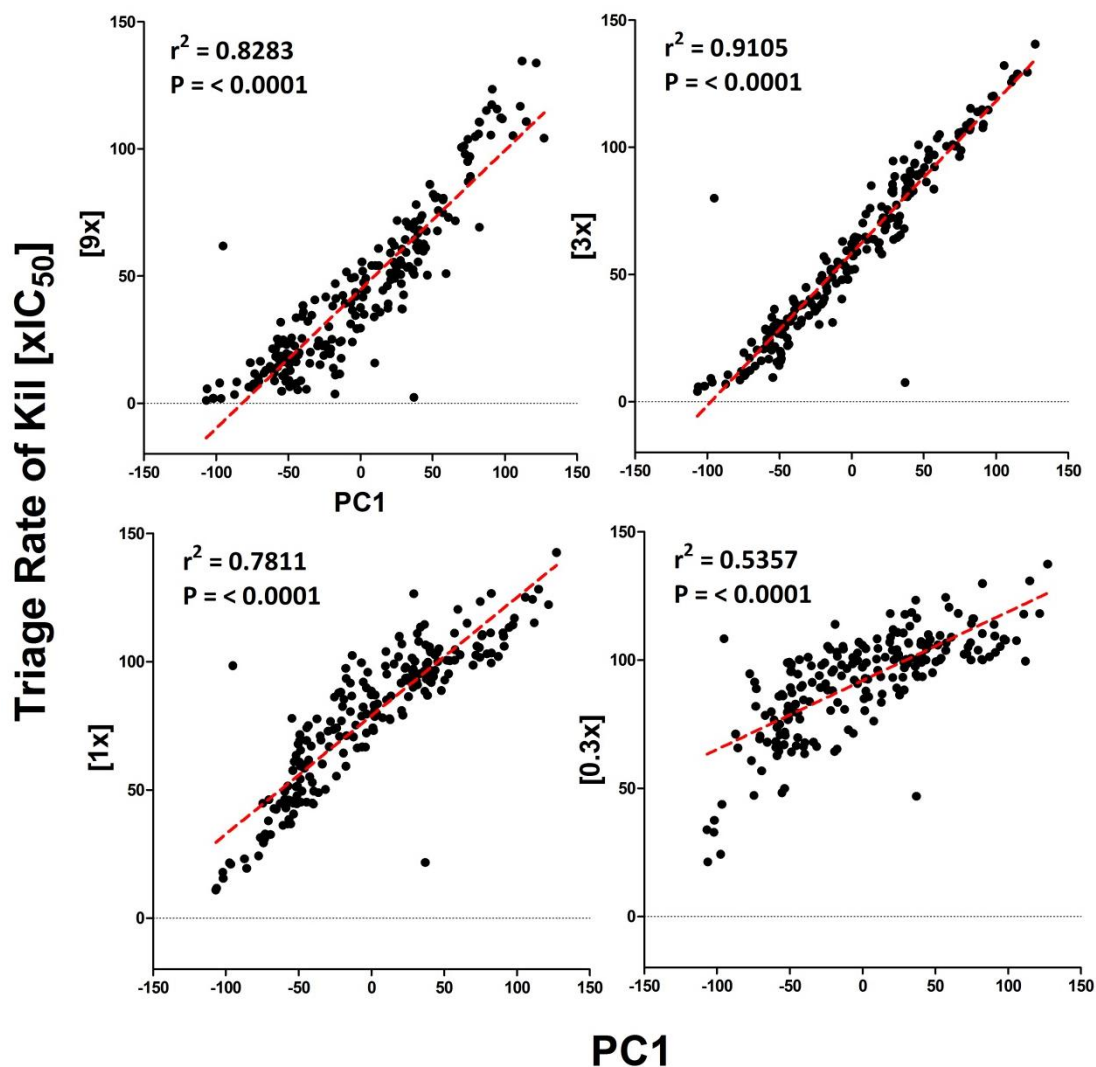
**Figure 4.7: Principle component Analysis**

(A) Data in three dimensions is distributed within the grey oval-with dotted lines representing their distribution in the three dimensions. (B) The greatest variance within the grey oval is reported as PC1 (comprising of components from all three of the original dimensions). (C) Representing the grey box on the new PC1 (C1) axis, the second principle component (PC2) is at orthogonal to PC1 and again comprises of components of these original dimensions. This is repeated to describe all the principle components, with each iteration reporting less of the variance in the dataset.

	Variance Explained	Cumulative Variance Explained
<b>3-HOURS</b>		
PC1	0.89	0.89
PC2	0.08	0.97
PC3	0.02	0.99
PC4	0.01	1.00
<b>6-HOURS</b>		
PC1	0.86	0.86
PC2	0.11	0.97
PC3	0.02	0.99
PC4	0.01	1.00

**Table 4.2: PCA on the estimates of rate of kill data**

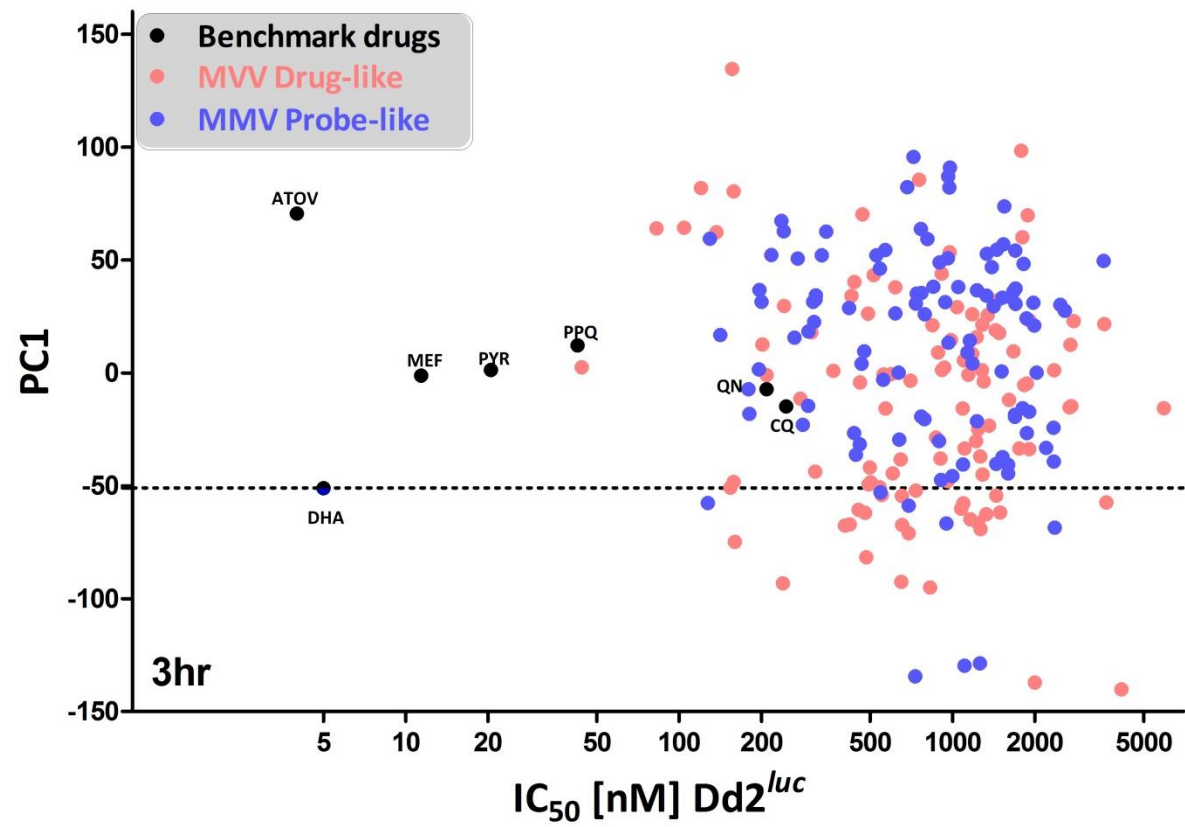
This table reports PCA on the estimates of rate of kill data at 3 and 6hr time points respectively (Source-Raman Sharma, LSTM).



**Figure 4.8: Comparison between PC1 and loss of bioluminescent signal in the BRoK assay**  
 Linear regression plots between the PC1 determined for each of the 217 Malaria Box compounds and seven benchmark antimalarial drugs and each equipotent dose (9 to 0.33xIC<sub>50</sub> at 6 hrs). The red line shows a linear regression curve.

To represent this data graphically, the PC1 determined for each of the 217 Malaria Box compounds and seven benchmark antimalarial drugs were zero meaned and plotted against their IC<sub>50</sub> for the 3hr and 6hr assays (Figure 4.9). This analysis provides a novel and simple means to explore the correlation between the IC<sub>50</sub> potency and initial rate of kill of

the MMV Malaria Box compounds tested here against a series of known antimalarial drug benchmarks. Potent, low  $IC_{50}$ , compounds with an initial rapid rate of kill are exemplified by artemisinins (i.e. DHA) and occupy the bottom left quadrant of this plot. Atovaquone, whilst potent in terms of its  $IC_{50}$ , is slow acting drug and occupies the upper left hand quadrant. This analysis quickly reveals that whilst the 224 Malaria Box compounds display a full range of initial rate of kill relative to the benchmarks shown, these compounds are, at best, lead development targets ( $IC_{50}$  potency is below that expected of an antimalarial drug). It would therefore not be expected to see a distribution of data towards the more potent  $IC_{50}$ s as reported here for the benchmark antimalarial drugs used. That said, using the PC1 value for DHA as the upper limit, 33 and 17 compounds tested demonstrated an initial rate of kill greater than that of DHA following PC1 in the 3hr and 6hr datasets, respectively. There is a considerable overlap between these two groups, with 14 of the 17 compounds identified at 6hr shared with the 3hr group (the remaining 3 sit just above the PC1 cut-off for DHA). As predicted, there is no correlation between rate of kill, expressed here as PC1, and  $IC_{50}$  at either time points (all  $R^2 < 0.01$ ).



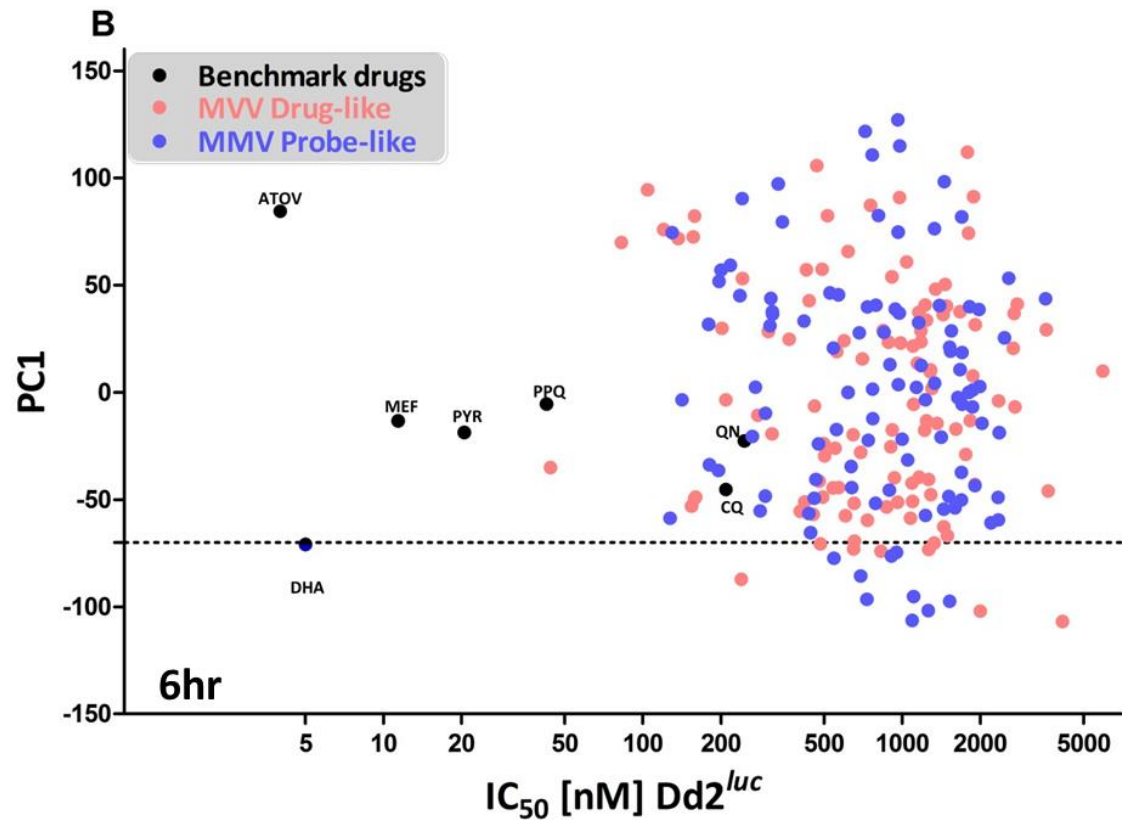


**Figure 4.9: Exploring RoK (PC1) against the IC<sub>50</sub> potency of the MMV Malaria Box compounds**

Graphical representation of the (A) 3hr and (B) 6hr PC1 (RoK) data compared to the IC<sub>50</sub> potency of the 224 MMV Malaria Box compounds tested in the bioluminescence rate of kill assay. The filled black circles represent known antimalarial drugs, pink and blue circles shows drug-like and probe-like compounds, respectively. Cutoffs (dotted line) based on PC1 of DHA at (A) 3hr and (B) 6hr respectively. Each data point represents mean from three biological repeats of three technical replicates (n=9).

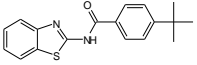
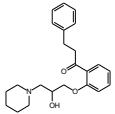
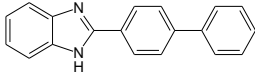
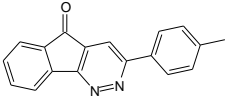
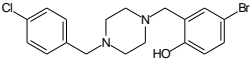
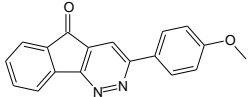
At 6hr using the PC1 values, the 36 and 17 compounds met the minimum essential (RoK > CQ) and ideal (RoK >DHA) criteria respectively for TCP1 candidates are reported below in Table 4.3, with the full dataset provided at the end of this thesis in appendix 2.

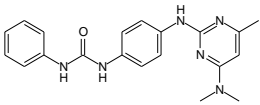
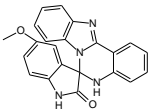
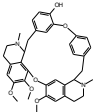
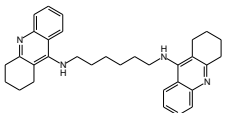
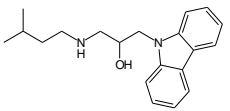
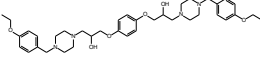
TCP1 candidates					
PC1 > -70 > DHA - PC1= > -45 > CQ (> DHA)					
MMV_ID	PC1 (6hr)	MMV_ID	PC1 (6hr)	MMV_ID	PC1 (6hr)
MMV142383	-106.9	MMV007617	-66.8	MMV665805	-53.0
MMV009015	-106.3	MMV667491	-65.4	MMV006764	-51.8
MMV665891	-102.1	MMV665796	-62.6	MMV019017	-51.7
MMV666021	-101.8	MMV666109	-60.8	MMV011795	-51.2
MMV665809	-97.5	MMV396736	-59.6	MMV665929	-51.1
MMV666026	-96.6	MMV000444	-59.5	MMV000839	-50.9
MMV020243	-95.2	MMV665831	-58.8	MMV000917	-50.2
MMV396749	-87.2	MMV001049	-58.8	MMV665878	-49.5
MMV007474	-85.6	MMV019127	-57.5	MMV006656	-49.3
MMV019555	-77.4	MMV667490	-57.4	MMV008455	-49.0
MMV006787	-76.2	MMV000848	-56.8	MMV006429	-48.8
MMV007092	-74.7	MMV665882	-56.5	MMV396794	-48.8
MMV665800	-74.1	MMV000248	-55.4	MMV007224	-48.5
MMV665826	-73.3	MMV020788	-55.3	MMV007181	-48.4
MMV665803	-73.0	MMV666079	-54.5	MMV000356	-47.7
MMV665806	-70.7	MMV007591	-53.9	MMV006704	-46.0
MMV020660	-70.3	MMV006172	-53.6	MMV665864	-45.6
MMV000483	-69.3	MMV006545	-53.4		

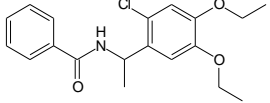
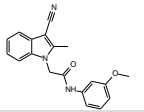
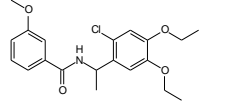
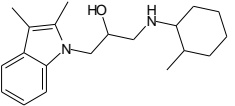
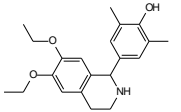
**Table 4.3: TCP1 candidates in the MMV Malaria Box**

This list reports the 53 TCP1 candidates identified with an initial rate of kill as good as, or better, than CQ (36 compounds) and DHA (17 compounds) respectively in the full bioluminescence rate of kill assay.

The 17 compounds that appear to exhibit an initial rate of kill as good as, or better, than DHA at 6hrs are shown in Table 4.4. This table also reports the available predicted biophysical data relevant to their potential oral bioavailability as a drug (hydrogen bond donors/acceptors, numbers of rotatable bonds, partition coefficient and molecular weight) as well as their MMV classification as a drug-like or probe-like compound. There is an apparent 50:50 proportion of drug-like and probe-like in these rates of kill hits.

Molecule	MMV number	PC1 (6hrs)	ALogP	Molecular Weight	Num_Rotatable Bonds	Num_H_Acceptors	Num_H_Donors	Classification
	MMV142383	-106.9	4.6	310.4	3	2	1	Drug-like
	MMV009015	-106.3	4.3	367.5	9	4	1	Probe-like
	MMV665891	-102.1	4.8	270.3	2	1	1	Drug-like
	MMV666021	-101.8	4.2	272.3	1	3	0	Probe-like
	MMV665809	-97.5	4.6	395.7	4	3	1	Probe-like
	MMV666026	-96.6	3.0	319.4	4	3	1	Probe-like

Molecule	MMV number	PC1 (6hrs)	ALogP	Molecular_Weight	Num_RotatableBonds	Num_H_Acceptors	Num_H_Donors	Classification
	MMV020243	-95.2	3.8	362.4	5	5	3	Probe-like
	MMV396749	-87.2	3.9	368.4	1	4	2	Drug-like
	MMV007474	-85.6	7.0	608.7	3	8	1	Probe-like
	MMV019555	-77.4	8.1	478.7	9	4	2	Probe-like
	MMV006787	-76.2	4.2	310.4	7	2	2	Probe-like
	MMV007092	-74.7	4.8	662.9	18	10	2	Probe-like

Molecule	MMV number	PC1 (6hrs)	ALogP	Molecular_Weight	Num_RotatableBonds	Num_H_Acceptors	Num_H_Donors	Classification
	MMV665800	-74.1	4.3	347.8	7	3	1	Drug-like
	MMV665826	-73.3	3.7	288.3	2	4	0	Drug-like
	MMV665803	-73.0	4.3	377.9	8	4	1	Drug-like
	MMV665806	-70.7	4.2	314.5	5	2	2	Drug-like
	MMV000483	-69.3	4.4	341.4	5	4	2	Drug-like

**Table 4.4: Biophysical parameters of hits**

This table reports the 17 hits identified with an initial rate of kill as good as, or better, than DHA in the full bioluminescence rate of kill assay, with key biophysical parameters for these compounds indicate (see main text).

#### 4.2.5 Single point assays using 3D7 IC<sub>50</sub> data: A simpler way forward?

The bioluminescence assay described here employs Dd2<sup>luc</sup> parasites, whilst high throughput screening IC<sub>50</sub> data are typically reported for the genetically distinct 3D7 clone (Barrows *et al.*, 2012; Spangenberg *et al.*, 2013). Thus, reconfirming the IC<sub>50</sub> data in Dd2<sup>luc</sup> parasites is a time-consuming limitation in the assay; in fact, it takes more time to determine the IC<sub>50</sub> values than in subsequently determining the RoK itself. This raises questions regarding the applicability of this assay as a high throughput tool in screening large compound libraries (i.e. TCAMS 13,000 compounds) as remeasuring Dd2<sup>luc</sup> IC<sub>50</sub> data would perhaps represent a too significant workload to make the approach viable. Here, a question is asked whether is it necessary to repeat IC<sub>50</sub> measurement in Dd2<sup>luc</sup> parasites prior to performing the RoK, or whether the widely available IC<sub>50</sub> data for the 3D7 clone can be used instead.

The Dd2<sup>luc</sup> IC<sub>50</sub> data obtained for the Malaria Box compounds (396 in total) were initially compared against the available 3D7 IC<sub>50</sub> data. Negative log-transformed IC<sub>50</sub> data (pIC<sub>50</sub>, to allow ready distribution of data across a wide range of concentrations) for each drug in the two clones were plotted and show a reasonable, but significant, correlation (Figure 4.10,  $r^2=0.4$ ,  $p<0.0001$ ). Critically, this correlation is comparable to the one established by Spangenberg *et al.*, (2013) between 3D7 and the K1 isolate of *P. falciparum*.

The difference in IC<sub>50</sub> values observed between 3D7 and Dd2<sup>luc</sup> could be attributed to variations in the different methodologies employed to measure this parameter, rather than their genetic background. The 3D7 IC<sub>50</sub> data reported by MMV with the Malaria Box were prepared during the massive chemical library screening, where compounds are screened rapidly for their IC<sub>50</sub> potency using large-fold dilution series (e.g. 10-fold

dilution), which imposes a limitation on the accuracy of the  $IC_{50}$  estimated from log dose response curves. In addition, there is no well-established single fixed endpoint for determining an  $IC_{50}$  value, with some laboratories preferring a 48hr assay format whilst others prefer a 72hr assay format. The 3D7  $IC_{50}$  data of the Malaria Box compounds resulted from a 72hr assay using DAPI (Spangenberg *et al.*, 2013; Duffy, and Avery, 2012; www.mmv.org), which is distinct from the 48hr MSF assay used in this study.

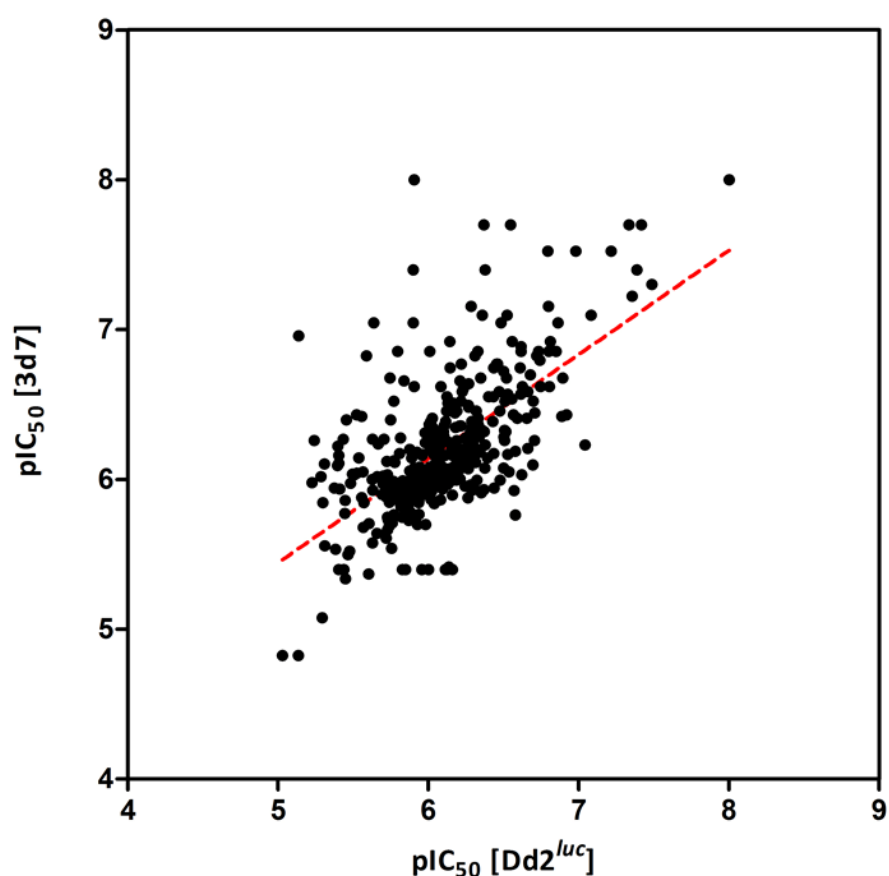


**Figure 4.10: Comparison of  $Dd2^{luc}$  and 3D7  $IC_{50}$  data**  
Regression analysis of the  $pIC_{50}$  ( $r^2 = 0.4$   $P < 0.0001$ ) determined for 396 compounds in the MMV Malaria Box for 3D7 (sourced from www.mmv.org) against those against  $Dd2^{luc}$  (developed in this study).

This level of correlation was determined not to be an issue as comparison between two sets of 3D7  $IC_{50}$  data available for Malaria Box compounds, developed using distinct methodologies (DAPI and high content imaging) actually showed a weaker correlation (Figure 4.11,  $r^2 = 0.2$ ,  $p < 0.0001$ ) than observed here,  $r$  when comparing the two fluorescence

assay datasets from two genetically distinct clones. This suggests that more variation in data can be attributed to the assay method employed than based on the genetic background of the parasite.

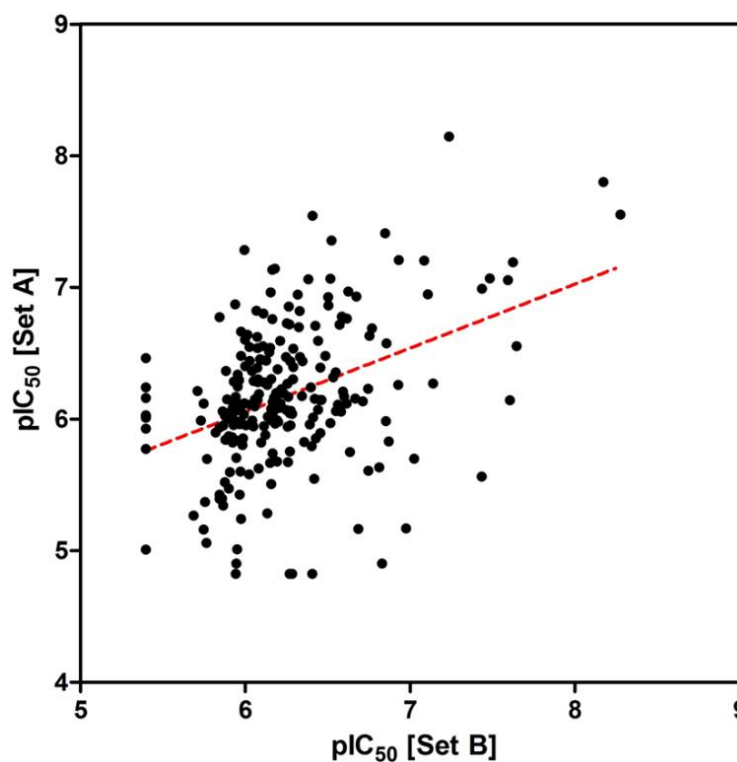


**Figure 4.11: Comparison of two independent 3D7 IC<sub>50</sub> datasets**

A linear regression plot between two independent 3D7 IC<sub>50</sub> datasets [Set A (ChEMBL, high content imaging) and set B (Avery, DAPI)] compared against each other. ( $r^2=0.2$ ,  $p$  value < 0.0001).

Based on the observation that Dd2<sup>luc</sup> and 3D7 IC<sub>50</sub> data showed limited variation, the loss in bioluminescence signal in Dd2<sup>luc</sup> parasites using the available 3D7 IC<sub>50</sub> data (DAPI fluorescent assay data provided with the Malaria Box) was determined. All 400 Malaria Box compounds were screened at a single-dose/single-time (i.e. 9xIC<sub>50</sub> of drug for 6hrs) using their 3D7 IC<sub>50</sub> concentration, including the 7 benchmark drugs previously employed (using 3D7 IC<sub>50</sub> data available from Hasenkamp *et al.*, 2013). This bioluminescence rate of kill data was plotted against the corresponding 3D7 IC<sub>50</sub> values (Figure 4.12).

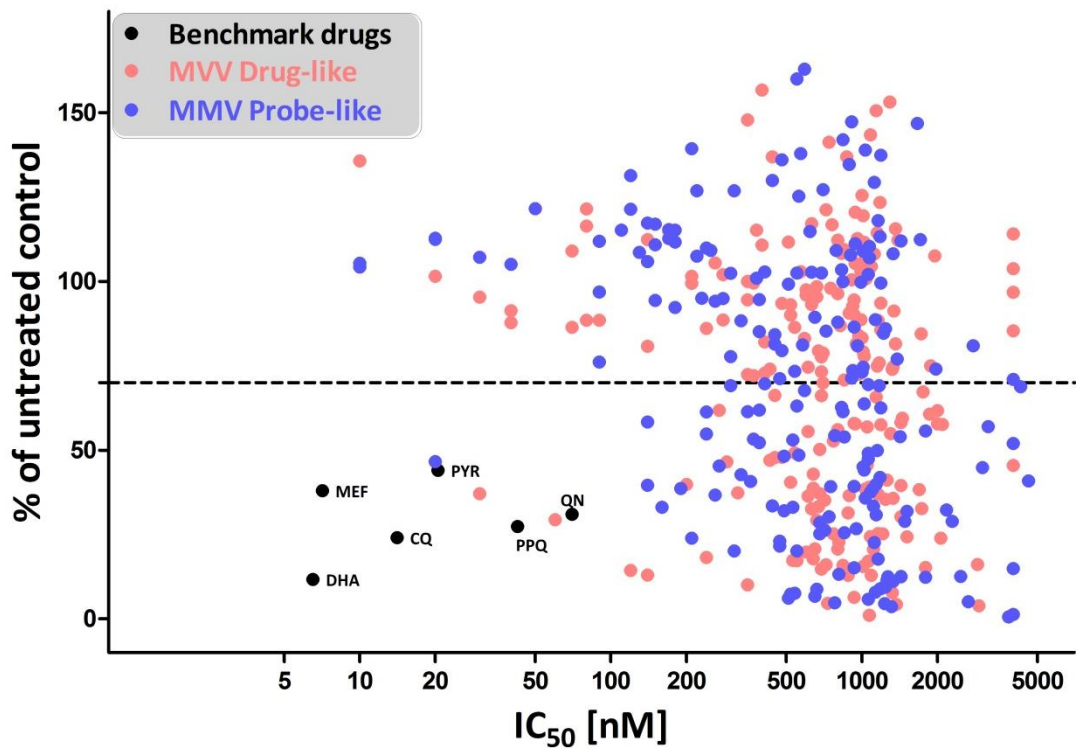


**Figure 4.12: Correlating the RoK against the corresponding IC<sub>50</sub> data from 3D7**  
 Scatter plot illustrating rate of kill data (9XIC<sub>50</sub> concentration of drug for 6hrs) against the corresponding IC<sub>50</sub> data from 3D7. The threshold line in the middle split compounds into fast acting and slow acting. Each data point represents mean percent from three biological repeats (n=9). Note, there is no apparent correlation ( $r^2=0.06$ ) between the estimates of rate of kill and IC<sub>50</sub> of these compounds.

This distribution of data based on the 3D7 IC<sub>50</sub> values was compared to those obtained from using their corresponding Dd2 IC<sub>50</sub> value (Figure 4.13) in the Dd2<sup>luc</sup> triage assay data described in Figure 4.4. This analysis shows a strong and significant linear correlation ( $r^2=0.88$ ,  $p<0.0001$ ) between the triage datasets generated using the two different sets of IC<sub>50</sub> data. This would appear to suggest that an initial triage to identify compounds likely to exert a measurable initial rate of kill can be performed using IC<sub>50</sub> data from a genetically unrelated *P. falciparum* clone/isolate. To explore the applicability of the triage assay, using either Dd2 or 3D7 IC<sub>50</sub> data, these data were compared against the 53 compounds identified in the full bioluminescence rate of kill assay to have initial rates of kill (lower PC1 values) greater than chloroquine (i.e. meeting the TCP1 criteria). The

percentage of these 53 compounds that would be “discovered” using triage assay thresholds set between 10-70% (in 10% increments) was determined and plotted in Figure 4.14. Importantly it is observed that, irrespective of the IC<sub>50</sub> dataset tested, when a 70% threshold was set (the original threshold selected) all the 53 compounds that were determined to meet the TCP1 criteria of better than chloroquine were identified (the actual minimal threshold value is 62%). As this threshold is lowered, the proportion of these 53 compounds identified in either triage assay decreases – with the reliability of detection falling off more quickly when 3D7 IC<sub>50</sub> triage data is used.

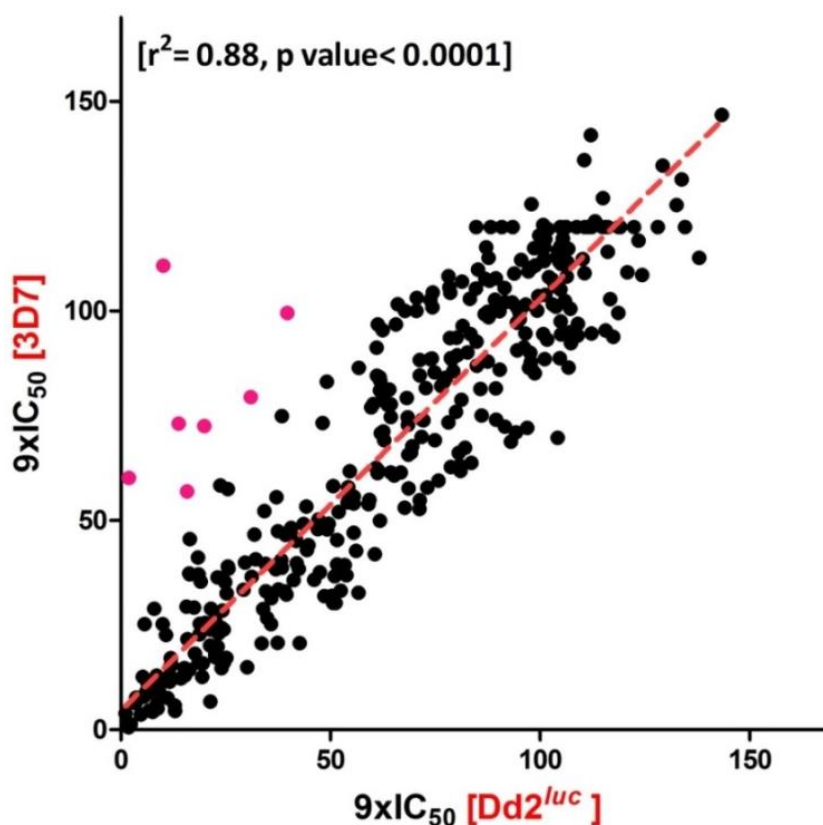


**Figure 4.13: Comparison between the RoK obtained using Dd2<sup>luc</sup> and 3D7 IC<sub>50</sub> values**  
A linear regression plot between the triage rates of kill data obtained using Dd2<sup>luc</sup> and 3D7 IC<sub>50</sub> values respectively. The red line shows linear regression curve and the pink data points illustrates outliers (see discussion).

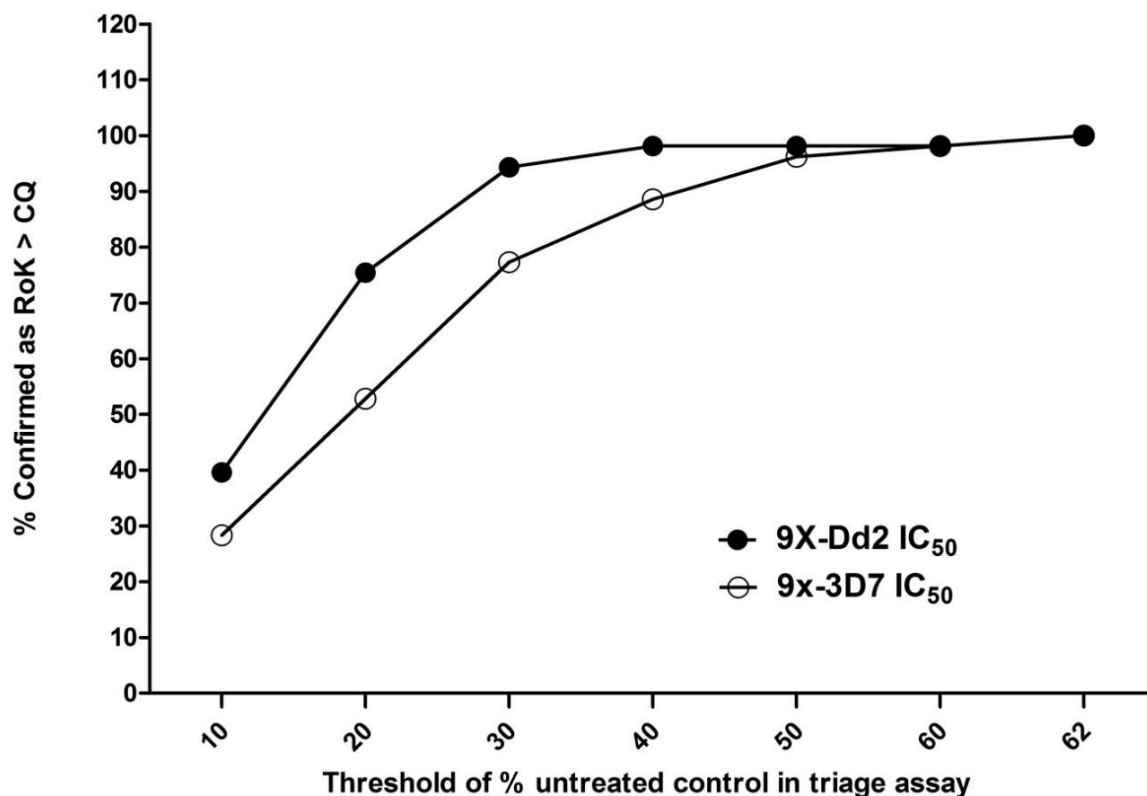


**Figure 4.14: Single dose and single timepoint triage assay**

Effectiveness of the triage assays in identifying compounds subsequently shown in the full bioluminescence rate of kill assay to have rates of kill greater than chloroquine. The y-axis reports the proportion of the 54 compounds with rate of kill (RoK) activity > CQ identified against the various threshold (x-axis) values applied for the single dose (9XIC<sub>50</sub>) and single timepoint (6hr) triage assay using IC<sub>50</sub> data from either 3D7 or Dd2.

Given these observations, it would appear that a threshold of 50% in a triage assay, using either IC<sub>50</sub> value, would identify >90% of the compounds subsequently shown to have an initial rate of kill greater than that of chloroquine. Interestingly, lowering that threshold to 25% and considering the 17 compounds determined to have an initial rate of kill greater than DHA; the Dd2 IC<sub>50</sub> triage assay would identify 16 of the 17 (94%), whereas the 3D7 IC<sub>50</sub> triage assay would identify 14 of the 17 compounds (82%).

Together these data would suggest that compounds with an initial rate of kill that meets the challenge of a TCP1 candidate can be rapidly screened, with >90% hit rate, using a single dose (without the need to remeasure the IC<sub>50</sub> in Dd2) and single timepoint assay.

### 4.3 Discussion

The gold standard for the determination of a rate of kill *in vitro* is based on the recrudescence growth of parasites following a bolus of drug exposure (Sanz *et al.*, 2012). Whilst this assay is complex (multiple wash steps, dilution, and sterile long-term culture) and requires a prolonged assay time (21-28 days), it provides a true rate – an effect determined over time – and reports both PRR and PCT, values that can be readily compared to available *in vivo* data. That said, the strength of this assay lies mainly in a lead validation/development role as the throughput is not sufficient to screen the necessary number of compounds to make it a valuable hit/lead discovery assay.

The bioluminescence assay employed here offers a compromise that meets the challenge of a reliable assay, with a good dynamic range of cytotoxic effect that is readily scalable due to its ease of use in a simple plate-based assay format over 6 hours. The limitation that it does not provide absolute data that can be directly compared to PRR and PCT parameters is balanced against its ability to readily generate relative data – and it is worth noting again that the TCP1 requirements for drugs that are at least as fast as CQ, and preferably better than artemisinin, are relative targets. The ease of use of the bioluminescence assay and the short time taken to provide the relative rate of kill data for the MMV Malaria Box compounds suggest that the utility of this assay lies mainly as a tool to complement current hit discovery assays (i.e. screening of many hundreds and more compounds) to ask not only what are the most potent hits, but also what are the fastest hits. The recrudescence PRR/PCT *in vitro* assay, along with the *in vivo* mouse modelling of rate of kill will continue to play a leading role in lead development, but with

the understanding that compounds being tested have already shown some potential as rapidly acting cytotoxic compounds in the bioluminescence screen.

In chapter 3, a comparison of bioluminescence assay data developed for a range of IC<sub>50</sub>-fold exposures using against the *in vitro* PRR and PCT data available for a range of benchmark antimalarials suggest a good correlation. Here, using the PC1 data for the same benchmark antimalarials, an analysis that combines the data from four different drug concentrations, this comparison was explored again (Figure 4.15). The PC1 data shows a strong and significant correlation with the PCT, as was the case for the loss of bioluminescence signal at higher multiple IC<sub>50</sub> doses in chapter 3. This was also the case with the analysis in chapter 3; the correlation was stronger using the 6hr assay format. Comparison of PC1 against the PRR suggests a reasonable, but not yet significant, trend, which also strengthens using the longer 6hr assay format. Again, the same caveats regarding the lack of variance in the available PRR data, and the requirement to exclude DHA as the PRR is only reported as >8, are true in this analysis.

It would perhaps not be reasonable to extrapolate an *in vitro* PRR or PCT from the PC1 data available, not at least due to the limitations in the diversity of drug classes tested and numbers of compounds compared. Access to more *in vitro* PCT and PRR data, or ideally more *in vivo* data, would be useful in taking bioluminescence PC1 data and making predictions regarding their PRR and PCT *in vitro* or even *in vivo*.

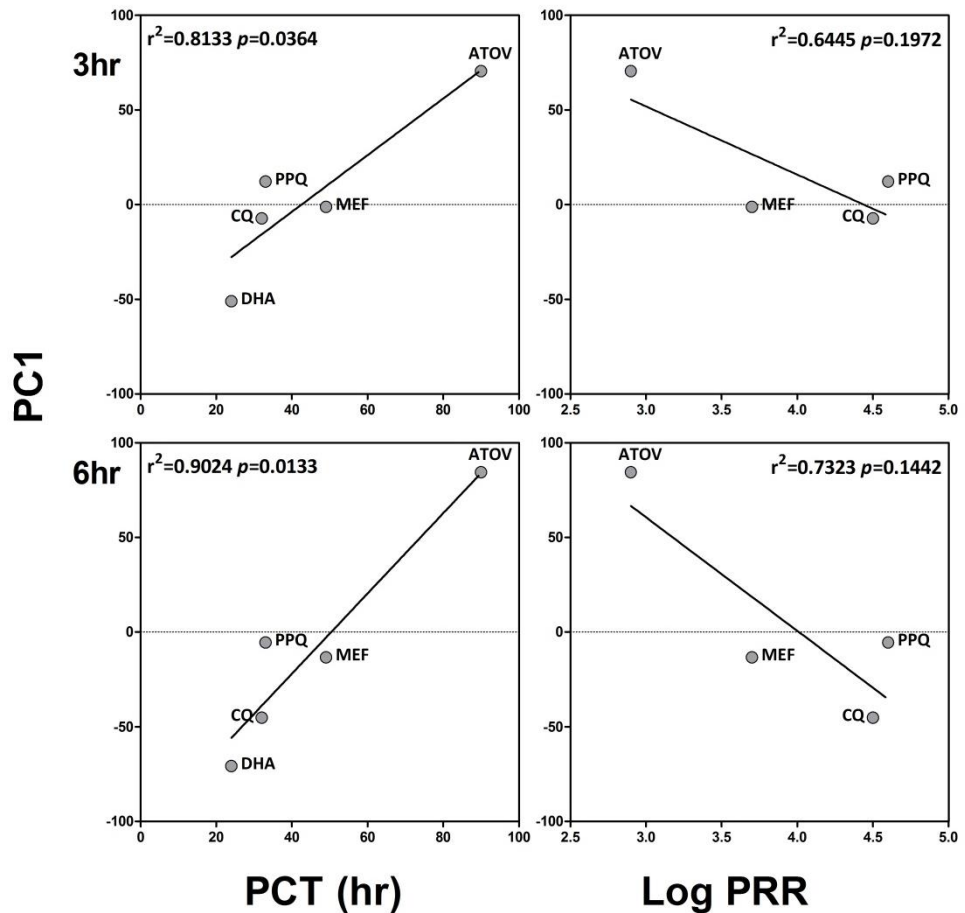


**Figure 4.15: Correlation of PC1 against PCT and PRR**  
 Correlation of PC1 data against available in vitro PCT (hr) and log PRR data (Sanz et al., 2012).

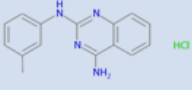
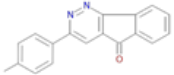
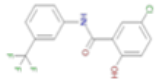
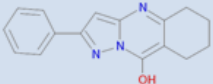
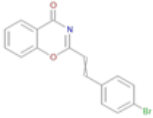
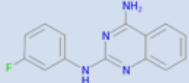
The limitations imposed by the temporal peak of luciferase expression during the trophozoite stage directs the use here of a 3hr and 6hr assay format. This is certainly a problem if the mode of action of a compound is outside this stage of development (and is an issue picked up in the next chapter). However, a 6hr assay window may be relevant for two reasons. A dramatic reduction of parasitaemia (>99%) in patients is required over a short period of time, usually 24 hours. As such, a reduction in parasite load (loss of viability) of >80% in 6hr period typically needs to be achieved, and is within the detection limits for this assay (i.e. that observed for DHA). Moreover, in the absence of any indication of the pharmacokinetic/pharmacodynamics (PK/PD) properties of the MMV

Malaria Box compounds *in vivo*, this assumption that they will have a long serum half-life cannot be made, a limitation with the current fast-acting artemisinins. This assay format of 6 hours assumes the worst case PK/PD scenario that a drug has to exert its cytotoxic action within a narrow time of peak plasma accumulation.

If, as proposed above, the bioluminescence rate of kill assay has a role to play in hit discovery, an important limitation could be the time spent in reconfirming the  $IC_{50}$  of each compound to be tested in the Dd2<sup>luc</sup> clone used here. Single dose/timepoint triage assay ( $9 \times IC_{50}$  for 6hrs either using Dd2<sup>luc</sup> or 3D7  $IC_{50}$  values) data developed here showed a significant correlation. Moreover, exploring how the threshold for the triage assay needs to be set to ensure discovery of the TCP1 candidates, here full bioluminescence assays report with PC1 values less than that of chloroquine, suggest that a 50% threshold would be sufficient to “discover” >90% of the TCP1 candidates irrespective of whether Dd2<sup>luc</sup> or 3D7  $IC_{50}$  data is used in the triage assay. With the general availability of 3D7  $IC_{50}$  data for large compound datasets, for example the TCAMS library of some 20,000 compounds or even the proposed new MMV Pathogens Box ([pathogensbox.org](http://pathogensbox.org)), this assay offers a simple and rapid means to quickly triage and then test compounds of interest as TCP1 candidates.

The comparison of triage assay datasets prepared using the Dd2<sup>luc</sup> and 3D7  $IC_{50}$  values in Figure 4.13 identified seven outliers (in pink). The majority of these compounds, except MMV665807, showed an apparent 2-14 fold increase in  $IC_{50}$  in Dd2<sup>luc</sup> compared to 3D7. The simplest explanation for their apparently greater cytotoxic effect in Dd2<sup>luc</sup> would be that a higher concentration of compound was used in the assay. Yet this is perhaps an oversimplification as the fold-change in  $IC_{50}$  doesn't correlate with the change in rate of

kill. These seven compounds are listed in Table 4.5. Of note, is that the IC<sub>50</sub> from other clones of *P. falciparum* (reported in Van-Voorhis *et al.*, manuscript in preparation) is more similar to that of Dd2<sup>luc</sup> reported here than for 3D7. Given that Dd2<sup>luc</sup> is chloroquine resistant, and 3D7 is chloroquine sensitive, these compounds were compared against the  $\beta$ -haematin inhibitors reported by Lee *et al.*, (2015) to be in the Malaria Box. These two groups of compounds are completely distinct from one another and provide no simple explanation for the differences in IC<sub>50</sub> based on  $\beta$ -haematin. However, given that chloroquine resistance is principally mediated through Pfcr1, a putative transport protein on the digestive vacuole membrane (Ecker *et al.*, 2012; Gaviria *et al.*, 2013; Roepe, 2010; Summers *et al.*, 2012), interactions between, or transport by, these seven compounds and the different forms of Pfcr1 in Dd2 and 3D7 cannot be excluded.

Molecule	MMV_ID	IC <sub>50</sub> in Dd2 <sup>luc</sup> (nM)	RoK (9XIC <sub>50</sub> ) in Dd2 <sup>luc</sup> using Dd2 IC <sub>50</sub>	IC <sub>50</sub> in 3D7 (nM)	RoK (9XIC <sub>50</sub> ) in Dd2 <sup>luc</sup> using 3D7 IC <sub>50</sub>
	MMV019110	3500.0	10.1	400.0	110.8
	MMV666021	1259.0	1.9	90.0	60.1
	MMV665948	2992.0	39.7	370.0	99.5
	MMV665807	1088.0	19.9	970.0	72.5
	MMV008270	1556.0	31.0	670.0	79.4
	MMV666599	5930.0	15.8	1050.0	56.9
	MMV080034	2366.0	13.8	1000.0	73.1

**Table 4.5: Seven outliers in the Malaria Box compounds**

Illustrate seven MMV Malaria Box compounds that are outliers when comparing the triage data following screens of Dd2<sup>luc</sup> with Dd2 and IC<sub>50</sub> concentrations.

In table 4.4 the 17 compounds identified during this study that appear to exhibit an initial rate of kill as good as, or better, than DHA at 6hrs are shown. This table also reports biophysical data relevant to their potential oral bioavailability based on the Rule of 5 initially described by Lipinski. These data are also represented for these 17 compounds using a radarplot (Figure 4.16) and include the polar surface area (PSA, Å<sup>2</sup>). The PSA is included as a PSA > 130 is generally regarded as an issue for the lipid solubility, and thus

bioavailability (particularly through an oral route of administration) due to the extent of the charged surface area of these compounds. Within the radarplot, a blue background illustrates the optimal region for a compound's properties in terms of predicted bioavailability. As such it can be noted that the majority of these 17 compounds would initially appear to be promising in terms of their biophysical properties. However, three compounds MMV007474 (LogP and Mw violation), MMV019555 (LogP violation) and MMV007092 (Mw and number of rotatable bonds violation) do not fall within this optimal region on the radar plot. It is not surprising therefore that these compounds are all listed as probe-like in the MMV Malaria Box.

Through a contribution of data to the MMV Malaria Box manuscript, preliminary access to additional data is available for these compounds. This includes high content imaging data originally contributed by the Ayoung group in which they have evaluated stage-specific activity of the MMV Malaria Box compounds against the clearly morphologically distinguishable intraerythrocytic stages of early rings, late rings, trophozoites and schizonts (Van-Vooris *et al.*, manuscript in preparation). In their work, they evaluated the effect of a fixed dose of 10  $\mu$ M of each of the 400 MMV Malaria Box compounds on these stages, with their effect on subsequent development also monitored.

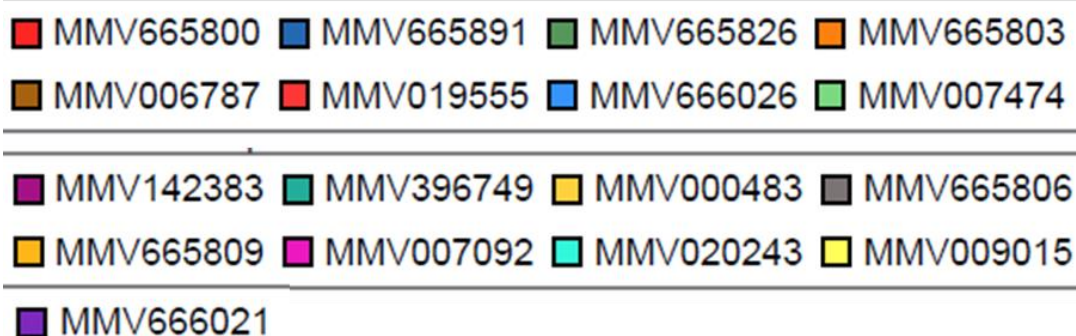
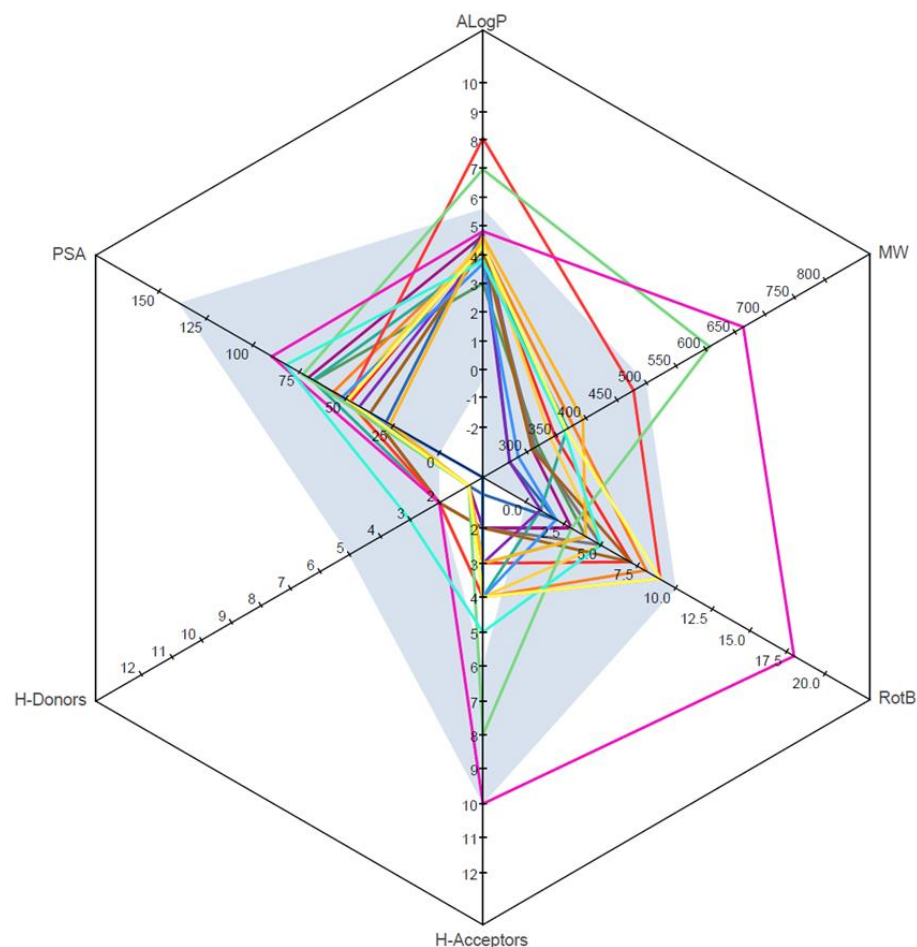


**Figure 4.16: Physicochemical property radar plot of the 17 hits compounds.**  
**ALogP** = Octanol-water partition coefficient. **PSA** = Polar surface area. **H-Donors** = Hydrogen bond donors  
**H-Acceptors** = Hydrogen bond acceptors. **MW**= Molecular weight. **RotB** = Rotatable bonds

Their application of a fixed dose of 10  $\mu$ M is distinct to the approach adopted in this study of using fold- $IC_{50}$  concentrations, however, for any compound with an  $IC_{50}$ >1  $\mu$ M, here  $9 \times IC_{50}$  dose would offer a close approximation. A brief summary of the intraerythrocytic

stage during which the 17 active compounds highlighted in this study are shown in Figure 4.17. Of note is that whilst this study specifically explored the cidal activity of these compounds in the trophozoite stage, data reported by the Ayoung group clearly reveals a preferential stage-specific activity within early rings (9 compounds) or mature rings (12 compounds) with only five compound reported in their study as affecting trophozoites.

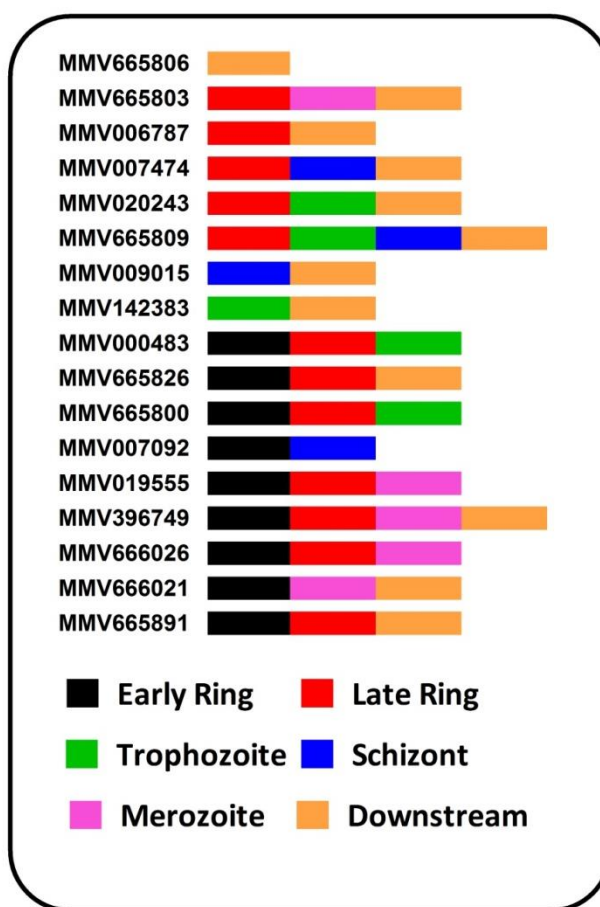


**Figure 4.17: Stage specific action of MMV Malaria Box compounds**  
 Stage specific action of MMV Malaria Box compounds as reported by Ayoung group. The coloured bar, see key, reports the morphological stage activity is reported or if occurring subsequently (downstream) to ring-stage application.

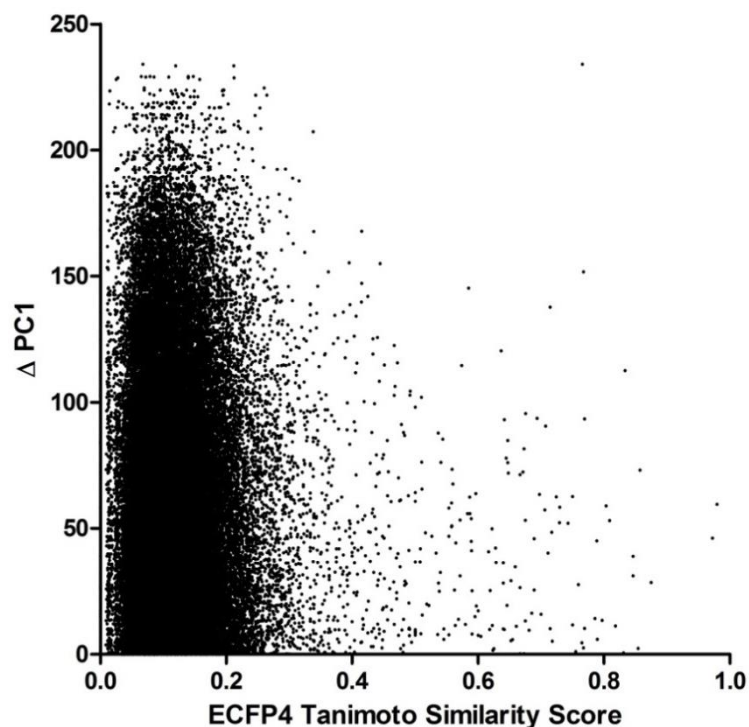
A detailed interpretation cannot be done prior to the full public release of this data; however, the ability to integrate the rate of kill data with additional datasets, such as the

stage-specificity of action here, illustrates how this process offers a value-added step in evaluating the MMV Malaria Box compound's as potential leads for further development. Another example of comparing these hits against existing data for the MMV Malaria Box is illustrated with a comparison against activity to a known target, in this case the plasma membrane P-type ATPase (PfATP4) that is involved in sodium ion and osmotic homeostasis (Jimenez-Diaz *et al.*, 2014; Lehane *et al.*, 2014; White *et al.*, 2014b). Of the 28 PfATP4 inhibitors identified in the MMV Malaria Box, data for 26 compounds are reported here. Of these, here this study has confirmed rapid action for 21 compounds with an initial rate of kill at least as good as, or better, than that of CQ. Of the 17 compounds reported here with an initial rate of kill greater than DHA, four compounds (MMV396749, MMV665800, MMV665826 and MMV665803) are apparent PfATP4 inhibitors (Lehane *et al.*, 2014). This is a promising observation given that clinical trials of the PfATP4 inhibitor NITD609/KAE609 suggest an *in vivo* rate of kill greater than artesunate. The *in vitro* rate of kill of PfATP4 inhibitors is perhaps not as rapid as the *in vivo* rate (and may thus fall between DHA and CQ), this suggested to be as a result of increased iRBC membrane rigidity and exposure of phosphatidylserine following exposure to PfATP4 inhibitors enhancing clearance *in vivo*. Interestingly, the best hit described here, in terms of initial rate of kill and IC<sub>50</sub> potency is MMV396749 with the second fastest kill and an IC<sub>50</sub> of 239nM. This compound is a PfATP4 inhibitor and is closely related to the NITD609/KAE609 spiroindolone, previously shown to rapidly inhibit ring stage parasites *in vitro* – as has also been shown for MMV396749 (Figure 4.17) .

The compounds within the MMV Malaria Box were originally selected to represent a diversity of chemotypes (Spangenberg *et al.*, 2013). With the structures readily available

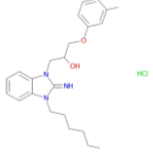
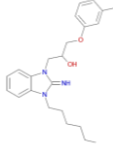
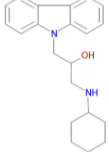
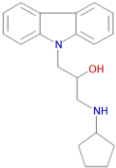
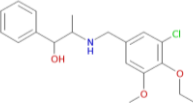
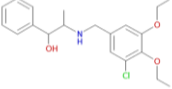
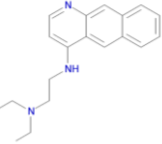
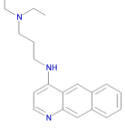
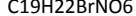
along with initial rate of kill data, an exploration of whether a chemical informatics approach could provide any useful information relating to a compounds likely initial rate of kill was carried out with Raman Sharma of the Liverpool School of Tropical Medicine. To describe each compounds relatedness to one another, an Extended Connectivity Fingerprint (ECFP4) analysis was performed to provide a binary “barcode” for each compound, with these barcodes used in a pairwise comparison to provide a Tanimoto similarity score for every pair of MMV Malaria Box compounds (80200 pairs). Of these, 23653 pairs had PC1 data available for both compounds. Taking these pairs, the Tanimoto similarity score was plotted against the  $\Delta PC1$  – asking only if the compounds shared a similar initial rate of kill, not whether they had a fast or slow rate of kill (Figure 4.18). This analysis revealed, not unexpectedly, the general unrelatedness of the compounds (with Tanimoto similarity scores predominantly  $<0.3$ ) in the MMV Malaria Box. As such, the analysis reveals that unrelated compounds show both a similar and dissimilar initial rate of kill to one another. This perhaps best equates to a comparison of chloroquine and atovaquone to DHA, all are structurally unrelated, but chloroquine has an initial rate of kill more similar to that of DHA than does atovaquone.

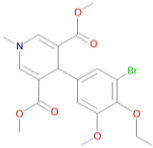
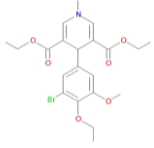
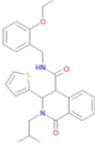
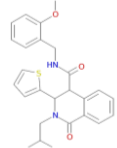
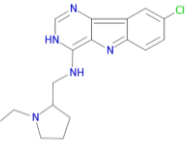
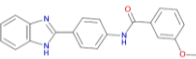
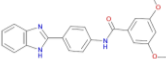
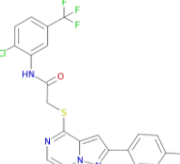
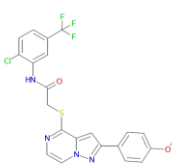
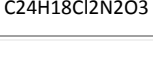
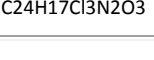
A Tanimoto similarity score of  $>0.8$  is typically regarded as showing significant structural similarity. In the MMV Malaria Box, 22 pairs of compounds show such a similarity score. For these 22 pairs, Dd2 triage assay data are available for all compounds, with PC1 data available for only 9 pairs of compounds (Table 4.6).

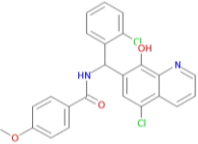
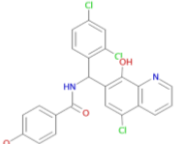
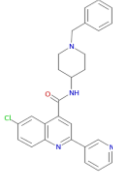
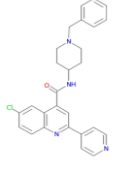
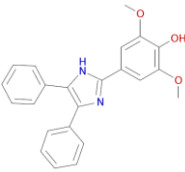
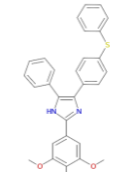
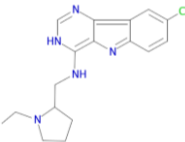
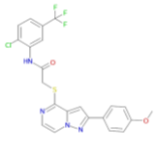


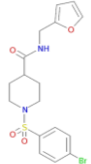
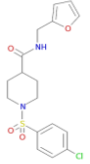
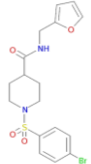
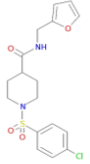
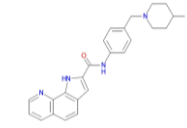
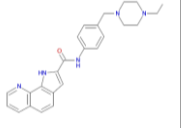
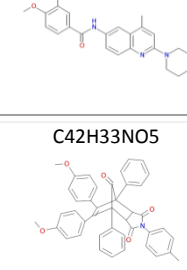
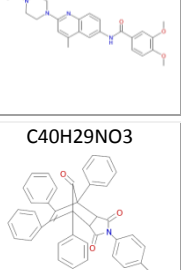
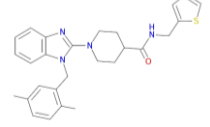
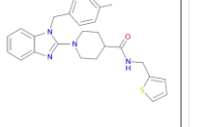
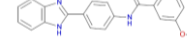
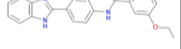
**Figure 4.18: Comparison of Tanimoto similarity score against differences in PC1**  
 Scatterplot illustrating the similarity between MMV compound pairs (Tanimoto similarity score based on their ECFP4 barcode) and the difference in initial rate of kill of these pair of compounds ( $\Delta PC1$ ).

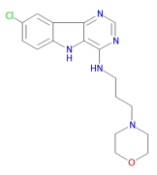
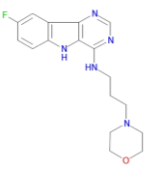
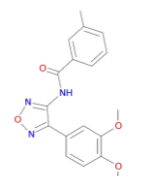
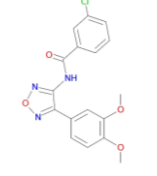
These 22 pairs of more related compounds were investigated more closely, specifically asking whether if more closely related compounds are more likely to share a similar initial rate of kill. The differences in bioluminescence data from the triage assay ( $\Delta RoK$  at  $9 \times IC_{50}$ ) for these 22 pairs and the  $\Delta PC1$  for the 9 pairs were plotted against their Tanimoto similarity score (Figure 4.19). This analysis, however, reveals no significant correlation. In Table 4.6, the  $IC_{50}$  for all the 44 compounds are recorded, showing a fold- $IC_{50}$  difference of between 1 and 4.4 between the 22 pairs of compounds. Given these differences, one explanation for any difference in initial rate of kill between these pairs is that a higher concentration of one of the two related compounds provides for a faster initial rate of kill.

MMV_Code (I)	Molecule (I)	MMV_Code (II)	Molecule (2)	IC <sub>50</sub> (nM) (I)	Triage RoK (I)	IC <sub>50</sub> (nM) (II)	Triage RoK (II)	PC1 (I)	PC1 (II)	Similarity score
MMV000445	C23H32ClN3O2 	MMV000444	C23H31N3O2 	1805	29.59	2346	8.75	-0.01	-59.54	0.980
MMV009063	C21H26N2O 	MMV000848	C20H24N2O 	277.9	39.24	452.7	17.45	-10.68	-56.82	0.972
MMV665857	C19H24ClNO3 	MMV396633	C20H26ClNO3 	1362	24.10	1908	19.02	-14.47	-42.99	0.875
MMV006303	C19H23N3 	MMV665783	C20H25N3 	464.9	34.19	60.75	87.89			0.857
MMV006764	C19H22BrNO6 	MMV006656	C21H26BrNO6 	789.1	8.55	458.1	9.00	-51.75	-49.34	0.854

										
MMV000653	C27H30N2O3S 	MMV000648	C26H28N2O3S 	1220	3.65	1143	35.78	-17.64	13.57	0.846
MMV396678	C17H20ClN5 	MMV396680	C22H16ClF3N4OS 	1451	111.79	327.7	100.95	98.18	31.50	0.846
MMV019762	C21H17N3O2 	MMV019124	C22H19N3O3 	831.5	49.05	521	74.37			0.840
MMV396680	C22H16ClF3N4OS 	MMV396679	C22H16ClF3N4O2S 	327.7	100.95	2300	109.02			0.838
MMV666022	C24H18Cl2N2O3 	MMV666054	C24H17Cl3N2O3 	977.9	78.67	511.9	86.77			0.833

										
MMV020490	C27H25ClN4O	MMV020275	C27H25ClN4O	1225	68.16	1480	60.18	40.77	40.20	0.831
										
MMV086103	C21H16O4	MMV006753	C20H14O4	846.4	104.84	606.7	116.09			0.826
										
MMV020750	C23H20N2O3	MMV007273	C29H24N2O3S	1544	60.54	734.5	66.75	28.63	39.86	0.818
										
MMV396678	C17H20ClN5	MMV396679	C22H16ClF3N4O2S	1451	111.79	2300	109.02			0.809
MMV007430	C17H19BrN2O4S	MMV006188	C17H19ClN2O4S	901.3	100.75	878.1	94.55			0.808

										
MMV020549	C25H26N4O 	MMV020548	C25H27N5O 	242.1	81.02	664.9	99.28			0.803
MMV019758	C24H27N3O3 	MMV019074	C25H30N4O3 	614.1	78.70	1854	65.20			0.800
MMV666101	C42H33NO5 	MMV666062	C40H29NO3 	190.3	98.85	397.1	107.14			0.800
MMV019741	C27H30N4OS 	MMV007564	C26H28N4OS 	1156	53.38	825.6	72.73			0.797
MMV019762	C21H17N3O2 	MMV019202	C22H19N3O2 	831.5	49.05	1207	78.31			0.796

MMV006587	C17H20ClN5O 	MMV019871	C17H20FN5O 	617.4	71.75	334.7	91.62			0.789
MMV665890	C18H17N3O4 	MMV020660	C17H14ClN3O4 	903.8	18.77	1328	8.54	-25.33	-70.32	0.788

**Table 4.6: Similarity scores for 22 pairs of the Malaria Box compounds**

This table reports molecule structure, their respective  $IC_{50}$ s, triage rate of kill ( $9 \times IC_{50}$ ), PC1 and similarity scores for 22 pairs of the Malaria Box compounds (44 compounds in total). Note that PC1 data are available only for 9 pairs.

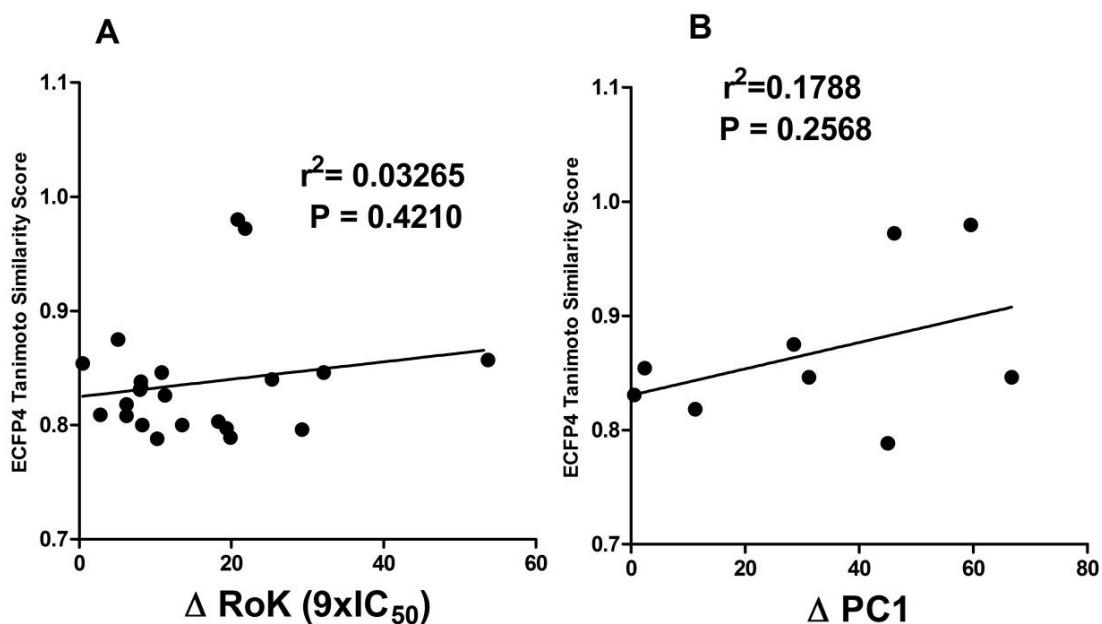


**Figure 4.19: Correlation of Tanimoto similarity score against difference in RoK**  
 The difference in the initial rate of kill derived from (A) the triage assay dataset ( $\Delta \text{RoK } 9 \times \text{IC}_{50}$ )  $n=22$  pairs and (B) PC1 dataset ( $\Delta \text{PC1}$ )  $n=9$  pairs.

Whilst data in chapters 3 and 4 does not suggest that the initial rate of kill correlates with the  $\text{IC}_{50}$ , these comparisons were based on compounds with very different structures. Plotting the fold- $\text{IC}_{50}$  difference between the 22 and 9 pairs of compounds against difference in triage assay and PC1 data, respectively, however, did not reveal any significant correlation, supporting the finding that initial rate of kill is apparently independent of the  $\text{IC}_{50}$  of the compound tested (Figure 4.20).

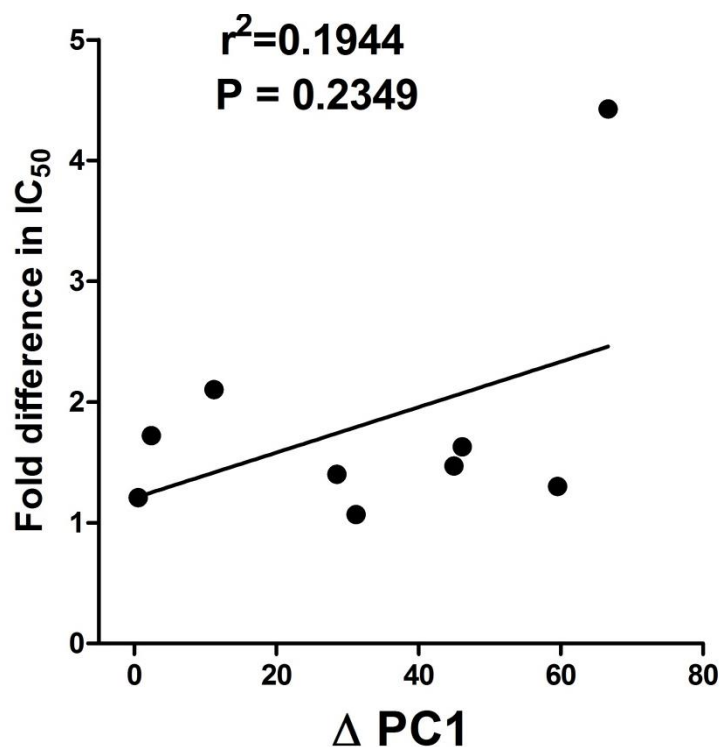


**Figure 4.20: Comparison of PC1 dataset ( $\Delta PC1$ ) against the fold- $IC_{50}$  difference**  
 PC1 dataset ( $\Delta PC1$ )  $n=9$  pairs against the fold- $IC_{50}$  difference between the compounds in each structurally related pair.

Whilst the results of this initial chemical informatics approach are perhaps initially disappointing, they are perhaps not surprising. The diversity of chemotypes within this collection of 400 compounds is likely a limiting factor in a more meaningful chemical informatics study. Screening additional libraries, particularly larger libraries that contain a higher proportion of related compounds, such as the 20000 compounds in the TCAMS library would be more useful. Moreover, future analyses would be enhanced by exploring properties of compounds beyond their immediate structural similarity. For example, compounds with biophysical properties that would enhance their immediate access to their target may influence their initial rate of kill. For example, more basic compounds may have more immediate access to targets in the digestive vacuole, or compounds with increased lipophilicity may access targets within subcellular organelles. Exploring these

attributes, in light of the simplicity of this assay to readily determine their initial rate of kill, offers a potentially novel approach to understanding how compounds can be modified to affect their rate of kill.

## CHAPTER 5: Exploring the Slow Acting Compounds in the Malaria Box Using a 48-Hours Bioluminescence-Rate of Kill (BRoK) Assay

---

### 5.1 Introduction

In chapter 4 fast-acting cytotoxic compounds acting against the trophozoite stages of intraerythrocytic development were identified in the MMV Malaria Box. The restriction to the trophozoite stage results from the use of 5' and 3' flanking sequences from the *Pfpcna* (*P. falciparum* proliferating cell nuclear antigen, PF3D7\_1361900) in the luciferase expression cassette (Wong *et al.*, 2011; Hasenkamp *et al.*, 2012). *Pfpcna*, encoding a processivity co-factor for DNA polymerase  $\delta$  on the leading strand during DNA synthesis, shows a strong temporal profile of stage-specific transcription linked to the S-phase of intraerythrocytic development (Kilbey *et al.*, 1993; Horrocks *et al.*, 1996, Horrocks and Kilbey, 1996; Wong *et al.*, 2011). The strong temporal transcription of the luciferase reporter protein from *Pfpcna* flanking sequences offers advantages in the excellent signal to noise ratio for bioluminescence based assays using this expression cassette (see Fig 5.1, Hasenkamp *et al.*, 2012). However, the narrow window for this strong reporter expression in the Dd2<sup>luc</sup> parasite line, limits the immediate utility of similar assays of drug-induced loss in parasite cell viability at other major developmental stages during intraerythrocytic development. Dd2<sup>luc</sup> can, therefore, be usefully used for the 3hr and 6hr bioluminescence assays in trophozoites reported in chapter 4. This can even usefully be extended to explore the loss of viability up to 9hrs (data not shown), however, beyond this, the lack of expression of luciferase and the relatively rapid turnover of this reporter protein results in greatly diminished bioluminescence signals.

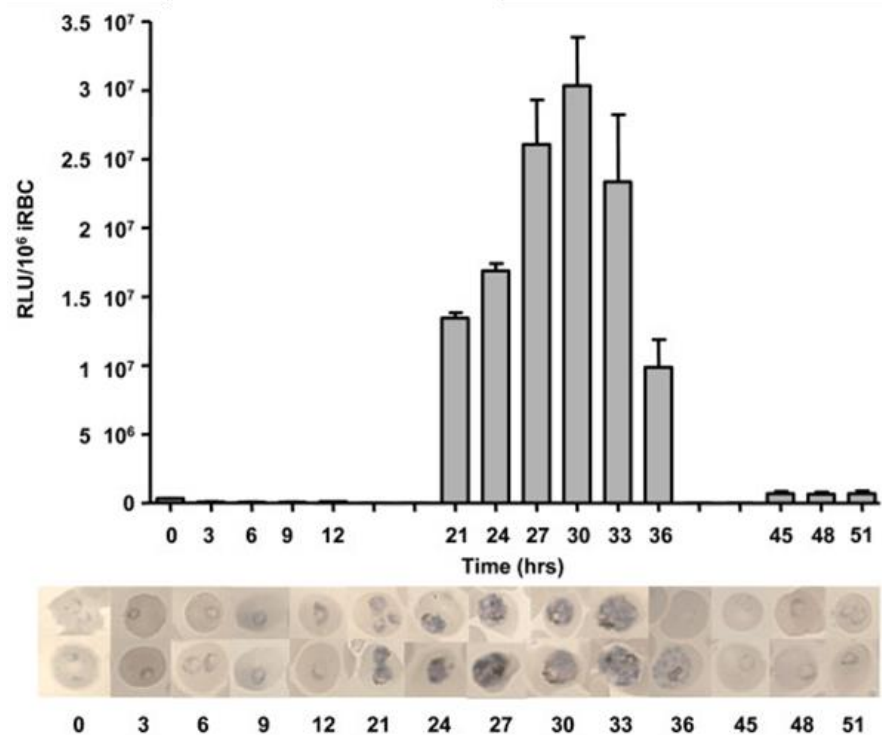


**Figure 5.1: Strong temporal regulation of the *Pfpcna*-luciferase promoter cassette during intraerythrocytic development.**

The morphological stages of intraerythrocytic development of *P. falciparum* are shown at below the chart, with the numbering representing hour's post-erythrocyte invasion. RLU, relative light units (Source-Hasenkamp *et al.*, 2012).

These limits likely have an impact when two aspects of drug action during intraerythrocytic development are considered. First is that of the lag phase; a period of time apparent for some classes of drugs, during which maximal kills rates (or sometimes even any killing if only cytostatic within the lag phase). The lag phase is not observed in all drug profiles, but some drugs have a variable lag phase lasting from 24 to as long as 48 hours (Sanz *et al.*, 2012; White, 2014) (Table 5.1). The recrudescence rate of kill assay, with its application of drugs for between 24 to 120hr allows the effect of these lag phase on the determination of PRR and PCT *in vitro* (Sanz *et al.*, 2012).

	lag phase (h)
artemisinin	0
pyronaridine	0
lumefantrine	0
piperaquine	0
chloroquine	0
mefloquine	0
pyrimethamine	24
atovaquone	48

**Table 5.1: The *in vitro* lag phase of known antimalarial drugs**  
(Source-Sanz *et al.*, 2012).

The second issue is the stage during intraerythrocytic development during which the applied drug is cytotoxic. The arsenal of antimalarial drugs that have been, or are being, applied are primarily active against the later stages of intraerythrocytic development with the majority having little appreciable effect against early ring stages (see Table 5.2). This would support the application of BRoK that is a trophozoite-stage based viability assay. However, it is considered useful to have antimalarial drugs that are also effective against early intraerythrocytic parasites. For example, part of the success of artemisinin has been linked to its substantial ring-stage activity (White, 1997; White *et al.*, 2011; Wilson *et al.*, 2013) with the new PfATP4 inhibitors (i.e. NITD609/KAE609 spiroindolone) also demonstrating activity against ring-stage parasites (Lehane *et al.*, 2014). To date, only artemisinin inhibits parasite egress with no antimalarial drug apparently affecting merozoite invasion (Wilson *et al.*, 2013). The ability to target erythrocytic stages of development beyond the trophozoite stage potentially offers opportunities in the design of novel chemotypes that hit, as yet, novel parasite targets.

Drug	Stage of activity			
	Merozoite invasion	Ring development	Growth to late stages	Schizont rupture
Chloroquine	No	Unlikely	Yes	Poor
Amodiaquine	No	Unlikely	Yes	Poor
Piperaquine	No	Unlikely	Yes	Poor
Quinine	No	Unlikely	Yes	Poor
Halofantrine	No	Unlikely	Yes	Poor
Lumefantrine	No	Unlikely	Yes	Poor
Mefloquine	No	Unlikely	Yes	Poor
Artemisinin	No	Likely	Yes	Yes
Artesunate	No	Likely	Yes	No
Atovaquone	No	No	Yes	No
Trichostatin A	No	Yes	NA	Yes
Cycloheximide	No	Yes	NA	Yes

**Table 5.2: Stage specific activity of known antimalarial drugs**  
*Inhibitory activity of antimalarial drugs during the intraerythrocytic development of P. falciparum (Source-Wilson et al., 2013).*

In chapter 4, it was apparent that almost half the MMV Malaria Box compounds showed little cytotoxic effects against trophozoites in a 6hr assay format. This assay format, however, doesn't account for any potential effect of lag phase or rapid cytotoxic activity at ring, late schizonts, and erythrocyte rupture or erythrocyte invasion. As the MMV Malaria Box compounds capture a diverse range of chemotypes, the potential for these apparently slow-acting compounds having a delayed or alternative stage-specific cytotoxic activity was considered in the following results chapter. In recognising the limitations of the current 6hr BRoK assay, the activity of these slow-acting schizonticides was explored in a 48hr assay format; trophozoites to trophozoites. Importantly, assays on these

compounds were carried out at 6hr and 48hr. The addition of the 6hr assay for these slow-acting compounds allowed an almost complete set of 6hr BRoK assay data to be developed for the MMV Malaria Box.

## 5.2 Results

### 5.2.1 Summary of the experimental approach

Sufficient materials were available for 178 of the compounds originally determined to be slow acting in the  $9 \times \text{IC}_{50}/6\text{hr}$  triage assays. These compounds were subjected to a full BRoK assay ( $9 \times$  to  $0.33 \times \text{IC}_{50}$ ) over 48hr to ensure completion of one full intraerythrocytic cycle. Bioluminescence assays were done at 6hr and 48hr, each with three technical replicates and with three biological replicates done. Two additional sets of compounds were included in the 48hr BRoK assay; seven benchmark antimalarials (DHA, CQ, MEF, QN, PPQ, PYR and ATOVA) and ten MMV compounds originally characterised as having a fast-acting cytocidal effect on trophozoites. A schematic representing the analysis of these data, along with that available from chapter 4, is shown below (Figure 5.2). Example plots of the dose-response curves are illustrated in Figure 5.3, with the remaining data recorded in Appendix 1.

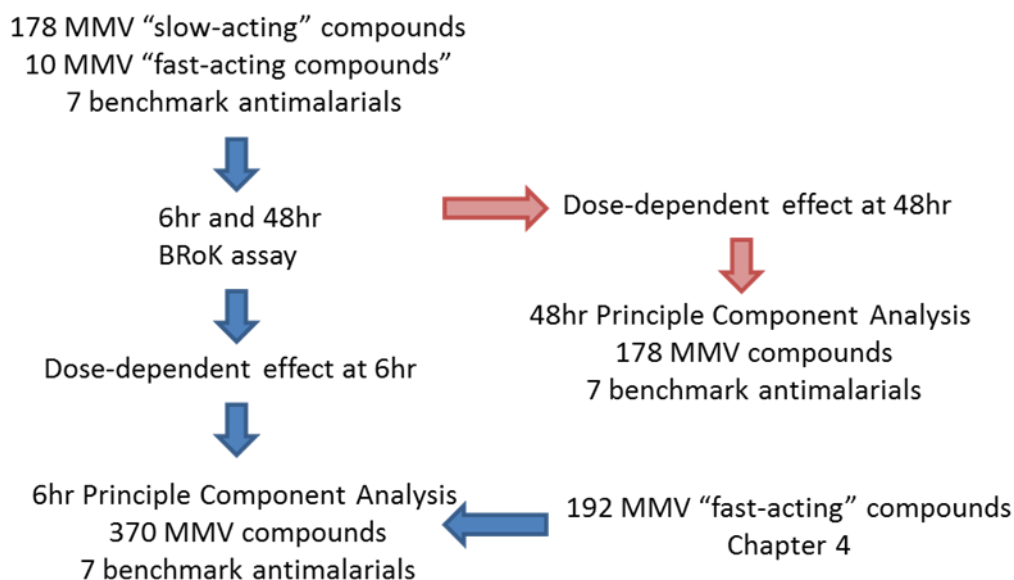


**Figure 5.2: A schematic for the analysis of the BRoK data**  
Schematic representing the analysis of the 6hr and 48hr BRoK assay data developed in chapter 5.

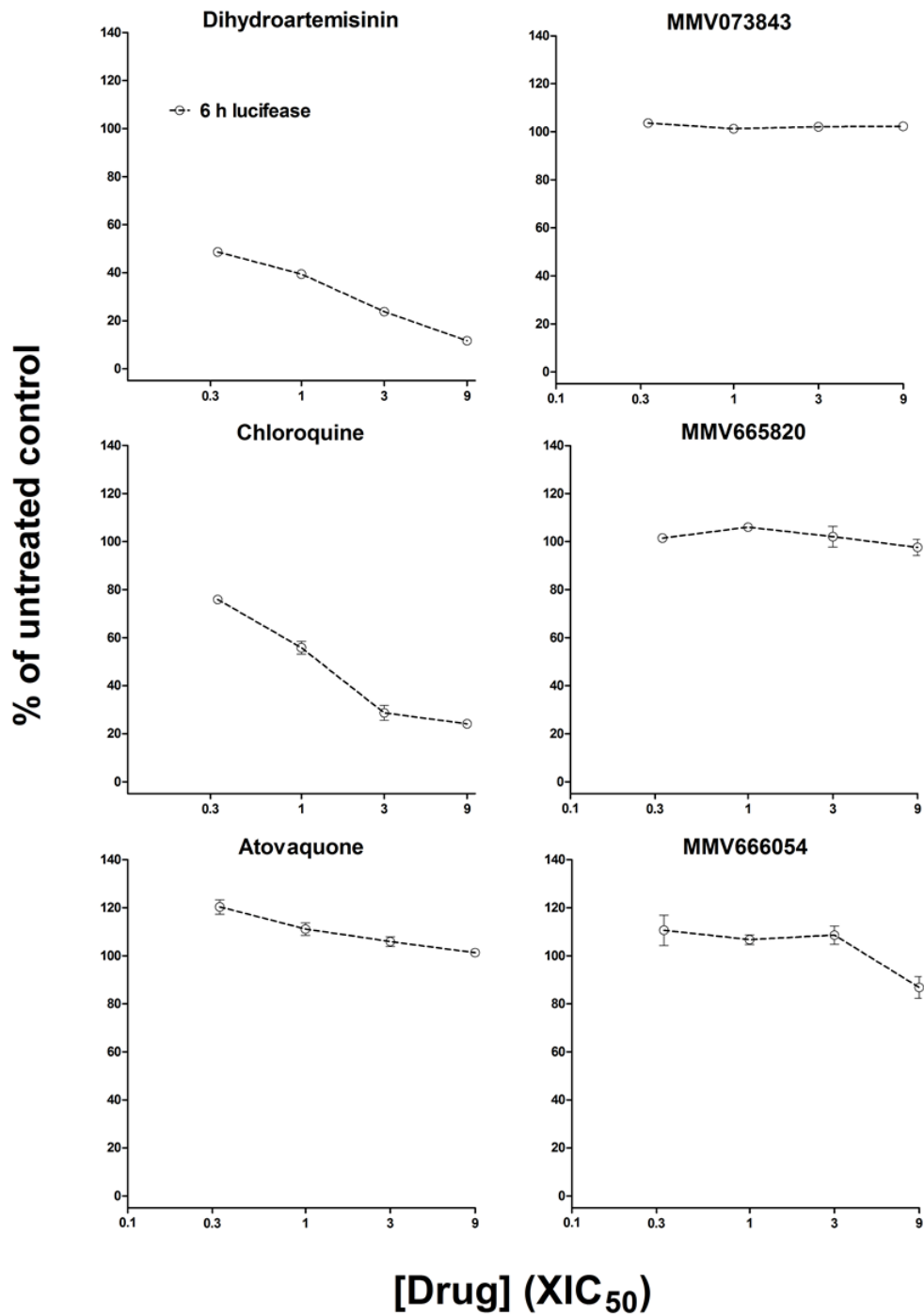


**Figure 5.3: Dose-dependent rate of kill of the Malaria Box candidates**  
 Exemplars dose-dependent rate of kill of the Malaria Box candidates at 6hr against a set of “benchmark” controls (DHA, CQ and ATOVA). Note – this level of data has been developed for 178 compounds and is reported in Appendix 1.

### 5.2.2 Provision of a full 6hr BRoK assay dataset for the MMV Malaria Box

Initial scatterplot analysis between the bioluminescence signals obtained following 6hr exposure to the different doses of “slow-acting” MMV Malaria Box compounds reports, as expected, minimal changes in trophozoite stage viability at all doses tested (Figure 5.4). The results for the ten “fast-acting” MMV Malaria Box compounds as well as the majority of the benchmark antimalarials show dose-dependent loss in parasite viability in line with data previously reported in chapter 4. Whilst not as apparent as the same analysis performed in chapter 4 for the “fast-acting” compounds, comparison of the bioluminescent data (normalised against untreated control) between the different fold- $IC_{50}$  concentrations used reveal better correlation when more similar concentrations are used e.g. effects at 9x v. 3x $IC_{50}$  are more closely related than those between 9x v. 0.33x $IC_{50}$  (Figure 5.4).

This new dataset for 178 “slow-acting” compounds initial rate of kill at 6hr was pooled together with the equivalent 6hr data reported for 192 “fast-acting” compounds reported in chapter 4. As before, to capture the concentration rate relationship in a single parameter, a PCA analysis was conducted (in collaboration with Raman Sharma, LSTM) to provide an initial rate of kill assay for a total of 370 of the 400 MMV Malaria Box compounds, as well as seven common benchmark antimalarials included in both analyses. Here PC1 describes 89% of the variation of the BRoK data (Table 5.3) with PC1 determined to comprise of;  $0.63(9X IC_{50}) + 0.62(3X IC_{50}) + 0.41(1X IC_{50}) + 0.22(0.3X IC_{50})$ . These values were zero-meanded to allow a final plot of PC1 against the  $IC_{50}$  for the majority of the MMV Malaria Box (Figure 5.5).

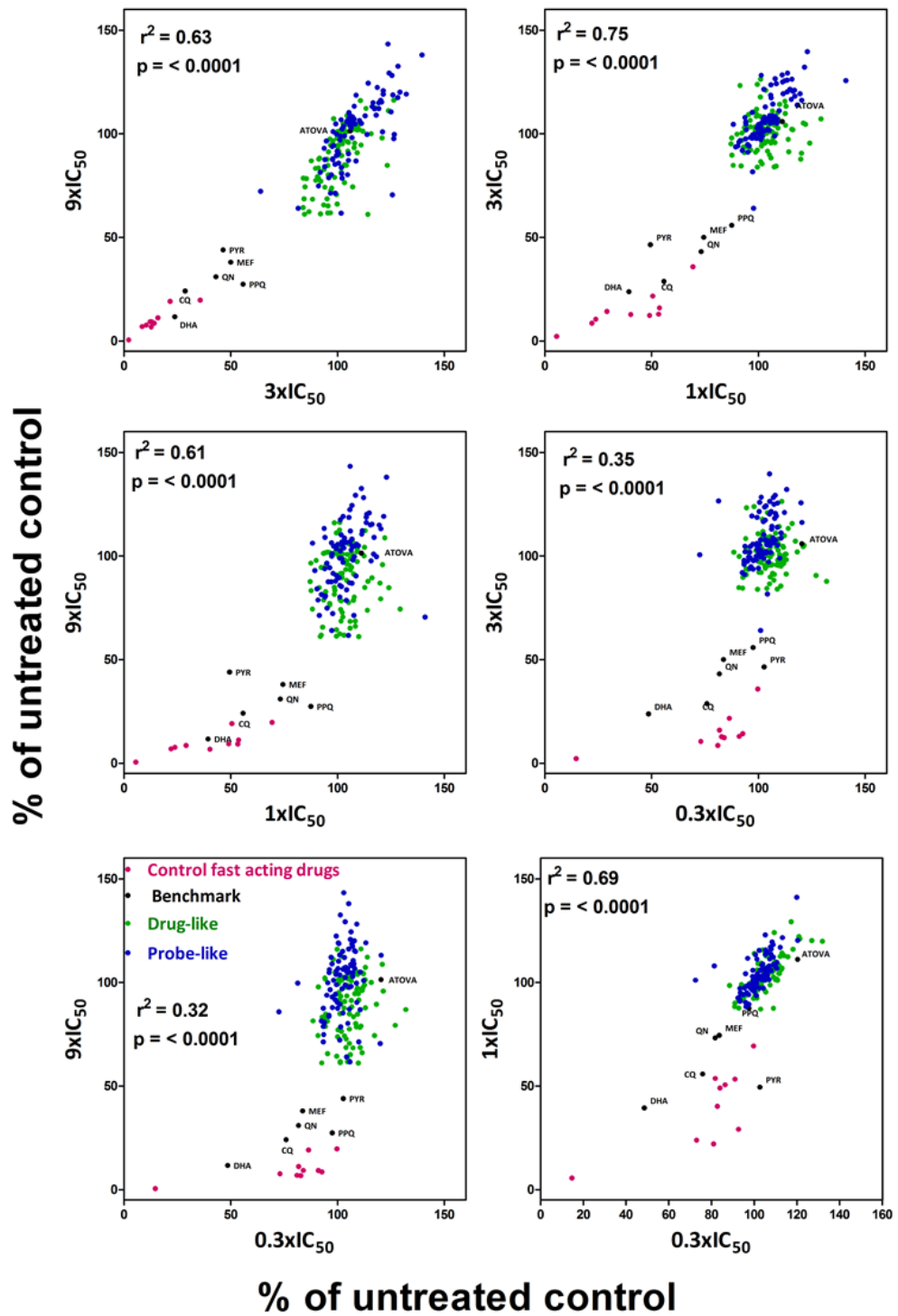


**Figure 5.4: Correlation between dose-dependent effects in a 6hr BRoK assay**  
 Comparisons between 9xIC<sub>50</sub>, 3xIC<sub>50</sub>, 1xIC<sub>50</sub> and 0.3xIC<sub>50</sub> at 6hrs for 178 slow acting compounds, ten control fast acting drugs and seven benchmark antimalarial drugs. The filled black circles represent known antimalarial drugs, green and blue circles show drug-like and probe-like MMV Malaria Box compounds, respectively. The pink circles represent fast-acting compounds used as an additional control.

	<b>% Variance Explained</b>	<b>% Cumulative Variance Explained</b>
<b>PC1</b>	0.89	0.89
<b>PC2</b>	0.08	0.97
<b>PC3</b>	0.02	0.99
<b>PC4</b>	0.01	1.00

**Table 5.3: Principle Component for 370 MMV Malaria Box compounds (6hr)**  
*The proportion of the variance, and cumulative variance, of the 6hr BRoK assay data reported in each Principle Component for 370 MMV Malaria Box compounds.*

To illustrate the relative contributions of PC1 and PC2, accounting for an accumulated variance of 97% of the data, these were plotted against each other to illustrate the continuation in the distribution of the data i.e. discrete groups were not observed. As expected based on the observations made in chapter 4, there was no correlation between the initial rate of kill, expressed here as PC1, and IC<sub>50</sub> in this more complete PCA of the 6hr BRoK assay data (Figure 5.5A).

Comparison of the 53 TCP1 candidates (initial rate of kill > CQ) reported in chapter 4 were compared against the proposed TCP1 candidates following this new PCA. Comparison of the two lists (Table 5.4) indicates that all 17 compounds indicated to have an initial rate of kill greater than DHA in chapter 4 are similarly reported in this new PCA. Comparison of the lists for compounds with an initial rate of kill greater than CQ but less than DHA reveal that three additional compounds are now included in this space following this new PCA (Table 5.4, a full new PCA list for 370 compounds is provided at the end of this thesis in appendix 3). It is important to note, however, that these same compounds only just did not make the list in chapter 4. Thus, this reanalysis of the data does not significantly change the list of potential TCP1 candidates provided from the initial triage assay

employed in chapter 4 and supports the assertion that this simplified assay format is sufficient for the discovery of potential TCP1 candidates.

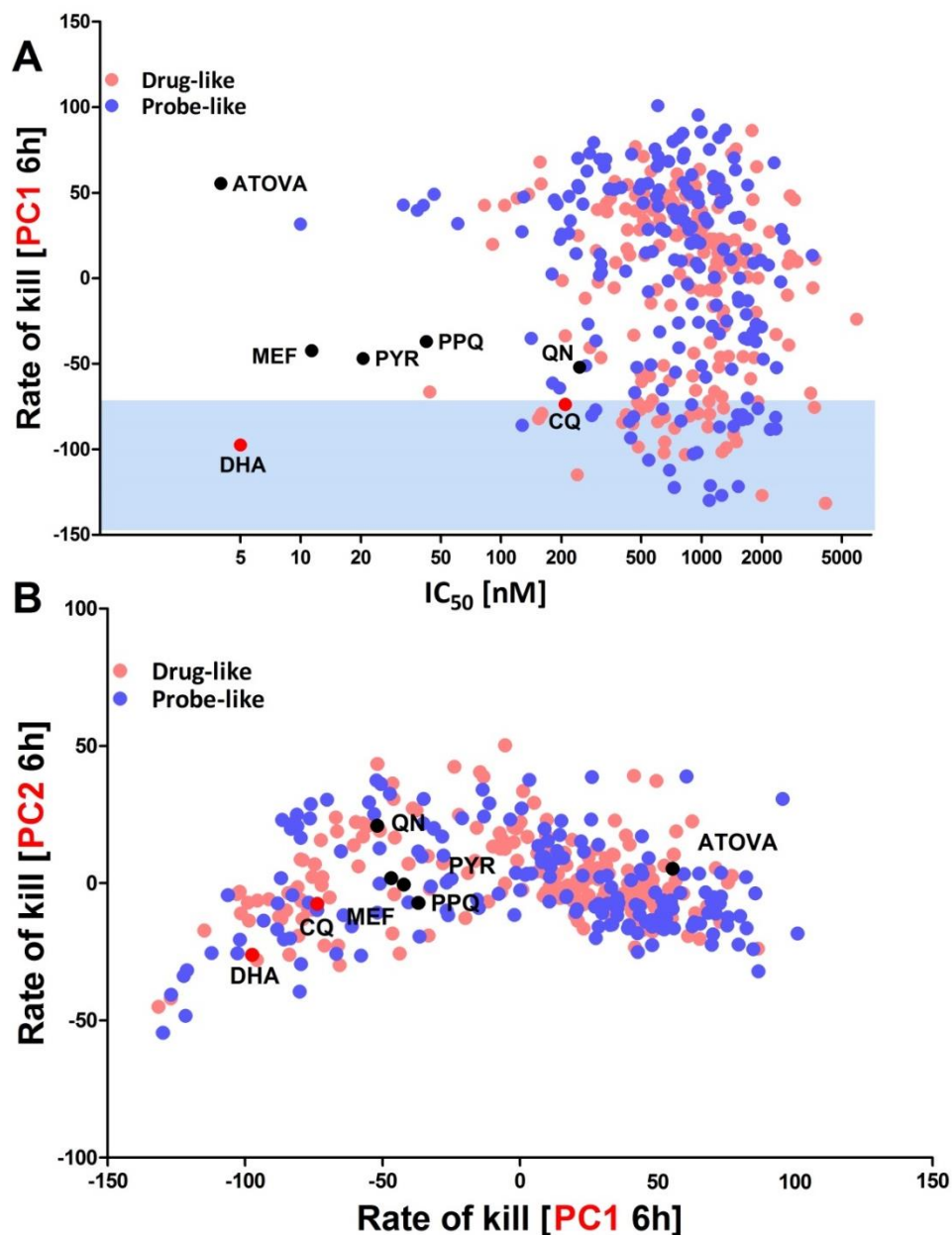


**Figure 5.5: Correlating RoK (PC1) for 370 Malaria Box compounds with  $IC_{50}$  and PC2**  
 (A) 6hr PC1 BRoK data plotted against the  $IC_{50}$  potency for 370 Malaria Box compounds. The blue shadowing represents the space occupied by compounds with an initial rate of kill faster than that of chloroquine. (B) PC1 data plotted against PC2 illustrating the continuous distributions of rate of kill data across these two components (accounting for 97% of the total variance in data). The filled pink, blue and black circles represent drug-like, probe-like and benchmark antimalarial drugs respectively. The red filled circles highlight DHA and CQ (i.e. TCP1 standards).

6hr PC1 (chapter 4)				6hr PC1 (chapter 5)			
MMV_ID	PC1	MMV_ID	PC1	MMV_ID	PC1	MMV_ID	PC1
MMV142383	-106.9	MMV665882	-56.5	MMV142383	-131.5	MMV000248	-84.3
MMV009015	-106.3	MMV000248	-55.4	MMV009015	-129.9	MMV019127	-83.9
MMV665891	-102.1	MMV020788	-55.3	MMV665891	-127.0	MMV665882	-83.6
MMV666021	-101.8	MMV666079	-54.5	MMV666021	-126.9	MMV006764	-83.4
MMV665809	-97.5	MMV007591	-53.9	MMV666026	-122.4	MMV007591	-82.8
MMV666026	-96.6	MMV006172	-53.6	MMV665809	-121.7	MMV665805	-82.1
MMV020243	-95.2	MMV006545	-53.4	MMV011522	-121.2	MMV000917	-82.1
MMV396749	-87.2	MMV665805	-53.0	MMV396749	-114.9	MMV008455	-81.2
MMV007474	-85.6	MMV006764	-51.8	MMV007474	-112.2	MMV006656	-81.0
MMV019555	-77.4	MMV019017	-51.7	MMV019555	-106.3	MMV019017	-80.9
MMV006787	-76.2	MMV011795	-51.2	MMV665800	-103.1	MMV006545	-80.6
MMV007092	-74.7	MMV665929	-51.1	MMV006787	-102.8	MMV020788	-80.2
MMV665800	-74.1	MMV000839	-50.9	MMV665803	-102.1	MMV007224	-79.8
MMV665826	-73.3	MMV000917	-50.2	MMV007092	-101.9	MMV665878	-79.8
MMV665803	-73.0	MMV665878	-49.5	MMV665826	-101.5	MMV665929	-79.8
MMV665806	-70.7	MMV006656	-49.3	MMV020660	-99.0	MMV006172	-79.6
MMV020660	-70.3	MMV008455	-49.0	MMV665806	-98.6	MMV000839	-79.5
DHA	-70.9	MMV006429	-48.8	DHA	-97.4	MMV011795	-79.1
MMV000483	-69.3	MMV396794	-48.8	MMV000483	-95.7	MMV006429	-79.0
MMV007617	-66.8	MMV007224	-48.5	MMV007617	-95.5	MMV396794	-77.1
MMV667491	-65.4	MMV007181	-48.4	MMV667491	-93.3	MMV007181	-76.9
MMV665796	-62.6	MMV000356	-47.7	MMV665796	-91.4	MMV007113	-76.4
MMV666109	-60.8	MMV006704	-46.0	MMV666109	-88.3	MMV665949	-76.1
MMV396736	-59.6	MMV665864	-45.6	MMV000444	-88.1	MMV000356	-75.9
MMV000444	-59.5	CQ	-45.3	MMV396736	-87.6	MMV006704	-75.6
MMV665831	-58.8			MMV667490	-87.0	MMV665918	-74.7
MMV001049	-58.8			MMV001049	-86.8	MMV665864	-73.8
MMV019127	-57.5			MMV666079	-86.5	CQ	-73.7
MMV667490	-57.4			MMV665831	-85.9		
MMV000848	-56.8			MMV000848	-85.0		

**Table 5.4: Comparison TCP1 candidates (Chapter 4 vs 5)**  
Comparison of the 53 TCP1 candidates (initial rate of kill > CQ) reported in chapter 4 against the proposed TCP1 candidates following this new PCA. The PC1 data for the TCP1 candidates (rate of kill > CQ) are reported in this table while a full list of the new PCA analysis for 370 compounds is provided at the end of this thesis in Appendix 4.

### 5.2.2 Exploring the slow acting compounds in a 48hr assay format

Accepting the limitations in the 6hr trophozoite assay format applied up to here, the rationale of the 48hr assay format was to explore what cytotoxic effects could be seen following 48hr incubation with drug. In addition to the 178 compounds previously characterised as “slow acting” in the 6hr assay, 7 known antimalarial drugs and 10 “fast

acting” compounds were tested. Log dose-normalised bioluminescence signal plots for all these compounds are provided in appendix 1. As with previous BRoK assays, correlations between the loss of bioluminescent signal following incubation at the different fold-doses of compounds were first explored (Figure 5.6).

As expected from previous assays, significant correlations ( $P < 0.001$ ) between loss in bioluminescent signals for all comparisons between fold-dose concentrations were observed, with stronger correlations between more similar concentrations i.e.  $9 \times IC_{50}$  v  $3 \times IC_{50}$  correlates better than the data for  $9 \times IC_{50}$  and  $0.33 \times IC_{50}$ . Importantly, the control “fast-acting” compounds, as well as the faster acting benchmark antimalarials, show between 95-98% loss in bioluminescence signal compared to untreated controls at the two highest doses tested. Interestingly, for the highest doses ( $3 \times$  and  $9 \times IC_{50}$ ) the most potent drug appeared to be pyronaridine, not the artemisinin DHA. DHA was actually less potent than CQ over the 48hr assay format. This was also seen in the 72hr assay format proposed by Sanz *et al.*, (2012) for their recrudescence assay, here they attributed this to the DHA being unstable after prolonged incubation at  $37^{\circ}C$  in an aqueous environment.

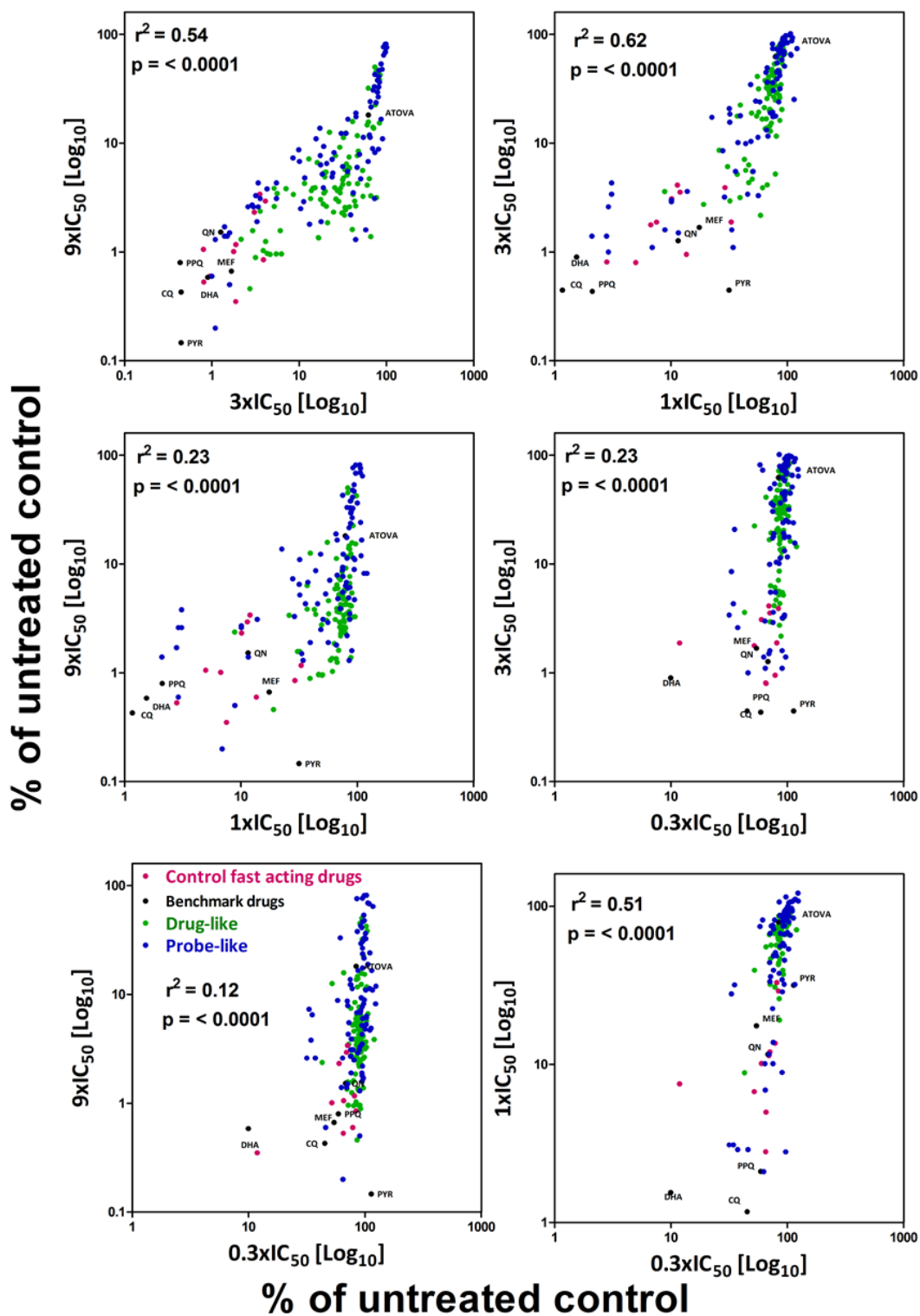


**Figure 5.6: Correlation between dose-dependent effects in the 48hr BRoK assay**  
 Correlations between loss of bioluminescence signal, compared to untreated control, following incubation with 9, 3, 1 and 0.3x IC<sub>50</sub> at 48hrs. The filled black circles represent known antimalarial drugs, green and blue circles represent drug-like and probe-like compounds, respectively. The pink circles represent ten “fast-acting” MMV Malaria Box compounds included as an additional control.

This same level of loss of bioluminescent signal was not observed for >90% of the 178 MMV Malaria Box compounds tested (Figure 5.6). These instead appear to split into two groups. Group-A shows a dose-dependent loss in bioluminescence signal, falling between CQ and ATOV. Group-B instead appears to show no appreciable cytotoxic effect at any concentration used over 48hrs, these then all falling above and to the right of ATOVA in Figure 5.6.

To provide a more meaningful comparison between these dose-dependent data, the 48hr BRoK assay for 178 “slow-acting” and ten “fast-acting” MMV Malaria Box compounds along with the seven benchmarks were analysed by Principle Component Analysis. Here PC1 describes 84% of the variation of the BRoK data (Table 5.5) with PC1 determined to comprise of;  $PC1 = 0.27(9X IC_{50}) + 0.64(3X IC_{50}) + 0.66(1X IC_{50}) + 0.29(0.3X IC_{50})$ . Note that compared to the 6hr PCA carried out to date, the 48hr PCA was more weighted to data provided from the 3x and 1x  $IC_{50}$  assays.

	<b>% Variance Explained</b>	<b>% Cumulative Variance Explained</b>
<b>PC1</b>	0.78	0.78
<b>PC2</b>	0.14	0.92
<b>PC3</b>	0.06	0.97
<b>PC4</b>	0.03	1.00

**Table 5.5: Principle Component for 370 MMV Malaria Box compounds (48hr)**  
*Reports the proportion of the variance, and cumulative variance, of the 48hr BRoK assay data reported in each Principle Component for 188 MMV Malaria Box compounds.*

These values were zero-meant to allow a final plot of PC1 against the  $IC_{50}$  for these “slow-acting” MMV Malaria Box compounds (Figure 5.7) after 48hr.

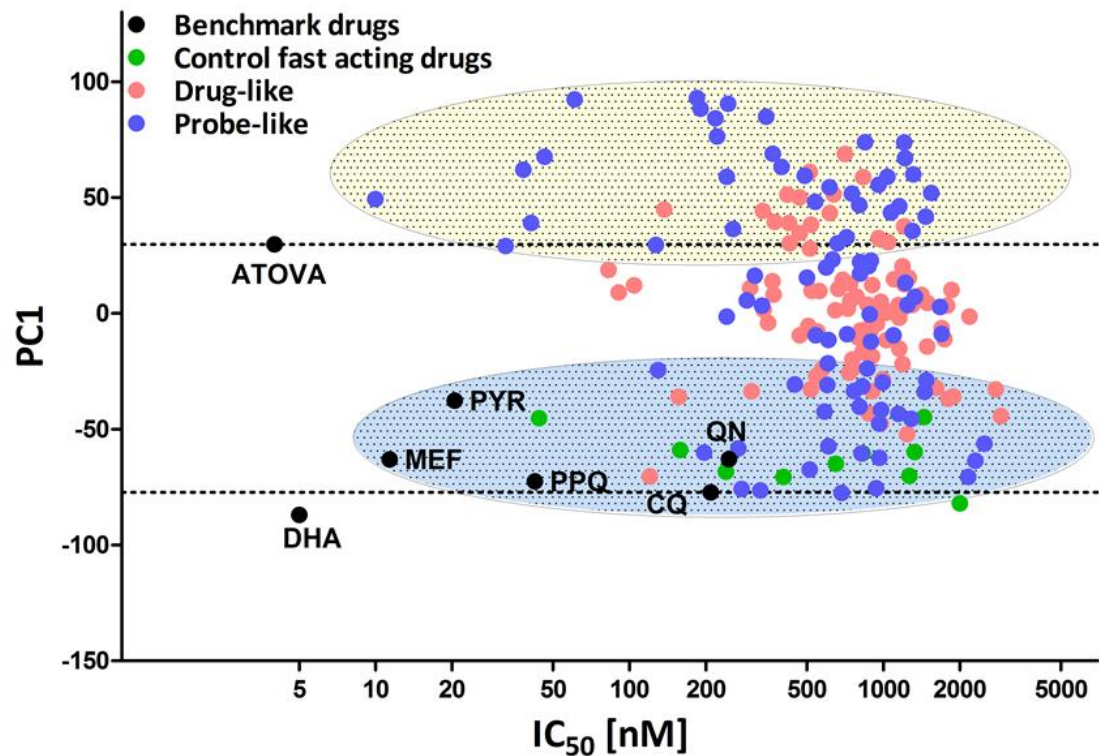


**Figure 5.7: PC1 (48hr) data plotted against their IC<sub>50</sub> potency- separating “slow-cytocidal” from those with no appreciable cytocidal effect**  
 Illustrates 48hr PC1 (RoK) data plotted against the IC<sub>50</sub> potency for 188 Malaria Box compounds and seven benchmark antimalarials. The filled pink and blue circles represent drug-like and probe-like, respectively compounds initially determined to be “slow-acting” MMV compounds. Black and green circles represent MMV “fast-acting” controls and benchmark antimalarial drugs, respectively. The dotted lines in the middle represent CQ and ATOVA PC1 thresholds. The light blue and yellow shaded areas highlight the apparent Group-A and B, respectively, outcomes for the 178 “slow-acting” MMV compounds discussed in the main text.

Importantly, the PC1 analysis reveals that after a 48hr assay only one additional compound, MMV006250, could be potentially added to the list of TCP1 candidates (Table 5.6). This compound only just meets the TCP1 threshold, with all others slower than CQ and the majority slower than the more moderately acting amino alcohols.

MMV_ID	PC1_48hrs										
DHA	-87.0	MMV001344	-35.9	MMV665886	-9.4	MMV008127	4.5	MMV009085	22.8	MMV007041	51.7
MMV006250	-77.5	MMV396678	-33.9	MMV011438	-9.4	MMV019066	5.0	MMV011832	23.2	MMV396723	51.9
CQ	-77.3	MMV666103	-33.6	MMV666070	-9.4	MMV019670	5.6	MMV009060	28.0	MMV666600	54.4
MMV396680	-76.5	MMV011256	-33.6	MMV006457	-9.0	MMV645672	5.6	MMV006309	29.0	MMV396652	55.5
MMV665827	-75.8	MMV006389	-33.5	MMV007228	-8.9	MMV007557	7.1	MMV665980	29.5	MMV019762	58.8
MMV000699	-75.5	MMV665916	-32.8	MMV665798	-8.2	MMV007906	7.2	ATOVA	29.7	MMV396665	59.0
PPQ	-72.5	MMV006278	-32.8	MMV007571	-7.8	MMV006820	8.0	MMV019241	30.3	MMV665923	59.0
MMV665797	-70.7	MMV665909	-32.2	MMV665799	-7.4	MMV007839	8.1	MMV666693	30.3	MMV666601	59.4
MMV008956	-70.4	MMV008416	-31.6	MMV006188	-6.4	MMV000963	9.1	MMV665939	30.7	MMV498479	60.0
MMV666054	-67.4	MMV665994	-30.9	MMV665954	-6.4	MMV019700	9.7	MMV665820	32.3	MMV011576	61.1
MMV396679	-63.6	MMV665977	-30.7	MMV006767	-5.9	MMV019124	9.7	MMV665901	32.5	MMV007160	62.0
MEF	-63.0	MMV084434	-29.9	MMV665883	-5.5	MMV019074	10.1	MMV007384	32.9	MMV666062	63.3
QN	-62.9	MMV007577	-28.9	MMV008212	-4.5	MMV020548	10.6	MMV020439	34.7	MMV667489	67.0
MMV000720	-62.4	MMV403679	-28.4	MMV019258	-4.1	MMV006427	11.0	MMV396770	35.5	MMV000642	67.5
MMV007127	-60.5	MMV006319	-27.2	MMV007881	-1.8	MMV020492	12.2	MMV666692	36.5	MMV020942	68.7
MMV665875	-60.1	MMV084940	-25.5	MMV666607	-1.4	MMV075490	12.2	MMV000911	37.5	MMV020885	68.8
MMV667492	-58.3	MMV666125	-24.5	MMV396681	-1.4	MMV019202	12.6	MMV666093	38.3	MMV019690	73.8
MMV006753	-57.4	MMV000788	-24.1	MMV666106	-0.5	MMV665940	12.8	MMV666023	39.0	MMV086103	73.9
MMV665908	-56.3	MMV665879	-24.1	MMV000972	0.3	MMV666095	13.2	MMV665961	39.0	MMV638723	76.3
MMV665874	-52.2	MMV006962	-23.8	MMV007116	1.4	MMV007808	13.8	MMV396703	39.5	MMV396664	84.2
MMV000787	-47.6	MMV666067	-22.0	MMV665876	1.6	MMV007374	14.5	MMV396594	41.7	MMV073843	84.9
MMV666105	-47.5	MMV666691	-21.5	MMV665904	1.6	MMV666075	14.7	MMV019758	43.3	MMV666101	88.3
MMV007764	-45.5	MMV666072	-19.9	MMV665850	1.8	MMV396595	15.1	MMV665814	43.5	MMV007695	90.5
MMV007791	-44.3	MMV007430	-18.5	MMV000563	2.0	MMV000662	15.3	MMV019871	44.2	MMV665783	92.4
MMV007574	-43.3	MMV007564	-16.8	MMV007977	2.1	MMV009127	15.4	MMV011259	44.8	MMV666596	93.0
MMV665843	-43.2	MMV396705	-15.3	MMV665898	2.8	MMV665836	16.3	MMV085471	46.2		
MMV006861	-42.5	MMV006913	-14.3	MMV006937	3.3	MMV007396	17.2	MMV396726	46.7		
MMV666022	-41.7	MMV008160	-12.2	MMV665810	3.4	MMV008149	18.8	MMV008294	48.2		
MMV665927	-40.3	MMV666108	-11.6	MMV666009	3.6	MMV666688	19.8	MMV085203	49.3		
PYR	-37.7	MMV396693	-11.5	MMV019746	3.6	MMV665899	20.3	MMV396672	50.0		
MMV001246	-36.8	MMV020651	-11.1	MMV665840	3.7	MMV665934	20.4	MMV665782	51.3		
MMV011099	-36.0	MMV020700	-10.4	MMV666057	3.7	MMV007199	22.2	MMV666081	51.3		

**Table 5.6: Ranking of the 48hr PC1 data**

This list reports the relative order (fastest first) 48hr PC1 data for 178 Malaria Box compounds and known antimalarial drugs.

The apparent lack of new “fast-acting” MMV compounds after this extended 48hr incubation would suggest that a 6 hr BRoK assay is sufficient to quickly identify rapid acting cytotoxic compounds. Whilst this may need to be tested against a wider range of chemotypes, this assertion is certainly true for the MMV Malaria Box compounds.

Whilst the 48hr assay does not appear to offer any new indications for rapid acting cytotoxic drugs, the presence of two apparently distinct extremes in 48hr bioluminescence assay data was shown (Figure 5.7). To better represent these two groups, the 6hr and 48hr PC1 data for these 178 “slow-acting” MMV Malaria Box compounds was plotted against each other (Figure 5.8A). This figure readily identifies Group-A and B extremes in the 48hr BRoK assay data; with group A showing cytotoxic potency similar to benchmark antimalarial drugs and the “fast-acting” MMV Malaria Box controls and group B displaying no apparent cytotoxic activity even after 48hrs of incubation. The 48hr dose-dependent loss in bioluminescence of the top 20 members in each group clearly shows the difference in cytotoxic activity of the compounds in each group (Figure 5.8B). Whilst these are readily identified from the 48hr assay, the relative distribution of these groups within the 6hr BRoK assay data was done to see if this earlier assay data can provide some predictive indication of compounds that fall into these two groups. As both groups are initially defined using the 6hr PC1 data, the 20 compounds from each group were mapped on a plot where PC1 was plotted against the second principle component PC2 (6hr) data (Figure 5.9C). Note that PC1 and PC2 explained 89% and 8% variance in the 6hr data respectively. There is no apparent discrete distribution of group-A and B in this analysis and would suggest that no useful predictive information regarding cytotoxic activity after 48hrs can be determined for these 178 MMV Malaria Box compounds based on data available from a 6hr BRoK assay.

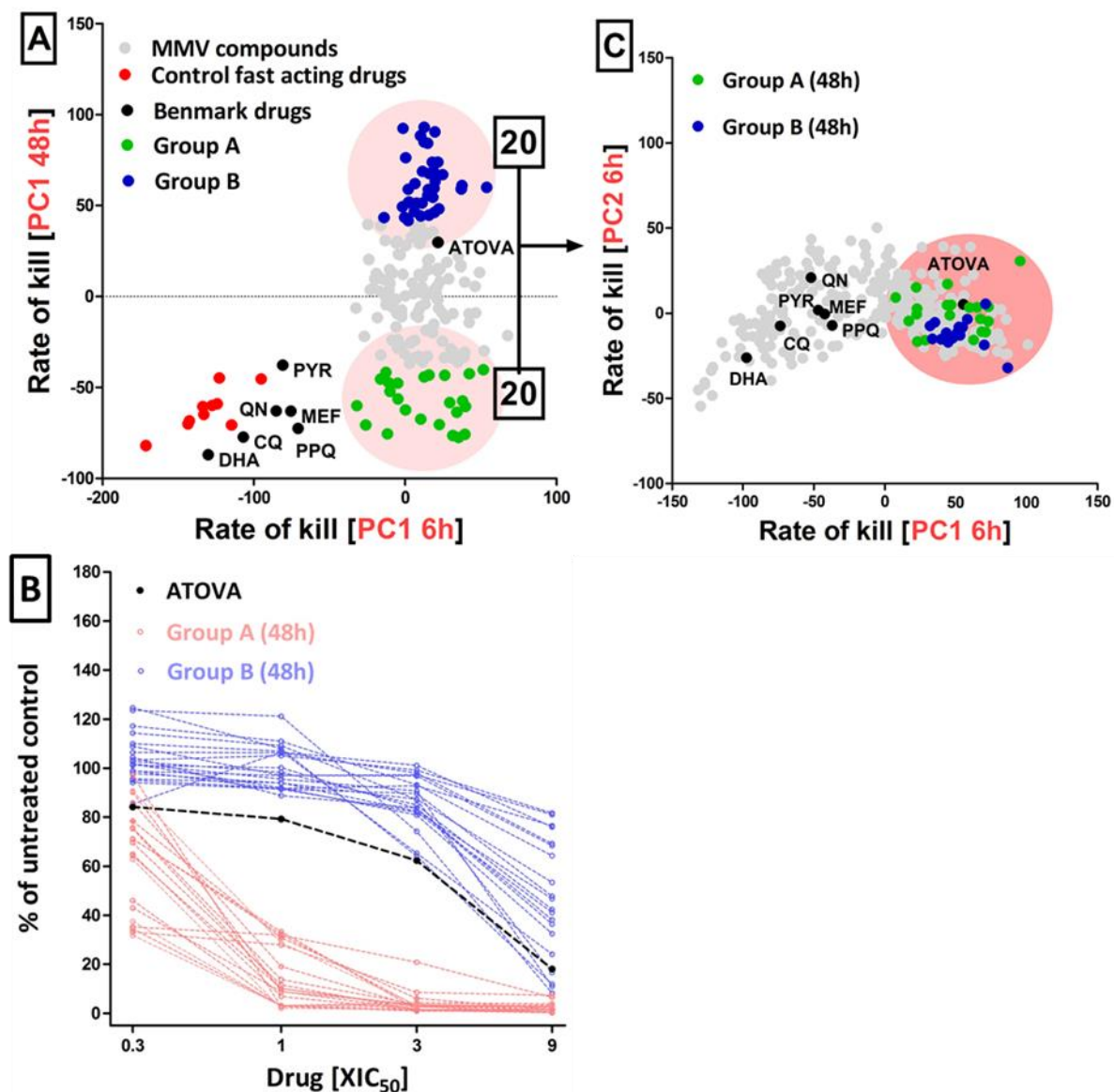


**Figure 5.8: Exploring the top 20 compounds with "slow-cytocidal" activity or no appreciable cytotoxic effect**

(A) Correlation between 6 and 48hr PC1 data for 178 Malaria Box compounds ( $r^2=0.148$ ,  $P < 0.0001$ ). Both Group A (green filled circles) and B (blue filled circles) are highlighted in light shaded pink circles. (B) The 48 hr dose-response curves of the top 20 members in each group (Group A and B), which shows the difference in cytotoxic activity of the compounds in each group. The black dotted curve represents ATOVA. (C) PC1 6hr data plotted against PC2 and 20 members of each group (Group A and B) are mapped (dark pink shaded circle).

### 5.3 Discussion

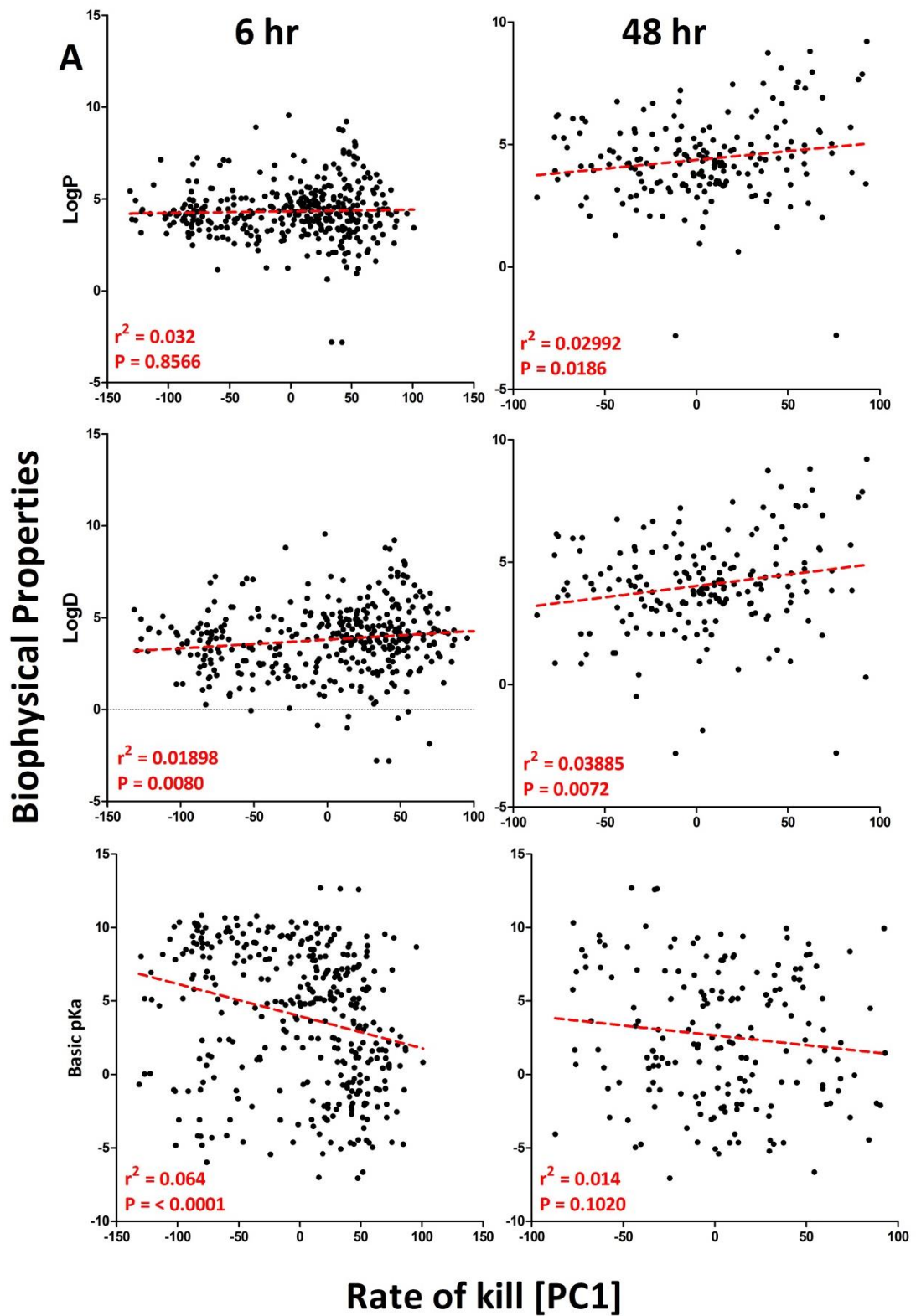
Together with the data developed in chapter 4, work described in this chapter provides an analysis of the immediate cytotoxic action of 370 (92.5%) of the 400 MMV Malaria Box compounds. When the 6hr BRoK assay data were pooled together (i.e. 178 “slow-acting” compounds from this chapter with 192 “fast-acting” compounds reported in chapter 4) a single Principle Component Analysis was done. This analysis showed that the 53 TCP1 candidates (i.e. an immediate rate of kill > CQ) reported in chapter 4, were subsequently confirmed to be TCP1 candidates when all 370 compounds were analysed. In addition, three compounds that were initially determined to be just below the CQ threshold in chapter 4 were classified in the second PCA to just fall on the other side of the CQ threshold. This is perhaps not unexpected as data for 178 compounds were added to the PCA that stretched out the distribution of the PC1 data on the plot, and those compounds that fell on either side of CQ do so very closely. Importantly, the 17 ideal TCP1 candidates (i.e. immediate rate of kill > DHA) that were reported in chapter 4 were also re-confirmed in this analysis with no other MMV compounds moving into this category. The minimal change to the classification of potential TCP1 candidates from the MMV Malaria Box based on these two PCA of the BRoK data suggests that this is a robust assay for the determination of rapidly acting cytotoxic compounds against the trophozoite intraerythrocytic stage.

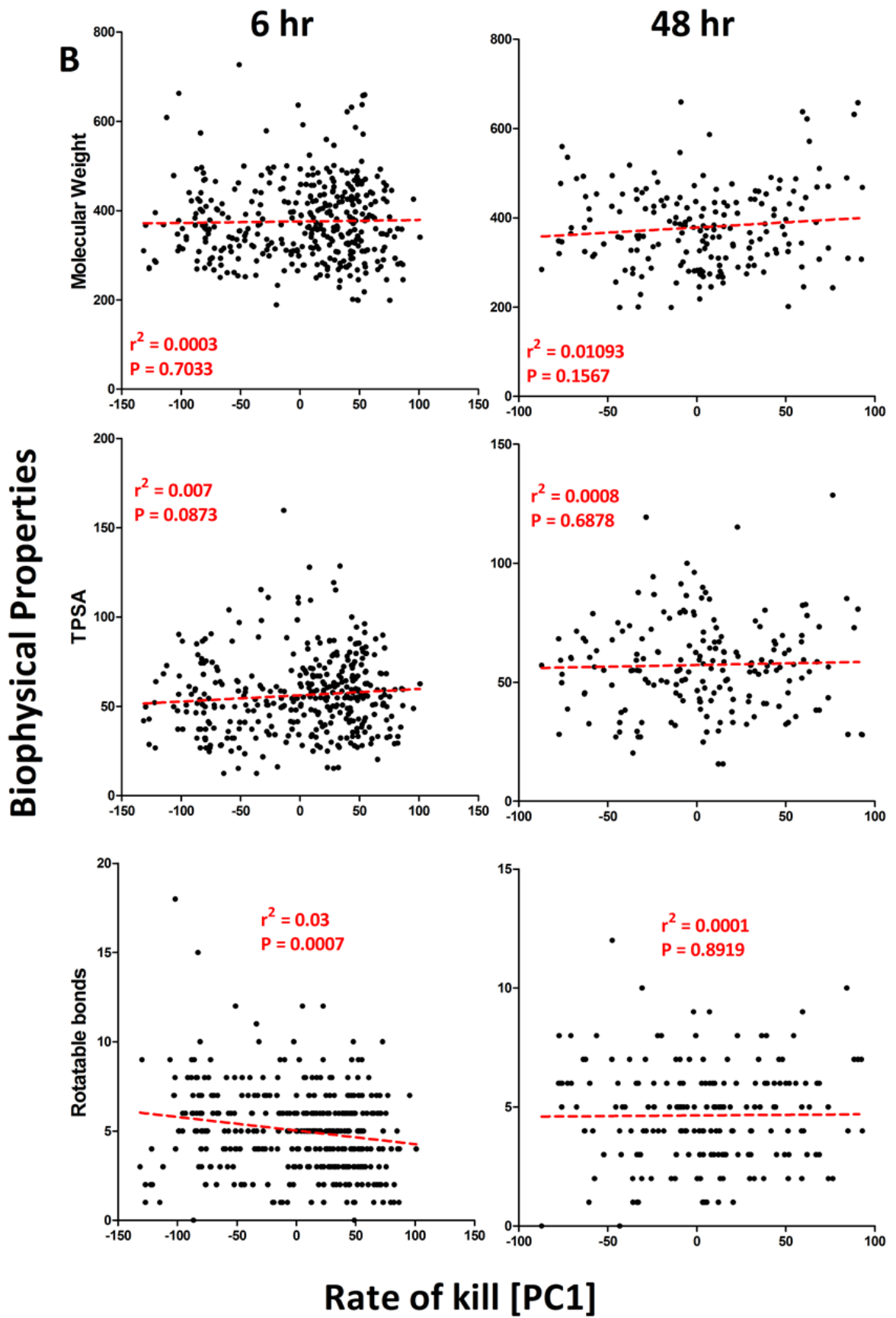
This rapid initial cytotoxic activity likely results from two principle contributing aspects of the drug’s action. The first aspect considers the target of the drug and how quickly a deficit in this target’s function will lead to cell death – perhaps best termed “mode of action”. Sanz *et al.*, (2012) considered in their recrudescence assay that compounds with

a similar mode of action would result in similar rates of kill. This is certainly supported by the evidence presented for the benchmark antimalarial compounds with artemisinins > 4 amino quinolones > amino alcohols. But this is a limited pool of drugs and also a collection of drugs that have been through development to enhance their pharmacodynamic/pharmacokinetic properties for optimal clinical use. Given the very short timeframe for determining cytotoxic action in the 6hr BRoK assay, and the early stage of development for the MMV Malaria Box compounds, a second attribute of these compounds may influence their immediate rate of kill – ease of access to their target. Within this *in vitro* assay, the compounds need to migrate through up to four membranes to access their target, and biophysical parameters based on their size, hydrophobicity and charge may contribute significantly to how easily they access their target. Another consideration, and one that is important for compounds with a basic charge at physiological pH, is that of potential access and concentration within the digestive vacuole in the trophozoite parasite, irrespective of whether this is the final site of their target. These biophysical properties are considered in predictions of *in vivo* bioavailability through the oral route, again considering that size, hydrophobicity and charge of a compound are important in the absorption and distribution of a drug. A set of rules to predict compounds most likely to act as an orally active drug was described by Lipinski in 1997 based on his analysis that demonstrated that commercial drugs tended to be small and moderately lipophilic (Lipinski *et al.*, 2001; Lipinski *et al.*, 2012; Lipinski, 2004). These analyses developed the Rules-of-5 (Ro5); a molecular weight of less than 500, no more than five hydrogen bond donors, less than ten hydrogen bond acceptors and an octanol-water partition coefficient (LogP) of less than five (Leo *et al.*, 1971). These rules have been

slightly modified with other factors considered more informative, e.g. total polar surface area, in refining these rules (Ghose *et al.*, 1999; Veber *et al.*, 2002). Given the importance of these biophysical parameters in the development of drugs and their potential effect in providing access for compounds to their targets, the following parameters were determined for the 370 MMV Malaria Box compounds and plotted against the 6hr and 48hr PC1; molecular weight, Log P, number of hydrogen bond donors and acceptors, total polar surface area ( $\text{\AA}^2$ ), number of rotatable bonds and most basic pKa. In addition, common modification of LogP was explored, the distribution coefficient (LogD) which considers the octanol-water distribution of the ionized and non-ionized forms of the compound at physiological pH (Figure 5.9, appendix 4).

Regression analyses of these data typically reveal a weak correlation between 6hr, and 48hr rate of kill and the biophysical properties explored. This is perhaps not surprising given the diverse range of chemotypes apparently available in the MMV Malaria Box and the potential for a large number of biological processes being targeted. The utility of this approach in understanding whether modifications to biophysical properties affect the rate of kill will perhaps be best done through the isolation of these properties from the intrinsic rate of kill provided when different targets are investigated. Therefore, modifications around a core chemical scaffold that presumably hits the same target may offer the means to look at how biophysical properties affect rate of kill. Unfortunately, the ECFP4/Tanimoto Similarity approach to exploring chemotypes relatedness proved fruitless in chapter 4. This issue will be revisited in chapter 6 where medicinal chemist expertise was used to cluster related compounds based on their chemotype.





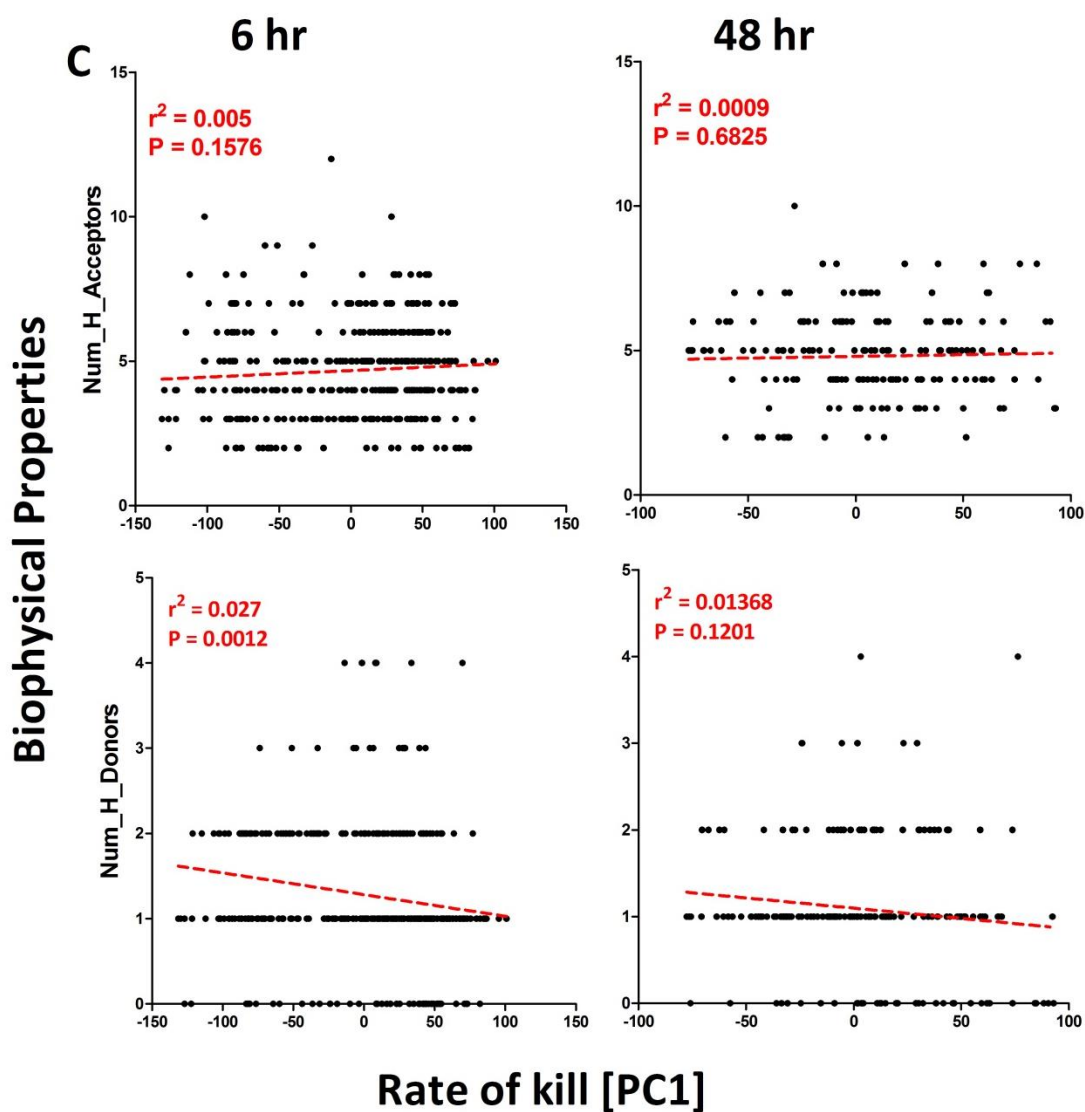


**Figure 5.9: Correlating biophysical properties against the RoK**  
 A, B and C reports linear regression plots of biophysical data plotted against rate of kill (PC1). ALogP/D = Octanol-water partition coefficient. TPSA = Total Polar surface area. H-Donors = Hydrogen bond donors. H-Acceptors = Hydrogen bond acceptors. PKa= Acid-base dissociation constant.

Comparison of the relative order of rate of kill of the MMV compounds after 6hr and 48hr, compared to the benchmark antimalarials, revealed only one additional compound that had been characterised as “slow-acting” in the 6hr assay format as now having a 48hr cytotoxic activity similar to CQ. This would suggest that for the determination of rapidly acting cytotoxic drugs (i.e. potential TCP1 candidates); the 6hr format is sufficient to provide a list of potential targets. The 48hr assay does not provide any further information in the selection of potential TCP1 candidates, and therefore means that the additional time and costs of this 48hr format are not necessary. The key information provided by the 48hr assay seems to be the description of two distinct groups of compounds. The first, group A, are compounds that after 48hr show a cytotoxic activity comparable to the “fast-acting” and benchmark antimalarial controls. Group B, by contrast, shows little cytotoxic activity up to  $3 \times \text{IC}_{50}$  doses of drug after 48hr and anything between 0-80 % kill at  $9 \times \text{IC}_{50}$ .

Given the potential for cytotoxic activity at intraerythrocytic stages other than trophozoites in the 48hr assay, the stage-specific activity data available from a high content imaging screen (Ayoung *et al*, in the Van Hooris publication) was compared for the top 20 compounds in each of group A and B (Figure 5.10). Of immediate note is that that 45% of group A and 20% of group B compounds report trophozoite stage activity, contrasting with my own observation of the apparent lack of cytotoxic activity at this stage. Both groups report a range of stage-specificities that would be captured in the 48hr assay format, but no clear correlation that could help understand the different cytotoxic activities between these two groups. One observation of note, however, is that a

classification of no activity was made for 25% of group B with no compounds showing no activity in group A.

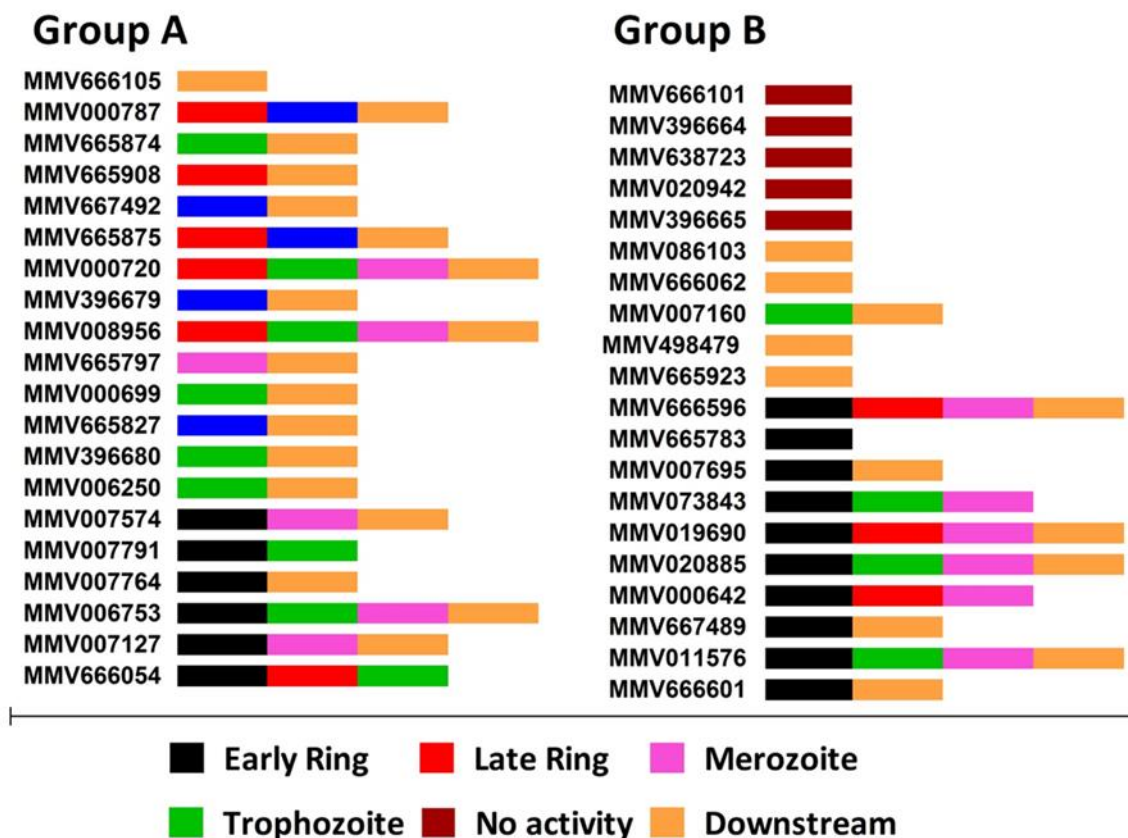


**Figure 5.10: Stage specific action of Group A and B compounds**

Stage specific action was reported by Ayoung group. The coloured bar, see key, reports the morphological stage activity is reported or if occurring subsequently (downstream) to ring-stage application.

These data would suggest that the cytotoxic activity observed in group A cannot be readily attributed to a specific stage-specific activity. Whilst it may well be the case that the different compounds in group A target a range of different developmental cycles – the similar distribution of stage-specific activities recorded for group B, where no appreciable cytotoxic activity was shown, would perhaps place a caution on this interpretation. Instead, it may well be that group A compounds are those that have a mode of action that includes a lag phase, after which the compound shows good cytotoxic

activity (e.g. pyrimethamine, Sanz *et al.*, 2012). Thus, given the absence of apparent activity after 6 hours, and the known lag phase for ATOVA, an estimate would suggest a lag phase of between 6 and 48 hrs may account for the rate of kill activity of the group A compounds. The implication for this is that whilst these compounds may not be suitable as a rapid-acting TCP1 component of a SERCaP medicine, these compounds may, depending upon their PK/PD properties, be able to act as a “long lasting” TCP2 component. Alternatively, if they show an excellent clinical safety profile, they may meet the TCP4 requirement for a long lasting TPP2 for potential mass drug administration.

Group B compounds may be subject to a prolonged lag phase of up to 48hr (one complete cycle of development), noting that these compounds are slower than ATOVA which has a 48hr lag phase. A clue to their apparent lack of cytotoxic activity after 48hr is provided by the comparison of the 48hr dose response in Figure 5.8B. Here it is clear that cytotoxic activities were only shown for some compounds when a  $9 \times IC_{50}$  dose was applied. In chapter 3 it was shown that whilst the apparent rate of kill doesn't correlate with the inhibitory or lethal doses of the antimalarial compounds tested, the rate of kill did correlate with the lethal dose/inhibitory ( $LD_{50}/IC_{50}$ ) dose ratio. Fast acting compounds like artemisinins have an  $LD_{50}/IC_{50}$  of 1, 4-aminoquinolines of between 5 to 10 and that of atovaquone is greater than 50. For those compounds that are exceptionally slow, the  $9 \times IC_{50}$  dose applied for 48hr may not reach the threshold for lethal activity of the drug – and thus, whilst the inhibitory effect can be measured (i.e. in a standard 48hr MSF assay) the cytotoxic activity cannot. Confirmation of this proposal, however, requires that the BRoK assay be utilised at much higher concentrations (likely, at least, up to  $100 \times IC_{50}$ ) and currently insufficient materials are available in my MMV Malaria Box resource (or the

concentration available is too low) to test this hypothesis. The implications for this group of compounds, however, are clear. These are not TCP1 candidates, nor, given their apparent lack of significant cytotoxic activity at up to  $9\times IC_{50}$  doses, are they likely to be TCP2 or TCP4 candidates. Outside of the scope of this thesis, is their potential as a compound that target either the intrahepatic (TCP3a) or gametocyte (TCP3b) stages of the *P. falciparum* lifecycle.

## CHAPTER: 6 Discussion

---

Massive phenotypic screens using some 2 million compounds from the small molecule libraries of GlaxoSmithKline (GSK), Novartis and St. Jude have identified a set of 20,000 compounds that exhibit sub-micromolar potency against the intraerythrocytic stages of *P. falciparum* (Gamo *et al.*, 2010; Guiguemde *et al.*, 2010; Plouffe *et al.*, 2008). These compounds, particularly novel chemotypes, are required to seed the antimalarial development pipeline to meet the demands for future antimalarial medicines such as the Single Exposure Radical Cure and Prophylaxis (SERCaP) target product profile outlined by MMV. Whilst these screens have pump-primed the drug development pipeline, efficiently exploiting this new resource relies on new assays for candidate components of a future SERCaP. Whilst these include assays for gametocidal and hepatocyte stages (Burrows *et al.*, 2013), this thesis has focused on Target Candidate Profile 1 (TCP1), drugs that exhibit rapid and potent cytocidal activity.

There are a number of rate of kill assays that offer the opportunity to identify TCP1 candidates. The first *in vitro* rate of kill assay was the recrudescence assay developed at the GSK Tres Cantos site (Sanz *et al.*, 2012). This assay perhaps represents the gold standard in the *in vitro* assay of rate of kill, providing data on PRR, PCT and lag phase. These data allow for the discrimination between minimum TCP1 candidates (better than chloroquine) and ideal candidates (better than artemisinins), although the challenging technical aspects of the dilution and parasite recrudescence over a 21-28 day assay limits the applicability of this assay to small scale lead validation assays (Baragaña *et al.*, 2015; Hameed *et al.*, 2015; Mcconville *et al.*, 2015). A South Africa/Swiss collaboration led to

the report of a rate of kill and stage specificity assay based on repeated daily determination of  $IC_{50}$  over three days using the highly sensitive [ $^3H$ ]-hypoxanthine incorporation assay (Le Manach *et al.*, 2013). Whilst offering the advantage of a relatively simple assay format, the assay does not discriminate between minimum and ideal TCP1 candidates as well as having limited appeal based on the requirements for scintillation counting equipment and disposal of radioactive waste.

The GSK team have developed two further rate of kill assays, one published just as this thesis was being completed (Bahamontes-Rosa *et al.*, 2012; Linares *et al.*, 2015). The first, based on real-time PCR of mRNA isolated from drug-treated parasites proved useful only in discriminating between cidal and static activities. The 10 day assay, as well as the technical molecular processing steps, has limited the development and application of this assay. More recently, Linares *et al.*, (2015) reported a rate of kill assay based on reinvasion of parasites that have been subjected to a 24hr or 48hr  $10 \times IC_{50}$  drug bolus. These drug-treated parasites are used to infect uninfected fluorophore labelled erythrocytes, with flow cytometry used to identify the proportion of living parasites that are capable of invading on the basis of their dual labelling with a DAPI nuclear stain. As with the original recrudescence assay, the assay is not dependent on changes in metabolic activity in dead and dying cells, a concern for some chemotypes, particularly those that inhibit DNA metabolism (Sanz *et al.*, 2012). The assay does, however, take between 3-4 days to complete and again offers no ability to discriminate between the minimum and ideal categories of TCP1 candidates. The report describing the invasion rate of kill assay provided data on the relative (fast, moderate, slow) rate of kill for a small number of MMV Malaria Box compounds as well as benchmark antimalarial drugs used in

this study. To explore the correlation between the bioluminescence and invasion rate of kill assays, a scatterplot of PC1 data from 6hr and 48hr BRoK assay data was plotted and the reinvasion assay data overlaid. Figure 6.1 clearly shows the related distribution of data using these two assay techniques and provides a second independent validation of the BRoK assay (in addition to that presented in Chapter 3).

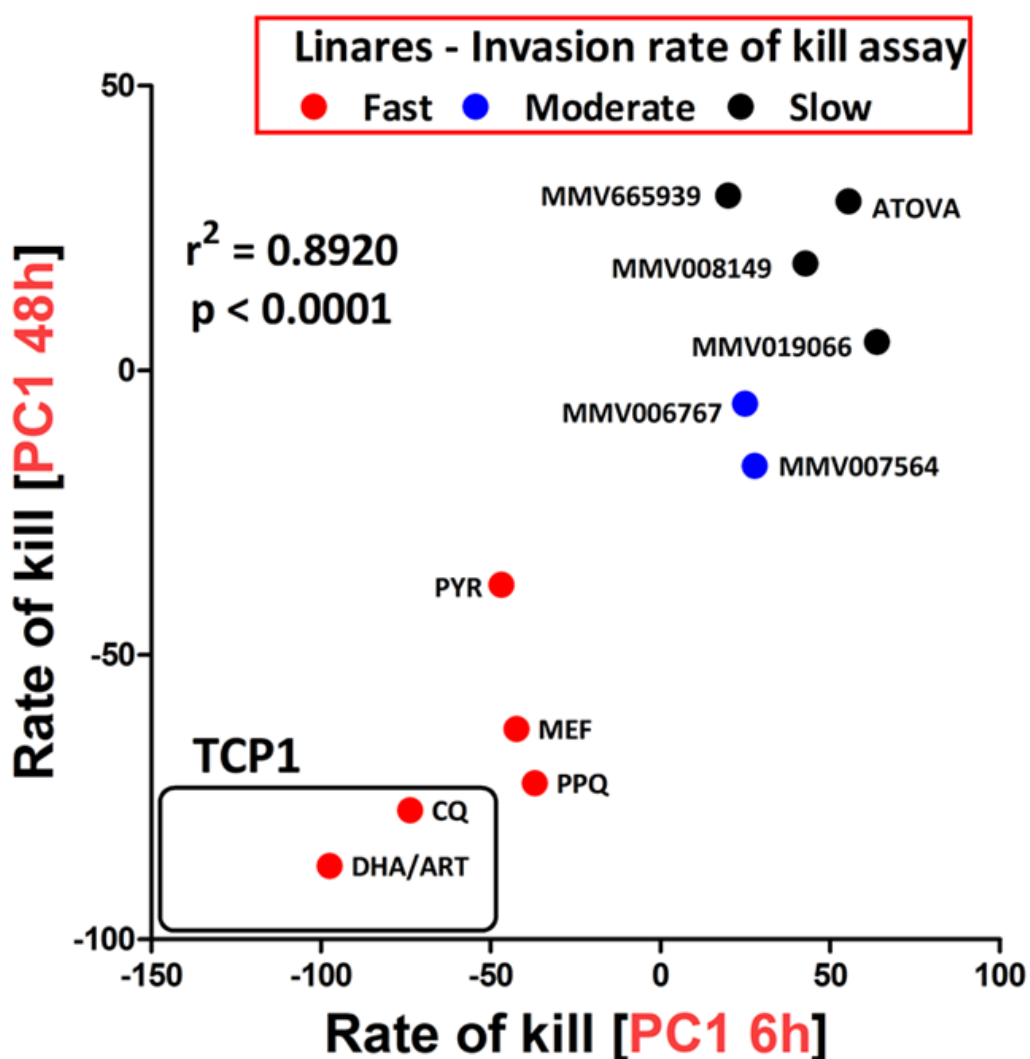


**Figure 6.1: Comparison between BroK and reinvasion rate of kill assay data.**  
The 6hr and 48hr BRoK PC1 for compounds also assayed using the reinvasion assay (Linares et al., 2015) are plotted and then overlaid with the invasion assay rate of kill outcome (see Key; black, blue and red filled circles show slow, moderate and fast definitions in the invasion assay). The box at the bottom left quadrant of the plot to represent the region that the BroK assay would define as being TCP1 candidates (note this box does not include all compounds categorized as “fast” in the invasion assay).

It is perhaps worth noting that the issue regarding the ability to discriminate between minimum and ideal TCP1 candidates is not limited to the assays described above. The same issue is also evident in the 48hr BRoK assay data (Chapter 5). This would suggest that there is some merit in exploring the utility of a reinvasion type assay that specifically uses a 6hr drug bolus prior to reinvasion – much like that initially explored here in Chapter 3 with the lethal dose estimation assays.

These varied assay formats offer a range of advantages and disadvantages (Table 6.1). The bioluminescence rate of kill assay developed here, validated in Chapter 3 and tested against the MMV Malaria Box compounds in Chapters 4 and 5, appears to offer a quick, robust and reliable assay for rapid cytotoxic activity. Importantly, this 6 hr assay offers the level of discrimination between minimum and ideal TCP1 candidates that are only offered elsewhere in the 21-28 day recrudescence assay. The BRoK assay scalability was demonstrated in Chapter 4 by the application of a single timepoint/single  $IC_{50}$  dose triage assay to the MMV Malaria Box. Currently, this is a 96-well microplate assay, using 200 $\mu$ l of a 2% haematocrit and 1% parasitaemia trophozoite stage culture, where only 40 $\mu$ l is taken for any bioluminescence assay. Given that 30 $\mu$ l cultures can be readily maintained for 6hr in a 384-well microplate, this offers significant opportunities for semi-automation of the BRoK assay to scale up to screen the 20,000 Tres Cantos Antimalarial Set (TCAMS). A quick calculation in Horrocks laboratory suggested that an investment of £250,000 would provide semi-skilled users and consumable costs to determine the TCP1 candidates in this library. In a facility with automation and bioluminescence detection for 1536-well microplates, the 10 $\mu$ l capacity of these wells, will likely still provide the robustness and sensitivity levels necessary for a successful high throughput assay. The opportunity

afforded through the rate of kill data for this compound library, with wider and deeper coverage of the chemotypes currently available in the MMV Malaria Box, is exciting given the potential to apply a chemical informatics approach to this important pharmacodynamic property of antimalarial drug action.

Assay type	Time for readout	Advantages	Limitations	Reference
Recrudescence growth	21-28 days	i) PRR, PCT and lag phase data ii) Differentiates between minimal/ideal TCP1 candidates iii) Not linked to cell metabolism	i) Low throughput ii) Technically difficult	Sanz <i>et al.</i> , (2012)
mRNA Real-time PCR	10 days	i) Readily determines cidal versus static activity	i) Low throughput ii) Technically difficult iii) Cannot differentiate between minimal/ideal TCP1 candidates	Bahamontes-Rosa <i>et al.</i> , (2012)
Timed series of IC <sub>50</sub> measurements	3-7 days	i) Simple assay format ii) Amenable for scaling	i) Cannot differentiate between minimal/ideal TCP1 candidates ii) Radioactive waste	Le Manach <i>et al.</i> , (2013)
Reinvasion	3-4 days	i) Simple assay format ii) Amenable for scaling iii) Not linked to cell metabolism	i) Cannot differentiate between minimal/ideal TCP1 candidates	Linares <i>et al.</i> , (2015)
Bioluminescence	6hr	i) Simple assay format ii) Amenable for scaling iii) Differentiates between minimal/ideal TCP1 candidates	i) Requires GM parasite ii) Currently only assays trophozoites	This thesis

**Table 6.1: Advantages and disadvantages of current *in vitro* rate of kill assays for *P. falciparum*.**

In 2011, the MMV launched the Malaria Box as an open access resource to pump-prime lead development from the TCAMS library. This scheme recognised that whilst medicinal chemistry expertise principally lay within the pharmaceutical industry sector, the academic sector provided expertise in the biology of malarial parasites (Spangenberg *et al.*, 2013). To facilitate this interaction, the Malaria Box provided free access to a subset of the TCAMS that was optimised to reflect the diversity of chemotypes available, but also triaged to identify those that were drug-like or probe-like. This library has now been

provided to some 200 groups worldwide for screens against malaria parasites, other parasites and even cancer cell lines (Van Voorhis submitted to PLoS Medicine). The significance of this resource will be demonstrated by comparison between the data freely shared by the many contributing laboratories on the same compound library. The Dd2 IC<sub>50</sub> data developed for 396 of the compounds during this study have shared with ChemBL data repository. Moreover, the 6hr BRoK data for 370 of the MMV Malaria Box compounds (92.5%) will be shortly submitted to ChemBL. Within chapters 4 and 5, the utility of this open access resource was shown by comparison of the BRoK data against what has been determined regarding the stage of kill data provided by the Ayoung team from high content imaging screens. As a second example of the utility of this sharing of data, Horrocks laboratory has collaborated with the LÍnas laboratory (Princeton University, USA) to compare the BRoK data against their metabolomic profiling data. The LÍnas team has mapped the metabolic profile of 65 metabolites following a 48hr exposure to a 10xIC<sub>50</sub> dose for 80 compounds from the MMV Malaria Box. From their work they have identified a metabolic fingerprint that they suggest is indicative of an atovaquone-like mode of action (Figure 6.2). Atovaquone inhibits the *bc1* mitochondrial complex blocking the transfer of electrons through the mitochondrial electron transfer chain. The enzyme dihydroorotate dehydrogenase (DHODH) requires a functioning electron transport chain to facilitate recycling of the FMN/FMNH<sub>2</sub> cofactor. Without this, DHODH no longer reduces dihydroorotate to orotate which blocks the *de novo* synthesis of pyrimidines. As *P. falciparum* lacks a pyrimidine salvage pathway, it is reliant on the *de novo* synthesis of pyrimidines for DNA metabolism. The LÍnas laboratory has shown that atovaquone inhibition results in the accumulation of dihydroorotate and its precursor N-

carbamoyl-L-aspartate. This metabolic-fingerprint was also observed in 22 other compounds they screened, and they have suggested that these compounds share a related mode of action to atovaquone. Here, BRoK data indicate that atovaquone is a slow acting drug. To provide independent support for this metabolic-fingerprint, the 6hr PC1 BRoK data for the same 80 compounds were plotted against fold-changes in the levels of dihydroorotate and N-carbamoyl-L-aspartate (Figure 6.3).

Here, this analysis offered data for 22 compounds, of which 21 compounds also share a slow rate of kill. Whilst, not absolute proof that these compounds inhibit the mitochondrial electron transfers chain, there is a circumstantial link provided by the BRoK data regarding the lack of an immediate cytotoxic kill. Interestingly, one compound demonstrates a rapid cytotoxic activity, MMV666021. It may be the case that this compound doesn't target the mitochondrial electron transport chain, but instead targets the DHODH itself. However, a recent report describing DSM265, a triazolopyrimidine-based inhibitor of *Pf*DHODH, the first DHODH inhibitor to reach clinical development for the treatment of malaria, indicates an *in vitro* rate of kill similar to that of atovaquone (Philips *et al.*, 2015).

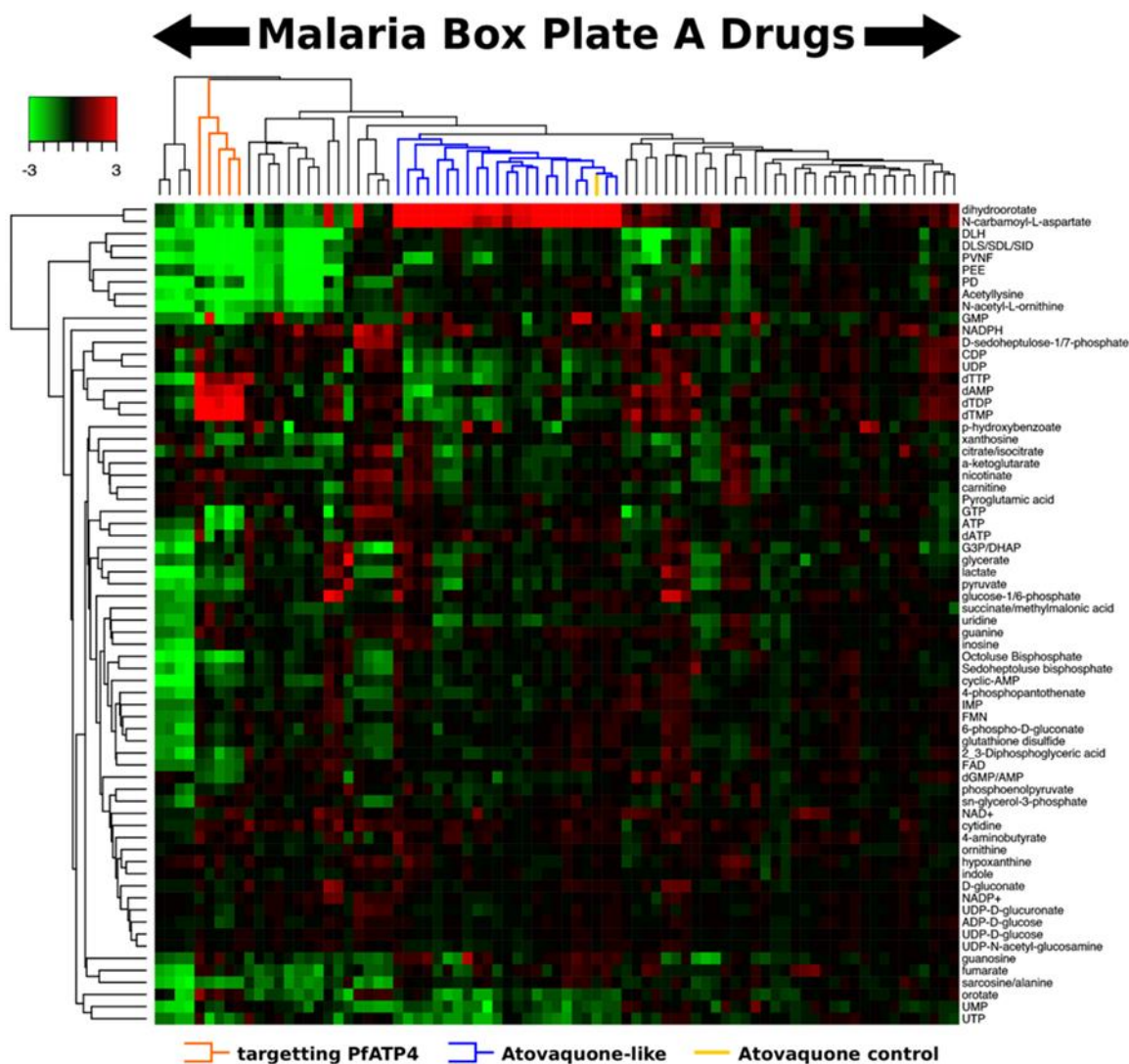


**Figure 6.2: Metabolic fingerprints of selected Malaria Box compounds**  
 Heat map showing metabolic fingerprints of Malaria Box plate A compounds and atovaquone control. Hierarchical clustering was performed on log<sub>2</sub> fold changes in metabolites scaled from -3 to +3. A large cluster of compounds exhibited an atovaquone-like signature (indicated in blue) characterized by dysregulation of pyrimidine biosynthesis. The atovaquone internal control is shown in yellow. (Figure kindly provided by the Línas laboratory).

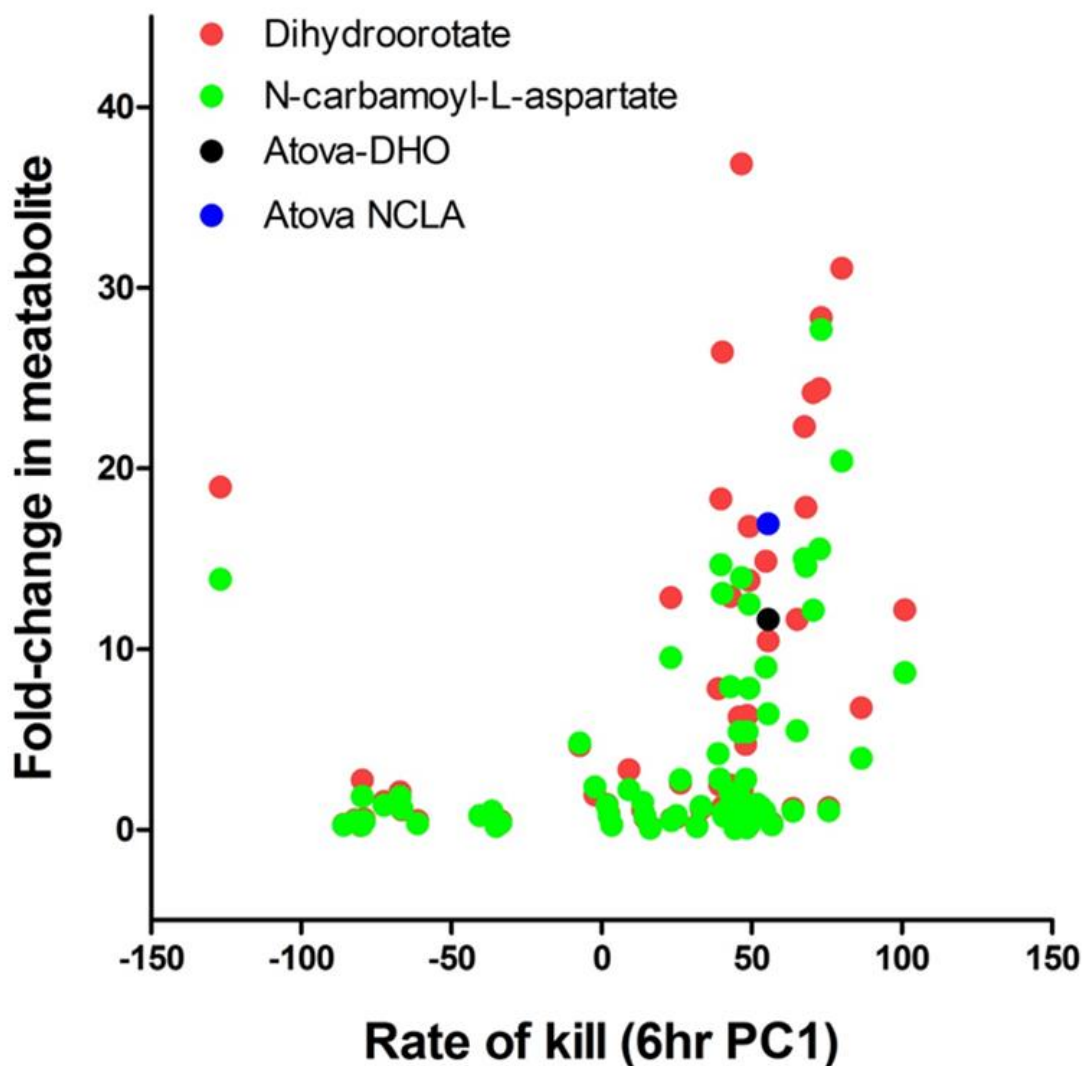


**Figure 6.3: Correlation between RoK and fold-changes in the metabolites DHO and NCLA**  
 This plot shows correlation between rate of kill (PC1 data from 6hrs) and the fold-change in dihydroorotate (DHO) and N-carbamoyl-L-aspartate (NCLA). Fold changes for these metabolites are shown for 80 MMV Malaria Box compounds (red and green, respectively) and atovaquone (black and blue, respectively).

This thesis has primarily considered the role for the BRoK assay in the hit identification stage of the drug development process. Here the utility of the screen provides a simple and quick means to identify rapid acting cytotoxic drugs from a large library dataset. The utility of the potency of a hit to be monitored in terms of both its  $IC_{50}$  and rate of kill potency simultaneously offers opportunities for this assay to be used in the latter stages of the pre-clinical drug development stages. Whilst the rate of kill is an intrinsic issue

related to the mode of action (Sanz *et al.*, 2012), biophysical properties that effect rapid access of drugs to the target are potentially important and can be readily explored in this simple cell based assay.

The principle for an intrinsic rate of kill is illustrated by a pilot study I conducted in the laboratory on four derivatives of 4-aminoalcohol quinolines for a collaborator Demailly-Mullié (University of Marseille, France). This class of compound includes mefloquine, a highly potent schizonticide with excellent PK/PD properties (Simpson *et al.*, 2000). Unfortunately, this drug consists of a racemic mix of stereoisomers, where the (-) *erythro* enantiomer is less potent against *P. falciparum* but does interact with the adenosine receptors within the central nervous system to cause neurological side-effects for this drug (Toovey, 2009). The Demailly-Mullié team has prepared stereospecific compounds to further explore the potential to develop new 4-aminoalcohol quinolones that lack these side effects and show greater potency than mefloquine (Dassonville-Klimpt *et al.*, 2013; Mullié *et al.*, 2012). However, given that these compounds all share the same target, just with different IC<sub>50</sub>, here this study collaborated to explore whether the iso-fold IC<sub>50</sub> doses used in the BRoK assay would mean that similar rates of kill would be observed for two stereoisomers of two compounds that have 5 carbon or 7 carbon chains added to the C11 position of a 4-aminoalcohol quinolones backbone. The BRoK assay data shown in Figure 6.4 would seem to support the assertion that these four related compounds share a similar immediate cytotoxic effect, supporting the proposal that they share a common target in the parasite.

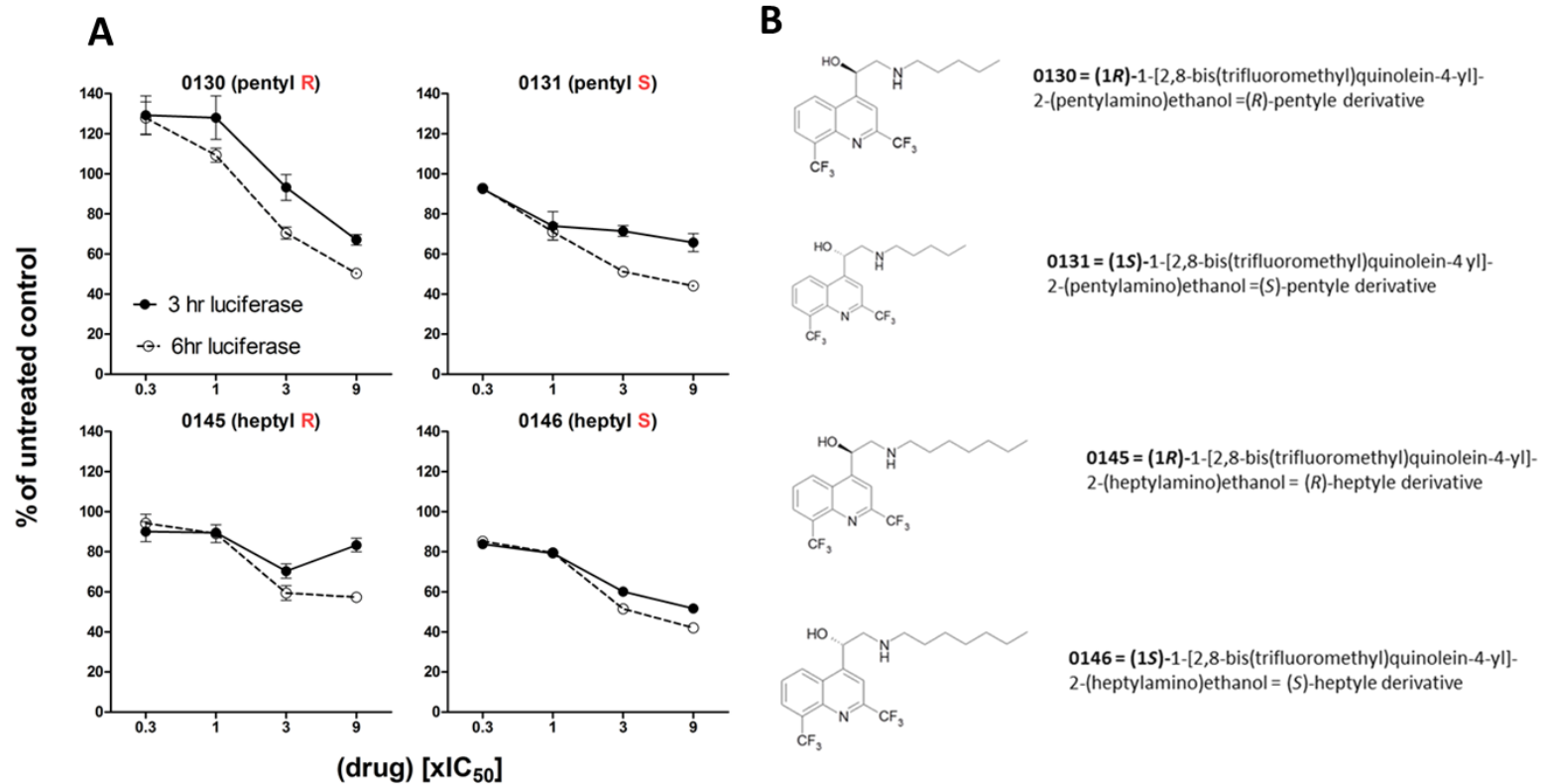
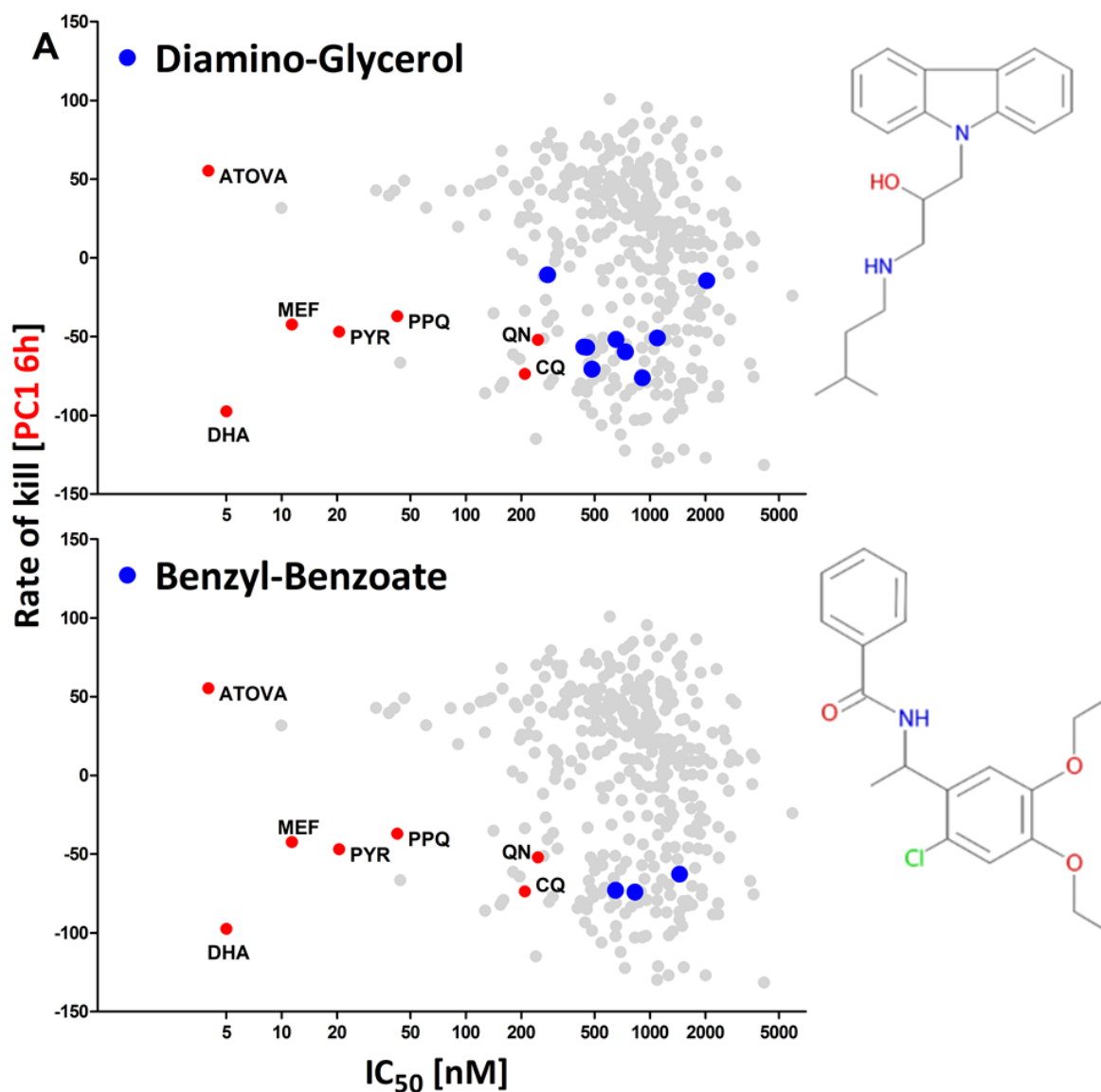


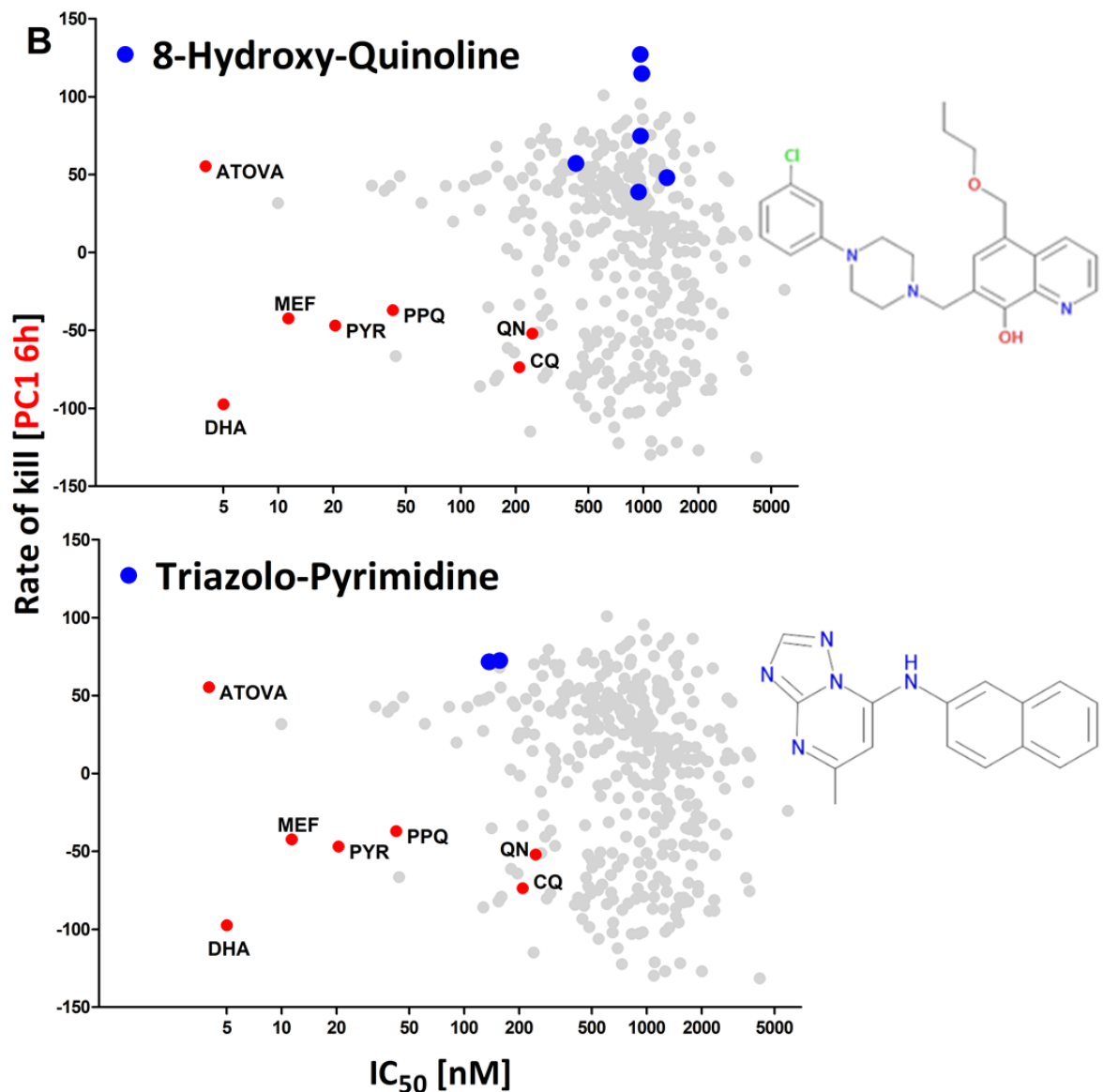
**Figure 6.4: Stereoisomers (R,S) of 4-aminoalcohol quinolines show the same rate of kill in the BRoK assay**  
 (A) BRoK plots for R and S isomers of pentyl or heptyl substituted 4-amino-quinolines with their (B) structures illustrated along with their IUPAC terms.

This observation was also extended into my work on the MMV Malaria Box compounds. In a recent collaboration with MedSynDesign Ltd, Dr Tony Mete, a medicinal chemist with over 20 years' experience within the pharmaceutical sector, has been working with Horrocks laboratory to provide a classification of the compound library by related core scaffold structure. This medicinal chemist "expert" view is distinct to the chemical informatics approach previously done in chapter 4, which was based on similarity scores of computationally-derived extended chemical fingerprints. As an example of this approach, the 6hr PC1/IC<sub>50</sub> plot of the 370 MMV compounds have been overlaid with four scaffold structures; diamino-glycerols, benzyl-benzoates, 8-hydroxyquinolines and triazolopyrimidine (Figure 6.5). These plots clearly reveal an intrinsic rapid cytotoxic mode of action for the diamino-glycerols and benzyl-benzoates, with slow acting/cytostatic action for the 8-hydroxyquinolines and triazolopyrimidine. It is noting that the slow acting DSM235 is based on the triazolopyrimidine scaffold.

Whilst still in its early stages, Dr Mete's classification has also described chemical scaffold clusters which contain compounds that exhibit a wide range of immediate rate of kill. This distribution of rates of kill would suggest that either (i) these very similar compounds have different targets with different rates of kill or (ii) that the intrinsic rate of kill of a target is also modified by factors that affect the access of the drug to the target (as discussed in the discussion to chapter 5). The second option suggests an interesting opportunity, that as well as using medicinal chemistry to optimise IC<sub>50</sub>, the same may also be true for rate of kill for some chemical scaffolds. This effect was also observed by Haddi Mybe, an MPhil student in the Horrocks laboratory (MPhil thesis entitled "The antimalarial properties of N-phenyl-3-(pyridyl)-4 substituted pyrazole scaffolds", 2015). In

her thesis, she initially characterised, using the same BRoK assay, the initial rate of kill for 28 compounds in three related pyrazole scaffolds with a range of minor substitutions to a phenyl ring substituent. Interestingly, the SAR for the  $IC_{50}$  did not correlate with that for the rate of kill, with amino substituted phenyl rings having some of the highest  $IC_{50}$ , but were potential TCP1 candidates in terms of their 6hr rate of kill.

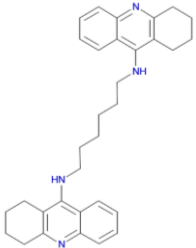
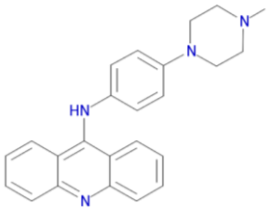
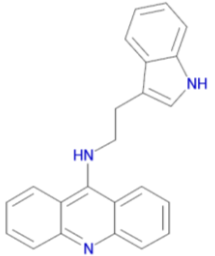
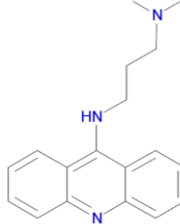
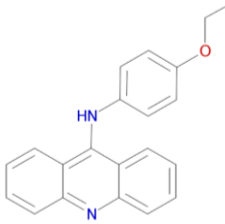
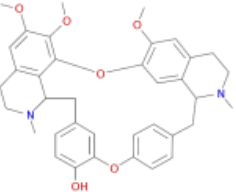
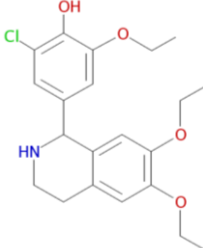
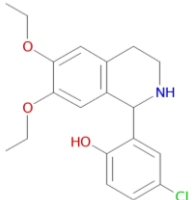
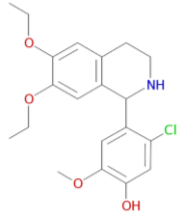
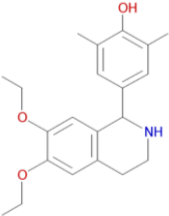




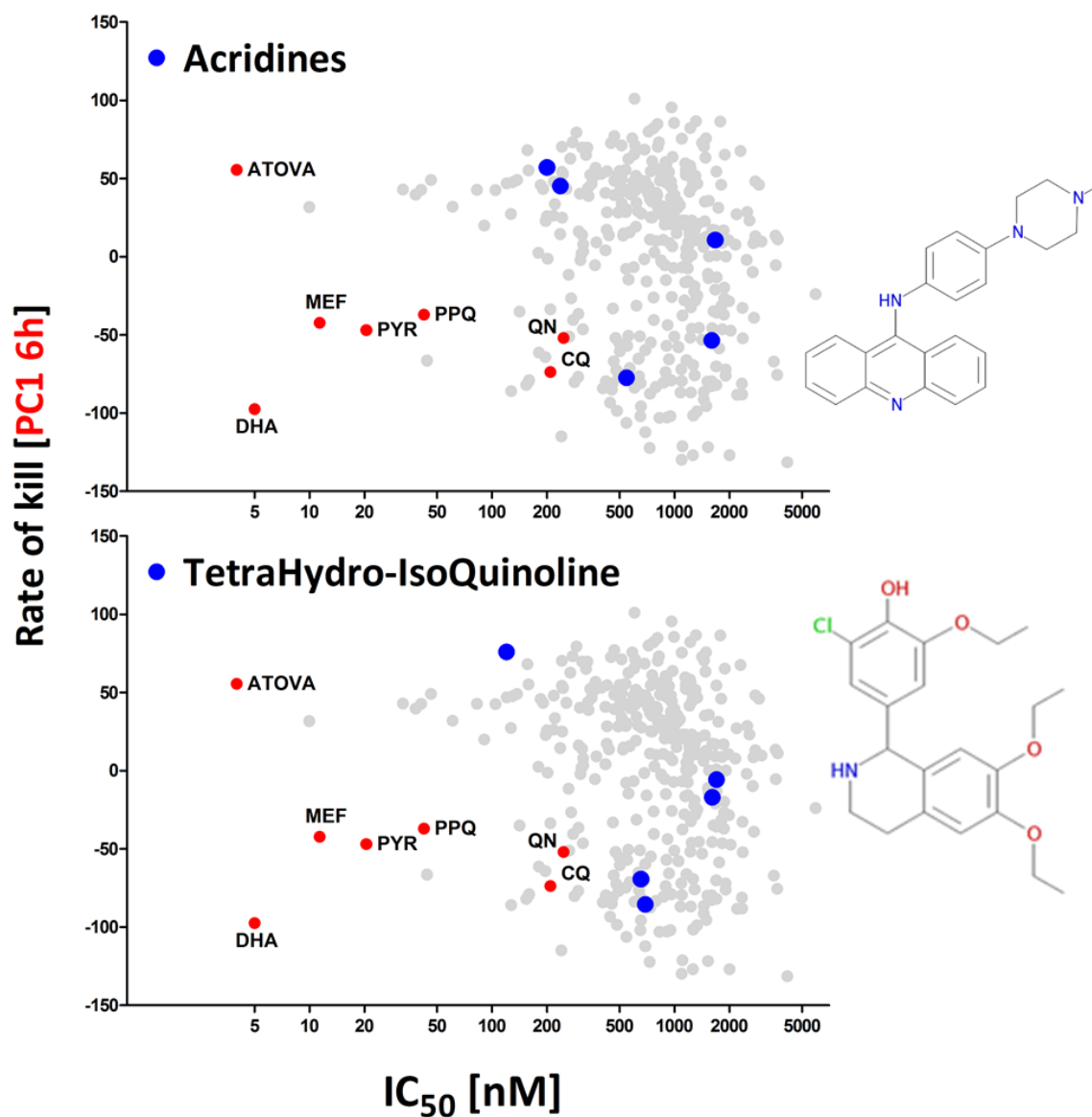
**Figure 6.5: Examples illustrating related compounds in the Malaria Box that share a similar rate of kill** (A) Represent two scaffolds that appear to show intrinsic rapid cytotoxic kill with (B) two scaffolds with intrinsic slow/cytostatic mode of action. The Blue circles represent the members of each scaffold projected against grey (370 compounds from MMV Malaria Box) and red (benchmark antimalarials) circles. Shown against each plot is an exemplar compound from this scaffold.

Plotting 6hr PC1/IC<sub>50</sub> plot of the 370 MMV compounds overlaid with information for two additional scaffolds (tetrahydroisoquinolines and acridines) show how the 5 compounds in each cluster are distributed between chloroquine and atovaquone in terms of their immediate rate of kill (Table 6.2). These clusters are shown in figure 6.6, with their

biophysical properties plotted against the 6hr PC1 rate of kill (Figure 6.7). Whilst these comparison plots reveal no significant correlations, as they only represent 5-6 compound clusters, some trends appear potentially interesting. The LogP and pKa, with LogD (a derivative of these values) for tetrahydroisoquinolines, show a potentially inverse trend between rate of kill and these parameters. That is, tetrahydroisoquinolines that are more basic and lipophilic are faster acting. Comparison between two, MMV008956 (IC<sub>50</sub> 120nM and PC1 of 75.9 [slower than atovaquone]) and MMV000483 (IC<sub>50</sub> 653nM and PC1 of -69.3 [similar to chloroquine]), share the same structure with minor substitutions to one phenyl ring (Table 6.2). Ideally, a TCP1 lead would have an IC<sub>50</sub> better than MMV008956 with an initial rate of kill better than MMV000483. As a starting point, additional tetrahydroisoquinolines in the TCAMS library would be sought to refine the IC<sub>50</sub> and PC1 SAR, using the IC<sub>50</sub> and PC1 plots first described in this thesis (19 related compounds in the TCAMS library). Using this information, a medicinal chemistry guided synthetic programme could design a series of compounds to test this SAR to design a viable lead. Of note, this may address the role for a bis-tetrahydroisoquinoline given the exceptional rate of kill, close to artemisinin, shown by MMV007474.

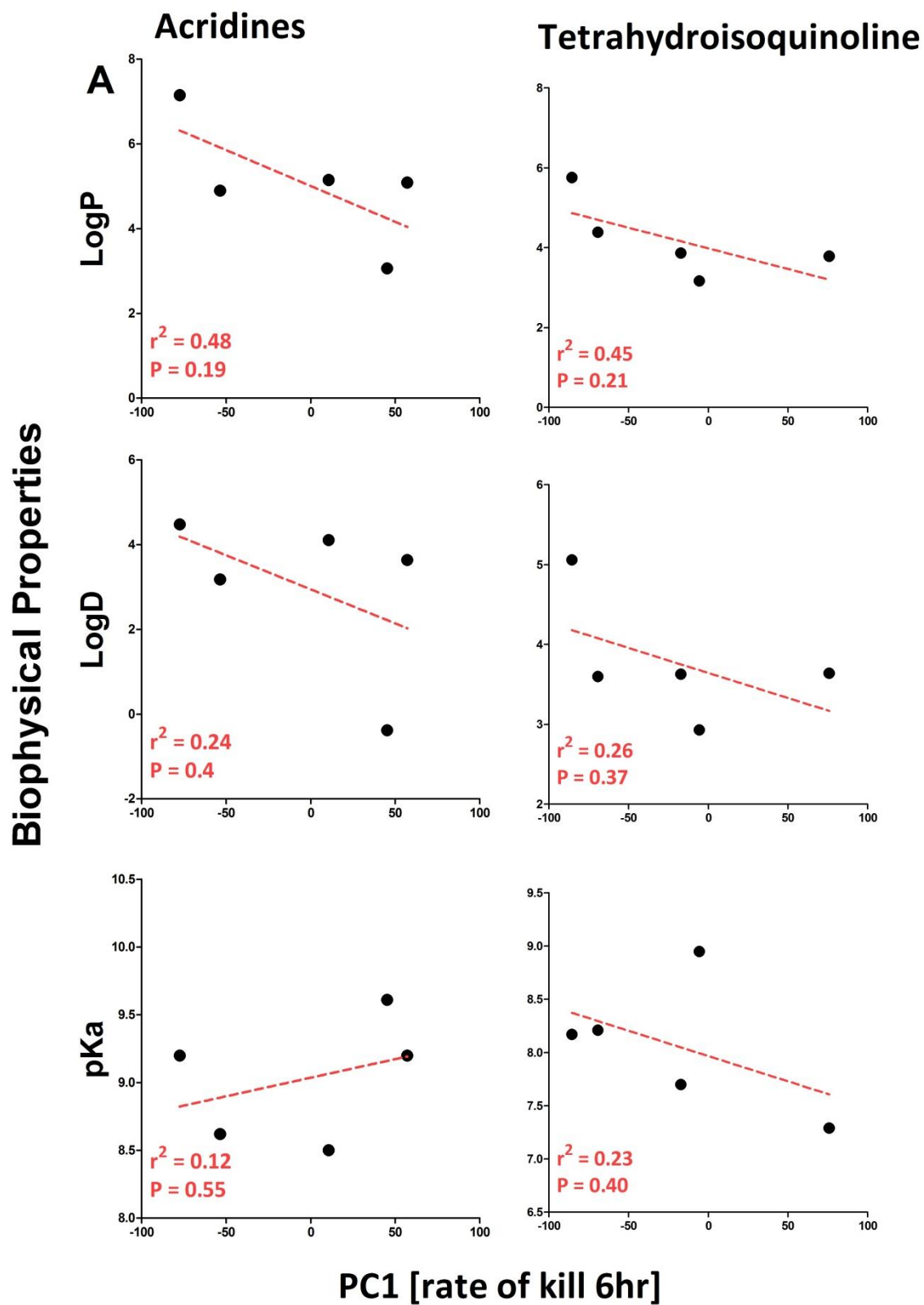
Acridines (Cluster 1)				
<b>MMV019555</b> <b>PC1 = -77.40</b> <b>IC<sub>50</sub> = 545.3 nM</b> 	<b>MMV006172</b> <b>PC1 = -53.56</b> <b>IC<sub>50</sub> = 1596.0 nM</b> 	<b>MMV006513</b> <b>PC1 = 57.09</b> <b>IC<sub>50</sub> = 200.0 nM</b> 	<b>MMV000448</b> <b>PC1 = 45.14</b> <b>IC<sub>50</sub> = 236.8 nM</b> 	<b>MMV000304</b> <b>PC1 = 10.62</b> <b>IC<sub>50</sub> = 1668.0 nM</b> 
TetraHydro-IsoQuinoline (Cluster 2)				
<b>MMV007474</b> <b>PC1 = -85.60</b> <b>IC<sub>50</sub> = 691.5 nM</b> 	<b>MMV000481</b> <b>PC1 = -17.13</b> <b>IC<sub>50</sub> = 1607.0 nM</b> 	<b>MMV000478</b> <b>PC1 = -5.60</b> <b>IC<sub>50</sub> = 1699.0 nM</b> 	<b>MMV008956</b> <b>PC1 = 75.91</b> <b>IC<sub>50</sub> = 120.1 nM</b> 	<b>MMV000483</b> <b>PC1 = -69.30</b> <b>IC<sub>50</sub> = 653.5 nM</b> 

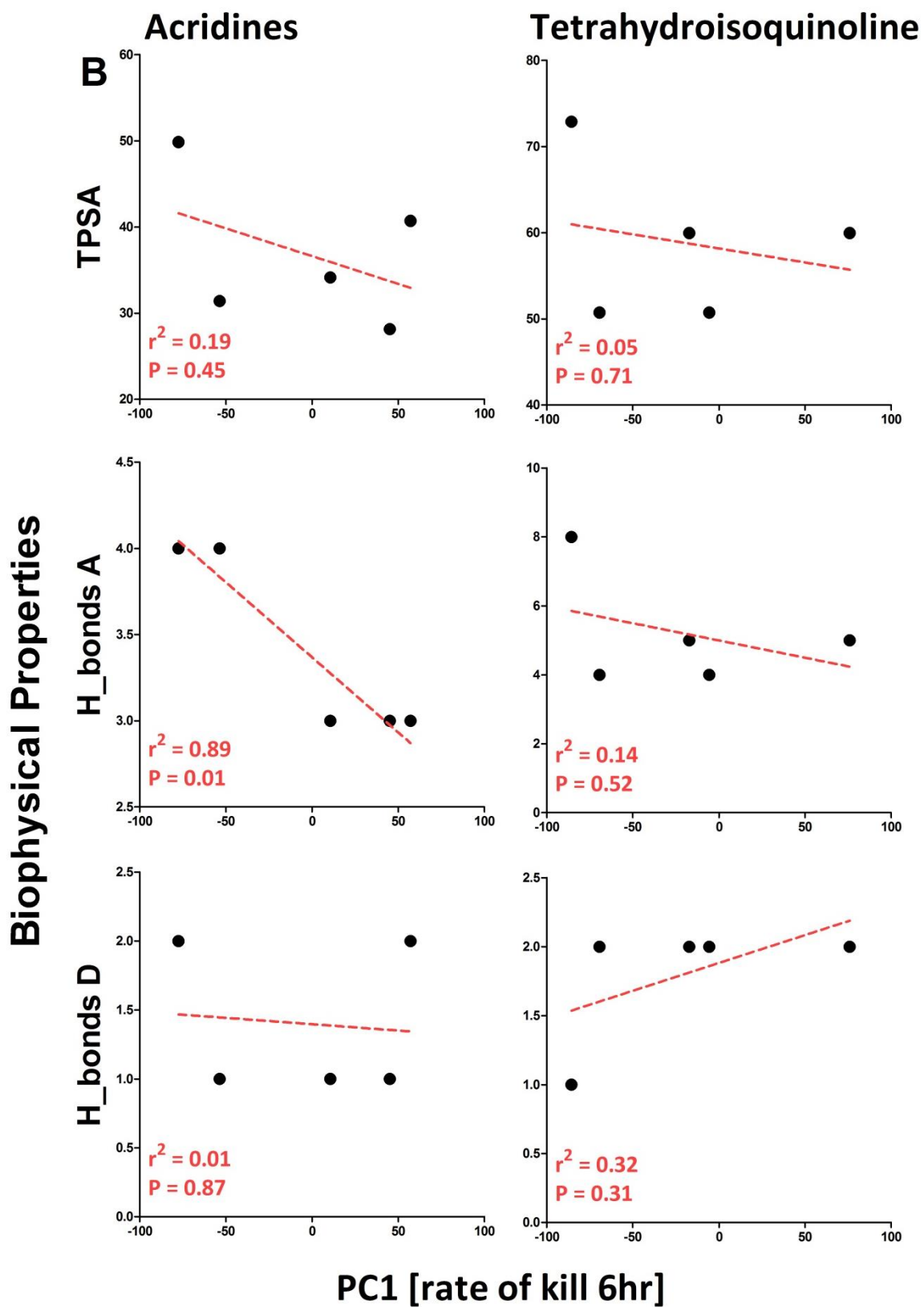
**Table 6.2: Structure of compounds within the acridines and tetrahydroisoquinoline clusters**  
The table reports MMV name, PC1 (rate of kill, 6hr) and IC<sub>50</sub> for each compound.



**Figure 6.6: Examples illustrating related compounds in the Malaria Box that show variation in their rates of kill**

The scaffolds appear to show both intrinsic rapid/cytocidal and slow/cytostatic mode of action. The Blue circles represent the members of each scaffold projected against grey (370 compounds from MMV Malaria Box) and red (benchmark antimalarials) circles. Shown against each plot is an exemplar compound from this scaffold.





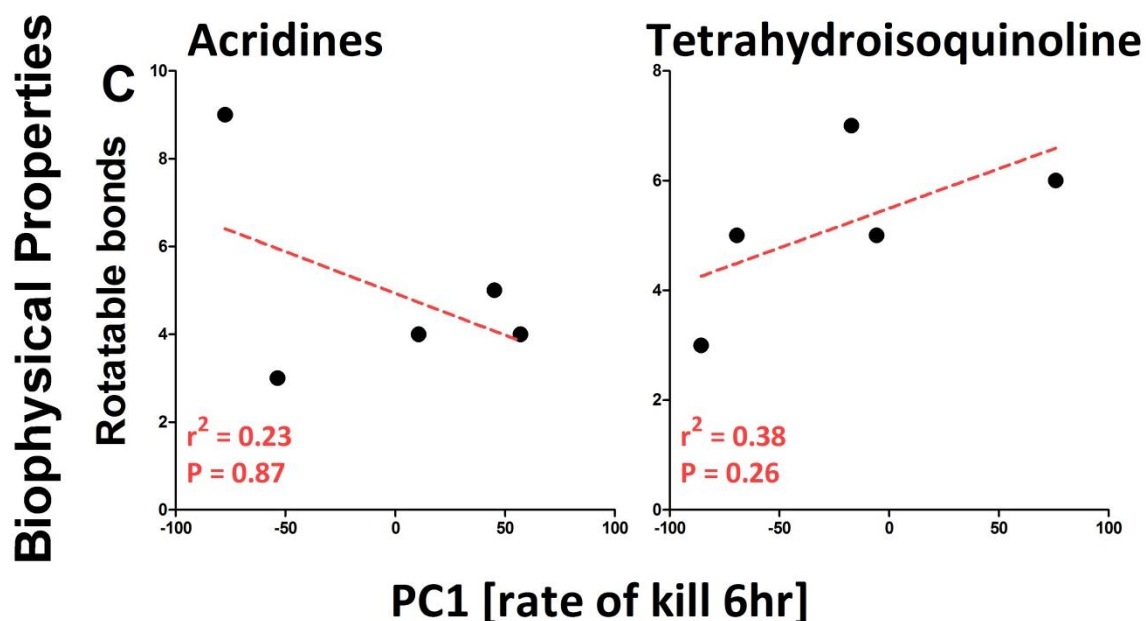


**Figure 6.7: Correlating biophysical data against rates of kill for Acridine and Tetrahydroisoquinoline scaffolds in the Malaria Box**

A, B and C - linear regression plots of biophysical properties plotted against the 6hr PC1 rate of kill for two scaffolds (tetrahydroisoquinoline and acridines) of medicinal chemistry interest. **LogP/D** = Octanol-water partition coefficient. **TPSA** = Total Polar surface area. **H-Bonds-D** = Hydrogen bond donors. **H-Bonds-A** = Hydrogen bond acceptors. **PKa**= Acid-base dissociation constant

The utility of this bioluminescent assay of cell viability has been demonstrated here for hit discovery, with the potential for hit-to-lead development illustrated. The ease of the bioluminescence assay to measure cytotoxic effects offers significant opportunities for the future development of this assay format. The current *Pfpcna* luciferase cassette limits the temporal window for assays to the trophozoite stage of intraerythrocytic action. Subcloning of 5' and 3' intergenic regions that flank a strongly expressed gene in the ring stage parasite, e.g. the gene expressing the knob associated histidine rich protein (*kahrp*), may provide a luciferase expression cassette to explore cytotoxic drug action at this stage (Lanzer *et al.*, 1992) – and may be of particular interest given artemisinin's predicted action at this developmental stage. In addition, the work described here is only reported for the multidrug resistant line Dd2. It would be of benefit to genetically modify

additional parasite clones (e.g. chloroquine sensitive 3D7) or even laboratory adapted field strains in future studies. These additional genetically modified parasites offer the opportunity to screen, or validate, the findings described here for the MMV Malaria Box compounds (or additional libraries screened in the future) in a different genetic (and potentially drug resistant) background. Moreover, the microplate format may allow more interesting studies that explore synergy in rate of kill to parallel the recent advances that have been made by Prof Paul Roepe of Georgetown University, USA, with his work on synergy with lethal doses of antimalarial drugs (Sherlach and Roepe, 2014). Of particular interest to my laboratory is the ability to use these bioluminescent parasites to define and titrate a cytotoxic kill within 6hr for a range of antimalarial drugs. This allows comparative studies on the ultrastructure, transcriptomic, proteomic, metabolomics and biochemical markers associated with cell death (mitochondrial membrane potential, nuclear DNA fragmentation, calcium redistribution, and caspase activity and phosphatidylserine redistribution) between different classes of antimalarial drugs – allowing the team to start to address just how parasites die when exposed to equivalent cytotoxic effects.

## References

---

- ADJALLEY, S.H., JOHNSTON, G.L., LI, T., EASTMAN, R.T., EKLAND, E.H., EAPPEN, A.G., RICHMAN, A., SIM, B.K., LEE, M.C., HOFFMAN, S.L. and FIDOCK, D.A., 2011. Quantitative assessment of *Plasmodium falciparum* sexual development reveals potent transmission-blocking activity by methylene blue. *Proceedings of the National Academy of Sciences of the United States of America*, **108**(47), pp. E1214-23.
- ALONSO, P.L. and TANNER, M., 2013. Public health challenges and prospects for malaria control and elimination. *Nature Medicine*, **19**(2), pp. 150-155.
- AMINO, R., GIOVANNINI, D., THIBERGE, S., GUEIRARD, P., BOISSON, B., DUBREMETZ, J., PRÉVOST, M., ISHINO, T., YUDA, M. and MÉNARD, R., 2008. Host cell traversal is important for progression of the malaria parasite through the dermis to the liver. *Cell Host & Microbe*, **3**(2), pp. 88-96.
- AMINO, R., THIBERGE, S., MARTIN, B., CELLI, S., SHORTE, S., FRISCHKNECHT, F. and MÉNARD, R., 2006. Quantitative imaging of *Plasmodium* transmission from mosquito to mammal. *Nature Medicine*, **12**(2), pp. 220-224.
- ANAND, A.C. and PURI, P., 2005. Jaundice in malaria. *Journal of Gastroenterology and Hepatology*, **20**(9), pp. 1322-1332.
- ANTINORI, S., GALIMBERTI, L., MILAZZO, L. and CORBELLINO, M., 2013. *Plasmodium knowlesi*: the emerging zoonotic malaria parasite. *Acta Tropica*, **125**(2), pp. 191-201.
- ANZALI, S., BARNICKEL, G., CEZANNE, B., KRUG, M., FILIMONOV, D. and POROIKOV, V., 2001. Discriminating between drugs and nondrugs by prediction of activity spectra for substances (PASS). *Journal of Medicinal Chemistry*, **44**(15), pp. 2432-2437.
- APONTE, J.J., MENENDEZ, C., SCHELLENBERG, D., KAHIGWA, E., MSHINDA, H., VOUNTASOU, P., TANNER, M. and ALONSO, P.L., 2007. Age interactions in the development of naturally acquired immunity to *Plasmodium falciparum* and its clinical presentation. *PLoS Med*, **4**(7), pp. e242.
- AUTINO, B., CORBETT, Y., CASTELLI, F. and TARAMELLI, D., 2012. Pathogenesis of malaria in tissues and blood. *Mediterranean Journal of Hematology and Infectious Diseases*, **4**(1), pp. e2012061.
- BAELL, J.B. and HOLLOWAY, G.A., 2010. New substructure filters for removal of pan assay interference compounds (PAINS) from screening libraries and for their exclusion in bioassays. *Journal of Medicinal Chemistry*, **53**(7), pp. 2719-2740.

- BAHAMONTES-ROSA, N., RODRÍGUEZ-ALEJANDRE, A., GONZÁLEZ-DEL-RIO, R., GARCÍA-BUSTOS, J.F. and MENDOZA-LOSANA, A., 2012. A new molecular approach for cidal vs static antimalarial determination by quantifying mRNA levels. *Molecular and Biochemical Parasitology*, **181**(2), pp. 171-177.
- BALMERT, N.J., RUND, S.S., GHAZI, J.P., ZHOU, P. and DUFFIELD, G.E., 2014. Time-of-day specific changes in metabolic detoxification and insecticide resistance in the malaria mosquito *Anopheles gambiae*. *Journal of Insect Physiology*, **64**, pp. 30-39.
- BANNISTER, L., HOPKINS, J., FOWLER, R., KRISHNA, S. and MITCHELL, G., 2000. Ultrastructure of rhoptry development in *Plasmodium falciparum* erythrocytic schizonts. *Parasitology*, **121**(03), pp. 273-287.
- BANNISTER, L.H. and MITCHELL, G.H., 2009. The malaria merozoite, forty years on. *Parasitology*, **136**(12), pp. 1435-1444.
- BARAGAÑA, B., HALLYBURTON, I., LEE, M.C., NORCROSS, N.R., GRIMALDI, R., OTTO, T.D., PROTO, W.R., BLAGBOROUGH, A.M., MEISTER, S. and WIRJANATA, G., 2015. A novel multiple-stage antimalarial agent that inhibits protein synthesis. *Nature*, **522**(7556), pp. 315-320.
- BARTOLONI, A. and ZAMMARCHI, L., 2012. Clinical aspects of uncomplicated and severe malaria. *Mediterranean Journal of Hematology and Infectious Diseases*, **4**(1), pp. e2012026.
- BARUCH, D.I., MA, X.C., SINGH, H.B., BI, X., PASLOSKE, B.L. and HOWARD, R.J., 1997. Identification of a region of *PfEMP1* that mediates adherence of *Plasmodium falciparum* infected erythrocytes to CD36: conserved function with variant sequence. *Blood*, **90**(9), pp. 3766-3775.
- BARUSCH, D., PASLOSKE, B., SINGH, H., BI, X., MA, X., FELDMAN, M., TARASCHI, T. and HOWARD, R., 1995. Cloning the *Plasmodium falciparum* gene encoding *PfEMP1*, a malaria variant antigen and adherence receptor on the surface of parasitized human erythrocytes. *Cell*, **82**, pp. 77-87.
- BATTLE, K.E., GETHING, P.W., ELYAZAR, I.R., MOYES, C.L., SINKA, M.E., HOWES, R.E., GUERRA, C.A., PRICE, R.N., BAIRD, K.J. and HAY, S.I., 2012. The global public health significance of *Plasmodium vivax*. *Advances in Parasitology*, **80**, pp. 1-111.
- BEIER, J.C., KILLEEN, G.F. and GITHURE, J.I., 1999. Short report: entomologic inoculation rates and *Plasmodium falciparum* malaria prevalence in Africa. *The American Journal of Tropical Medicine and Hygiene*, **61**(1), pp. 109-113.
- BEJON, P., WHITE, M.T., OLOTU, A., BOJANG, K., LUSINGU, J.P., SALIM, N., OTSYULA, N.N., AGNANDJI, S.T., ASANTE, K.P. and OWUSU-AGYEI, S., 2013. Efficacy of RTS, S malaria

vaccines: individual-participant pooled analysis of phase 2 data. *The Lancet Infectious Diseases*, **13**(4), pp. 319-327.

BELL, A., 2005. Antimalarial drug synergism and antagonism: mechanistic and clinical significance. *FEMS Microbiology Letters*, **253**(2), pp. 171-184.

BERTHOLD, M.R., CEBRON, N., DILL, F., GABRIEL, T.R., KÖTTER, T., MEINL, T., OHL, P., SIEB, C., THIEL, K. and WISWEDEL, B., 2008. KNIME: The Konstanz information miner. *Data analysis, machine learning and applications*. Springer, pp. 319-326.

BIRKETT, A.J., MOORTHY, V.S., LOUCQ, C., CHITNIS, C.E. and KASLOW, D.C., 2013. Malaria vaccine R&D in the Decade of Vaccines: breakthroughs, challenges and opportunities. *Vaccine*, **31**, pp. B233-B243.

BOUSEMA, T. and DRAKELEY, C., 2011. Epidemiology and infectivity of *Plasmodium falciparum* and *Plasmodium vivax* gametocytes in relation to malaria control and elimination. *Clinical Microbiology Reviews*, **24**(2), pp. 377-410.

BRAY, P., WARD, S. and O'NEILL, P., 2005. Malaria: drugs, disease and post-genomic biology. *Curr.Top.Microbiol.Immun*, **295**, pp. 3-38.

BUFFET, P.A., SAFEUKUI, I., DEPLAINE, G., BROUSSE, V., PRENDKI, V., THELLIER, M., TURNER, G.D. and MERCEREAU-PUIJALON, O., 2011. The pathogenesis of *Plasmodium falciparum* malaria in humans: insights from splenic physiology. *Blood*, **117**(2), pp. 381-392.

BURROWS, J., KOWALCZYK, P., MCDONALD, S., SPANGENBERG, T., WELLS, T. and WILLIS, P., 2012. The Malaria Box: a catalyst for drug discovery. *Malaria Journal*, **11**(Suppl 1), pp. P136.

BURROWS, J.N., BURLOT, E., CAMPO, B., CHERBUIN, S., JEANNERET, S., LEROY, D., SPANGENBERG, T., WATERSON, D., WELLS, T.N. and WILLIS, P., 2014. Antimalarial drug discovery—the path towards eradication. *Parasitology*, **141**(01), pp. 128-139.

BURROWS, J.N., LEROY, D., LOTHARIUS, J. and WATERSON, D., 2011. Challenges in antimalarial drug discovery. *Future Medicinal Chemistry*, **3**(11), pp. 1401-1412.

BURROWS, J.N., VAN HUIJSDUIJNEN, R.H., MÖHRLE, J.J., OEUVRAY, C. and WELLS, T.N., 2013. Designing the next generation of medicines for malaria control and eradication. *Malar J*, **12**(187), pp. 10.1186.

CHE, P., CUI, L., KUTSCH, O., CUI, L. and LI, Q., 2012. Validating a firefly luciferase-based high-throughput screening assay for antimalarial drug discovery. *Assay and Drug Development Technologies*, **10**(1), pp. 61-68.

- CHEN, Q., SCHLICHTERLE, M. and WAHLGREN, M., 2000. Molecular aspects of severe malaria. *Clinical Microbiology Reviews*, **13**(3), pp. 439-450.
- CH'NG, J., LIEW, K., GOH, A.S., SIDHARTHA, E. and TAN, K.S., 2011. Drug-induced permeabilization of parasite's digestive vacuole is a key trigger of programmed cell death in *Plasmodium falciparum*. *Cell Death & Disease*, **2**(10), pp. e216.
- CHONG, W., BASIR, R. and FEI, Y.M., 2013. Eradication of malaria through genetic engineering: the current situation. *Asian Pacific Journal of Tropical Medicine*, **6**(2), pp. 85-94.
- CLARK, I.A., BUDD, A.C., ALLEVA, L.M. and COWDEN, W.B., 2006. Human malarial disease: a consequence of inflammatory cytokine release. *Malaria Journal*, **5**, pp. 85.
- COLEMAN, R.E., SATTABONGKOT, J., PROMSTAPORM, S., MANEECHAI, N., TIPPAYACHAI, B., KENGLUECHA, A., RACHAPAEW, N., ZOLLNER, G., MILLER, R.S., VAUGHAN, J.A., THIMASARN, K. and KHUNTIRAT, B., 2006. Comparison of PCR and microscopy for the detection of asymptomatic malaria in a *Plasmodium falciparum/vivax* endemic area in Thailand. *Malaria Journal*, **5**, pp. 121.
- COLLINS, W.E. and JEFFERY, G.M., 2005. *Plasmodium ovale*: parasite and disease. *Clinical Microbiology Reviews*, **18**(3), pp. 570-581.
- COOKE, B., COPPEL, R. and WAHLGREN, M., 2000. Falciparum malaria: sticking up, standing out and out-standing. *Parasitology Today*, **16**(10), pp. 416-420.
- COWMAN, A.F. and CRABB, B.S., 2006. Invasion of red blood cells by malaria parasites. *Cell*, **124**(4), pp. 755-766.
- COWMAN, A.F., BERRY, D. and BAUM, J., 2012. The cellular and molecular basis for malaria parasite invasion of the human red blood cell. *The Journal of cell biology*, **198**(6), pp. 961-971.
- CRABB, B., TRIGLIA, T., WATERKEYN, J. and COWMAN, A., 1997a. Stable transgene expression in *Plasmodium falciparum*. *Molecular and Biochemical Parasitology*, **90**(1), pp. 131-144.
- CRABB, B.S., COOKE, B.M., REEDER, J.C., WALLER, R.F., CARUANA, S.R., DAVERN, K.M., WICKHAM, M.E., BROWN, G.V., COPPEL, R.L. and COWMAN, A.F., 1997b. Targeted gene disruption shows that knobs enable malaria-infected red cells to cytoadhere under physiological shear stress. *Cell*, **89**(2), pp. 287-296.
- CRAWLEY, J. and NAHLEN, B., 2004. Prevention and treatment of malaria in young African children, *Seminars in Pediatric Infectious Diseases* 2004, Elsevier, pp. 169-180.

CRAWLEY, J., CHU, C., MTOVE, G. and NOSTEN, F., 2010. Malaria in children. *The Lancet*, **375**(9724), pp. 1468-1481.

CUADROS, D.F., BRANSCUM, A.J. and CROWLEY, P.H., 2011. HIV-malaria co-infection: effects of malaria on the prevalence of HIV in East sub-Saharan Africa. *International Journal of Epidemiology*, **40**(4), pp. 931-939.

CUI, L., MIAO, J., WANG, J., LI, Q. and CUI, L., 2008. *Plasmodium falciparum*: development of a transgenic line for screening antimalarials using firefly luciferase as the reporter. *Experimental Parasitology*, **120**(1), pp. 80-87.

CUNNINGTON, A.J., RILEY, E.M. and WALTHER, M., 2013. Stuck in a rut? Reconsidering the role of parasite sequestration in severe malaria syndromes. *Trends in Parasitology*, **29**(12), pp. 585-592.

DANESHVAR, C., DAVIS, T.M., COX-SINGH, J., RAFA'EE, M.Z., ZAKARIA, S.K., DIVIS, P.C. and SINGH, B., 2010. Clinical and parasitological response to oral chloroquine and primaquine in uncomplicated human *Plasmodium knowlesi* infections. *Malaria Journal*, **9**, pp. 238-2875-9-238.

DAVID, P.H., HANDUNNETTI, S.M., LEECH, J.H., GAMAGE, P. and MENDIS, K.N., 1988. Rosetting: a new cytoadherence property of malaria-infected erythrocytes. *The American Journal of Tropical Medicine and Hygiene*, **38**(2), pp. 289-297.

DELVES, M., PLOUFFE, D., SCHEURER, C., MEISTER, S., WITTLIN, S., WINZELER, E.A., SINDEN, R.E. and LEROY, D., 2012. The activities of current antimalarial drugs on the life cycle stages of Plasmodium: a comparative study with human and rodent parasites. *PLoS Medicine*, **9**(2), pp. 227.

DESJARDINS, R.E., CANFIELD, C.J., HAYNES, J.D. and CHULAY, J.D., 1979. Quantitative assessment of antimalarial activity *in vitro* by a semiautomated microdilution technique. *Antimicrobial Agents and Chemotherapy*, **16**(6), pp. 710-718.

DONDORP, A.M., INCE, C., CHARUNWATTHANA, P., HANSON, J., VAN KUIJEN, A., FAIZ, M.A., RAHMAN, M.R., HASAN, M., BIN YUNUS, E., GHOSE, A., RUANGVEERAYUT, R., LIMMATHUROTSAKUL, D., MATHURA, K., WHITE, N.J. and DAY, N.P., 2008. Direct *in vivo* assessment of microcirculatory dysfunction in severe falciparum malaria. *The Journal of Infectious Diseases*, **197**(1), pp. 79-84.

DONDORP, A.M., LEE, S.J., FAIZ, M.A., MISHRA, S., PRICE, R., TJITRA, E., THAN, M., HTUT, Y., MOHANTY, S., YUNUS, E.B., RAHMAN, R., NOSTEN, F., ANSTEY, N.M., DAY, N.P. and WHITE, N.J., 2008. The relationship between age and the manifestations of and mortality associated with severe malaria. *Clinical infectious diseases : an official publication of the Infectious Diseases Society of America*, **47**(2), pp. 151-157.

DONDORP, A.M., NOSTEN, F., YI, P., DAS, D., PHYO, A.P., TARNING, J., LWIN, K.M., ARIEY, F., HANPITHAKPONG, W. and LEE, S.J., 2009. Artemisinin resistance in *Plasmodium falciparum* malaria. *New England Journal of Medicine*, **361**(5), pp. 455-467.

DOOLAN, D.L., DOBANO, C. and BAIRD, J.K., 2009. Acquired immunity to malaria. *Clinical Microbiology Reviews*, **22**(1), pp. 13-36.

DUFFY, S. and AVERY, V.M., 2012. Development and optimization of a novel 384-well anti-malarial imaging assay validated for high-throughput screening. *The American Journal of Tropical Medicine and Hygiene*, **86**(1), pp. 84-92.

ECKER, A., LEHANE, A.M., CLAIN, J. and FIDOCK, D.A., 2012. PfCRT and its role in antimalarial drug resistance. *Trends in Parasitology*, **28**(11), pp. 504-514.

EKLAND, E.H., SCHNEIDER, J. and FIDOCK, D.A., 2011. Identifying apicoplast-targeting antimalarials using high-throughput compatible approaches. *FASEB journal : official publication of the Federation of American Societies for Experimental Biology*, **25**(10), pp. 3583-3593.

ELABBADI, N., ANCELIN, M.L. and VIAL, H.J., 1992. Use of radioactive ethanolamine incorporation into phospholipids to assess *in vitro* antimalarial activity by the semiautomated microdilution technique. *Antimicrobial Agents and Chemotherapy*, **36**(1), pp. 50-55.

FAMIN, O. and GINSBURG, H., 2002. Differential effects of 4-aminoquinoline-containing antimalarial drugs on hemoglobin digestion in *Plasmodium falciparum*-infected erythrocytes. *Biochemical Pharmacology*, **63**(3), pp. 393-398.

FAMIN, O., KRUGLIAK, M. and GINSBURG, H., 1999. Kinetics of inhibition of glutathione-mediated degradation of ferriprotoporphyrin IX by antimalarial drugs. *Biochemical Pharmacology*, **58**(1), pp. 59-68.

FEACHEM, R.G., PHILLIPS, A.A., TARGETT, G.A. and SNOW, R.W., 2010. Call to action: priorities for malaria elimination. *The Lancet*, **376**(9752), pp. 1517-1521.

FIGTREE, M., LEE, R., BAIN, L., KENNEDY, T., MACKERTICH, S., URBAN, M., CHENG, Q. and HUDSON, B.J., 2010. *Plasmodium knowlesi* in human, Indonesian Borneo. *Emerging Infectious Diseases*, **16**(2), pp. 672-674.

FINNEY, O.C., KEITANY, G.J., SMITHERS, H., KAUSHANSKY, A., KAPPE, S. and WANG, R., 2014. Immunization with genetically attenuated *P. falciparum* parasites induces long-lived antibodies that efficiently block hepatocyte invasion by sporozoites. *Vaccine*, **32**(19), pp. 2135-2138.

FLOWER, D.R., 1998. DISSIM: a program for the analysis of chemical diversity. *Journal of Molecular Graphics and Modelling*, **16**(4), pp. 239-253.

- FOLEY, M. and TILLEY, L., 1997. Quinoline antimalarials: mechanisms of action and resistance. *International Journal for Parasitology*, **27**(2), pp. 231-240.
- FOLEY, M. and TILLEY, L., 1998. Quinoline antimalarials: mechanisms of action and resistance and prospects for new agents. *Pharmacology & Therapeutics*, **79**(1), pp. 55-87.
- FONG, K.Y., SANDLIN, R.D. and WRIGHT, D.W., 2015. Identification of  $\beta$ -hematin inhibitors in the MMV Malaria Box. *International Journal for Parasitology: Drugs and Drug Resistance*, **5**(3), pp. 84-91.
- FRANKE-FAYARD, B., DJOKOVIC, D., DOOREN, M., RAMESAR, J., WATERS, A., FALADE, M., KRANENDONK, M., MARTINELLI, A., CRAVO, P. and JANSE, C., 2008. Simple and sensitive antimalarial drug screening *in vitro* and *in vivo* using transgenic luciferase expressing *Plasmodium berghei* parasites. *International Journal for Parasitology*, **38**(14), pp. 1651-1662.
- FREESE, J.A., SHARP, B., NGXONGO, S. and MARKUS, M., 1988. *In vitro* confirmation of chloroquine-resistant *Plasmodium falciparum* malaria in KwaZulu. *South African Medical Journal/Suid-Afrikaanse Mediese Tydskrift*, **74**(11), pp. 576-579.
- FREVERT, U., 2004. Sneaking in through the back entrance: the biology of malaria liver stages. *Trends in Parasitology*, **20**(9), pp. 417-424.
- FUEHRER, H.P., STARZENGRUBER, P., SWOBODA, P., KHAN, W.A., MATT, J., LEY, B., THRIEMER, K., HAQUE, R., YUNUS, E.B., HOSSAIN, S.M., WALOCHNIK, J. and NOEDL, H., 2010. Indigenous *Plasmodium ovale* malaria in Bangladesh. *The American Journal of Tropical Medicine and Hygiene*, **83**(1), pp. 75-78.
- GAMO, F., SANZ, L.M., VIDAL, J., DE COZAR, C., ALVAREZ, E., LAVANDERA, J., VANDERWALL, D.E., GREEN, D.V., KUMAR, V. and HASAN, S., 2010. Thousands of chemical starting points for antimalarial lead identification. *Nature*, **465**(7296), pp. 305-310.
- GATTI, S., GRAMEGNA, M., BISOFFI, Z., RAGLIO, A., GULLETTA, M., KLERSY, C., BRUNO, A., MASERATI, R., MADAMA, S. and SCAGLIA, M., 2007. A comparison of three diagnostic techniques for malaria: a rapid diagnostic test (NOW<sup>®</sup> Malaria), PCR and microscopy. *Annals of Tropical Medicine and Parasitology*, **101**(3), pp. 195-204.
- GAVIRIA, D., PAGUIO, M.F., TURNBULL, L.B., TAN, A., SIRIWARDANA, A., GHOSH, D., FERDIG, M.T., SINAI, A.P. and ROEPE, P.D., 2013. A process similar to autophagy is associated with cytotoxic chloroquine resistance in *Plasmodium falciparum*. *PLoS ONE*, , pp. 8(11): e79059.
- GENTON, B., D'ACREMONT, V., LORRY, K., BAEA, K., REEDER, J. and MUELLER, I., 2005. *Plasmodium vivax* is associated with severe malaria in Papua New Guinean children, *AMERICAN JOURNAL OF TROPICAL MEDICINE AND HYGIENE* 2005, AMER SOC TROP MED & HYGIENE 8000 WESTPARK DR, STE 130, MCLEAN, VA 22101 USA, pp. 14-14.

GETHING, P.W., ELYAZAR, I.R., MOYES, C.L., SMITH, D.L., BATTLE, K.E., GUERRA, C.A., PATIL, A.P., TATEM, A.J., HOWES, R.E. and MYERS, M.F., 2012. A long neglected world malaria map: *Plasmodium vivax* endemicity in 2010. *PLoS Negl Trop Dis*, **6**(9), pp. e1814. doi:10.1371/journal.pntd.0001814.

GETHING, P.W., PATIL, A.P., SMITH, D.L., GUERRA, C.A., ELYAZAR, I., JOHNSTON, G.L., TATEM, A.J. and HAY, S.I., 2011. A new world malaria map: *Plasmodium falciparum* endemicity in 2010. *Malar J*, **10**(378), pp. 1475-2875.

GHOSE, A.K., VISWANADHAN, V.N. and WENDOLOSKI, J.J., 1999. A knowledge-based approach in designing combinatorial or medicinal chemistry libraries for drug discovery. 1. A qualitative and quantitative characterization of known drug databases. *Journal of Combinatorial Chemistry*, **1**(1), pp. 55-68.

GODFRAY, H.C.J., 2013. Mosquito ecology and control of malaria. *Journal of Animal Ecology*, **82**(1), pp. 15-25.

GOLDBERG, D.E. and COWMAN, A.F., 2010. Moving in and renovating: exporting proteins from *Plasmodium* into host erythrocytes. *Nature Reviews Microbiology*, **8**(9), pp. 617-621.

GORKA, A.P., JACOBS, L.M. and ROEPE, P.D., 2013. Cytostatic versus cytotoxic profiling of quinoline drug combinations via modified fixed-ratio isobologram analysis. *Malar J*, **12**, pp. 332.

GRAU, G.E., MACKENZIE, C.D., CARR, R.A., REDARD, M., PIZZOLATO, G., ALLASIA, C., CATALDO, C., TAYLOR, T.E. and MOLYNEUX, M.E., 2003. Platelet accumulation in brain microvessels in fatal pediatric cerebral malaria. *Journal of Infectious Diseases*, **187**(3), pp. 461-466.

GRIMBERG, B.T. and MEHLOTRA, R.K., 2011. Expanding the Antimalarial Drug Arsenal—Now, But How? *Pharmaceuticals*, **4**(5), pp. 681-712.

GROBUSCH, M. and KREMSNER, P., 2005. Uncomplicated malaria. *Curr Top Microbiol Immunol*, **295**, pp. 81-104.

GUERIN, P.J., OLLIARO, P., NOSTEN, F., DRUILHE, P., LAXMINARAYAN, R., BINKA, F., KILAMA, W.L., FORD, N. and WHITE, N.J., 2002. Malaria: current status of control, diagnosis, treatment, and a proposed agenda for research and development. *The Lancet Infectious Diseases*, **2**(9), pp. 564-573.

GUIGUEMDE, W.A., SHELAT, A.A., BOUCK, D., DUFFY, S., CROWTHER, G.J., DAVIS, P.H., SMITHSON, D.C., CONNELLY, M., CLARK, J. and ZHU, F., 2010. Chemical genetics of *Plasmodium falciparum*. *Nature*, **465**(7296), pp. 311-315.

GUILBRIDE, D.L., GAWLINSKI, P. and GUILBRIDE, P.D., 2010. Why functional pre-erythrocytic and bloodstage malaria vaccines fail: a meta-analysis of fully protective immunizations and novel immunological model.

GUILBRIDE, D.L., GAWLINSKI, P. and GUILBRIDE, P.D., 2010. Why functional pre-erythrocytic and bloodstage malaria vaccines fail: a meta-analysis of fully protective immunizations and novel immunological model. *PLoS ONE*, **5**(5), pp. e10685. doi:10.1371/journal.pone.0010685.

HALDAR, K., KAMOUN, S., HILLER, N.L., BHATTACHARJE, S. and VAN OOIJ, C., 2006. Common infection strategies of pathogenic eukaryotes. *Nature Reviews Microbiology*, **4**(12), pp. 922-931.

HAMEED P, S., CHINNAPATTU, M., SHANBAG, G., MANJREKAR, P., KOUSHIK, K., RAICHURKAR, A., PATIL, V., JATHEENDRANATH, S., RUDRAPATNA, S.S. and BARDE, S.P., 2014. Aminoazabenzimidazoles, a novel class of orally active antimalarial agents. *Journal of Medicinal Chemistry*, **57**(13), pp. 5702-5713.

HANN, M., HUDSON, B., LEWELL, X., LIFELY, R., MILLER, L. and RAMSDEN, N., 1999. Strategic pooling of compounds for high-throughput screening. *Journal of Chemical Information and Computer Sciences*, **39**(5), pp. 897-902.

HASENKAMP, S., SIDAWAY, A., DEVINE, O., ROYE, R. and HORROCKS, P., 2013. Evaluation of bioluminescence-based assays of anti-malarial drug activity. *Malar J*, **12**, pp. 58.

HASENKAMP, S., WONG, E.H. and HORROCKS, P., 2012. An improved single-step lysis protocol to measure luciferase bioluminescence in *Plasmodium falciparum*. *Malaria Journal*, **11**, pp. 42-2875-11-42.

HASLER, T., HANDUNNETTI, S.M., AGUIAR, J.C., VAN SCHRAVENDIJK, M.R., GREENWOOD, B.M., LALLINGER, G., CEGIELSKI, P. and HOWARD, R.J., 1990. *In vitro* rosetting, cytoadherence, and microagglutination properties of *Plasmodium falciparum*-infected erythrocytes from Gambian and Tanzanian patients. *Blood*, **76**(9), pp. 1845-1852.

HAY, S.I., GUERRA, C.A., TATEM, A.J., NOOR, A.M. and SNOW, R.W., 2004. The global distribution and population at risk of malaria: past, present, and future. *The Lancet Infectious Diseases*, **4**(6), pp. 327-336.

HEPPNER, D.G., 2013. The malaria vaccine—status quo 2013. *Travel Medicine and Infectious Disease*, **11**(1), pp. 2-7.

HILL, A.V., 2011. Vaccines against malaria. *Philosophical Transactions of the Royal Society of London. Series B, Biological Sciences*, **366**(1579), pp. 2806-2814.

HORROCKS, P. and KILBEY, B.J., 1996. Physical and functional mapping of the transcriptional start sites of *Plasmodium falciparum* proliferating cell nuclear antigen. *Molecular and Biochemical Parasitology*, **82**(2), pp. 207-215.

HORROCKS, P., JACKSON, M., CHEESMAN, S., WHITE, J.H. and KILBEY, B.J., 1996. Stage specific expression of proliferating cell nuclear antigen and DNA polymerase  $\delta$  from *Plasmodium falciparum*. *Molecular and Biochemical Parasitology*, **79**(2), pp. 177-182.

HURD, H., CARTER, V. and NACER, A., 2005. Interactions between malaria and mosquitoes: the role of apoptosis in parasite establishment and vector response to infection. *Role of Apoptosis in Infection*. Springer, pp. 185-217.

IDRO, R., NDIRITU, M., OGUTU, B., MITHWANI, S., MAITLAND, K., BERKLEY, J., CRAWLEY, J., FEGAN, G., BAUNI, E. and PESHU, N., 2007. Burden, features, and outcome of neurological involvement in acute falciparum malaria in Kenyan children. *Jama*, **297**(20), pp. 2232-2240.

JIMENEZ-DIAZ, M.B., EBERT, D., SALINAS, Y., PRADHAN, A., LEHANE, A.M., MYRAND-LAPIERRE, M.E., O'LOUGHLIN, K.G., SHACKLEFORD, D.M., JUSTINO DE ALMEIDA, M., CARRILLO, A.K., CLARK, J.A., DENNIS, A.S., DIEP, J., DENG, X., DUFFY, S., ENDSLEY, A.N., FEDEWA, G., GUIGUEMDE, W.A., GOMEZ, M.G., HOLBROOK, G., HORST, J., KIM, C.C., LIU, J., LEE, M.C., MATHENY, A., MARTINEZ, M.S., MILLER, G., RODRIGUEZ-ALEJANDRE, A., SANZ, L., SIGAL, M., SPILLMAN, N.J., STEIN, P.D., WANG, Z., ZHU, F., WATERSON, D., KNAPP, S., SHELAT, A., AVERY, V.M., FIDOCK, D.A., GAMO, F.J., CHARMAN, S.A., MIRSA LIS, J.C., MA, H., FERRER, S., KIRK, K., ANGULO-BARTUREN, I., KYLE, D.E., DERISI, J.L., FLOYD, D.M. and GUY, R.K., 2014. (+)-SJ733, a clinical candidate for malaria that acts through ATP4 to induce rapid host-mediated clearance of Plasmodium. *Proceedings of the National Academy of Sciences of the United States of America*, **111**(50), pp. E5455-62.

JOHNSON, J.D., DENNULL, R.A., GERENA, L., LOPEZ-SANCHEZ, M., RONCAL, N.E. and WATERS, N.C., 2007. Assessment and continued validation of the malaria SYBR green I-based fluorescence assay for use in malaria drug screening. *Antimicrobial Agents and Chemotherapy*, **51**(6), pp. 1926-1933.

KAKKILAYA, B., 2009. Malaria and pregnancy. Available at: <http://www.malariasite.com> [Accessed: 01/07/2015].

KANTELE, A. and JOKIRANTA, T.S., 2011. Review of cases with the emerging fifth human malaria parasite, *Plasmodium knowlesi*. *Clinical infectious diseases : an official publication of the Infectious Diseases Society of America*, **52**(11), pp. 1356-1362.

KARUNAMOORTHY, K., 2011. Vector control: a cornerstone in the malaria elimination campaign. *Clinical Microbiology and Infection*, **17**(11), pp. 1608-1616.

KAWAMOTO, F., MIYAKE, H., KANEKO, O., KIMURA, M., NGUYEN, T.D., NGUYEN, T.D., LIU, Q., ZHOU, M., LE, D.D., KAWAI, S., ISOMURA, S. and WATAYA, Y., 1996. Sequence variation in the 18S rRNA gene, a target for PCR-based malaria diagnosis, in *Plasmodium ovale* from southern Vietnam. *Journal of Clinical Microbiology*, **34**(9), pp. 2287-2289.

KILBEY, B.J., FRASER, I., MCALEESE, S., GOMAN, M. and RIDLEY, R.G., 1993. Molecular characterisation and stage-specific expression of proliferating cell nuclear antigen (PCNA) from the malarial parasite, *Plasmodium falciparum*. *Nucleic Acids Research*, **21**(2), pp. 239-243.

KYES, S., HORROCKS, P. and NEWBOLD, C., 2001. Antigenic variation at the infected red cell surface in malaria. *Annual Reviews in Microbiology*, **55**(1), pp. 673-707.

LANZER, M., DE BRUIN, D. and RAVETCH, J.V., 1992. A sequence element associated with the *Plasmodium falciparum* KAHRP gene is the site of developmentally regulated protein-DNA interactions. *Nucleic Acids Research*, **20**(12), pp. 3051-3056.

LE MANACH, C., SCHEURER, C., SAX, S., SCHLEIFERBÖCK, S., CABRERA, D.G., YOUNIS, Y., PAQUET, T., STREET, L., SMITH, P. and DING, X.C., 2013. Fast *in vitro* methods to determine the speed of action and the stage-specificity of anti-malarials in *Plasmodium falciparum*. *Malar.J*, **16**, pp. 424-430.

LEE, K.S., COX-SINGH, J. and SINGH, B., 2009. Morphological features and differential counts of *Plasmodium knowlesi* parasites in naturally acquired human infections. *Malaria Journal*, **8**, pp. 73-2875-8-73.

LEESON, P.D. and SPRINGTHORPE, B., 2007. The influence of drug-like concepts on decision-making in medicinal chemistry. *Nature Reviews Drug Discovery*, **6**(11), pp. 881-890.

LEHANE, A.M., RIDGWAY, M.C., BAKER, E. and KIRK, K., 2014. Diverse chemotypes disrupt ion homeostasis in the malaria parasite. *Molecular Microbiology*, **94**(2), pp. 327-339.

LEO, A., HANSCH, C. and ELKINS, D., 1971. Partition coefficients and their uses. *Chemical Reviews*, **71**(6), pp. 525-616.

LEROY, D., CAMPO, B., DING, X.C., BURROWS, J.N. and CHERBUIN, S., 2014. Defining the biology component of the drug discovery strategy for malaria eradication. *Trends in Parasitology*, **30**(10), pp. 478-490.

LIN, J.T., JULIANO, J.J. and WONGSRICHANALAI, C., 2010. Drug-resistant malaria: the era of ACT. *Current Infectious Disease Reports*, **12**(3), pp. 165-173.

LINARES, M., VIERA, S., CRESPO, B., FRANCO, V., GÓMEZ-LORENZO, M.G., JIMÉNEZ-DÍAZ, M.B., ANGULO-BARTUREN, Í., SANZ, L.M. and GAMO, F., 2015. Identifying rapidly

parasitocidal anti-malarial drugs using a simple and reliable *in vitro* parasite viability fast assay. *Malaria Journal*, **14**(1), pp. 441.

LIPINSKI, C., 2001. Avoiding investment in doomed drugs, is poor solubility an industry wide problem. *Curr. Drug Dis*, **4**, pp. 17-19.

LIPINSKI, C.A., 2000. Drug-like properties and the causes of poor solubility and poor permeability. *Journal of Pharmacological and Toxicological Methods*, **44**(1), pp. 235-249.

LIPINSKI, C.A., 2004. Lead-and drug-like compounds: the rule-of-five revolution. *Drug Discovery Today: Technologies*, **1**(4), pp. 337-341.

LIPINSKI, C.A., LOMBARDO, F., DOMINY, B.W. and FEENEY, P.J., 2012. Experimental and computational approaches to estimate solubility and permeability in drug discovery and development settings. *Advanced Drug Delivery Reviews*, **64**, pp. 4-17.

LIPINSKI, C.A., LOMBARDO, F., DOMINY, B.W. and FEENEY, P.J., 2012. Experimental and computational approaches to estimate solubility and permeability in drug discovery and development settings. *Advanced Drug Delivery Reviews*, **64**, pp. 4-17.

LUCANTONI, L., DUFFY, S., ADJALLEY, S.H., FIDOCK, D.A. and AVERY, V.M., 2013. Identification of MMV malaria box inhibitors of plasmodium falciparum early-stage gametocytes using a luciferase-based high-throughput assay. *Antimicrobial Agents and Chemotherapy*, **57**(12), pp. 6050-6062.

LUCUMI, E., DARLING, C., JO, H., NAPPER, A.D., CHANDRAMOHANADAS, R., FISHER, N., SHONE, A.E., JING, H., WARD, S.A., BIAGINI, G.A., DEGRADO, W.F., DIAMOND, S.L. and GREENBAUM, D.C., 2010. Discovery of potent small-molecule inhibitors of multidrug-resistant *Plasmodium falciparum* using a novel miniaturized high-throughput luciferase-based assay. *Antimicrobial Agents and Chemotherapy*, **54**(9), pp. 3597-3604.

MACKINTOSH, C.L., BEESON, J.G. and MARSH, K., 2004. Clinical features and pathogenesis of severe malaria. *Trends in Parasitology*, **20**(12), pp. 597-603.

MAIER, A.G., COOKE, B.M., COWMAN, A.F. and TILLEY, L., 2009. Malaria parasite proteins that remodel the host erythrocyte. *Nature Reviews Microbiology*, **7**(5), pp. 341-354.

MAKLER, M., PALMER, C. and AGER, A., 1998. A review of practical techniques for the diagnosis of malaria. *Annals of Tropical Medicine and Parasitology*, **92**(4), pp. 419-433.

MAKLER, M.T. and HINRICHS, D.J., 1993. Measurement of the lactate dehydrogenase activity of *Plasmodium falciparum* as an assessment of parasitemia. *The American Journal of Tropical Medicine and Hygiene*, **48**(2), pp. 205-210.

MALERA CONSULTATIVE GROUP ON VECTOR CONTROL, 2011. A research agenda for malaria eradication: vector control. *PLoS Med*, **8**(1), pp. e1000401.

MCCONVILLE, M., FERNANDEZ, J., ANGULO-BARTUREN, I., BAHAMONTES-ROSA, N., BALLELL-PAGES, L., CASTAÑEDA, P., DE COZAR, C., CRESPO, B., GUIJARRO, L. and JIMÉNEZ-DÍAZ, M.B., 2015. Carbamoyl Triazoles, Known Serine Protease Inhibitors, Are a Potent New Class of Antimalarials. *Journal of Medicinal Chemistry*, **58**(16), pp. 6448-6455.

Medicine for Malaria Venture (MMV). Available at: <http://www.mmv.org/> [Accessed: 01/06/2015].

MEISTER, S., PLOUFFE, D.M., KUHEN, K.L., BONAMY, G.M., WU, T., BARNES, S.W., BOPP, S.E., BORBOA, R., BRIGHT, A.T., CHE, J., COHEN, S., DHARIA, N.V., GAGARING, K., GETTAYACAMIN, M., GORDON, P., GROESSL, T., KATO, N., LEE, M.C., MCNAMARA, C.W., FIDOCK, D.A., NAGLE, A., NAM, T.G., RICHMOND, W., ROLAND, J., ROTTMANN, M., ZHOU, B., FROISSARD, P., GLYNNE, R.J., MAZIER, D., SATTABONGKOT, J., SCHULTZ, P.G., TUNTLAND, T., WALKER, J.R., ZHOU, Y., CHATTERJEE, A., DIAGANA, T.T. and WINZELER, E.A., 2011. Imaging of Plasmodium liver stages to drive next-generation antimalarial drug discovery. *Science (New York, N.Y.)*, **334**(6061), pp. 1372-1377.

MENENDEZ, C., FLEMING, A. and ALONSO, P., 2000. Malaria-related anaemia. *Parasitology Today*, **16**(11), pp. 469-476.

MESHNICK, S.R. and DOBSON, M.J., 2001. The history of antimalarial drugs. *Antimalarial chemotherapy*. Springer, pp. 15-25.

MILLER, L.H., BARUCH, D.I., MARSH, K. and DOUMBO, O.K., 2002. The pathogenic basis of malaria. *Nature*, **415**(6872), pp. 673-679.

MOLETTE, J., ROUTIER, J., ABLA, N., BESSON, D., BOMBRUN, A., BRUN, R., BURT, H., GEORGI, K., KAISER, M. and NWAKA, S., 2013. Identification and Optimization of an Aminoalcohol-Carbazole Series with Antimalarial Properties. *ACS Medicinal Chemistry Letters*, **4**(11), pp. 1037-1041.

MOORTHY, V.S., NEWMAN, R.D., DUCLOS, P., OKWO-BELE, J.M. and SMITH, P.G., 2013. Assessment of the RTS,S/AS01 malaria vaccine. *The Lancet Infectious Diseases*, **13**(4), pp. 280-282.

MORDECAI, E.A., PAAIJMANS, K.P., JOHNSON, L.R., BALZER, C., BEN-HORIN, T., MOOR, E., MCNALLY, A., PAWAR, S., RYAN, S.J. and SMITH, T.C., 2013. Optimal temperature for malaria transmission is dramatically lower than previously predicted. *Ecology Letters*, **16**(1), pp. 22-30.

MORRISSETTE, N.S. and SIBLEY, L.D., 2002. Cytoskeleton of apicomplexan parasites. *Microbiology and Molecular Biology Reviews : MMBR*, **66**(1), pp. 21-38.

MUELLER, I., ZIMMERMAN, P.A. and REEDER, J.C., 2007. *Plasmodium malariae* and *Plasmodium ovale*—the ‘bashful’ malaria parasites. *Trends in Parasitology*, **23**(6), pp. 278-283.

MULLIÉ, C., JONET, A., DESGROUAS, C., TAUDON, N. and SONNET, P., 2012. Differences in anti-malarial activity of 4-aminoalcohol quinoline enantiomers and investigation of the presumed underlying mechanism of action. *Malar J*, **11**(65), pp. 10.1186.

MURRAY, C.J., ROSENFELD, L.C., LIM, S.S., ANDREWS, K.G., FOREMAN, K.J., HARING, D., FULLMAN, N., NAGHAVI, M., LOZANO, R. and LOPEZ, A.D., 2012. Global malaria mortality between 1980 and 2010: a systematic analysis. *The Lancet*, **379**(9814), pp. 413-431. NÁJERA, J.A., GONZÁLEZ-SILVA, M. and ALONSO, P.L., 2011. Some lessons for the future from the Global Malaria Eradication Programme (1955–1969). *PLoS Med*, **8**(1), pp. e1000412.

NDIAYE, D., PATEL, V., DEMAS, A., LEROUX, M., NDIR, O., MBOUP, S., CLARDY, J., LAKSHMANAN, V., DAILY, J.P. and WIRTH, D.F., 2010. A non-radioactive DAPI-based high-throughput in vitro assay to assess *Plasmodium falciparum* responsiveness to antimalarials--increased sensitivity of *P. falciparum* to chloroquine in Senegal. *The American Journal of Tropical Medicine and Hygiene*, **82**(2), pp. 228-230.

NEWMAN, P.M., WANZIRA, H., TUMWINE, G., ARINAITWE, E., WALDMAN, S., ACHAN, J., HAVLIR, D., ROSENTHAL, P.J., DORSEY, G. and CLARK, T.D., 2009. Placental malaria among HIV-infected and uninfected women receiving anti-folates in a high transmission area of Uganda. *Malar J*, **8**(254), pp. 1475-2875.

NOEDL, H., SOCHEAT, D. and SATIMAI, W., 2009. Artemisinin-resistant malaria in Asia. *New England Journal of Medicine*, **361**(5), pp. 540-541.

NOEDL, H., WERNSDORFER, W.H., MILLER, R.S. and WONGSRICHANALAI, C., 2002. Histidine-rich protein II: a novel approach to malaria drug sensitivity testing. *Antimicrobial Agents and Chemotherapy*, **46**(6), pp. 1658-1664.

OCKENHOUSE, C.F., HO, M., TANDON, N.N., VAN SEVENTER, G.A., SHAW, S., WHITE, N.J., JAMIESON, G.A., CHULAY, J.D. and WEBSTER, H.K., 1991. Molecular basis of sequestration in severe and uncomplicated *Plasmodium falciparum* malaria: differential adhesion of infected erythrocytes to CD36 and ICAM-1. *The Journal of Infectious Diseases*, **164**(1), pp. 163-169.

OKELLO, P.E., VAN BORTEL, W., BYARUHANGA, A.M., CORREWYN, A., ROELANTS, P., TALISUNA, A., D'ALESSANDRO, U. and COOSEMANS, M., 2006. Variation in malaria transmission intensity in seven sites throughout Uganda. *The American Journal of Tropical Medicine and Hygiene*, **75**(2), pp. 219-225.

OLLIARO, P., 2001. Mode of action and mechanisms of resistance for antimalarial drugs. *Pharmacology & Therapeutics*, **89**(2), pp. 207-219.

OPREA, T.I., 2000. Property distribution of drug-related chemical databases\*. *Journal of Computer-Aided Molecular Design*, **14**(3), pp. 251-264.

- PAGUIO, M.F., BOGLE, K.L. and ROEPE, P.D., 2011. *Plasmodium falciparum* resistance to cytotoxic versus cytostatic effects of chloroquine. *Molecular and Biochemical Parasitology*, **178**(1), pp. 1-6.
- PAIARDINI, A., BAMERT, R.S., KANNAN-SIVARAMAN, K., DRINKWATER, N., MISTRY, S.N., SCAMMELLS, P.J. and MCGOWAN, S., 2015. Screening the Medicines for Malaria Venture "Malaria Box" against the *Plasmodium falciparum* aminopeptidases, M1, M17 and M18. *PLoS One*, **10**(2), pp. e0115859.
- PASTERNAK, N.D. and DZIKOWSKI, R., 2009. *PfEMP1*: an antigen that plays a key role in the pathogenicity and immune evasion of the malaria parasite *Plasmodium falciparum*. *The International Journal of Biochemistry & Cell Biology*, **41**(7), pp. 1463-1466.
- PATES, H. and CURTIS, C., 2005. Mosquito behavior and vector control. *Annu.Rev.Entomol.*, **50**, pp. 53-70.
- PERANDIN, F., MANCA, N., CALDERARO, A., PICCOLO, G., GALATI, L., RICCI, L., MEDICI, M.C., ARCANGELETTI, M.C., SNOUNOU, G., DETTORI, G. and CHEZZI, C., 2004. Development of a real-time PCR assay for detection of *Plasmodium falciparum*, *Plasmodium vivax*, and *Plasmodium ovale* for routine clinical diagnosis. *Journal of Clinical Microbiology*, **42**(3), pp. 1214-1219.
- PHILLIPS, M.A., LOTHARIUS, J., MARSH, K., WHITE, J., DAYAN, A., WHITE, K.L., NJOROGE, J.W., EL MAZOUNI, F., LAO, Y., KOKKONDA, S., TOMCHICK, D.R., DENG, X., LAIRD, T., BHATIA, S.N., MARCH, S., NG, C.L., FIDOCK, D.A., WITTLIN, S., LAFUENTE-MONASTERIO, M., BENITO, F.J., ALONSO, L.M., MARTINEZ, M.S., JIMENEZ-DIAZ, M.B., BAZAGA, S.F., ANGULO-BARTUREN, I., HASELDEN, J.N., LOUTTIT, J., CUI, Y., SRIDHAR, A., ZEEMAN, A.M., KOCKEN, C., SAUERWEIN, R., DECHERING, K., AVERY, V.M., DUFFY, S., DELVES, M., SINDEN, R., RUECKER, A., WICKHAM, K.S., ROCHFORD, R., GAHAGEN, J., IYER, L., RICCIO, E., MIRSALIS, J., BATHURST, I., RUECKLE, T., DING, X., CAMPO, B., LEROY, D., ROGERS, M.J., RATHOD, P.K., BURROWS, J.N. and CHARMAN, S.A., 2015. A long-duration dihydroorotate dehydrogenase inhibitor (DSM265) for prevention and treatment of malaria. *Science Translational Medicine*, **7**(296), pp. 296ra111.
- PIPER, R., LEBRAS, J., WENTWORTH, L., HUNT-COOKE, A., HOUZE, S., CHIODINI, P. and MAKLER, M., 1999. Immunocapture diagnostic assays for malaria using *Plasmodium* lactate dehydrogenase (pLDH). *The American Journal of Tropical Medicine and Hygiene*, **60**(1), pp. 109-118.
- PLOUFFE, D., BRINKER, A., MCNAMARA, C., HENSON, K., KATO, N., KUHEN, K., NAGLE, A., ADRIAN, F., MATZEN, J.T., ANDERSON, P., NAM, T.G., GRAY, N.S., CHATTERJEE, A., JANES, J., YAN, S.F., TRAGER, R., CALDWELL, J.S., SCHULTZ, P.G., ZHOU, Y. and WINZELER, E.A., 2008. *In silico* activity profiling reveals the mechanism of action of antimalarials discovered in a high-throughput screen. *Proceedings of the National Academy of Sciences of the United States of America*, **105**(26), pp. 9059-9064.

PORTH, C., 2011. *Essentials of pathophysiology: concepts of altered health states*. 8th edn. China: Lippincott Williams & Wilkins.

PRICE, R.N., TJITRA, E., GUERRA, C.A., YEUNG, S., WHITE, N.J. and ANSTEY, N.M., 2007. Vivax malaria: neglected and not benign. *The American Journal of Tropical Medicine and Hygiene*, **77**(6 Suppl), pp. 79-87.

PRUDÊNCIO, M., RODRIGUEZ, A. and MOTA, M.M., 2006. The silent path to thousands of merozoites: the Plasmodium liver stage. *Nature Reviews Microbiology*, **4**(11), pp. 849-856.

PUKRITTAYAKAMEE, S., CHANTRA, A., SIMPSON, J.A., VANIJANONTA, S., CLEMENS, R., LOOAREESUWAN, S. and WHITE, N.J., 2000. Therapeutic responses to different antimalarial drugs in vivax malaria. *Antimicrobial Agents and Chemotherapy*, **44**(6), pp. 1680-1685.

RANSON, H., N'GUESSAN, R., LINES, J., MOIROUX, N., NKUNI, Z. and CORBEL, V., 2011. Pyrethroid resistance in African anopheline mosquitoes: what are the implications for malaria control? *Trends in Parasitology*, **27**(2), pp. 91-98.

RISHTON, G.M., 1997. Reactive compounds and *in vitro* false positives in HTS. *Drug Discovery Today*, **2**(9), pp. 382-384.

ROEPE, P.D., 2010. PfCRT-mediated drug transport in malarial parasites. *Biochemistry*, **50**(2), pp. 163-171.

ROGERSON, S.J., CHAIYAROJ, S.C., NG, K., REEDER, J.C. and BROWN, G.V., 1995. Chondroitin sulfate A is a cell surface receptor for *Plasmodium falciparum*-infected erythrocytes. *The Journal of Experimental Medicine*, **182**(1), pp. 15-20.

ROLL BACK MALARIA., 2008. Key facts about malaria. Available at: [www.rollbackmalaria.org](http://www.rollbackmalaria.org) [Accessed: 21/06/2015].

ROLL BACK MALARIA., 2014. Key facts about malaria. Available at: [www.rollbackmalaria.org](http://www.rollbackmalaria.org) [Accessed: 21/06/2015].

ROTTMANN, M., MCNAMARA, C., YEUNG, B.K., LEE, M.C., ZOU, B., RUSSELL, B., SEITZ, P., PLOUFFE, D.M., DHARIA, N.V., TAN, J., COHEN, S.B., SPENCER, K.R., GONZALEZ-PAEZ, G.E., LAKSHMINARAYANA, S.B., GOH, A., SUWANARUSK, R., JEGLA, T., SCHMITT, E.K., BECK, H.P., BRUN, R., NOSTEN, F., RENIA, L., DARTOIS, V., KELLER, T.H., FIDOCK, D.A., WINZELER, E.A. and DIAGANA, T.T., 2010. Spiroindolones, a potent compound class for the treatment of malaria. *Science (New York, N.Y.)*, **329**(5996), pp. 1175-1180.

ROWE, J.A., CLAESSENS, A., CORRIGAN, R.A. and ARMAN, M., 2009. Adhesion of *Plasmodium falciparum*-infected erythrocytes to human cells: molecular mechanisms and therapeutic implications. *Expert Reviews in Molecular Medicine*, **11**, pp. e16.

- RUBIN, R. and STRAYER, D., 2011. *Rubin's Pathology: Clinicopathologic foundations of medicine*. 6th edn. Philadelphia: Lippincott Williams & Wilkins.
- SANZ, L.M., CRESPO, B., DE-CÓZAR, C., DING, X.C., LLERGO, J.L., BURROWS, J.N., GARCÍA-BUSTOS, J.F. and GAMO, F., 2012. *P. falciparum* *in vitro* killing rates allow to discriminate between different antimalarial mode-of-action. *PLoS ONE*, **7**(2), pp. e30949.
- SARALAMBA, S., PAN-NGUM, W., MAUDE, R.J., LEE, S.J., TARNING, J., LINDEGARDH, N., CHOTIVANICH, K., NOSTEN, F., DAY, N.P., SOCHEAT, D., WHITE, N.J., DONDORP, A.M. and WHITE, L.J., 2011. Intrahost modeling of artemisinin resistance in *Plasmodium falciparum*. *Proceedings of the National Academy of Sciences of the United States of America*, **108**(1), pp. 397-402.
- SARDA, V., KASLOW, D.C. and WILLIAMSON, K.C., 2009. Approaches to malaria vaccine development using the retrospectroscope. *Infection and Immunity*, **77**(8), pp. 3130-3140.
- SCHERF, A., LOPEZ-RUBIO, J.J. and RIVIERE, L., 2008. Antigenic variation in *Plasmodium falciparum*. *Annu.Rev.Microbiol.*, **62**, pp. 445-470.
- SCHNEIDER, N., JÄCKELS, C., ANDRES, C. and HUTTER, M.C., 2008. Gradual *in silico* filtering for druglike substances. *Journal of Chemical Information and Modeling*, **48**(3), pp. 613-628.
- SCHWARTZ, L., BROWN, G.V., GENTON, B. and MOORTHY, V.S., 2012. A review of malaria vaccine clinical projects based on the WHO rainbow table. *Malar J*, **11**(11), pp. 10.1186.
- SCHWENK, R.J. and RICHIE, T.L., 2011. Protective immunity to pre-erythrocytic stage malaria. *Trends in Parasitology*, **27**(7), pp. 306-314.
- SCIENTIFIC, T.F., 2009. Luciferase reporters. Thermo Scientific Pierce Protein Assay Technical Handbook. Available at : <https://www.lifetechnologies.com/uk/en/home/life-science/protein-biology/protein-biology-learning-center/protein-biology-resource-library/pierce-protein-methods/luciferase-reporters.html> [Accessed: 13/01/2013].
- SHANKS, G.D., 2010. For severe malaria, artesunate is the answer. *Lancet (London, England)*, **376**(9753), pp. 1621-1622.
- SHERLACH, K.S. and ROEPE, P.D., 2013. Determination of the Cytostatic and Cytocidal Activities of Antimalarial Compounds and Their Combination Interactions. *Current Protocols in Chemical Biology*, , pp. 237-248 DOI: 10.1002/9780470559277.ch140125.
- SILVIE, O., MOTA, M.M., MATUSCHEWSKI, K. and PRUDÊNCIO, M., 2008. Interactions of the malaria parasite and its mammalian host. *Current Opinion in Microbiology*, **11**(4), pp. 352-359.

- SIMONETTI, A.B., 1996. The biology of malarial parasite in the mosquito: a review. *Memórias Do Instituto Oswaldo Cruz*, **91**(5), pp. 519-541.
- SIMPSON, J.A., SILAMUT, K., CHOTIVANICH, K., PUKRITTAYAKAMEE, S. and WHITE, N.J., 1999. Red cell selectivity in malaria: a study of multiple-infected erythrocytes. *Transactions of the Royal Society of Tropical Medicine and Hygiene*, **93**(2), pp. 165-168.
- SIMPSON, J.A., WATKINS, E.R., PRICE, R.N., AARONS, L., KYLE, D.E. and WHITE, N.J., 2000. Mefloquine pharmacokinetic-pharmacodynamic models: implications for dosing and resistance. *Antimicrobial Agents and Chemotherapy*, **44**(12), pp. 3414-3424.
- SINGH, B. and DANESHVAR, C., 2013. Human infections and detection of *Plasmodium knowlesi*. *Clinical Microbiology Reviews*, **26**(2), pp. 165-184.
- SINGH, B., SUNG, L.K., MATUSOP, A., RADHAKRISHNAN, A., SHAMSUL, S.S., COX-SINGH, J., THOMAS, A. and CONWAY, D.J., 2004. A large focus of naturally acquired *Plasmodium knowlesi* infections in human beings. *The Lancet*, **363**(9414), pp. 1017-1024.
- SMILKSTEIN, M., SRIWILAIJAROEN, N., KELLY, J.X., WILAIRAT, P. and RISCOE, M., 2004. Simple and inexpensive fluorescence-based technique for high-throughput antimalarial drug screening. *Antimicrobial Agents and Chemotherapy*, **48**(5), pp. 1803-1806.
- SMITH, T., CHARLWOOD, J., KIHONDA, J., MWANKUSYE, S., BILLINGSLEY, P., MEUWISSEN, J., LYIMO, E., TAKKEN, W., TEUSCHER, T. and TANNER, M., 1993. Absence of seasonal variation in malaria parasitaemia in an area of intense seasonal transmission. *Acta Tropica*, **54**(1), pp. 55-72.
- SMITH, T.A., LEUENBERGER, R. and LENGELER, C., 2001. Child mortality and malaria transmission intensity in Africa. *Trends in Parasitology*, **17**(3), pp. 145-149.
- SMITH, J.D., CHITNIS, C.E., CRAIG, A.G., ROBERTS, D.J., HUDSON-TAYLOR, D.E., PETERSON, D.S., PINCHES, R., NEWBOLD, C.I. and MILLER, L.H., 1995. Switches in expression of *Plasmodium falciparum* var genes correlate with changes in antigenic and cytoadherent phenotypes of infected erythrocytes. *Cell*, **82**(1), pp. 101-110.
- SPANGENBERG, T., BURROWS, J.N., KOWALCZYK, P., MCDONALD, S., WELLS, T.N. and WILLIS, P., 2013. The open access malaria box: a drug discovery catalyst for neglected diseases. *PLoS ONE*, **8**(6), pp. e62906.
- STOUTE, J.A., ODINDO, A.O., OWUOR, B.O., MIBEI, E.K., OPOLLO, M.O. and WAITUMBI, J.N., 2003. Loss of red blood cell-complement regulatory proteins and increased levels of circulating immune complexes are associated with severe malarial anemia. *Journal of Infectious Diseases*, **187**(3), pp. 522-525.

STOUTE, J.A., SLAOUI, M., HEPNER, D.G., MOMIN, P., KESTER, K.E., DESMONS, P., WELLDE, B.T., GARÇON, N., KRZYCH, U. and MARCHAND, M., 1997. A preliminary evaluation of a recombinant circumsporozoite protein vaccine against *Plasmodium falciparum* malaria. *New England Journal of Medicine*, **336**(2), pp. 86-91.

SU, X., HAYTON, K. and WELLEMS, T.E., 2007. Genetic linkage and association analyses for trait mapping in *Plasmodium falciparum*. *Nature Reviews Genetics*, **8**(7), pp. 497-506.

SUMMERS, R.L., NASH, M.N. and MARTIN, R.E., 2012. Know your enemy: understanding the role of PfCRT in drug resistance could lead to new antimalarial tactics. *Cellular and Molecular Life Sciences*, **69**(12), pp. 1967-1995.

SUTHERLAND, C.J., TANOMSING, N., NOLDER, D., OGUIKE, M., JENNISON, C., PUKRITTAYAKAMEE, S., DOLECEK, C., HIEN, T.T., DO ROSARIO, V.E., AREZ, A.P., PINTO, J., MICHON, P., ESCALANTE, A.A., NOSTEN, F., BURKE, M., LEE, R., BLAZE, M., OTTO, T.D., BARNWELL, J.W., PAIN, A., WILLIAMS, J., WHITE, N.J., DAY, N.P., SNOUNOU, G., LOCKHART, P.J., CHIODINI, P.L., IMWONG, M. and POLLEY, S.D., 2010. Two nonrecombining sympatric forms of the human malaria parasite *Plasmodium ovale* occur globally. *The Journal of Infectious Diseases*, **201**(10), pp. 1544-1550.

TALISUNA, A., ADIBAKU, S., DORSEY, G., KAMYA, M.R. and ROSENTHAL, P.J., 2012. Malaria in Uganda: challenges to control on the long road to elimination. II. The path forward. *Acta Tropica*, **121**(3), pp. 196-201.

TARGETT, G.A. and GREENWOOD, B.M., 2008. Malaria vaccines and their potential role in the elimination of malaria. *Malaria Journal*, **7 Suppl 1**, pp. S10-2875-7-S1-S10.

TILLEY, L., DIXON, M.W. and KIRK, K., 2011. The *Plasmodium falciparum*-infected red blood cell. *The International Journal of Biochemistry & Cell Biology*, **43**(6), pp. 839-842.

TOOVEY, S., 2009. Mefloquine neurotoxicity: a literature review. *Travel Medicine and Infectious Disease*, **7**(1), pp. 2-6.

TOURÉ, Y. and ODUOLA, A., 2004. Focus: malaria. *Nature Reviews Microbiology*, **2**(4), pp. 276-277.

TRAGER, W. and JENSEN, J.B., 1976. Human malaria parasites in continuous culture. *Science (New York, N.Y.)*, **193**(4254), pp. 673-675.

VAN HELLEMOND, J.J., RUTTEN, M., KOELEWIJN, R., ZEEMAN, A.M., VERWEIJ, J.J., WISMANS, P.J., KOCKEN, C.H. and VAN GENDEREN, P.J., 2009. Human *Plasmodium knowlesi* infection detected by rapid diagnostic tests for malaria. *Emerging Infectious Diseases*, **15**(9), pp. 1478-1480.

- VEBER, D.F., JOHNSON, S.R., CHENG, H., SMITH, B.R., WARD, K.W. and KOPPLE, K.D., 2002. Molecular properties that influence the oral bioavailability of drug candidates. *Journal of Medicinal Chemistry*, **45**(12), pp. 2615-2623.
- VERMA, R., KHANNA, P. and CHAWLA, S., 2013. Malaria vaccine can prevent millions of deaths in the world. *Human Vaccines & Immunotherapeutics*, **9**(6), pp. 1268-1271.
- VLACHOU, D., SCHLEGELMILCH, T., RUNN, E., MENDES, A. and KAFATOS, F.C., 2006. The developmental migration of Plasmodium in mosquitoes. *Current Opinion in Genetics & Development*, **16**(4), pp. 384-391.
- WALKER, N.F., NADJM, B. and WHITTY, C.J.M., 2014. Malaria. *Medicine*, **42**(2), pp. 100-106.
- WALTERS, W.P. and NAMCHUK, M., 2003. Designing screens: how to make your hits a hit. *Nature Reviews Drug Discovery*, **2**(4), pp. 259-266.
- WANG, J., HUANG, L., LI, J., FAN, Q., LONG, Y., LI, Y. and ZHOU, B., 2010. Artemisinin directly targets malarial mitochondria through its specific mitochondrial activation. *PLoS ONE*, **5**(3), pp. e9582.
- WEATHERALL, D.J., MILLER, L.H., BARUCH, D.I., MARSH, K., DOUMBO, O.K., CASALS-PASCUAL, C. and ROBERTS, D.J., 2002. Malaria and the red cell. *Hematology / the Education Program of the American Society of Hematology*, , pp. 35-57.
- WELLS, T.N., VAN HUIJSDUIJNEN, R.H. and VAN VOORHIS, W.C., 2015. Malaria medicines: a glass half full? *Nature Reviews Drug Discovery*, **14**, pp. 424-442.
- WELSCH, M.E., SNYDER, S.A. and STOCKWELL, B.R., 2010. Privileged scaffolds for library design and drug discovery. *Current Opinion in Chemical Biology*, **14**(3), pp. 347-361.
- WESTLING, J., YOWELL, C.A., MAJER, P., ERICKSON, J.W., DAME, J.B. and DUNN, B.M., 1997. *Plasmodium falciparum*, *P. vivax*, and *P. malariae*: A comparison of the active site properties of plasmepsins cloned and expressed from three different species of the malaria parasite. *Experimental Parasitology*, **87**(3), pp. 185-193.
- WHITE, N.J., 1997. Assessment of the pharmacodynamic properties of antimalarial drugs *in vivo*. *Antimicrobial Agents and Chemotherapy*, **41**(7), pp. 1413-1422.
- WHITE, N.J., 2008. *Plasmodium knowlesi*: the fifth human malaria parasite. *Clinical infectious diseases : an official publication of the Infectious Diseases Society of America*, **46**(2), pp. 172-173.
- WHITE, N.J., 2011. The parasite clearance curve. *Malaria Journal*, **10**, pp. 278-2875-10-278.

WHITE, N.J., PUKRITTAYAKAMEE, S., HIEN, T.T., FAIZ, M.A., MOKUOLU, O.A. and DONDORP, A.M., 2014. Malaria. *The Lancet*, **383**(9918), pp. 723-735.

WHITE, N.J., PUKRITTAYAKAMEE, S., PHYO, A.P., RUEANGWEERAYUT, R., NOSTEN, F., JITTAMALA, P., JEEYAPANT, A., JAIN, J.P., LEFÈVRE, G. and LI, R., 2014b. Spiroindolone KAE609 for falciparum and vivax malaria. *New England Journal of Medicine*, **371**(5), pp. 403-410.

WHITE, N.J., TURNER, G.D., DAY, N.P. and DONDORP, A.M., 2013. Lethal malaria: Marchiafava and Bignami were right. *The Journal of Infectious Diseases*, **208**(2), pp. 192-198.

WHO., 2006. World Malaria Report. Available at: [http://apps.who.int/iris/bitstream/10665/43425/1/WHO\\_TRS\\_936\\_eng.pdf](http://apps.who.int/iris/bitstream/10665/43425/1/WHO_TRS_936_eng.pdf) [Accessed: 09/04/2015].

WHO., 2012. World Malaria Report. Available at: [http://www.who.int/malaria/publications/world\\_malaria\\_report\\_2012/en/](http://www.who.int/malaria/publications/world_malaria_report_2012/en/) [Accessed: 21/04/2015].

WHO., 2013. World Malaria Report. Available at: [http://www.who.int/malaria/publications/world\\_malaria\\_report\\_2013/en/](http://www.who.int/malaria/publications/world_malaria_report_2013/en/) [Accessed: 09/04/2015]. .

WHO., 2014. World Malaria Report. Available at: [http://www.who.int/malaria/publications/world\\_malaria\\_report\\_2014/report/en/](http://www.who.int/malaria/publications/world_malaria_report_2014/report/en/) [Accessed: 01/05/2015].

WIESNER, J., ORTMANN, R., JOMAA, H. and SCHLITZER, M., 2003. New antimalarial drugs. *Angewandte Chemie International Edition*, **42**(43), pp. 5274-5293.

WILSON, D.W., LANGER, C., GOODMAN, C.D., MCFADDEN, G.I. and BEESON, J.G., 2013. Defining the timing of action of antimalarial drugs against *Plasmodium falciparum*. *Antimicrobial Agents and Chemotherapy*, **57**(3), pp. 1455-1467.

WIN, T., LIN, K., MIZUNO, S., ZHOU, M., LIU, Q., FERREIRA, M., TANTULAR, I., KOJIMA, S., ISHII, A. and KAWAMOTO, F., 2002. Wide distribution of *Plasmodium ovale* in Myanmar. *Tropical Medicine & International Health*, **7**(3), pp. 231-239.

WONG, E.H., HASENKAMP, S. and HORROCKS, P., 2011. Analysis of the molecular mechanisms governing the stage-specific expression of a prototypical housekeeping gene during intraerythrocytic development of *P. falciparum*. *Journal of Molecular Biology*, **408**(2), pp. 205-221.

WONGSRICHANALAI, C., BARCUS, M.J., MUTH, S., SUTAMIHARDJA, A. and WERNSDORFER, W.H., 2007. A review of malaria diagnostic tools: microscopy and rapid diagnostic test (RDT). *The American Journal of Tropical Medicine and Hygiene*, **77**(6 Suppl), pp. 119-127.

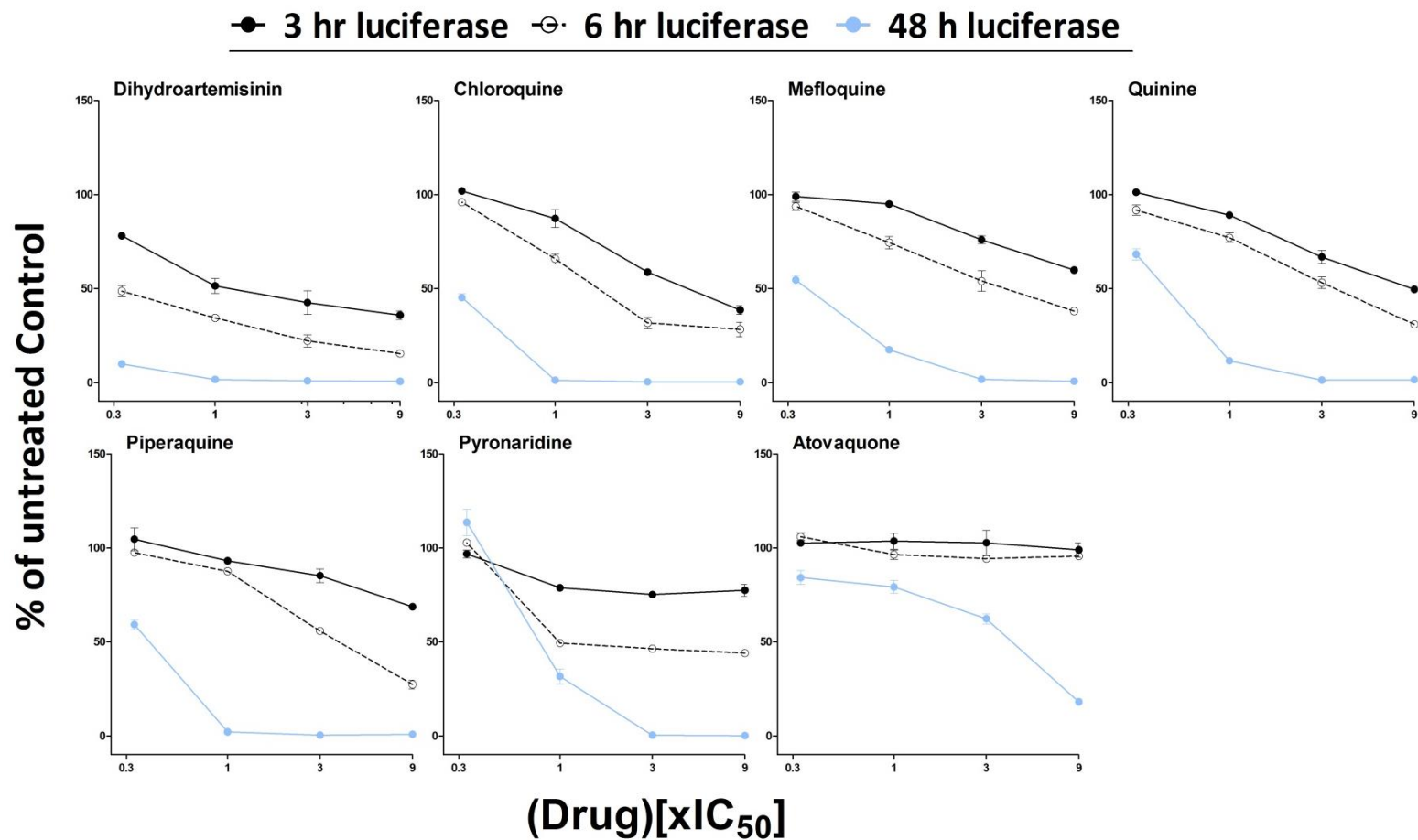
YAMANA, T.K. and ELTAHIR, E.A., 2013. Incorporating the effects of humidity in a mechanistic model of *Anopheles gambiae* mosquito population dynamics in the Sahel region of Africa. *Parasit Vectors*, **6**, pp. 235.

ZHANG, J.H., CHUNG, T.D. and OLDENBURG, K.R., 1999. A Simple Statistical Parameter for Use in Evaluation and Validation of High Throughput Screening Assays. *Journal of Biomolecular Screening*, **4**(2), pp. 67-73.

ZIMMERMAN, R.H., LOUNIBOS, L.P., NISHIMURA, N., GALARDO, A.K., GALARDO, C.D. and ARRUDA, M.E., 2013. Nightly biting cycles of malaria vectors in a heterogeneous transmission area of eastern Amazonian Brazil. *Malar J*, **12**, pp. 262.

## Appendix 1 (Chapter 4, Chapter 5)

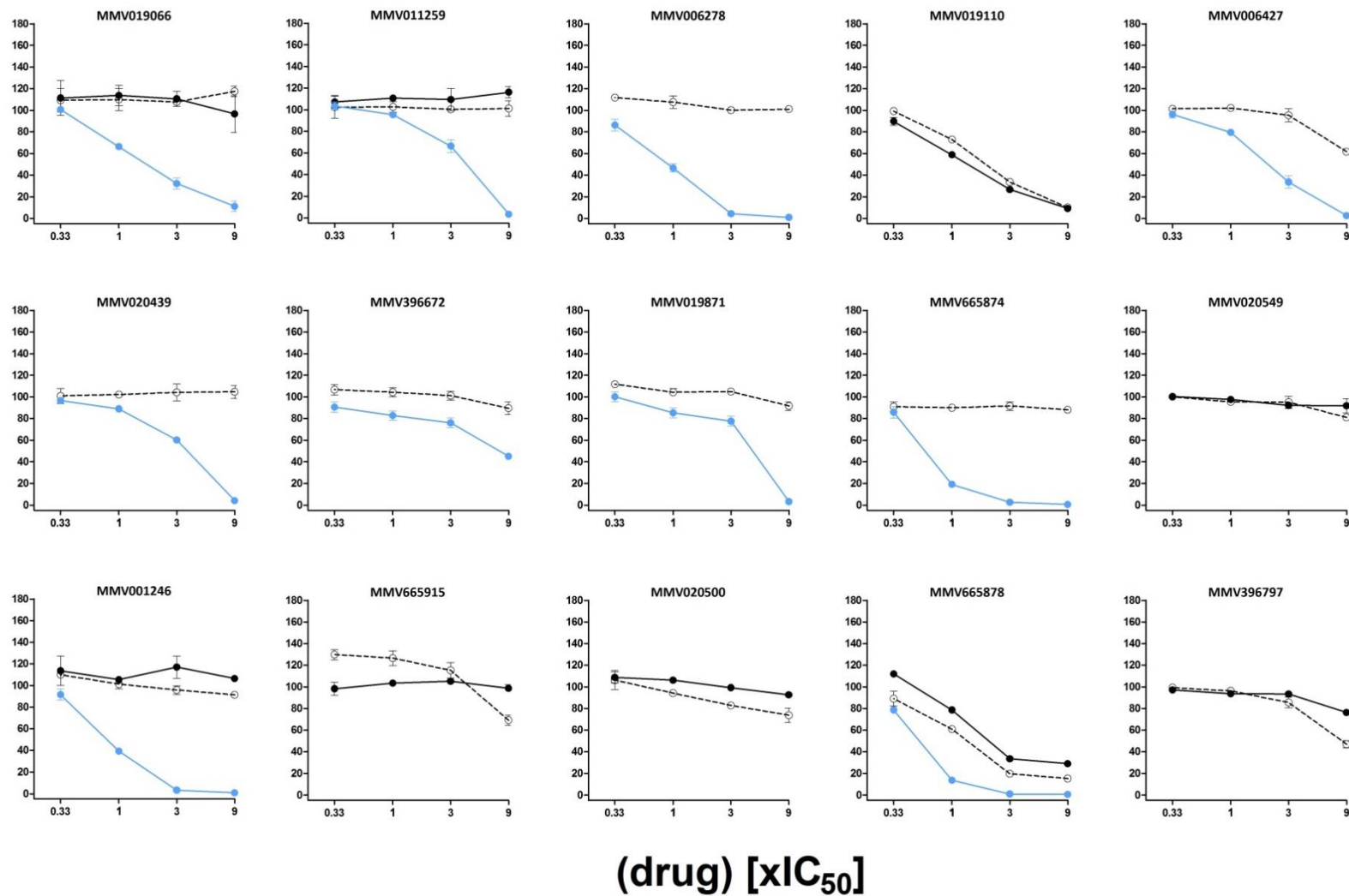
These graphs show dose (9 to 0.33 $\times$ IC<sub>50</sub>) and time response (3, 6 and 48hr) curves of the 370 Malaria Box compounds and 7 benchmark antimalarial drugs. D1-D13 and P1-P12 represents the drug-like and probe-like compounds. Each data point represents mean RLU  $\pm$  stdev (n>9).



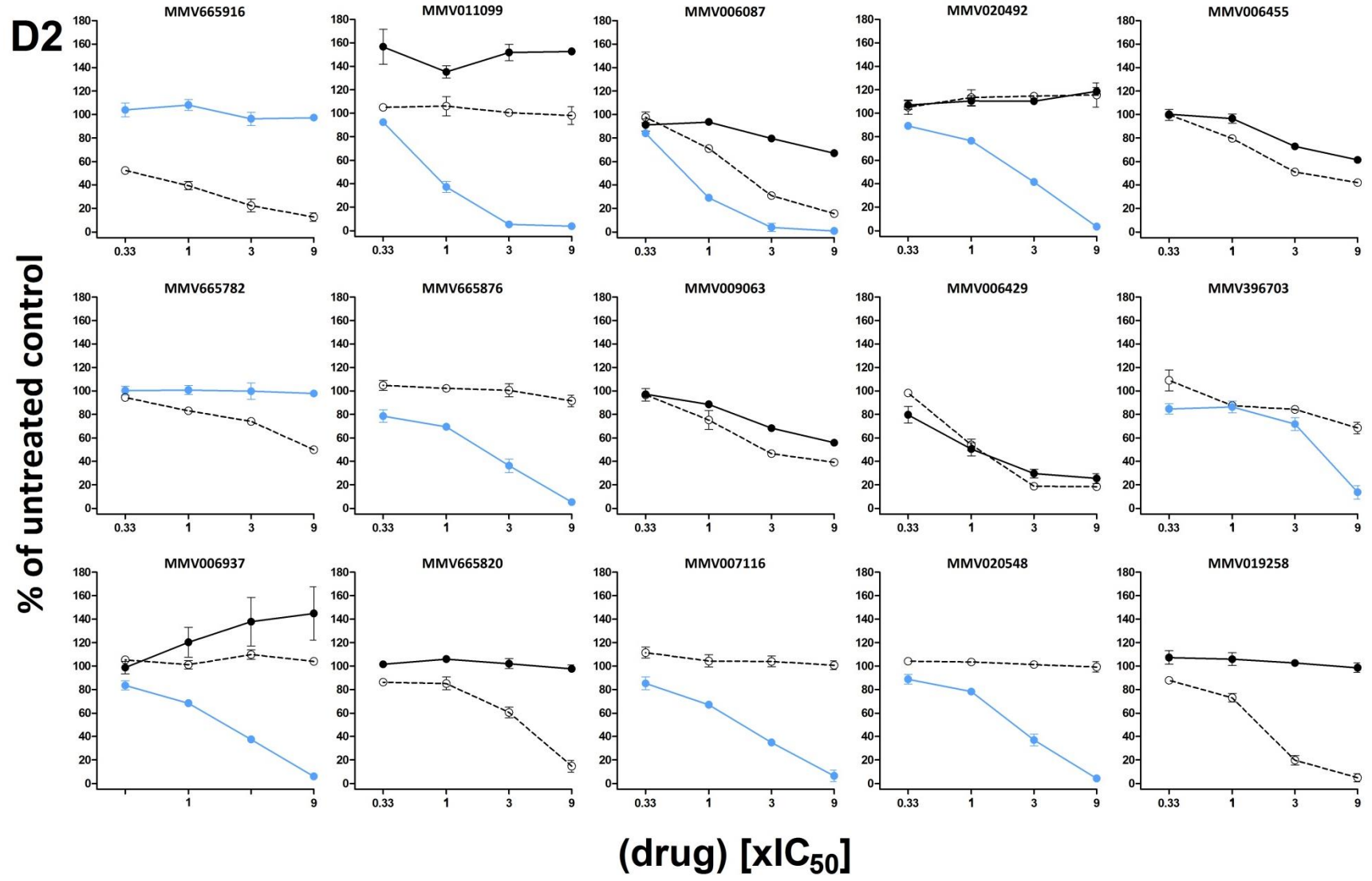
● 3 hr luciferase ○ 6 hr luciferase ● 48 hr luciferase

D1

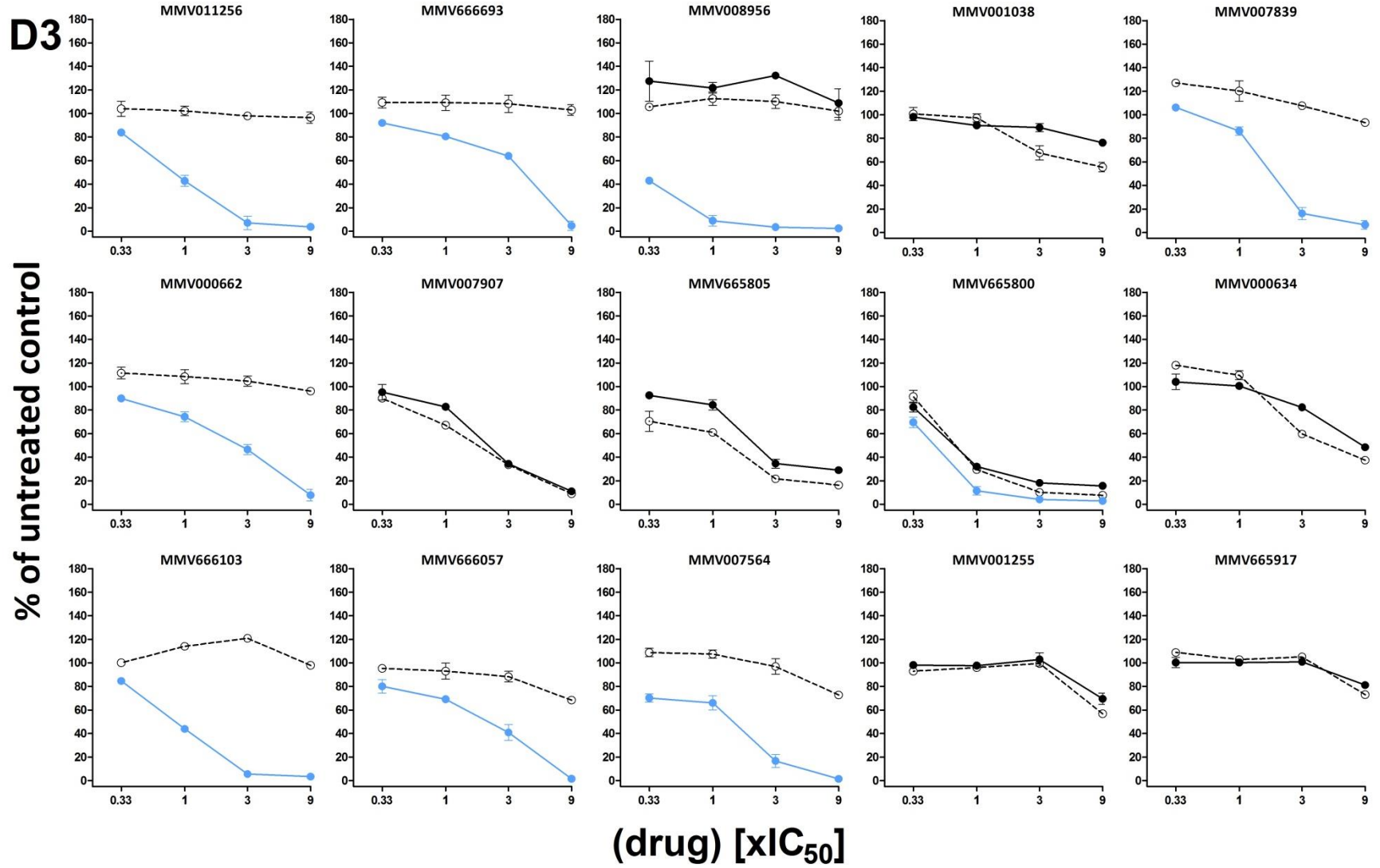
% of untreated control



● 3 hr luciferase ○ 6 hr luciferase ● 48 hr luciferase



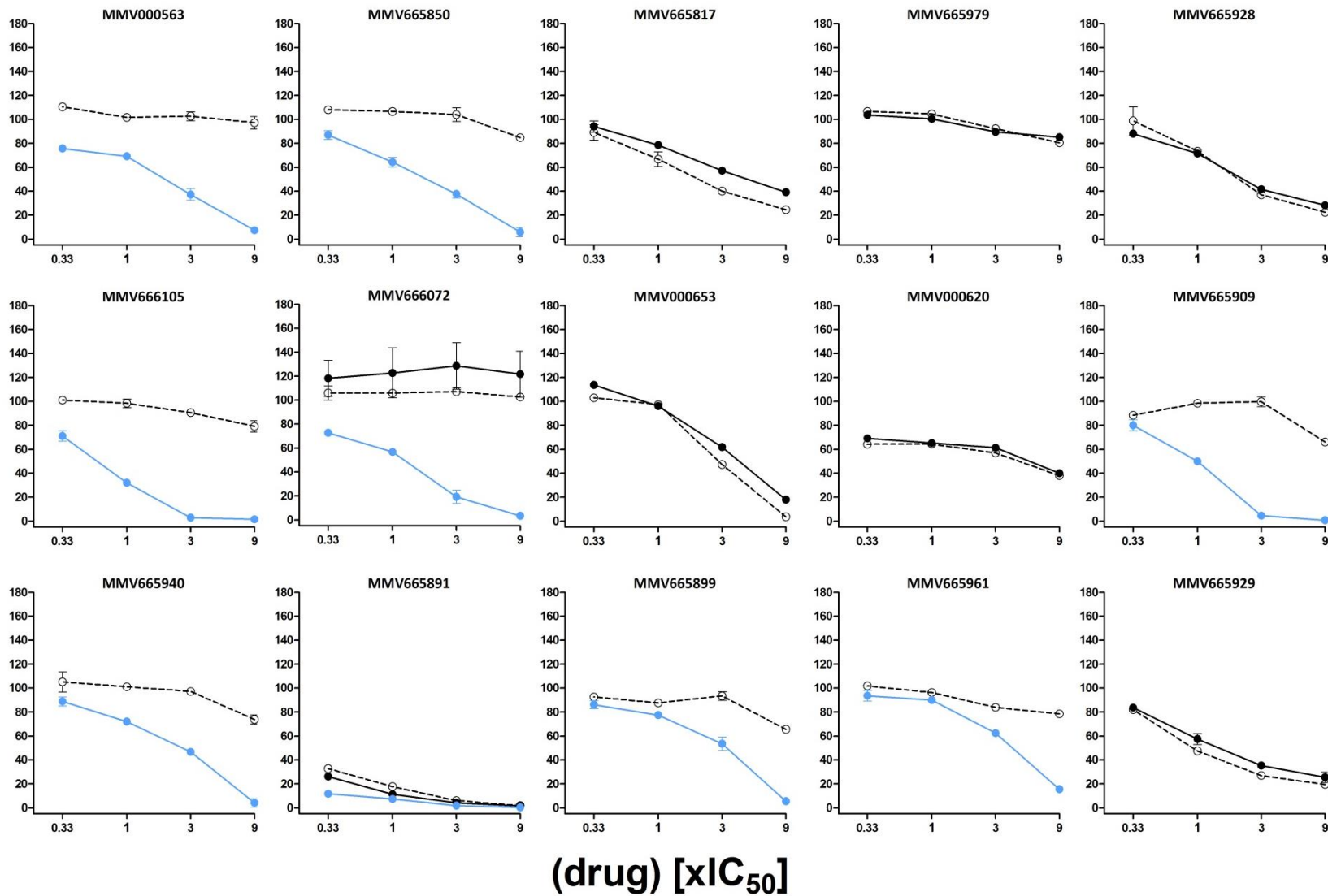
● 3 hr luciferase ○ 6 hr luciferase ● 48 hr luciferase



● 3 hr luciferase ○ 6 hr luciferase ● 48 hr luciferase

D4

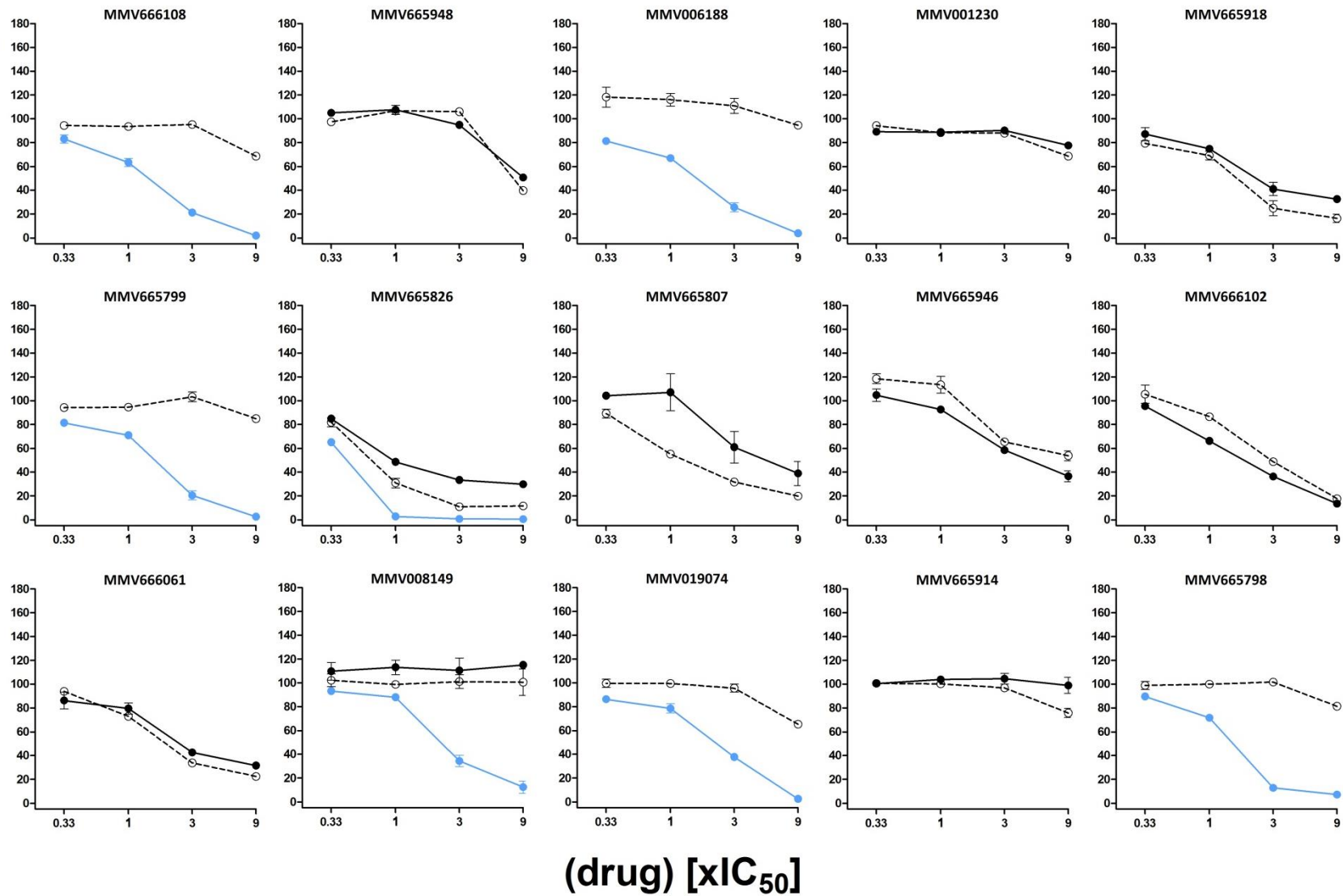
% of untreated control



● 3 hr luciferase ○ 6 hr luciferase ● 48 hr luciferase

D5

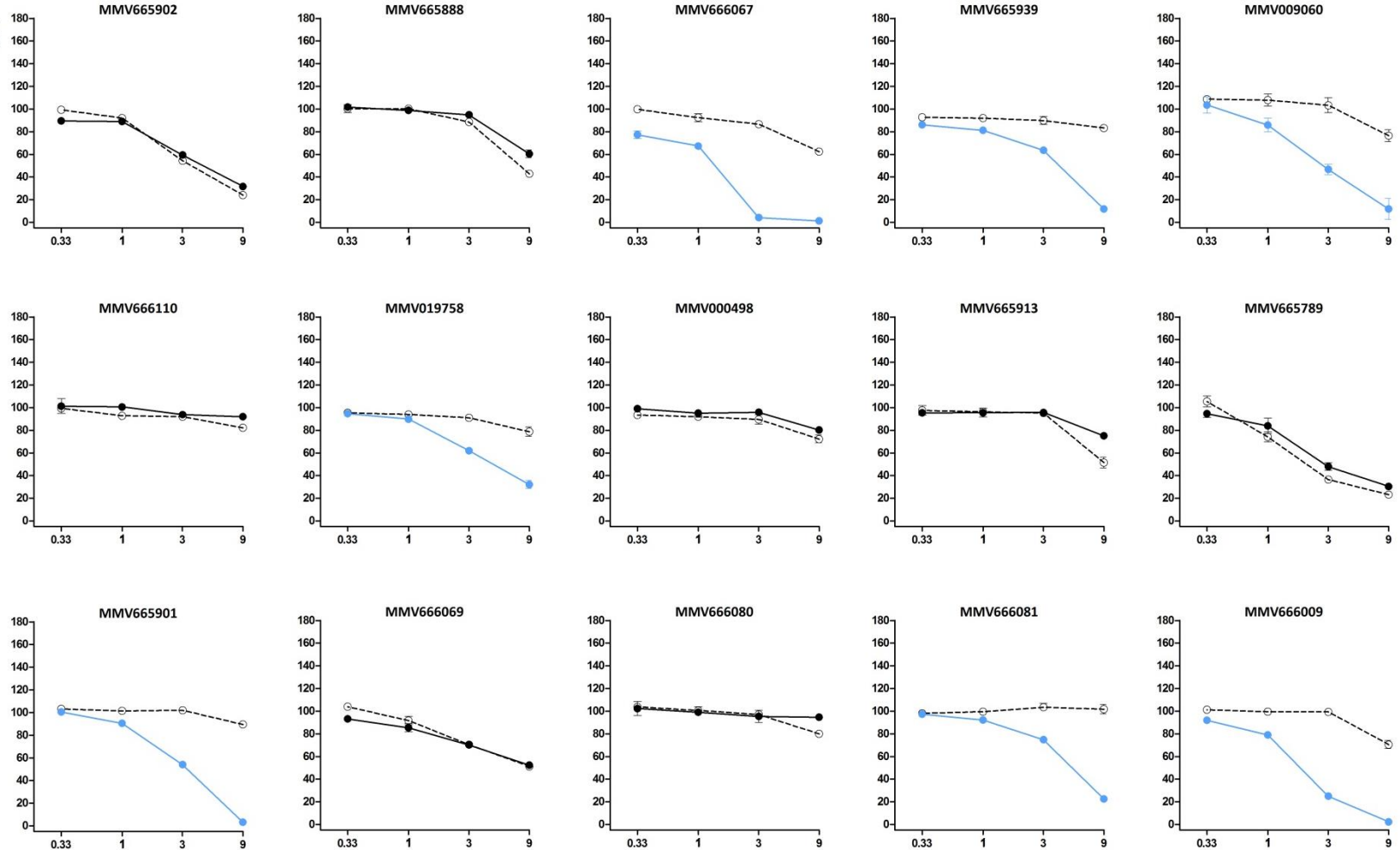
% of untreated control



● 3 hr luciferase ○ 6 hr luciferase ● 48 hr luciferase

D6

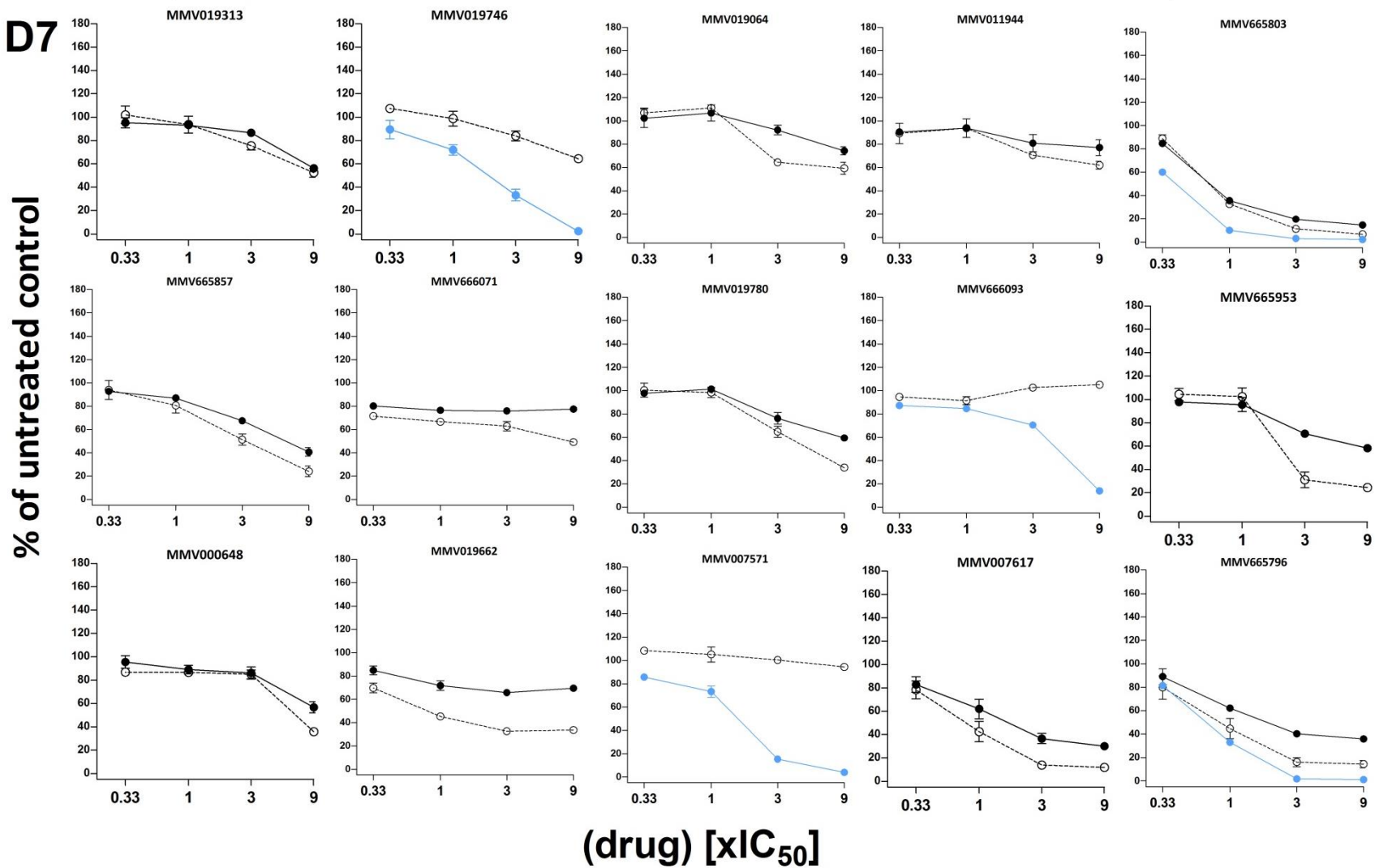
% of untreated control



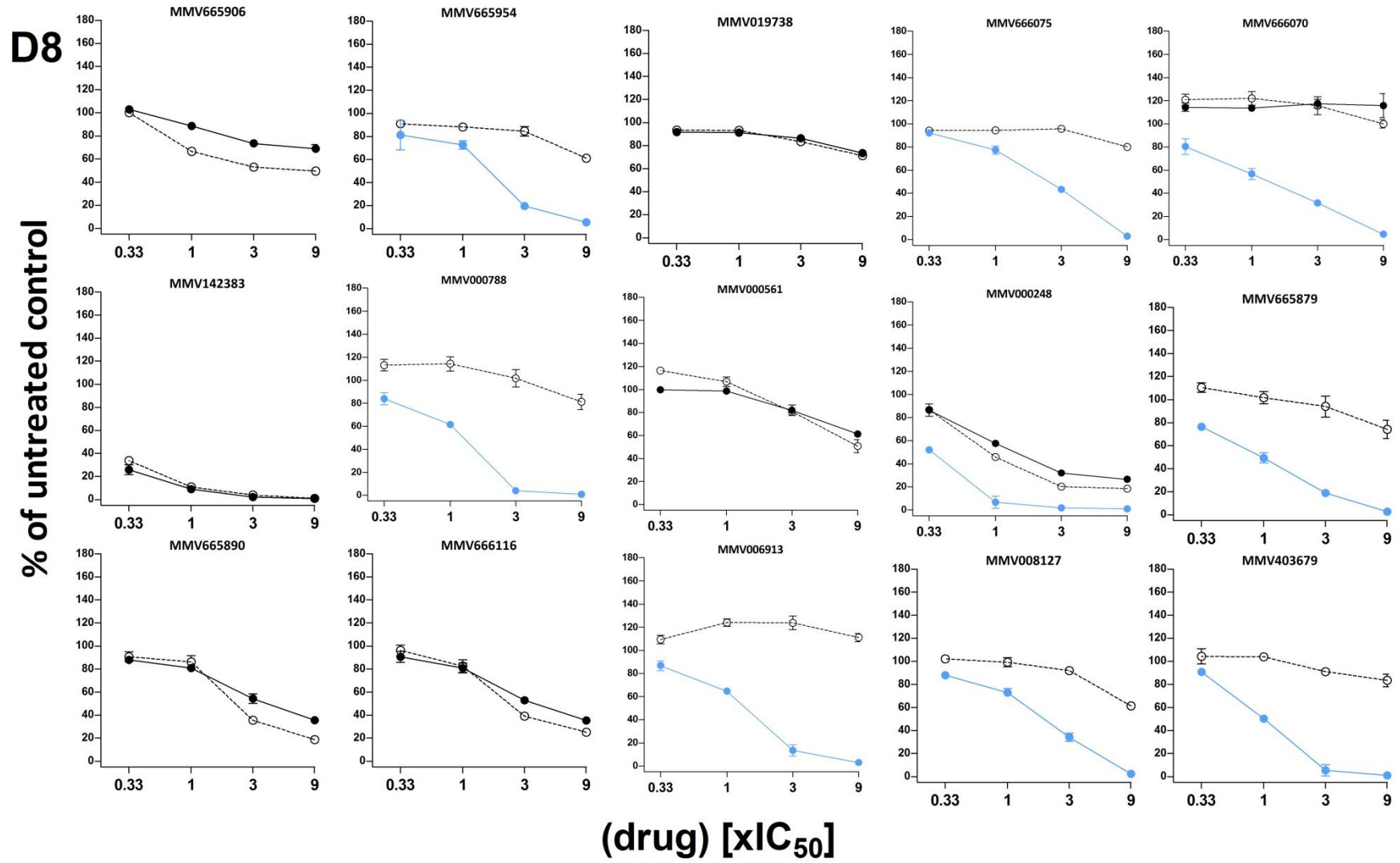
(drug) [ $\times IC_{50}$ ]

● 3 hr luciferase ○ 6 hr luciferase ● 48 hr luciferase

D7

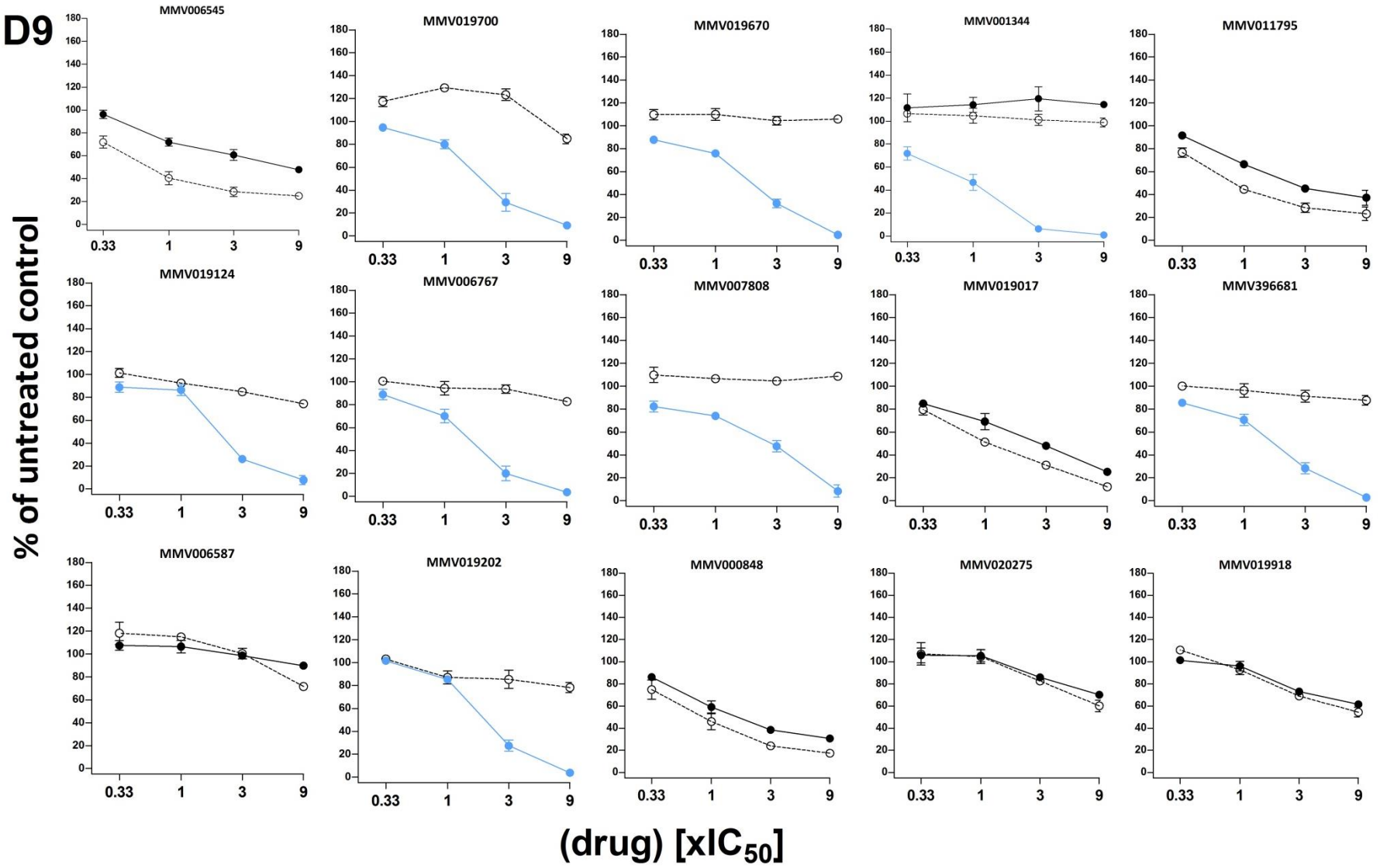


● 3 hr luciferase ○ 6 hr luciferase ● 48 hr luciferase



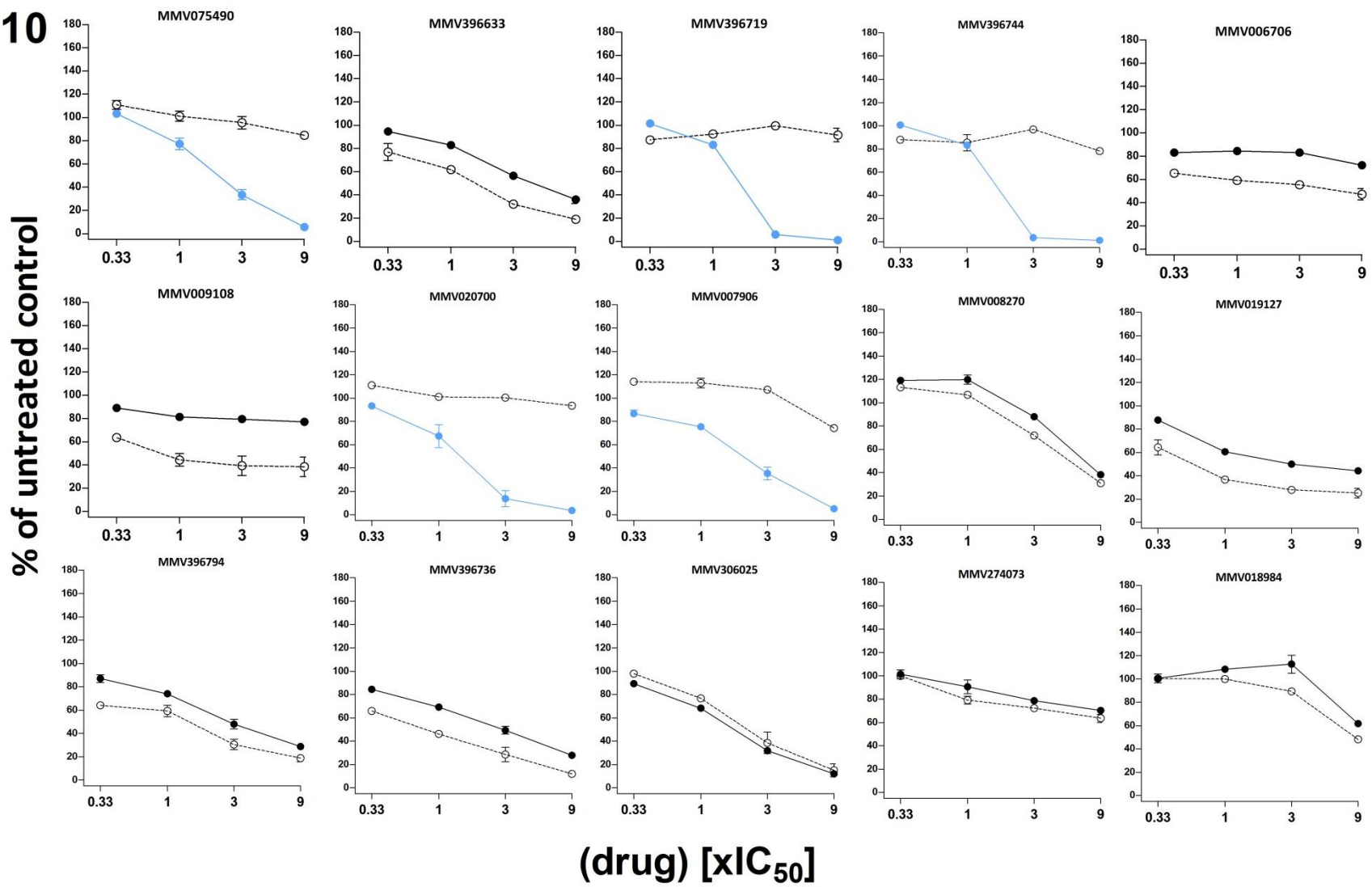
● 3 hr luciferase ○ 6 hr luciferase ● 48 hr luciferase

D9



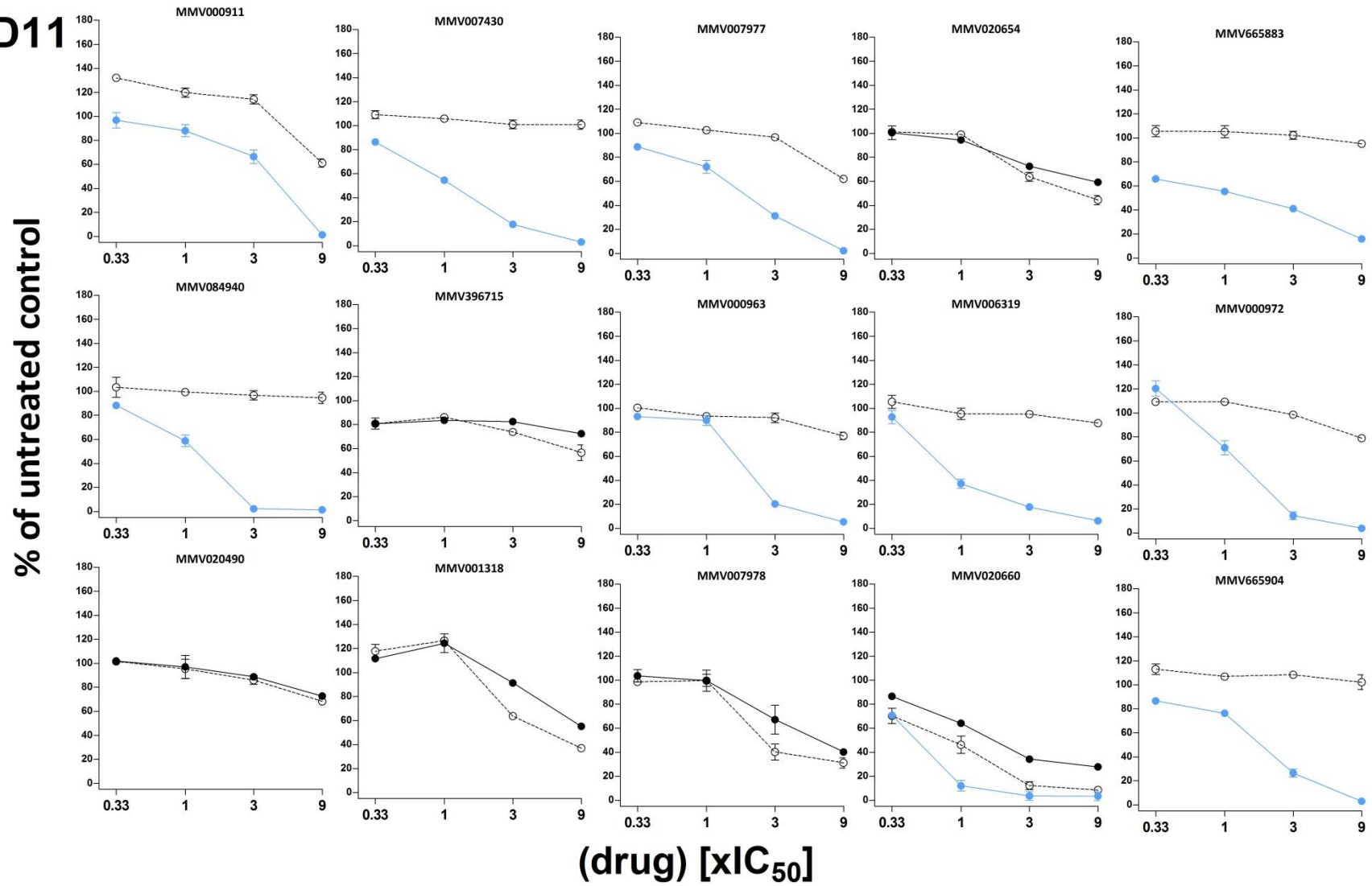
● 3 hr luciferase ○ 6 hr luciferase ● 48 hr luciferase

D10



● 3 hr luciferase ○ 6 hr luciferase ● 48 hr luciferase

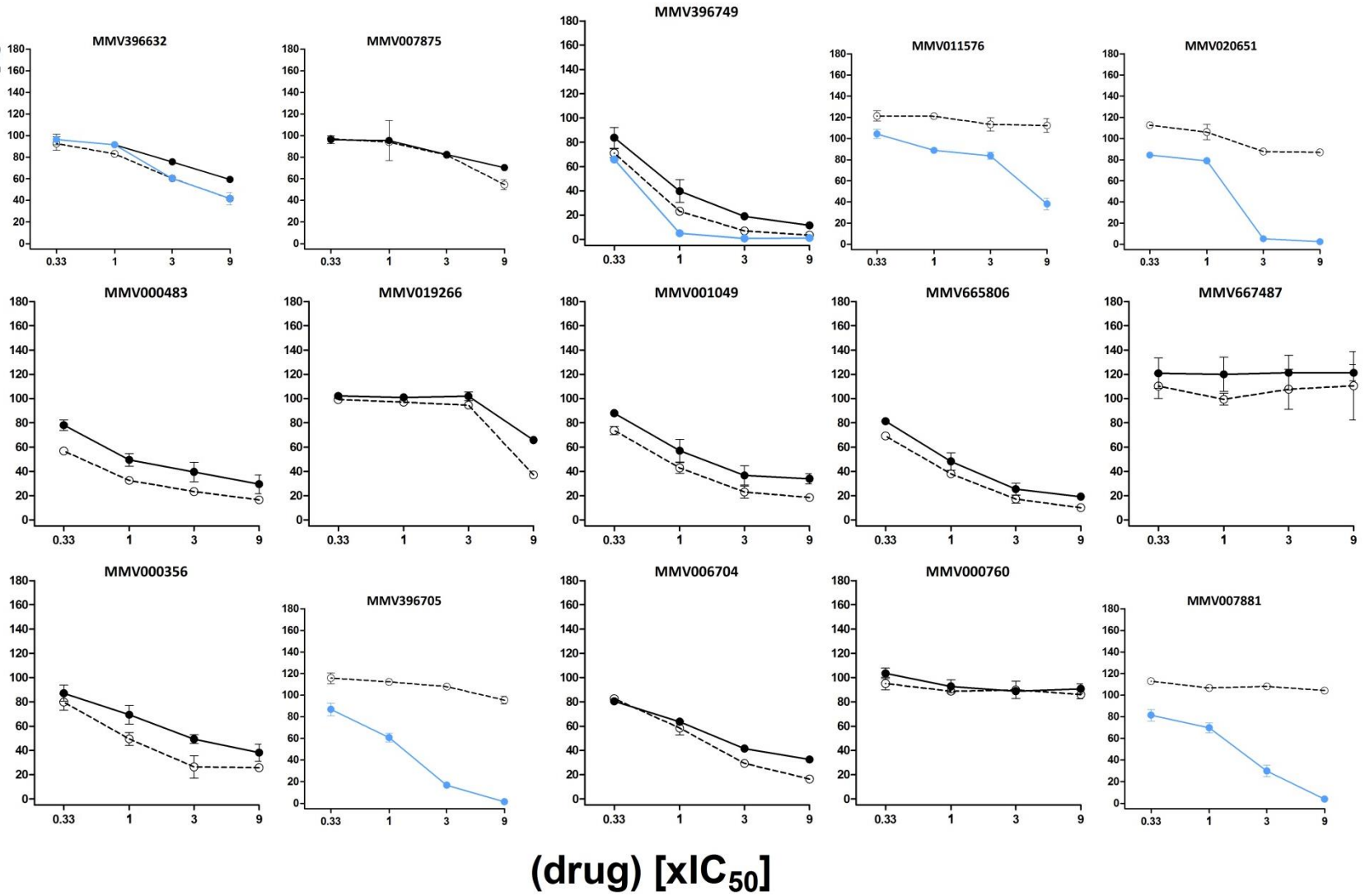
D11



● 3 hr luciferase ○ 6 hr luciferase ● 48 hr luciferase

D12

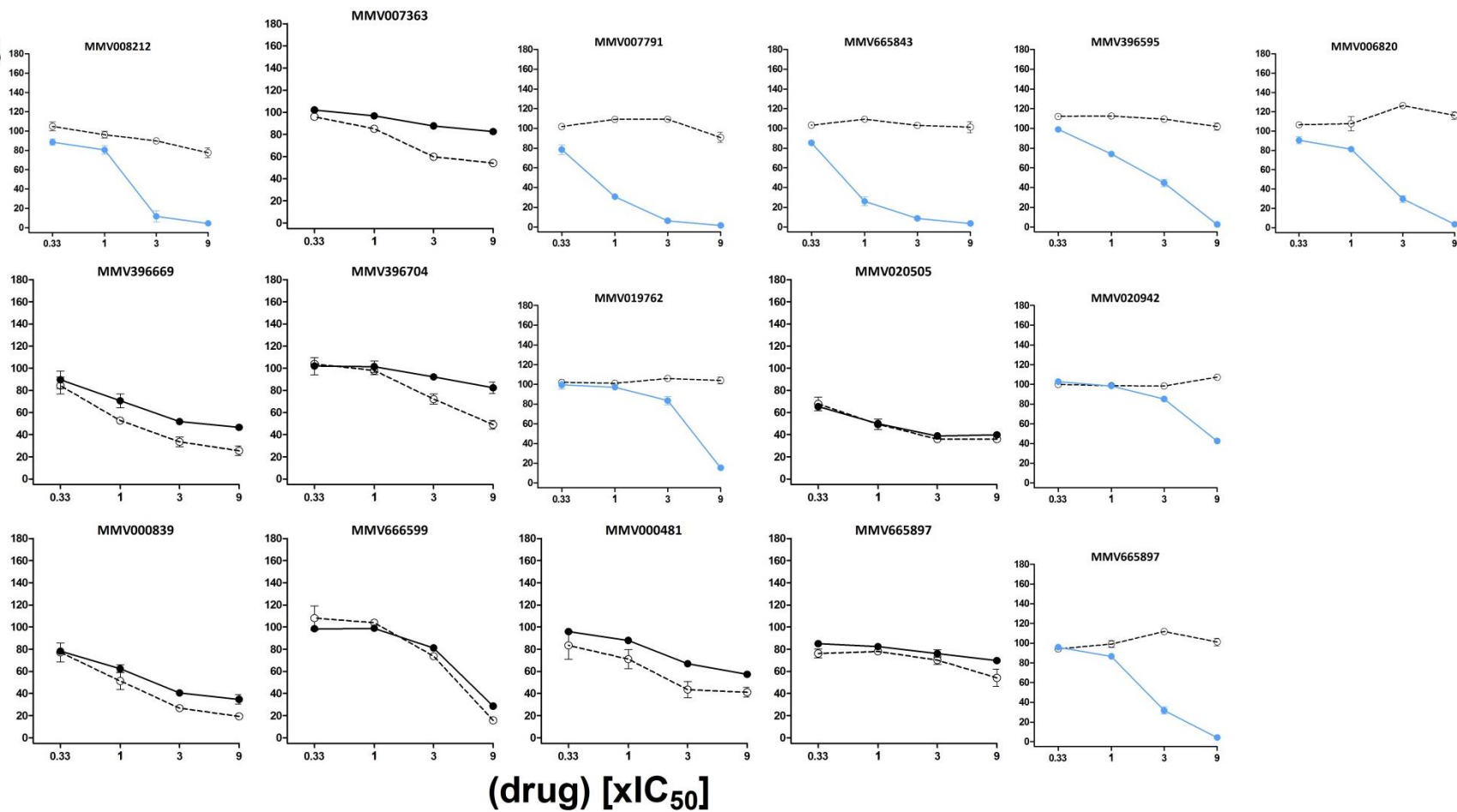
% of untreated control



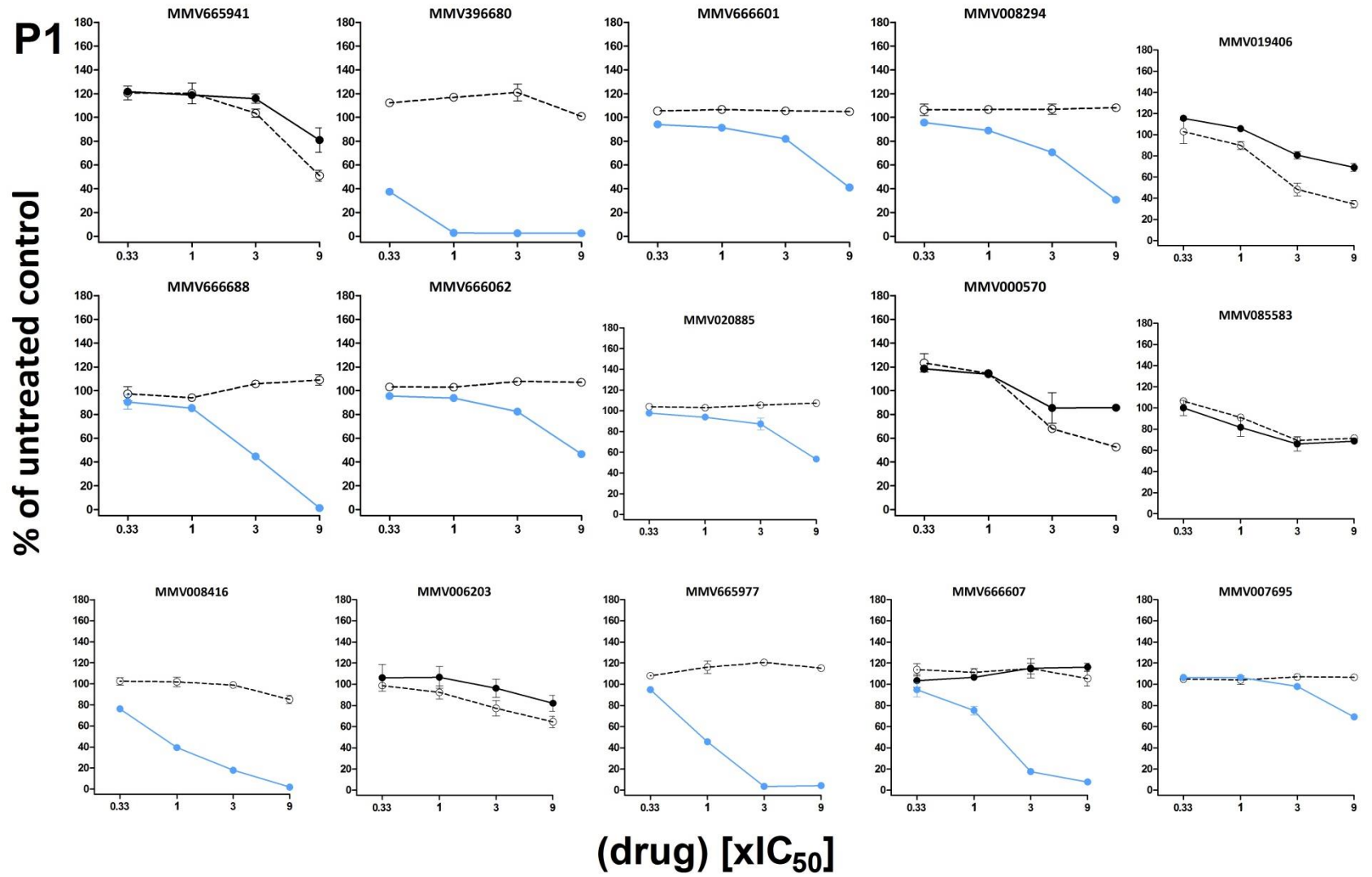
● 3 hr luciferase ○ 6 hr luciferase ● 48 hr luciferase

D13

% of untreated control



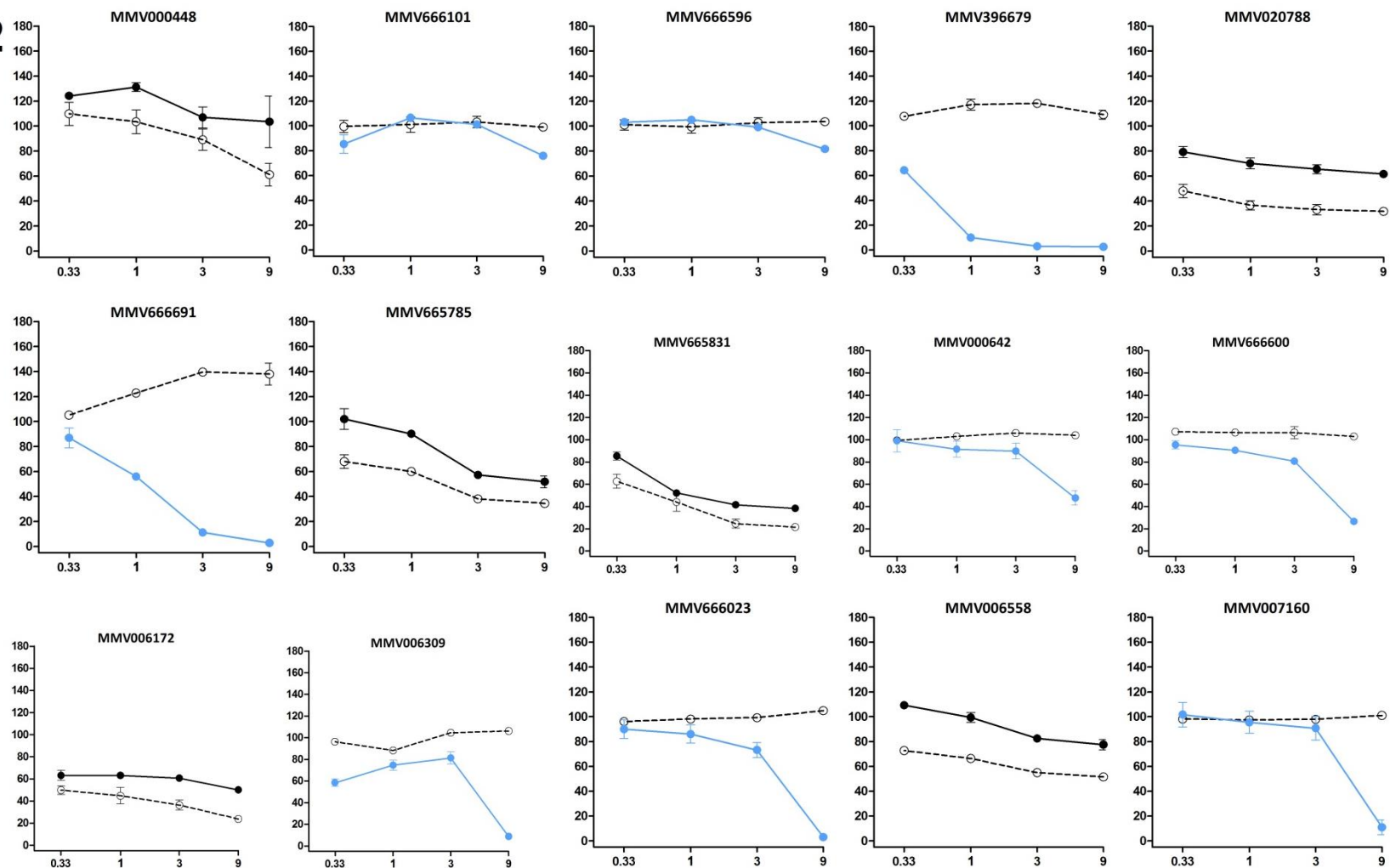
● 3 hr luciferase ● 48 hr luciferase ○ 6 hr luciferase



● 3 hr luciferase    ● 48 hr luciferase    ○ 6 hr luciferase

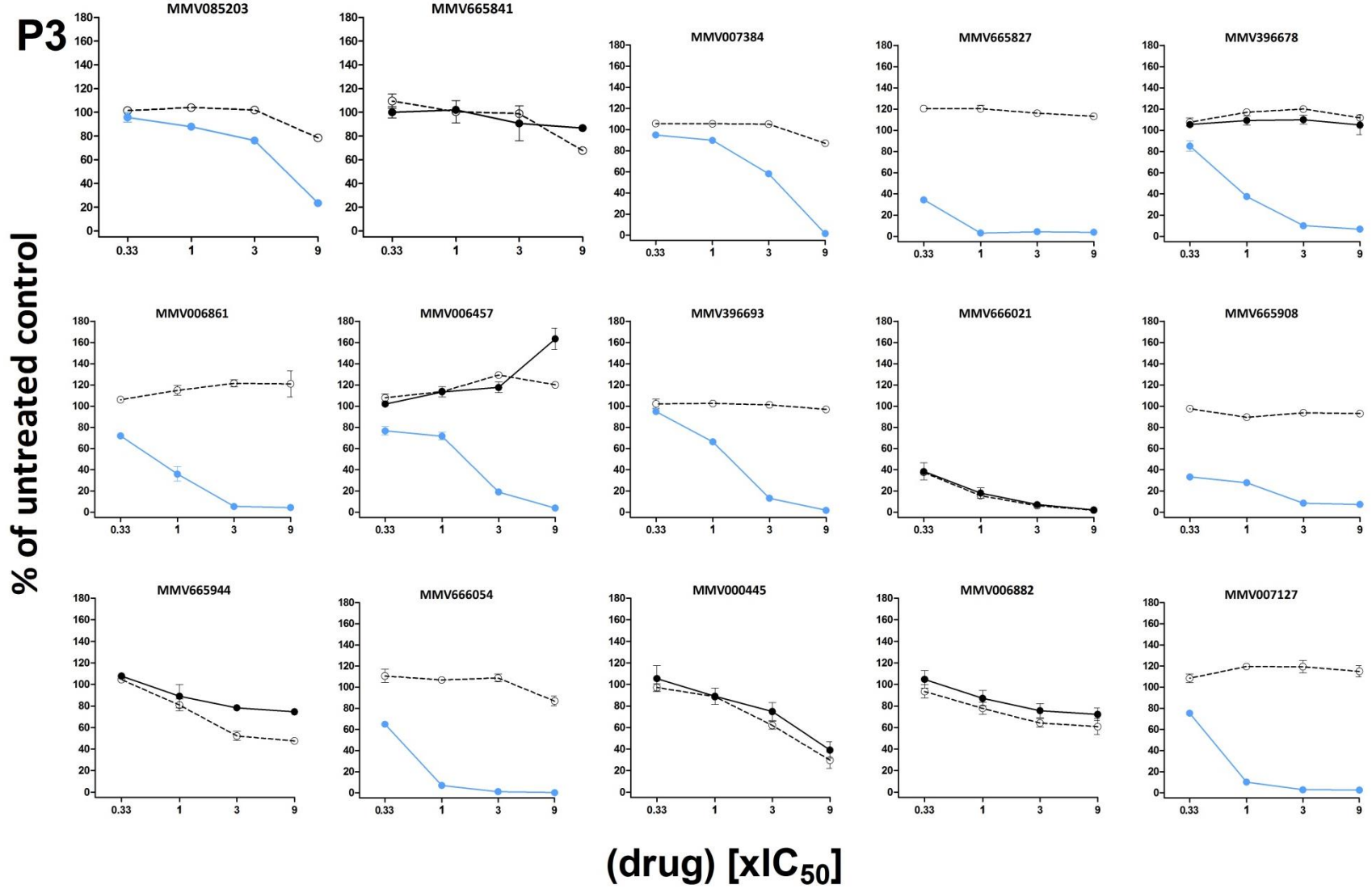
P2

% of untreated control



(drug) [ $xIC_{50}$ ]

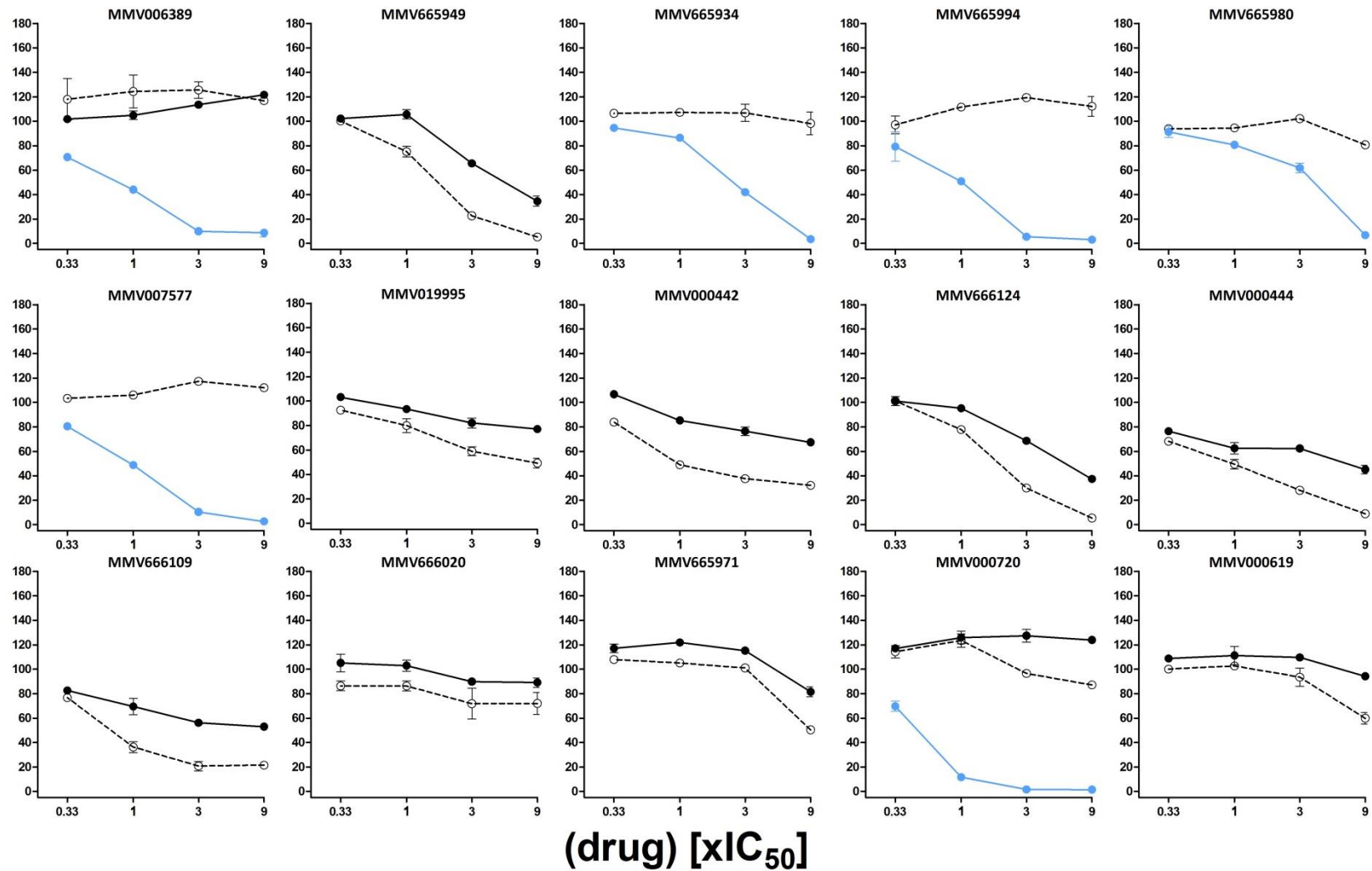
● 3 hr luciferase ● 48 hr luciferase ○ 6 hr luciferase



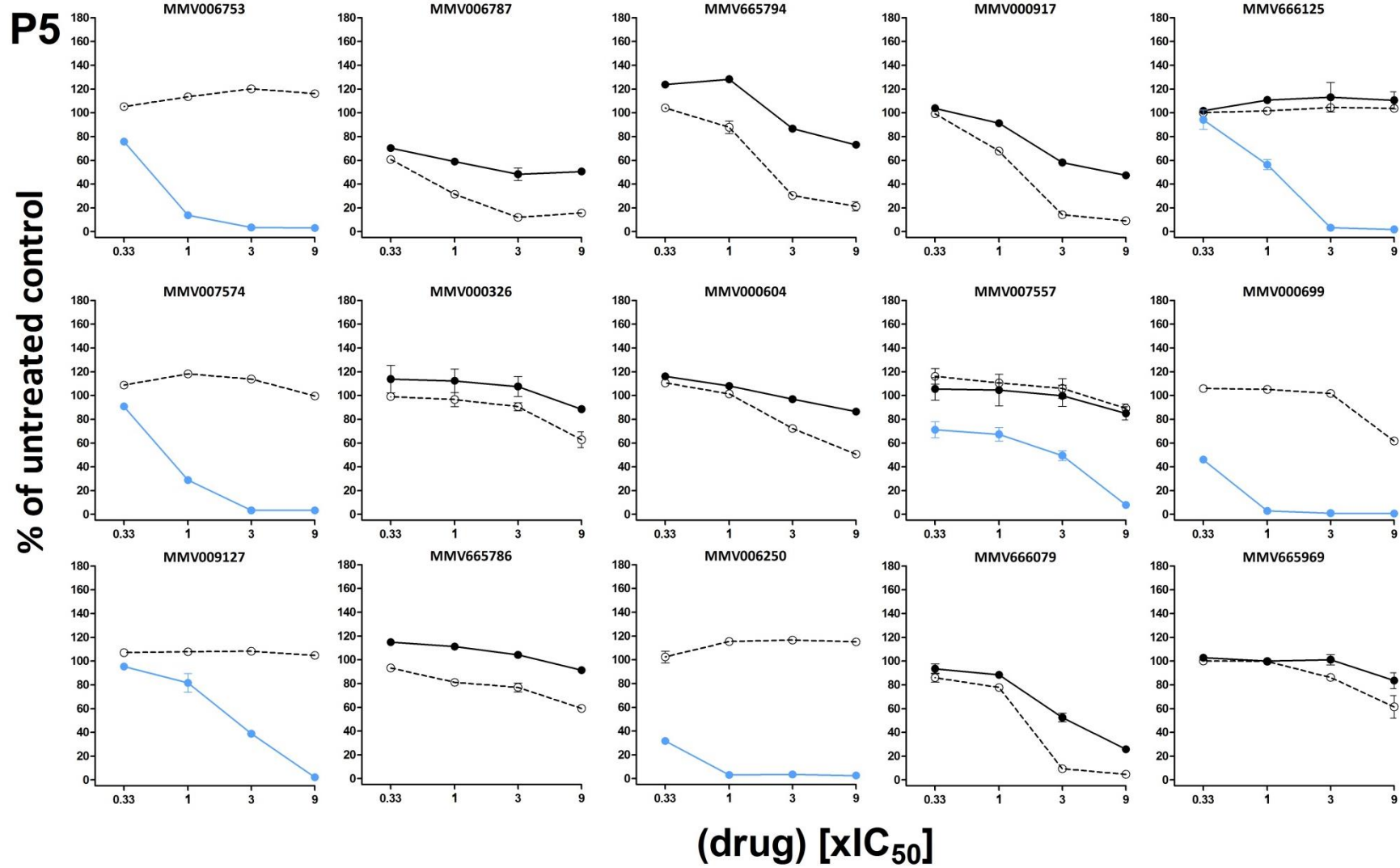
● 3 hr luciferase ● 48 hr luciferase ○ 6 hr luciferase

P4

% of untreated control



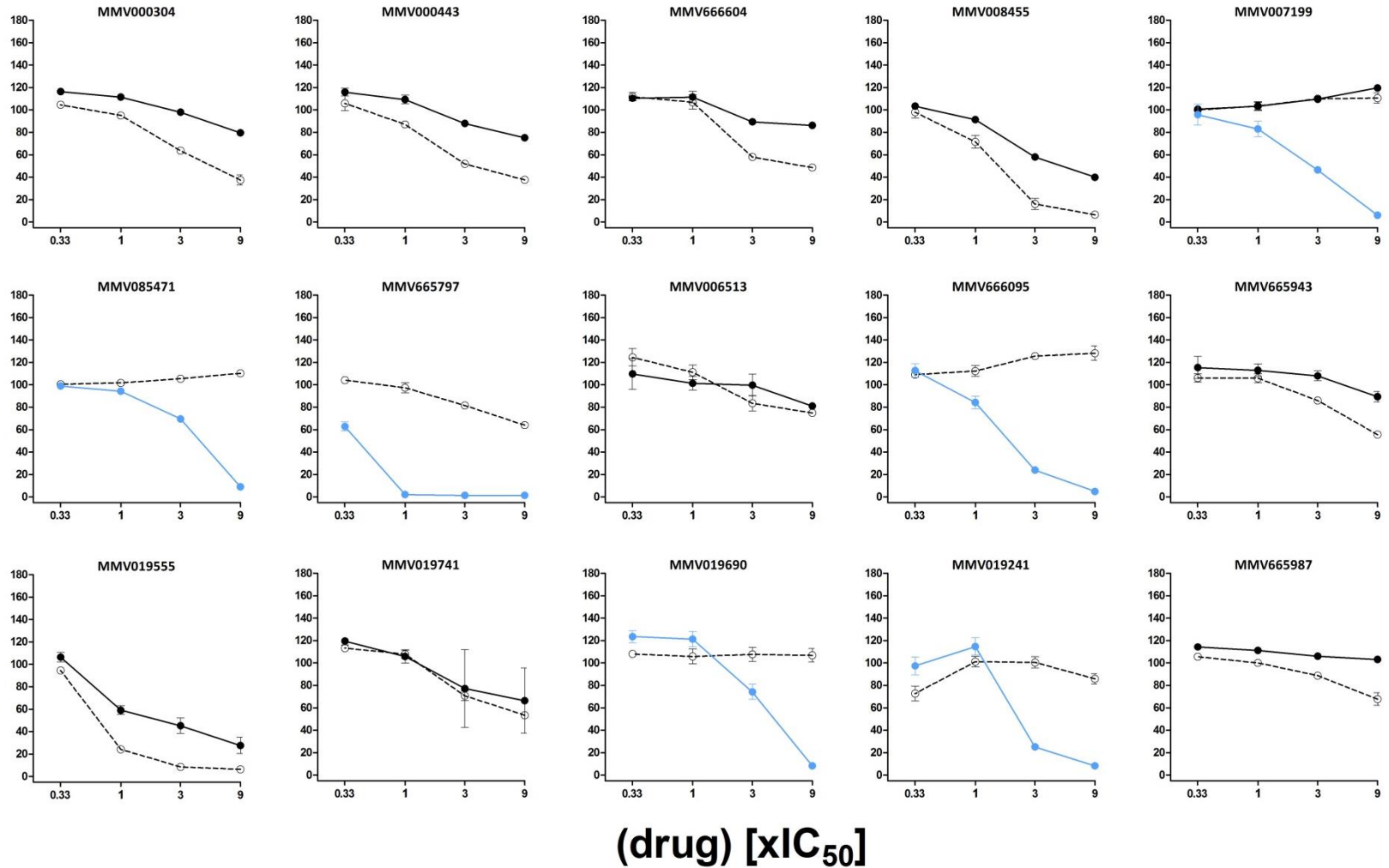
● 3 hr luciferase ● 48 hr luciferase ○ 6 hr luciferase



● 3 hr luciferase ● 48 hr luciferase ○ 6 hr luciferase

P6

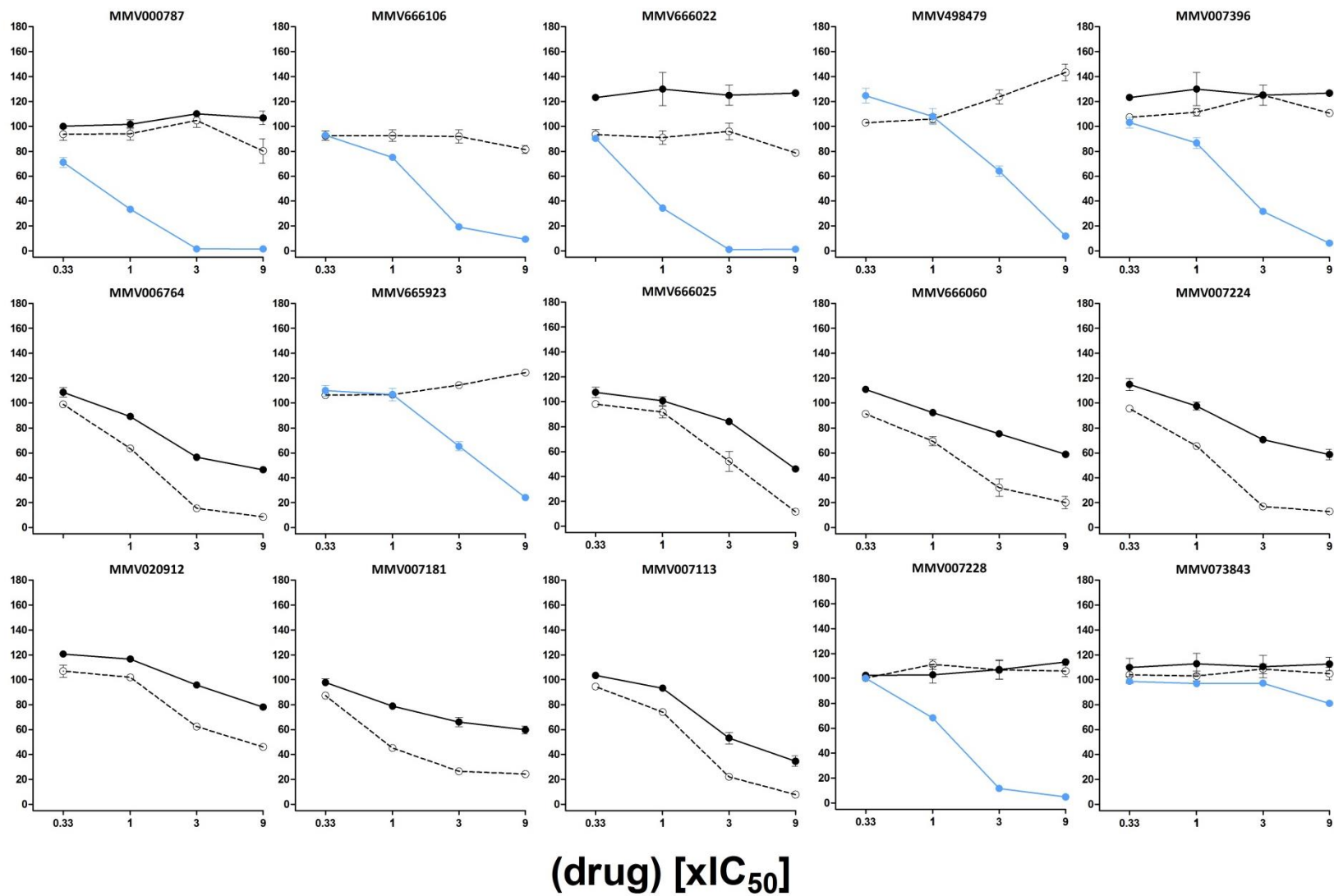
% of untreated control



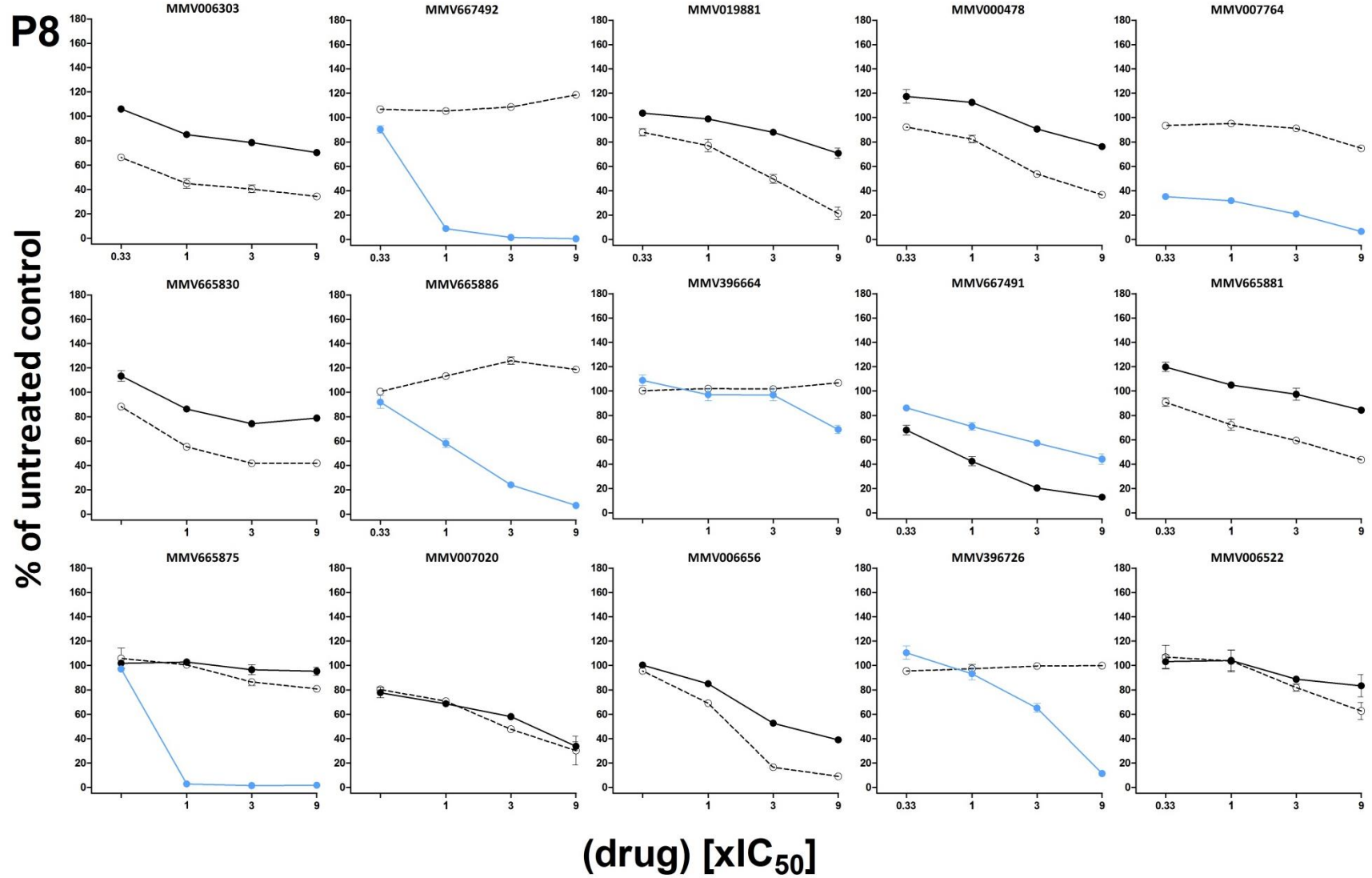
● 3 h luciferase ○ 6 h luciferase ● 48 h luciferase

P7

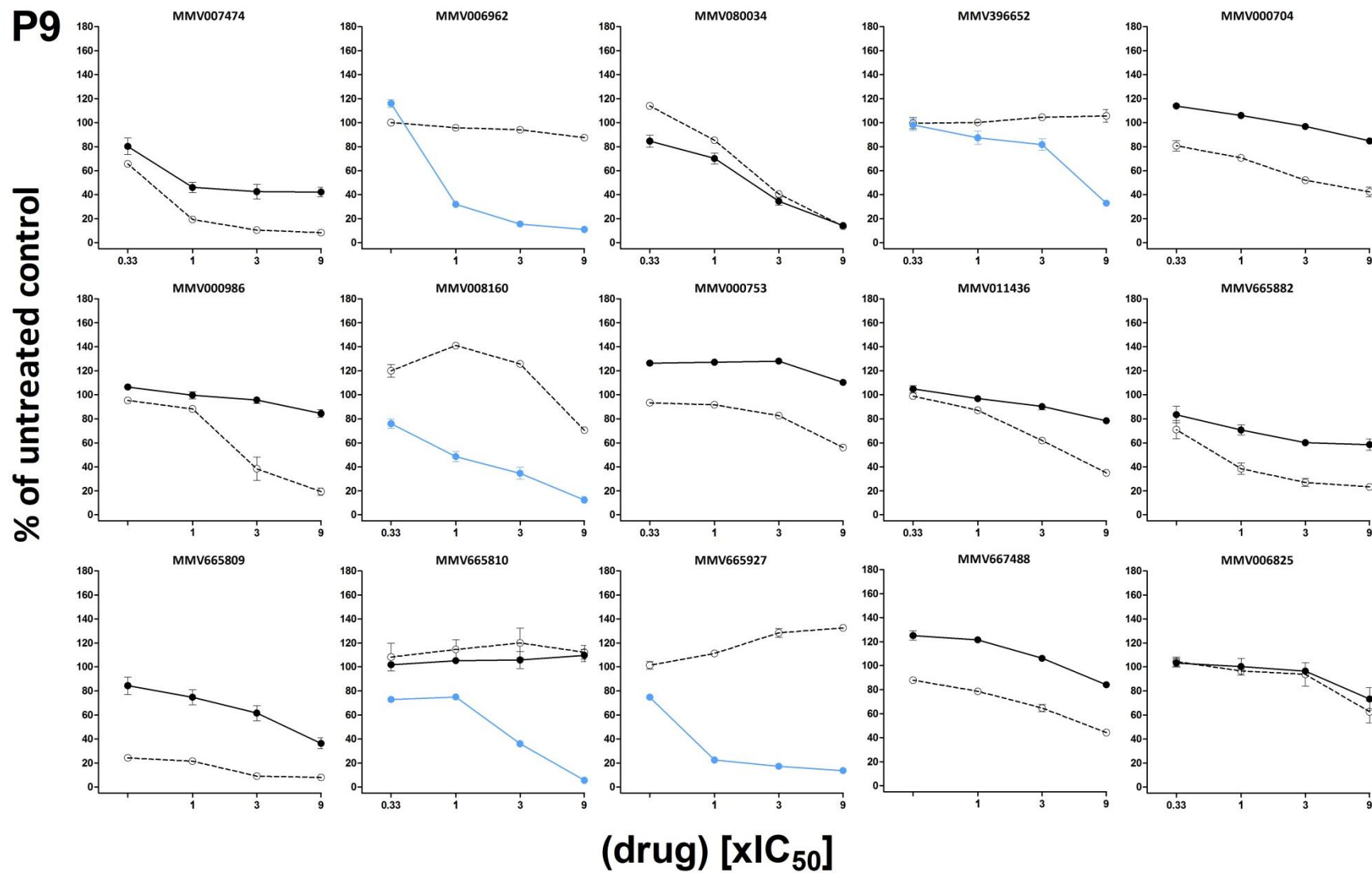
% of untreated control



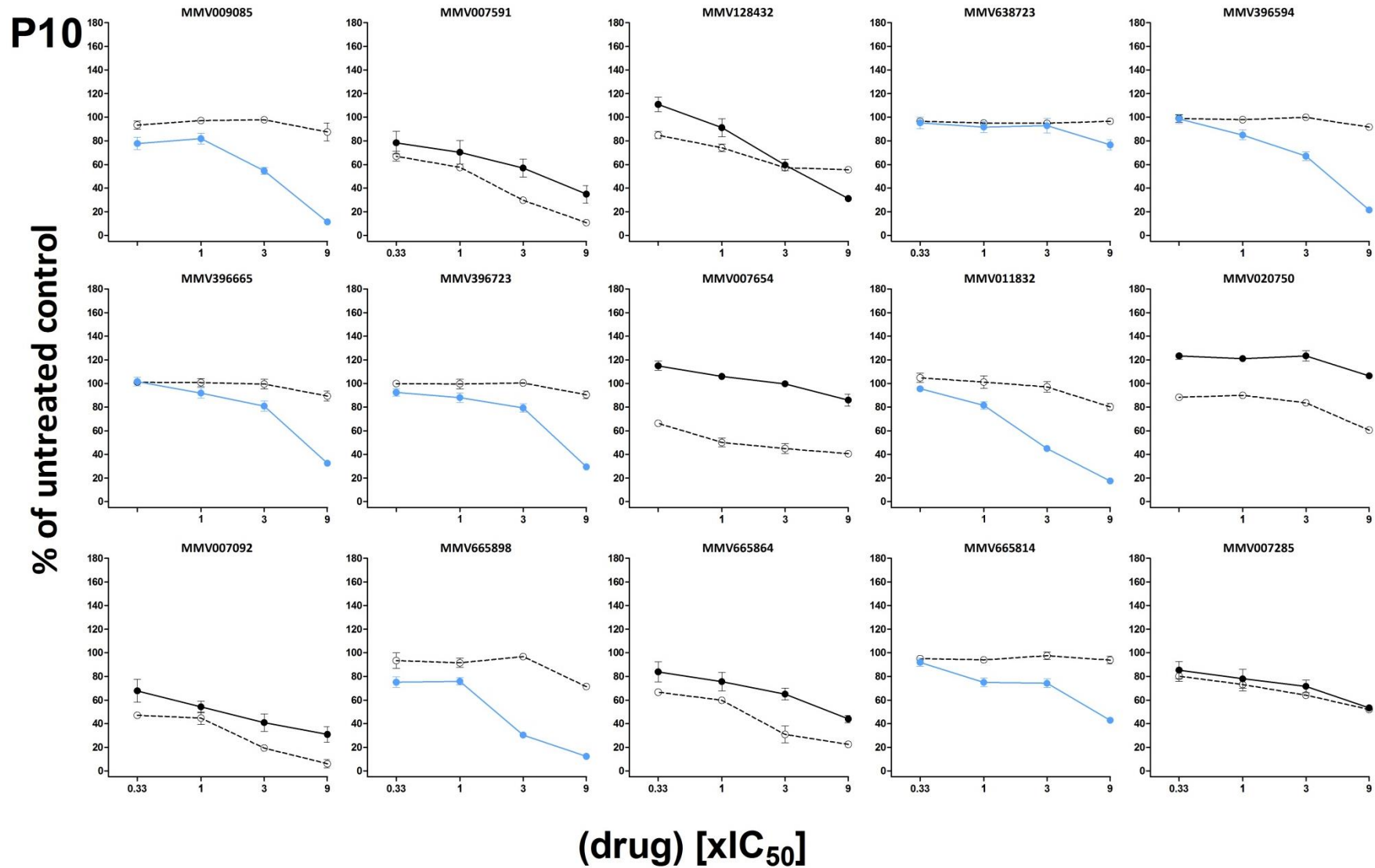
● 3 h luciferase ○ 6 h luciferase ● 48 h luciferase



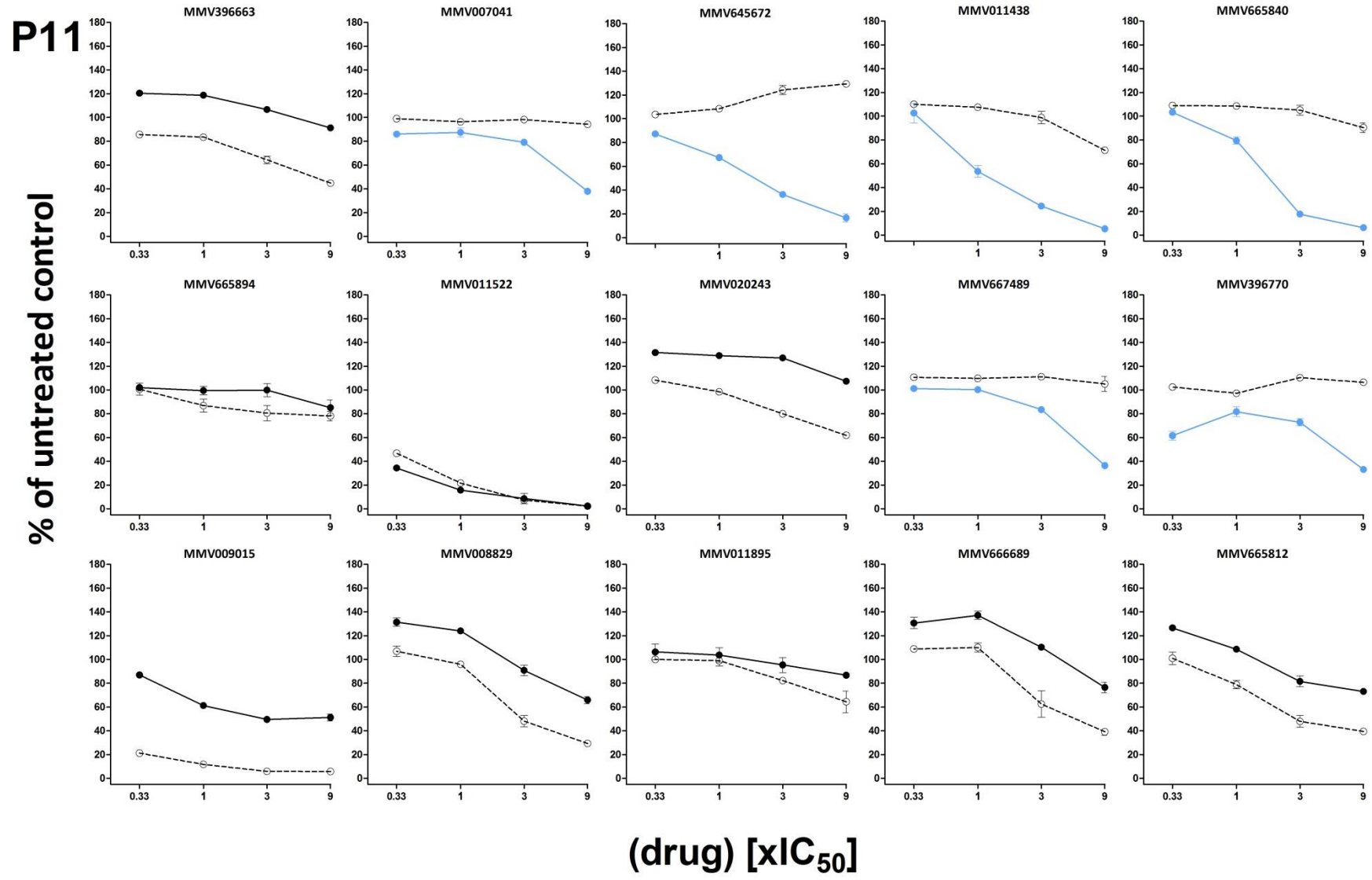
● 3 h luciferase ○ 6 h luciferase ● 48 h luciferase



● 3 h luciferase ○ 6 h luciferase ● 48 h luciferase



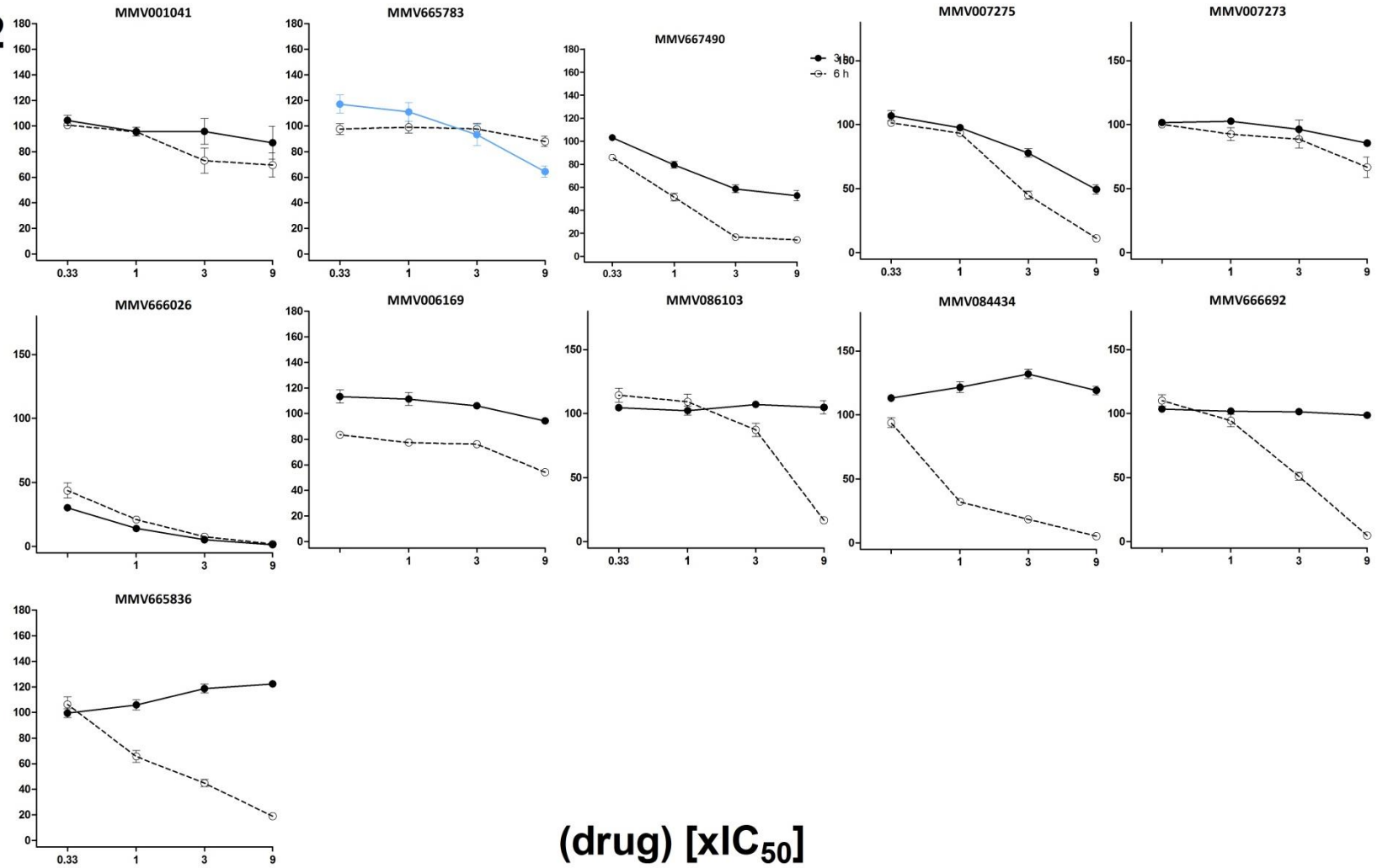
● 3 h luciferase ○ 6 h luciferase ● 48 h luciferase



● 3 h luciferase ○ 6 h luciferase ● 48 h luciferase

P12

% of untreated control



## Appendix 2 (Chapter 4)

This table reports full PC1 dataset of the Malaria Box compounds (data reported in Chapter 4). The compounds are categorised by RAG (Red, Amber and Green). **Green**-TCP1 candidates with initial rate of kill > DHA; **Amber** -TCP1 candidates with initial rate of kill > CQ and < DHA. **Red**- slow acting compounds.

6hr PC1 (Chapter 4)							
MMV_ID	PC1	MMV_ID	PC1	MMV_ID	PC1	MMV_ID	PC1
MMV142383	-106.9	MMV008455	-49.0	MMV665857	-14.5	MMV011944	23.4
MMV009015	-106.3	MMV006429	-48.8	MMV666025	-14.4	MMV396704	23.6
MMV665891	-102.1	MMV396794	-48.8	MMV666102	-13.4	MMV019918	24.1
MMV666021	-101.8	MMV007224	-48.5	MEF	-13.3	MMV019313	24.8
MMV665809	-97.5	MMV007181	-48.4	MMV665953	-13.1	MMV666020	25.4
MMV666026	-96.6	MMV000356	-47.7	MMV000704	-12.2	MMV000753	27.8
MMV020243	-95.2	MMV006704	-46.0	MMV009063	-10.7	MMV000604	28.0
MMV396749	-87.2	MMV665864	-45.6	MMV006558	-9.7	MMV396797	28.4
MMV007474	-85.6	CQ	-45.3	MMV007978	-6.8	MMV020750	28.6
MMV019555	-77.4	MMV665918	-44.6	MMV665812	-6.7	MMV007875	28.7
MMV006787	-76.2	MMV019662	-44.5	MMV666071	-6.3	MMV019266	28.8
MMV007092	-74.7	MMV007113	-44.4	MMV000478	-5.6	MMV001318	29.2
MMV665800	-74.1	MMV665949	-43.4	MMV665902	-5.5	MMV665888	29.9
MMV665826	-73.3	MMV396633	-43.0	PPQ	-5.5	MMV006203	31.1
MMV665803	-73.0	MMV665807	-42.4	MMV665906	-4.0	MMV019064	31.6
DHA	-70.9	MMV007907	-41.3	MMV019406	-3.5	MMV085583	31.7
MMV665806	-70.7	MMV396669	-40.6	MMV665881	-3.5	MMV019741	32.5
MMV020660	-70.3	MMV006303	-40.6	MMV006455	-3.4	MMV001041	33.3
MMV000483	-69.3	MMV009108	-39.8	MMV008829	-2.5	MMV665946	33.7
MMV007617	-66.8	MMV020505	-39.5	MMV000443	0.0	MMV665913	36.3
MMV667491	-65.4	MMV666124	-37.4	MMV000445	0.0	MMV000570	36.5
MMV665796	-62.6	MMV000442	-36.4	MMV128432	1.1	MMV001230	36.8
MMV666109	-60.8	MMV006087	-35.1	MMV007285	1.6	MMV011522	37.0
MMV396736	-59.6	MMV666060	-34.6	MMV396632	1.8	MMV000561	37.3
MMV000444	-59.5	MMV665785	-33.8	MMV665944	2.3	MMV019738	37.6
MMV665831	-58.8	MMV007654	-31.6	MMV667488	2.4	MMV011895	37.7
MMV001049	-58.8	MMV666061	-29.6	MMV011436	2.6	MMV665894	38.6
MMV019127	-57.5	MMV665817	-28.9	MMV019995	3.6	MMV665969	38.8
MMV667490	-57.4	MMV306025	-27.9	MMV396663	4.2	MMV007273	39.9
MMV000848	-56.8	MMV665928	-26.0	MMV665897	7.7	MMV665943	39.9
MMV665882	-56.5	MMV665890	-25.3	MMV019780	9.6	MMV020275	40.2
MMV000248	-55.4	MMV665830	-24.1	MMV666599	9.9	MMV000326	40.5
MMV020788	-55.3	MMV665789	-23.9	MMV007363	10.5	MMV006522	40.7
MMV666079	-54.5	QN	-22.6	MMV000304	10.6	MMV020490	40.8
MMV007591	-53.9	MMV665794	-22.4	MMV006882	12.5	MMV000498	41.2
MMV006172	-53.6	MMV007020	-21.9	MMV006169	13.0	MMV020500	42.8

MMV006545	-53.4	MMV000986	-21.0	MMV000648	13.6	MMV000619	43.6
MMV665805	-53.0	MMV019881	-20.5	MMV020654	15.5	MMV006825	43.8
MMV006764	-51.8	MMV666116	-19.7	MMV020912	18.6	MMV000448	45.1
MMV019017	-51.7	MMV000620	-19.3	MMV000634	19.0	MMV665987	45.5
MMV011795	-51.2	MMV080034	-18.8	MMV666689	19.2	MMV665971	46.4
MMV665929	-51.1	PYR	-18.7	MMV666069	20.6	MMV000760	48.1
MMV000839	-50.9	MMV000653	-17.6	MMV665786	20.7	MMV666110	50.4
MMV000917	-50.2	MMV006706	-17.5	MMV666604	21.1	MMV665875	51.8
MMV665878	-49.5	MMV007275	-17.3	MMV274073	21.7	MMV020549	53.1
MMV006656	-49.3	MMV000481	-17.1	MMV001038	23.1	MMV665841	53.2

MMV_ID	PC1	MMV_ID	PC1	MMV_ID	PC1	MMV_ID	PC1
MMV665914	53.9	MMV011099	72.5	MMV665915	82.4	MMV396678	98.2
MMV006513	57.1	MMV001246	74.3	MMV007199	82.5	MMV666070	105.7
MMV666080	57.2	MMV666125	74.5	ATOVA	84.4	MMV006389	110.7
MMV665979	57.5	MMV000720	74.8	MMV666072	87.2	MMV006937	112.0
MMV665941	59.3	MMV008956	75.9	MMV666607	90.4	MMV666022	114.9
MMV665917	60.9	MMV007557	76.3	MMV019066	90.9	MMV006457	121.7
MMV006587	65.7	MMV073843	79.5	MMV001344	91.3	MMV000787	127.2
MMV008149	69.9	MMV007228	81.9	MMV020492	94.5		
MMV011259	71.8	MMV667487	82.2	MMV665810	97.2		

### Appendix 3 (Chapter 5)

This table reports full PC1 dataset of the all the **370 Malaria Box compounds** (data reported in Chapter 5). The compounds are categorised by RAG (Red, Amber and Green). **Green**-TCP1 candidates with initial rate of kill > DHA: **Amber** -TCP1 candidates with initial rate of kill > CQ and < DHA. **Red**- slow acting compounds.

6hr PC1 data (Chapter 5)							
MMV Name	6hr PC1	MMV Name	6hr PC1	MMV Name	6hr PC1	MMV Name	6hr PC1
MMV142383	-131.5	MMV000839	-79.5	MMV665953	-46.4	MMV665786	-7.8
MMV009015	-129.9	MMV011795	-79.1	MMV666102	-46.0	MMV396704	-7.4
MMV665891	-127.0	MMV006429	-79.0	MMV000481	-45.8	MMV001038	-7.3
MMV666021	-126.9	MMV396794	-77.1	MMV665857	-45.5	MMV274073	-6.8
MMV666026	-122.4	MMV007181	-76.9	MMV006706	-43.7	MMV019918	-6.6
MMV665809	-121.7	MMV007113	-76.4	MEF	-42.4	MMV011944	-5.5
MMV011522	-121.2	MMV665949	-76.1	MMV009063	-40.5	MMV019313	-5.5
MMV396749	-114.9	MMV000356	-75.9	MMV000704	-40.5	MMV001318	-5.5
MMV007474	-112.2	MMV006704	-75.6	MMV007978	-39.0	MMV000604	-3.5
MMV019555	-106.3	MMV665918	-74.7	MMV665902	-37.7	MMV019266	-2.5
MMV665800	-103.1	MMV665864	-73.8	MMV665812	-37.1	MMV396797	-2.3
MMV006787	-102.8	CQ	-73.7	PPQ	-37.0	MMV666020	-2.1
MMV665803	-102.1	MMV007907	-72.5	MMV006558	-36.6	MMV000753	-1.5
MMV007092	-101.9	MMV396633	-72.2	MMV000478	-35.8	MMV665888	-1.3
MMV665826	-101.5	MMV665807	-71.9	MMV019406	-35.1	MMV007875	-1.1
MMV020660	-99.0	MMV019662	-71.2	MMV008829	-35.0	MMV020750	0.0
MMV665806	-98.6	MMV666124	-70.2	MMV006455	-33.6	MMV019064	0.2
DHA	-97.4	MMV396669	-69.2	MMV666071	-33.3	MMV019741	0.5
MMV000483	-95.7	MMV019110	-67.1	MMV665906	-32.8	MMV665954	0.9
MMV007617	-95.5	MMV006303	-66.9	MMV665881	-32.5	MMV665946	1.1
MMV667491	-93.3	MMV006087	-66.5	MMV000445	-31.4	MMV006203	1.9
MMV665796	-91.4	MMV020505	-66.2	MMV000443	-31.3	MMV085583	2.5
MMV666109	-88.3	MMV009108	-65.7	MMV011436	-28.4	MMV018984	2.7
MMV000444	-88.1	MMV666060	-65.2	MMV396632	-28.0	MMV000570	3.4
MMV396736	-87.6	MMV000442	-64.3	MMV665944	-27.9	MMV001041	4.1
MMV667490	-87.0	MMV665785	-61.2	MMV128432	-26.8	MMV000561	5.1
MMV001049	-86.8	MMV666061	-60.4	MMV667488	-26.7	MMV665913	6.2
MMV666079	-86.5	MMV306025	-59.7	MMV007285	-26.1	MMV020243	6.6
MMV665831	-85.9	MMV665817	-58.8	MMV019995	-25.7	MMV666067	6.6
MMV000848	-85.0	MMV007654	-57.8	MMV396663	-25.0	MMV665797	7.6
MMV000248	-84.3	MMV665928	-57.1	MMV666599	-24.0	MMV011895	8.0
MMV019127	-83.9	MMV665890	-57.1	MMV019780	-22.3	MMV001230	8.5
MMV665882	-83.6	MMV665789	-55.5	MMV000304	-21.1	MMV665969	8.9
MMV006764	-83.4	MMV665794	-55.0	MMV665897	-19.9	MMV665943	8.9
MMV007591	-82.8	MMV000986	-53.1	MMV007363	-18.9	MMV396703	9.1
MMV665805	-82.1	MMV080034	-52.2	MMV000648	-16.4	MMV019738	9.2
MMV000917	-82.1	QN	-52.0	MMV020654	-15.8	MMV020275	9.4

MMV008455	-81.2	MMV665830	-52.0	MMV006882	-15.7	MMV665899	9.5
MMV006656	-81.0	MMV000653	-51.9	MMV006169	-15.0	MMV665948	9.7
MMV019017	-80.9	MMV019881	-51.1	MMV000634	-14.6	MMV006522	10.1
MMV006545	-80.6	MMV007020	-51.1	MMV666689	-13.6	MMV019746	10.6
MMV020788	-80.2	MMV666116	-51.1	MMV008270	-13.3	MMV665894	10.7
MMV007224	-79.8	MMV007275	-50.6	MMV020912	-13.1	MMV666057	10.7
MMV665878	-79.8	MMV666025	-47.4	MMV396715	-11.6	MMV007273	10.8
MMV665929	-79.8	PYR	-46.9	MMV666604	-11.1	MMV000326	11.0
MMV006172	-79.6	MMV000620	-46.4	MMV666069	-9.8	MMV001255	11.1

MMV Name	6hr PC1						
MMV020490	11.5	MMV403679	28.4	MMV666692	43.4	MMV666693	54.7
MMV008127	12.7	MMV011438	28.5	MMV665883	43.5	MMV009127	54.8
MMV000498	13.0	MMV006962	28.5	MMV019871	43.9	MMV019690	54.9
MMV019124	13.4	MMV665908	28.6	MMV666054	44.0	MMV007808	55.0
MMV000619	13.5	MMV011832	29.1	MMV000720	44.3	MMV007881	55.2
MMV020500	13.7	MMV009085	29.9	MMV666081	44.3	MMV667487	55.2
MMV006825	14.0	MMV006319	30.3	MMV665820	44.4	ATOVA	55.4
MMV000448	14.4	MMV665799	30.8	MMV665840	44.4	MMV008294	55.5
MMV019202	14.5	MMV665798	31.0	MMV020548	44.6	MMV006188	55.9
MMV665971	15.0	MMV665917	31.1	MMV020942	44.6	MMV007199	56.0
MMV666108	15.1	MMV020651	31.3	MMV000563	44.8	MMV396595	56.6
MMV665987	15.7	MMV085203	31.7	MMV666596	45.8	MMV007839	56.8
MMV006427	16.1	MMV665783	31.9	MMV007791	45.9	MMV667489	58.2
MMV665898	16.8	MMV075490	32.2	MMV001246	46.0	MMV666103	59.2
MMV019074	16.9	MMV665814	32.8	MMV019258	46.6	MMV007574	59.6
MMV007764	17.0	MMV008416	33.1	MMV007557	46.7	MMV008160	60.6
MMV665909	17.2	MMV638723	33.5	MMV008956	46.9	MMV666072	61.0
MMV665961	17.2	MMV000972	33.6	MMV007430	47.2	MMV019700	62.6
MMV007977	18.9	MMV009060	34.1	MMV666125	47.5	MMV667492	62.7
MMV019758	19.3	MMV006587	34.5	MMV396664	48.0	MMV007577	63.3
MMV000963	19.9	MMV396594	35.3	MMV666688	48.0	MMV019066	63.7
MMV665939	19.9	MMV007041	35.3	MMV396652	48.0	MMV396680	65.1
MMV666106	20.4	MMV396665	35.4	MMV006278	48.2	MMV001344	65.3
MMV666022	20.6	MMV396723	35.8	MMV007374	48.2	MMV665994	65.5
MMV008212	20.9	MMV084940	36.8	MMV000662	48.3	MMV396679	67.5
MMV000760	21.0	MMV665901	37.6	MMV020439	48.4	MMV011099	68.0
MMV000699	22.2	MMV007906	38.5	MMV019762	48.6	MMV006250	68.4
MMV666110	22.5	MMV665876	38.8	MMV665843	48.9	MMV665810	69.6
MMV666105	22.6	MMV396726	39.3	MMV000642	49.1	MMV665836	69.7
MMV665875	22.8	MMV396672	39.3	MMV011259	49.1	MMV665923	70.2
MMV666009	23.0	MMV665850	39.3	MMV007116	49.1	MMV007396	70.3
MMV666075	23.0	MMV007160	39.6	MMV665934	49.2	MMV396678	70.4
MMV665874	23.1	MMV000788	39.8	MMV665915	49.6	MMV006753	71.1
MMV665841	23.2	MMV011256	40.1	MMV086103	51.3	MMV011576	71.2
MMV006767	24.9	MMV007384	40.4	MMV396770	51.6	MMV665977	72.6

MMV020549	24.9	MMV020700	40.7	MMV666600	51.7	MMV006820	72.8
MMV665914	24.9	MMV665782	40.7	MMV020885	51.9	MMV665827	73.0
MMV665879	24.9	MMV000911	41.4	MMV666601	52.3	MMV007127	73.1
MMV665940	25.2	MMV666093	41.7	MMV073843	52.3	MMV665886	75.3
MMV006513	25.8	MMV396693	42.0	MMV085471	52.3	MMV006913	75.6
MMV665941	26.2	MMV665916	42.2	MMV396705	52.5	MMV006861	75.6
MMV396681	27.2	MMV007571	42.5	MMV007695	52.9	MMV666070	77.0
MMV665980	27.3	MMV020492	42.6	MMV666062	53.1	MMV645672	79.4
MMV019241	27.5	MMV666023	42.7	MMV665904	54.1	MMV006457	80.0
MMV007564	27.7	MMV008149	42.7	MMV666607	54.3	MMV006389	82.2
MMV665979	28.2	MMV006309	42.8	MMV007228	54.4	MMV666095	82.4
MMV666080	28.4	MMV666101	43.4	MMV019670	54.5	MMV665927	84.8
MMV084434	85.54573	MMV006937	86.45927	MMV498479	86.74462	MMV000787	95.48005
MMV666691	100.8948						

## Appendix 4 (Chapter 5)

Table reports biophysical properties for the 400 Malaria Box compounds. **MW**= Molecular weight, **LogP/D** = Octanol-water partition coefficient, **TPSA** = Total Polar surface area, **RotB** = Rotatable bonds, **PKa**= Acid-base dissociation constant, **LE**= Ligand efficiency, **LLE**= ligand-lipophilicity efficiency, **H-D** = Hydrogen bond donors, **H-A** = Hydrogen bond acceptors and **Ro5-V**= rule of 5 violation.

MMV-Code	MW	LogP	LogD	TPSA	Rt_B	pKa	LE	LLE	H_A	H_D	Ro5_V
MMV000248	421.4	4.2	2.7	53.8	8	8.9	0.3	1.9	5	2	0
MMV000340	216.3	2.8	-0.6	27.1	1	11.7	0.5	3.4	2	1	0
MMV000356	379.3	3.8	3.9	26.7	4	7.0	0.4	2.2	3	1	0
MMV000443	303.8	4.2	4.2	21.7	4	3.9	0.4	2.1	3	0	0
MMV000444	367.5	4.5	4.4	59.8	9	6.5			5	2	0
MMV000448	279.4	3.1	-0.4	28.2	5	9.6	0.4	3.6	3	1	0
MMV000478	347.8	3.2	2.9	50.7	5	9.0	0.4	3.0	4	2	0
MMV000481	391.9	3.9	3.6	60.0	7	7.7	0.3	2.0	5	2	0
MMV000483	341.5	4.4	3.6	50.7	5	8.2	0.3	1.8	4	2	0
MMV000498	363.5	5.0	4.9	54.5	6	6.6			5	1	0
MMV000561	458.6	4.3	1.5	68.6	12	10.3	0.3	1.5	7	1	0
MMV000563	371.5	5.0	3.7	41.8	2	0.5	0.3	1.1	3	1	0
MMV000620	343.9	4.7	2.5	23.5	5	9.6			2	1	0
MMV000634	450.6	4.5	2.5	49.6	6	9.5	0.3	1.7	5	1	0
MMV000648	448.6	4.6	4.6	58.6	7	-1.1			5	1	0
MMV000653	462.6	5.0	5.0	58.6	8	-1.1	0.2	0.9	5	1	0
MMV000662	434.6	4.9	4.9	58.6	6	-1.1	0.3	2.5	5	1	0
MMV000704	420.5	5.0	4.3	66.9	7	8.0	0.3	0.9	7	1	0
MMV000760	416.3	4.1	4.0	39.6	3	6.8			4	1	0
MMV000787	426.0	4.2	3.9	48.8	7	8.7	0.3	2.2	5	1	0
MMV000788	426.0	4.1	3.8	48.8	6	8.7	0.3	2.1	5	1	0
MMV000839	330.4	4.0	2.5	37.2	6	8.9	0.3	1.9	3	2	0
MMV000848	308.4	3.7	1.1	37.2	5	10.1	0.4	2.5	3	2	0
MMV000911	278.7	4.4	4.4	41.1	2	-4.7			3	2	0
MMV000917	398.5	4.6	4.6	51.1	3	1.1	0.3	1.3	5	0	0
MMV000963	356.4	5.2	5.2	59.1	6	5.1	0.3	1.1	5	2	0
MMV000972	282.2	2.8	2.0	46.5	2	-5.1			3	1	0
MMV000986	335.4	3.8	3.4	64.5	3	7.6	0.3	2.1	6	2	0
MMV001038	308.4	3.9	3.9	70.1	5	5.1	0.4	2.4	5	3	0
MMV001041	349.2	4.1	4.1	70.1	5	4.8	0.4	2.1	5	3	0
MMV001049	269.4	3.9	2.3	32.3	6	9.0	0.4	2.0	2	2	0
MMV001230	395.5	4.7	4.7	55.3	6	4.8			5	0	0

MMV001239	400.5	4.0	4.0	79.1	5	4.8				6	0	0
MMV001241	414.5	4.5	4.5	79.1	5	4.8				6	0	0
MMV001246	327.4	4.2	4.2	54.9	4	1.2	0.4	2.4	4	1	0	0
MMV001255	384.5	3.8	3.7	66.5	5	-3.5	0.3	2.5	5	1	0	0
MMV001318	325.6	4.5	4.5	41.1	2	-4.6			3	2	0	0
MMV001344	286.2	4.1	4.1	20.3	1	-1.1	0.5	2.1	2	0	0	0
MMV006087	277.8	2.9	0.7	28.2	6	9.4	0.5	4.3	3	1	0	0
MMV006169	326.4	5.3	5.3	49.8	5	4.9	0.3	0.8	4	2	0	0
MMV006188	382.9	1.9	1.9	79.6	4	-1.3	0.3	4.1	6	1	0	0
MMV006203	319.5	3.6	1.6	28.2	4	9.1	0.4	2.9	3	1	0	0
MMV006250	348.4	5.3	5.3	68.3	6	5.8	0.4	1.2	5	1	0	0
MMV006278	200.3	2.9	-0.5	27.1	1	12.6	0.6	3.5	2	1	0	0
MMV006303	293.4	3.3	0.8	28.2	6	9.4	0.4	3.1	3	1	0	0
MMV006309	292.3	3.3	3.3	41.9	3	4.7	0.5	4.0	4	0	0	0
MMV006319	308.4	4.2	4.1	49.8	5	7.1	0.4	1.9	4	2	0	0
MMV006427	464.0	3.5	3.5	72.9	4	-4.1	0.3	3.6	6	0	0	0
MMV006429	409.5	4.2	4.2	75.4	5	-0.5	0.4	3.3	6	1	0	0
MMV006455	370.5	4.1	1.7	61.8	11	9.8	0.3	2.7	5	2	0	0
MMV006457	293.3	4.2	4.2	59.4	4	2.0	0.4	2.7	4	1	0	0
MMV006522	357.3	4.7	4.0	34.2	4	8.0	0.4	1.6	3	1	0	0
MMV006545	362.3	3.1	1.2	56.8	6	9.3	0.4	3.0	5	2	0	0
MMV006558	287.8	5.1	5.1	12.5	2	4.5	0.5	1.5	2	0	0	0
MMV006587	345.8	2.1	1.9	66.1	5	7.2	0.4	4.1	6	2	0	0
MMV006656	468.3	3.6	3.6	74.3	10	-4.2	0.3	2.6	7	0	0	0
MMV006704	291.4	3.7	1.9	28.2	5	8.9	0.3	1.7	3	1	0	0
MMV006706	359.5	3.9	2.5	47.6	2	8.8	0.3	2.2	5	0	0	0
MMV006753	318.3	4.1	4.1	56.5	2	-2.9			4	0	0	0
MMV006764	440.3	2.9	2.9	74.3	8	-4.2	0.3	3.4	7	0	0	0
MMV006767	323.4	3.3	3.3	86.5	4	5.4	0.4	2.7	6	2	0	0
MMV006787	310.4	3.9	1.4	37.2	7	10.0	0.4	2.4	3	2	0	0
MMV006820	245.3	3.6	3.6	42.4	4	2.2	0.4	1.7	3	1	0	0
MMV006825	320.4	3.9	3.8	59.1	6	7.1	0.4	2.4	5	2	0	0
MMV006861	355.4	4.4	4.3	37.4	3	7.1	0.3	2.2	4	1	0	0
MMV006882	335.8	3.3	1.3	54.5	8	9.4	0.4	2.6	5	1	0	0
MMV006913	199.3	3.1	3.1	33.1	2	3.1	0.6	2.8	2	1	0	0
MMV006937	279.3	4.3	4.3	50.4	1	1.8	0.4	2.1	4	1	0	0
MMV007020	321.4	4.0	3.3	37.4	5	8.1	0.3	1.4	4	1	0	0
MMV007041	341.4	5.1	4.5	63.6	3	0.9	0.3	0.3	5	1	0	0

MMV007116	245.3	3.8	3.8	59.4	4	1.7	0.5	2.7	4	1	0
MMV007285	298.8	4.4	4.3	34.2	4	6.5	0.4	1.0	3	1	0
MMV007363	232.7	3.2	3.0	16.1	1	7.2	0.5	2.8	2	0	0
MMV007374	267.3	3.3	3.3	55.1	3	1.2	0.4	2.1	5	1	0
MMV007430	427.3	2.1	2.1	79.6	4	-1.3	0.3	4.0	6	1	0
MMV007564	444.6	5.6	5.6	50.2	6	5.9	0.3	0.4	5	1	0
MMV007571	301.4	3.3	3.3	42.2	6	-2.7	0.4	2.9	3	1	0
MMV007591	496.7	5.0	0.3	76.7	15	10.1			6	2	0
MMV007617	335.5	3.7	3.7	46.9	6	5.2	0.3	2.0	4	1	0
MMV007686	334.4	3.2	3.2	67.4	8	-6.6	0.4	3.7	5	2	0
MMV007764	256.4	4.7	1.3	27.1	5	12.7	0.5	1.4	2	1	0
MMV007791	357.4	1.3	1.3	75.0	6	4.5			7	1	0
MMV007808	274.3	4.3	4.3	69.2	5	-0.3	0.4	1.7	6	1	0
MMV007839	312.2	2.7	2.0	55.8	3	-4.7	0.4	3.9	4	1	0
MMV007875	298.8	4.1	3.4	34.2	3	8.0	0.4	1.6	3	1	0
MMV007881	378.5	3.8	3.8	79.6	9	-3.1			6	1	0
MMV007906	274.3	3.4	3.4	64.4	6	-0.7			5	1	0
MMV007907	267.4	4.5	4.5	37.8	3	1.2	0.5	2.0	3	1	0
MMV007977	283.7	3.8	3.8	38.7	2	-5.4	0.4	2.2	3	0	0
MMV007978	319.4	3.4	3.4	47.6	8	-2.2			4	1	0
MMV008127	331.4	3.1	2.6	47.6	1	7.8	0.3	2.3	5	0	0
MMV008138	361.2	1.9	1.6	65.1	2	7.6	0.4	4.6	4	3	0
MMV008149	376.4	4.7	4.7	47.2	5	-1.1			4	1	0
MMV008212	280.3	3.1	2.5	54.4	3	8.0	0.4	2.9	4	2	0
MMV008270	265.3	3.8	3.8	50.4	1	1.8			4	1	0
MMV008294	380.4	5.9	5.9	69.7	7	5.9	0.3	0.7	6	1	0
MMV008416	228.3	3.8	0.4	27.1	3	12.6	0.5	2.8	2	1	0
MMV008474	405.5	3.6	3.1	54.9	6	7.6			6	0	0
MMV008829	393.5	2.5	2.5	88.9	4	1.0	0.3	3.4	7	2	0
MMV008956	377.9	3.8	3.6	60.0	6	7.3	0.3	2.6	5	2	0
MMV009015	367.5	3.9	3.2	49.8	9	8.0	0.3	2.3	4	1	0
MMV009060	274.4	3.8	3.8	32.3	5	5.4			3	1	0
MMV009063	322.5	4.1	1.4	37.2	5	10.2	0.4	2.4	3	2	0
MMV009085	410.4	0.6	0.6	115.2	8	-2.4	0.3	5.5	8	2	0
MMV009108	415.6	5.6	5.6	62.3	6	2.4	0.3	0.6	5	1	0
MMV009127	406.5	3.4	3.4	62.7	3	9.4	0.3	2.6	5	1	0
MMV011099	275.3	2.9	2.9	55.1	2	0.4	0.4	3.8	5	1	0
MMV011256	327.7	4.0	4.0	55.1	3	-0.6	0.4	2.7	5	1	0

MMV011259	321.3	4.4	4.4	55.1	3	-0.5	0.4	2.6	5	1	0
MMV011522	284.8	4.4	4.4	63.8	2	5.1	0.4	1.0	4	2	0
MMV011567	389.8	3.4	3.4	95.7	6	-3.1	0.3	2.9	8	1	0
MMV011576	445.5	2.6	2.6	82.7	6	-2.0	0.3	3.3	7	1	0
MMV011795	358.5	4.4	4.1	26.7	5	8.0	0.3	1.8	3	1	0
MMV011832	289.3	3.8	3.7	60.9	3	6.9	0.4	2.4	4	3	0
MMV011944	310.4	2.8	2.8	79.3	6	4.8	0.4	3.3	6	3	0
MMV018984	278.3	3.9	3.9	55.1	3	-0.7	0.4	2.3	4	1	0
MMV019017	367.3	3.5	1.7	46.4	7	9.2	0.3	2.5	4	2	0
MMV019064	493.6	4.5	4.5	62.6	7	6.0	0.2	1.3	7	1	0
MMV019066	359.4	2.2	2.2	87.7	6	-2.2	0.4	4.6	7	2	0
MMV019074	434.5	4.3	3.6	66.9	6	8.0	0.3	1.4	7	1	0
MMV019110	250.3	3.8	3.8	63.8	2	5.1	0.5	2.6	4	2	0
MMV019124	373.4	4.1	4.1	76.2	5	5.2	0.3	1.9	6	2	0
MMV019127	403.4	3.2	2.4	26.7	6	9.8	0.3	3.0	3	1	0
MMV019199	266.3	3.2	3.2	73.1	3	5.0	0.4	2.2	5	2	0
MMV019202	357.4	4.6	4.6	67.0	5	5.2			5	2	0
MMV019258	397.5	4.4	4.4	65.4	7	4.8	0.3	2.4	6	1	0
MMV019266	312.4	5.2	5.2	54.5	2	3.7	0.4	1.0	4	1	0
MMV019313	397.5	3.0	0.8	52.7	5	9.6	0.3	3.2	5	1	0
MMV019406	367.5	4.0	3.3	41.5	7	10.8	0.4	2.8	3	2	0
MMV019662	465.6	4.3	4.3	63.3	7	6.6	0.2	1.6	7	1	0
MMV019670	377.5	4.7	3.9	35.6	5	8.0	0.3	1.3	4	1	0
MMV019700	383.7	4.2	4.2	45.5	3	2.1	0.4	2.0	4	1	0
MMV019738	391.5	3.8	2.6	48.1	5	8.5	0.3	2.3	4	2	0
MMV019746	495.1	4.5	4.0	67.5	7	7.7	0.2	1.4	7	2	0
MMV019758	405.5	5.0	4.9	63.7	5	6.6			6	1	0
MMV019762	343.4	4.2	4.2	67.0	4	5.2			5	2	0
MMV019780	497.8	4.4	1.7	51.7	7	10.0	0.2	1.8	6	1	0
MMV019871	329.4	1.6	1.4	66.1	5	7.2	0.4	4.8	6	2	0
MMV019918	383.7	3.6	-0.9	37.2	5	10.4	0.4	2.5	3	2	0
MMV019995	462.4	2.8	0.1	44.8	6	10.0	0.3	3.5	5	1	0
MMV020243	362.4	4.1	4.1	82.2	5	6.1	0.3	1.8	7	3	0
MMV020275	457.0	4.4	3.3	58.1	5	8.5	0.3	1.6	5	1	0
MMV020439	459.6	4.4	4.1	53.4	7	7.5	0.3	1.9	6	1	0
MMV020490	457.0	4.4	3.3	58.1	5	8.5	0.3	1.6	5	1	0
MMV020492	309.8	3.5	3.5	29.5	1	-2.4	0.5	4.1	3	0	0
MMV020500	249.7	1.9	-1.0	37.0	5	10.2	0.6	5.2	3	2	0

MMV020505	310.8	3.0	0.9	28.4	7	9.5	0.4	3.1	3	1	0
MMV020548	413.5	3.4	2.6	64.3	5	8.1	0.3	3.1	6	2	0
MMV020549	398.5	4.2	2.6	61.0	4	9.1	0.3	2.4	5	2	0
MMV020651	431.3	4.6	4.5	54.7	5	6.8	0.3	1.1	5	1	0
MMV020654	368.7	4.6	4.6	49.3	4	-3.1	0.4	1.6	3	2	0
MMV020660	359.8	3.6	3.6	86.5	5	-3.1			7	1	0
MMV020700	349.5	5.2	5.2	54.9	5	-1.5	0.4	0.9	4	1	0
MMV020788	271.4	2.5	1.8	32.3	4	10.8	0.5	5.2	2	2	0
MMV020942	307.4	2.0	2.0	73.3	6	-0.3			6	1	0
MMV056726	279.4	3.0	3.0	29.5	3	-1.1	0.4	2.4	3	0	0
MMV073843	309.4	3.8	3.8	28.1	4	4.5			4	0	0
MMV075490	268.4	4.3	4.3	15.7	3	-2.0	0.4	1.8	3	0	0
MMV080034	254.3	3.5	3.5	63.8	2	4.9	0.4	2.5	4	2	0
MMV084434	358.4	3.5	3.5	59.9	4	-1.1	0.3	2.7	5	1	0
MMV084940	287.3	2.1	2.1	72.3	2	0.8	0.4	3.9	6	1	0
MMV085203	362.4	4.0	3.0	62.1	3	2.4	0.4	4.3	5	1	0
MMV128432	321.8	2.9	1.8	50.7	7	9.7	0.4	2.8	4	2	0
MMV142383	310.4	5.4	5.4	42.0	3	-0.7			3	1	0
MMV274073	280.3	3.1	2.6	54.4	3	8.0	0.4	3.0	4	2	0
MMV306025	341.3	1.1	1.1	104.0	4	-4.2	0.3	5.0	9	0	0
MMV396595	380.5	4.1	4.0	62.9	5	5.9	0.3	1.9	6	1	0
MMV396632	335.8	3.3	2.1	50.7	8	8.6	0.4	2.7	4	2	0
MMV396633	363.9	4.0	2.8	50.7	9	8.7	0.3	1.9	4	2	0
MMV396665	420.5	5.0	5.0	69.7	5	-0.7	0.3	1.1	6	1	0
MMV396669	401.5	4.9	4.9	70.2	7	6.1	0.3	1.0	6	2	0
MMV396672	396.5	4.8	4.0	32.3	6	8.1	0.3	1.6	3	1	0
MMV396681	472.4	5.2	5.2	78.3	5	2.5	0.3	0.8	7	1	0
MMV396693	254.3	-2.8	-2.8	49.0	3	2.1	0.5	9.3	4	2	0
MMV396703	317.8	3.0	1.1	56.8	6	9.3	0.4	3.4	5	2	0
MMV396704	301.8	2.7	2.3	48.1	1	7.6	0.4	3.2	5	1	0
MMV396705	392.4	3.2	3.2	76.9	5	-3.7	0.3	2.7	8	0	0
MMV396715	311.4	5.1	5.1	29.9	1	4.7	0.3	0.7	3	1	0
MMV396719	341.4	4.9	4.9	39.1	2	4.7	0.3	1.0	4	1	0
MMV396723	431.4	4.5	3.6	50.6	6	8.2	0.3	1.4	5	1	0
MMV396736	393.3	3.9	2.0	46.4	6	9.4	0.3	2.0	4	2	0
MMV396744	405.5	4.8	4.8	85.8	6	1.7	0.3	1.3	6	2	0
MMV396749	368.4	4.2	4.2	68.2	1	4.7	0.3	1.9	6	2	0
MMV396770	352.4	3.9	3.9	73.4	5	5.8	0.3	2.0	7	2	0

MMV396794	348.3	4.6	2.1	41.5	8	10.0	0.4	1.3	3	2	0
MMV396797	309.3	1.2	1.2	98.5	3	2.5	0.4	5.1	7	1	0
MMV403679	465.5	3.2	3.2	119.3	4	2.5	0.2	2.8	10	2	0
MMV498479	245.3	3.8	3.8	59.4	4	1.6			4	1	0
MMV638723	243.2	-2.8	-2.8	128.6	2	-0.1	0.5	9.2	8	4	0
MMV645672	341.4	4.4	1.4	29.1	1	-2.5	0.3	1.6	2	1	0
MMV665782	324.4	2.4	1.0	45.6	4	8.9	0.4	4.9	4	1	0
MMV665783	307.4	3.4	0.3	28.2	7	9.9			3	1	0
MMV665785	261.4	3.4	2.4	32.3	4	10.6	0.5	3.4	2	2	0
MMV665786	396.9	3.9	2.0	41.6	6	9.3	0.3	2.2	4	1	0
MMV665789	261.8	2.9	2.6	32.3	4	9.3	0.5	3.3	2	2	0
MMV665796	422.3	4.2	4.2	56.8	8	-1.1	0.3	1.6	5	1	0
MMV665798	366.3	5.7	5.7	50.7	4	0.9			4	1	0
MMV665799	381.8	3.4	3.4	80.3	5	5.6			6	2	0
MMV665800	347.8	4.2	4.2	47.6	7	-1.0	0.3	1.7	4	1	0
MMV665803	377.9	4.0	4.0	56.8	8	-1.1	0.3	2.1	5	1	0
MMV665805	367.4	4.2	4.2	86.5	7	-3.1	0.4	2.7	7	1	0
MMV665806	314.5	4.2	1.4	37.2	5	10.4	0.4	1.9	3	2	0
MMV665807	315.7	4.2	3.9	49.3	3	-4.3			3	2	0
MMV665809	395.7	4.3	4.4	26.7	4	6.9			3	1	0
MMV665810	348.4	1.6	-1.9	89.9	4	9.5	0.3	4.4	7	4	0
MMV665812	255.4	3.6	2.0	32.3	6	9.0			2	2	0
MMV665813	336.4	4.2	4.1	60.5	7	6.6			5	1	0
MMV665817	319.5	4.4	1.9	41.5	8	10.0			3	2	0
MMV665820	293.5	2.9	2.9	35.5	2	-4.7	0.5	3.4	3	0	0
MMV665824	286.3	4.3	4.3	34.9	2	3.0			3	0	0
MMV665826	319.4	3.1	3.1	67.1	4	-4.8	0.3	2.9	5	1	0
MMV665827	346.4	3.6	3.6	49.9	5	0.7	0.4	3.4	5	0	0
MMV665830	292.5	3.4	-0.1	15.3	6	10.6	0.4	2.6	2	1	0
MMV665831	426.5	4.2	4.1	78.9	9	10.3	0.3	2.5	6	2	0
MMV665836	310.4	3.5	3.5	50.7	3	-0.5	0.4	2.8	4	1	0
MMV665841	273.3	2.1	2.1	49.8	2	7.1	0.5	4.8	4	1	0
MMV665843	199.3	3.2	3.2	33.1	0	3.3			2	1	0
MMV665850	273.7	3.3	3.3	60.9	3	6.9			4	3	0
MMV665857	349.9	3.7	2.4	50.7	8	8.7			4	2	0
MMV665864	294.4	3.7	3.1	74.8	8	8.0	0.4	2.4	6	3	0
MMV665874	341.7	4.5	4.5	55.1	3	-0.6	0.5	3.7	5	1	0
MMV665875	395.9	2.8	1.2	60.5	6	8.8	0.3	3.4	6	2	0

MMV665876	326.4	4.6	4.6	43.1	4	-0.9	0.4	2.0	4	0	0
MMV665878	367.4	3.8	3.8	87.7	5	-4.8	0.4	3.0	7	2	0
MMV665879	412.5	5.4	5.4	86.9	5	5.1			6	3	0
MMV665881	479.5	3.0	3.0	98.1	7	1.0	0.2	3.0	8	2	0
MMV665883	422.4	4.5	4.5	100.0	5	5.1	0.3	1.6	7	3	0
MMV665886	385.9	5.2	5.2	55.4	6	-4.6	0.3	0.8	4	1	0
MMV665888	440.5	5.1	5.0	107.9	6	-3.4			7	4	0
MMV665890	339.4	3.5	3.5	86.5	5	-3.1			7	1	0
MMV665891	270.3	4.9	4.9	28.7	2	5.1	0.4	1.0	2	1	0
MMV665894	303.4	3.3	3.3	71.1	3	-1.8	0.4	3.0	5	2	0
MMV665897	189.2	1.2	1.2	61.0	1	5.0			4	1	0
MMV665898	403.4	3.9	3.9	85.5	6	5.2	0.3	2.0	7	2	0
MMV665899	340.8	4.8	4.8	33.2	4	2.5			3	0	0
MMV665901	441.3	4.2	4.1	54.7	5	6.8	0.3	1.7	5	1	0
MMV665902	443.4	3.9	2.3	53.8	6	9.0	0.3	2.1	5	2	0
MMV665904	218.3	1.0	1.0	41.9	3	3.3			4	0	0
MMV665906	440.5	3.4	3.4	115.4	4	1.2	0.3	2.8	8	3	0
MMV665908	453.6	3.9	3.9	63.3	8	6.6			7	1	0
MMV665909	360.2	4.4	4.4	54.9	3	1.2	0.4	1.5	4	1	0
MMV665913	416.5	4.1	4.1	85.4	6	-0.5			6	1	0
MMV665914	487.0	3.6	3.6	74.8	7	5.6			7	1	0
MMV665915	420.5	4.2	4.2	85.4	6	-0.5	0.3	2.2	6	1	0
MMV665916	353.4	2.3	2.3	87.7	6	-2.2	0.4	4.8	7	2	0
MMV665917	357.8	2.0	2.0	78.7	2	1.7			8	1	0
MMV665918	423.4	3.3	3.3	90.6	5	1.3			8	1	0
MMV665923	290.2	4.7	4.7	51.8	2	-1.0			4	1	0
MMV665924	286.8	4.2	4.2	26.3	4	-4.8	0.4	1.8	2	0	0
MMV665927	282.6	2.6	2.6	38.3	5	-4.8	0.5	3.7	3	1	0
MMV665928	338.3	4.9	2.6	32.3	6	9.7	0.4	1.3	2	2	0
MMV665929	338.3	4.9	2.7	32.3	7	9.7	0.4	1.1	2	2	0
MMV665934	337.2	4.1	4.1	42.9	1	0.0	0.4	1.9	3	0	0
MMV665935	290.2	3.4	3.4	50.7	3	0.4			4	1	0
MMV665939	346.4	4.6	4.6	58.2	4	-2.2			4	2	0
MMV665940	293.3	3.4	3.4	47.9	4	-4.6	0.4	2.9	4	0	0
MMV665941	389.5	5.0	5.0	30.0	6	5.2	0.3	1.6	4	1	0
MMV665944	312.4	2.6	2.4	35.9	5	7.8	0.4	3.4	4	1	0
MMV665946	388.5	4.4	2.9	61.0	5	8.9	0.3	1.6	5	2	0
MMV665948	348.2	4.6	4.6	62.5	3	-3.1			4	2	0

MMV665949	281.1	4.3	4.3	40.5	2	-6.0			2	2	0
MMV665953	333.6	5.1	5.1	41.1	2	-4.6	0.4	0.6	3	2	0
MMV665954	390.5	4.6	4.6	51.2	4	4.7	0.3	1.2	4	1	0
MMV665961	368.9	5.3	2.8	41.1	8	9.9			4	1	0
MMV665971	485.0	4.9	4.9	88.4	6	2.4	0.3	1.4	7	1	0
MMV665977	456.5	4.4	4.4	68.3	10	0.6	0.3	2.3	7	0	0
MMV665979	362.4	4.4	2.2	15.3	7	9.5	0.3	1.7	2	1	0
MMV665994	268.1	3.8	3.8	33.1	2	3.0	0.5	2.3	2	1	0
MMV666009	268.3	3.7	3.7	24.9	1	-2.3	0.4	2.3	4	0	0
MMV666020	265.4	3.3	0.7	41.5	10	10.0			3	2	0
MMV666021	272.3	3.8	3.8	42.9	1	0.0	0.5	3.2	3	0	0
MMV666025	500.2	5.5	5.5	55.9	4	0.5	0.3	0.4	5	1	0
MMV666026	288.3	3.2	3.2	52.1	2	0.1			4	0	0
MMV666057	420.7	4.8	4.7	71.1	4	5.6			5	2	0
MMV666060	393.4	3.7	3.3	49.8	6	9.0			4	1	0
MMV666061	384.5	2.9	2.0	35.9	5	9.7	0.3	3.4	4	1	0
MMV666067	480.0	4.8	3.0	62.8	8	9.2	0.3	1.3	6	2	0
MMV666069	418.6	4.3	1.5	33.5	9	9.4	0.3	1.5	5	0	0
MMV666070	445.5	4.8	2.9	44.4	7	9.3			4	2	0
MMV666071	413.5	4.3	3.5	61.3	5	8.1			5	2	0
MMV666072	438.9	3.5	3.3	50.8	8	7.0			5	1	0
MMV666075	254.3	3.9	3.9	15.7	2	-2.0			3	0	0
MMV666079	287.4	4.7	4.7	51.8	0	5.8	0.4	1.2	3	1	0
MMV666080	354.4	4.4	4.4	62.2	4	4.4	0.3	1.5	4	2	0
MMV666081	201.3	3.4	3.4	33.1	2	3.5			2	1	0
MMV666093	386.5	2.7	2.7	80.3	6	4.8			8	0	0
MMV666095	280.2	4.1	4.1	33.1	2	2.6	0.5	1.8	2	1	0
MMV666102	252.3	2.6	2.5	57.9	2	6.8			4	2	0
MMV666103	441.9	4.8	4.8	61.8	6	1.6	0.3	1.2	5	1	0
MMV666105	494.7	4.8	4.8	67.9	12	-3.1	0.2	1.2	6	1	0
MMV666108	401.0	3.7	2.2	45.5	7	8.9	0.3	2.2	4	1	0
MMV666109	383.5	3.8	3.0	59.0	8	8.4			5	1	0
MMV666110	411.6	3.8	1.0	35.6	9	10.0	0.3	1.9	4	1	0
MMV666116	354.5	2.8	1.9	26.7	4	10.1	0.3	3.5	3	1	0
MMV666124	403.9	4.6	4.6	72.0	6	-0.2			5	1	0
MMV666125	335.3	3.1	3.1	94.4	4	-7.1	0.4	3.3	6	0	0
MMV666599	328.2	4.0	4.0	38.7	2	-5.4			3	0	0
MMV666607	281.3	3.7	3.7	96.2	4	5.7	0.5	3.1	7	2	0

MMV666686	334.4	3.9	3.9	73.9	6	5.0	0.3	2.2	5	1	0
MMV666687	394.4	3.6	3.6	92.4	8	5.0	0.3	2.5	7	1	0
MMV666691	340.4	3.4	3.4	62.6	4	0.8	0.4	3.3	5	1	0
MMV666693	309.3	2.9	2.9	57.1	4	-4.5	0.5	4.7	5	0	0
MMV667486	261.3	1.3	0.3	89.2	3	8.4			6	2	0
MMV667487	260.3	1.2	-0.1	83.2	2	8.8			6	2	0
MMV667488	494.6	2.2	2.2	111.0	7	4.8	0.2	4.2	9	2	0
MMV667490	493.6	3.8	3.8	85.0	7	6.8	0.2	1.9	8	1	0
MMV667491	440.5	4.1	3.0	61.2	6	8.5	0.3	1.8	6	1	0
MMV667492	313.4	2.1	2.1	78.8	4	-1.0	0.4	3.8	6	1	0
MMV000304	314.4	5.1	4.1	34.2	4	8.5	0.3	0.8	3	1	1
MMV000326	316.3	5.1	4.3	24.9	3	8.1	0.4	0.8	2	1	1
MMV000442	315.8	5.6	5.6	12.5	3	4.2	0.4	0.9	2	0	1
MMV000445	381.5	4.9	4.9	59.8	10	6.5	0.3	1.0	5	2	1
MMV000570	278.4	5.3	5.2	45.2	3	6.6	0.4	1.4	3	2	1
MMV000604	417.4	4.6	4.6	48.0	4	3.9	0.3	1.5	5	0	1
MMV000617	432.0	5.2	4.9	41.9	9	7.3			4	1	1
MMV000619	422.4	5.6	5.4	32.7	8	7.3	0.3	0.2	3	1	1
MMV000621	399.6	5.5	5.2	32.7	10	7.4			3	1	1
MMV000642	469.0	5.5	5.5	58.6	6	-1.1	0.3	2.2	5	1	1
MMV000720	447.5	6.1	6.0	67.3	7	7.3	0.2	-0.1	5	2	1
MMV006172	368.5	4.9	3.2	31.4	3	8.6	0.3	2.0	4	1	1
MMV006389	359.4	5.5	5.5	29.4	1	0.6	0.3	0.9	2	0	1
MMV006513	337.4	5.1	3.6	40.7	4	9.2	0.4	1.4	3	2	1
MMV007092	662.9	4.0	3.3	90.3	18	7.8	0.2	1.9	10	2	1
MMV007113	358.4	7.2	7.2	24.7	2	0.6	0.3	-1.1	2	0	1
MMV007127	420.3	5.9	4.4	32.6	1	0.5	0.3	0.3	2	1	1
MMV007181	356.4	5.9	5.9	54.4	5	6.6	0.3	0.2	4	2	1
MMV007199	434.5	5.3	5.3	62.6	6	0.8	0.3	1.0	5	1	1
MMV007224	470.2	6.9	6.9	49.8	4	2.3	0.3	-0.9	4	2	1
MMV007273	480.6	7.0	7.0	67.4	7	4.9	0.3	-0.6	5	2	1
MMV007275	354.8	7.1	7.1	41.1	4	-1.6	0.4	-0.8	3	2	1
MMV007384	460.5	6.4	6.4	75.8	6	5.7	0.3	0.4	6	2	1
MMV007396	426.6	6.3	6.3	51.2	7	1.1	0.3	-0.2	4	1	1
MMV007574	413.6	6.8	6.8	29.1	4	-5.0	0.3	-0.7	2	1	1
MMV007577	420.6	6.4	6.4	51.2	7	1.1	0.3	-0.5	4	1	1
MMV007654	308.4	6.8	6.8	24.9	3	2.4			2	1	1
MMV008160	387.5	6.2	6.2	31.9	2	3.5	0.3	0.1	3	1	1

MMV008173	480.6	5.2	5.2	76.2	6	-4.5	0.2	0.6	7	0	1
MMV008455	484.6	5.4	5.4	67.9	6	-1.0	0.2	0.5	6	1	1
MMV019241	442.3	6.1	6.1	57.8	3	5.0	0.3	0.2	4	2	1
MMV019555	478.7	7.2	4.5	49.8	9	9.2	0.2	-0.7	4	2	1
MMV019690	470.6	5.0	3.8	43.5	5	8.4	0.2	1.0	5	2	1
MMV019741	458.6	6.2	6.1	50.2	6	5.9	0.2	-0.3	5	1	1
MMV019881	727.0	4.5	1.1	97.0	12	9.0	0.2	1.7	9	3	1
MMV020403	496.0	6.8	6.8	47.7	5	-3.9			5	1	1
MMV020750	372.4	4.9	4.9	67.4	5	4.9	0.3	1.1	5	2	1
MMV020912	420.5	6.8	6.8	58.3	6	3.0			4	2	1
MMV085471	465.6	8.1	8.1	39.9	7	6.5	0.2	-2.3	4	0	1
MMV086103	332.4	4.6	4.6	56.5	2	-2.9	0.3	1.4	4	0	1
MMV396594	490.7	6.9	6.9	58.6	4	4.0	0.2	-0.9	6	0	1
MMV396652	487.7	7.5	7.3	35.6	6	7.4	0.2	-1.6	4	1	1
MMV396663	485.7	6.5	5.9	58.4	7	7.9	0.2	-0.5	5	1	1
MMV396664	489.5	5.7	5.7	85.2	10	-4.5	0.2	0.5	8	0	1
MMV396678	462.9	5.6	5.6	59.3	6	1.6	0.3	1.0	5	1	1
MMV396679	492.9	5.5	5.5	68.5	7	1.7	0.3	1.6	6	1	1
MMV396680	476.9	6.1	6.1	59.3	6	1.7	0.3	0.9	5	1	1
MMV396717	492.0	5.9	5.8	78.5	6	1.1	0.2	0.2	6	2	1
MMV396726	484.6	6.7	6.4	56.3	6	7.2	0.2	-0.7	5	0	1
MMV665794	448.4	7.1	7.1	49.8	6	2.2	0.3	-0.6	4	2	1
MMV665797	364.4	4.9	4.2	60.5	8	8.0	0.3	1.4	5	1	1
MMV665814	419.5	5.7	5.6	67.3	6	6.5	0.3	0.3	5	2	1
MMV665840	382.2	5.6	5.6	57.8	3	5.2	0.3	0.5	4	2	1
MMV665852	350.0	5.5	5.5	41.1	2	-4.7	0.4	0.4	3	2	1
MMV665936	460.6	6.2	6.2	78.3	7	0.5			6	0	1
MMV665943	430.5	5.0	5.0	109.4	4	5.8	0.2	0.8	6	4	1
MMV665969	432.9	5.4	5.3	71.5	5	3.6	0.3	1.0	5	2	1
MMV665972	401.9	5.8	5.8	49.3	5	-2.6	0.3	0.1	3	2	1
MMV665980	332.5	4.5	4.5	44.3	3	-2.8			3	3	1
MMV665987	314.4	5.6	5.4	46.5	5	-7.0	0.4	0.6	3	1	1
MMV666022	453.3	5.5	5.4	71.5	5	3.6	0.3	0.6	5	2	1
MMV666023	453.5	8.7	8.7	54.6	6	1.6	0.3	-1.3	5	1	1
MMV666054	487.8	6.1	6.0	71.5	5	3.6	0.3	0.2	5	2	1
MMV666106	436.6	4.9	4.9	62.6	8	-3.0	0.3	1.1	5	1	1
MMV666123	412.0	5.8	5.8	46.9	4	1.2			4	1	1
MMV666596	468.1	9.2	9.2	28.0	4	1.5	0.3	-2.3	3	0	1

MMV666597	451.6	8.2	8.0	70.5	7	4.2	0.3	-2.0	5	2	1
MMV666600	459.9	7.3	7.3	57.5	8	-6.7	0.3	-0.7	5	0	1
MMV666688	476.0	7.5	7.5	37.6	4	3.2	0.3	-0.9	4	0	1
MMV666689	472.5	6.1	6.0	159.7	9	3.6	0.3	0.2	12	4	1
MMV666692	431.6	7.5	7.2	59.4	8	-0.5	0.3	-1.1	4	1	1
MMV667489	389.9	5.6	5.6	38.3	3	1.0	0.3	0.4	3	1	1
MMV000699	559.6	6.2	6.1	53.4	6	7.0	0.2	0.1	6	1	2
MMV000753	636.7	9.6	9.5	111.0	6	5.3	0.2	-3.1	7	4	2
MMV006962	501.4	6.7	6.7	86.9	5	5.1			6	3	2
MMV007160	621.8	8.8	8.8	78.0	3		0.2	-1.2	7	0	2
MMV007208	554.5	6.7	6.7	55.8	4	-1.1	0.2	-0.7	5	0	2
MMV007228	659.7	7.2	7.2	91.4	5	-2.0	0.2	-0.7	8	0	2
MMV007474	608.7	5.8	5.1	72.9	3	8.2	0.2	0.1	8	1	2
MMV007557	586.7	5.7	5.7	84.9	9	-1.3	0.2	0.5	7	1	2
MMV007695	657.8	7.9	7.9	80.8	7	-2.1	0.2	-1.1	6	0	2
MMV011436	579.1	8.9	8.8	52.9	4	1.8	0.2	-2.9	4	1	2
MMV011438	546.6	6.8	6.6	79.2	5	1.8	0.2	-0.3	6	1	2
MMV011895	524.6	5.9	5.9	127.9	6	5.8	0.2	0.1	8	4	2
MMV020885	510.4	6.9	6.9	38.3	3	2.2	0.3	-0.2	3	1	2
MMV085583	592.7	7.4	7.2	71.4	9	1.8	0.2	-0.7	6	1	2
MMV396635	520.0	5.2	4.2	62.5	6	8.4	0.2	0.8	6	1	2
MMV665882	574.2	6.0	3.3	37.2	5	10.2	0.3	0.4	3	2	2
MMV666062	571.7	8.0	8.0	54.5	5	-2.0	0.2	-1.4	4	0	2
MMV666101	631.7	7.6	7.6	72.9	7	-2.0	0.2	-0.8	6	0	2
MMV666601	637.7	7.3	7.3	82.4	9	3.1	0.2	-0.5	8	0	2
MMV666604	500.6	5.3	5.3	88.4	6	2.9	0.2	0.6	7	1	2